UNIVERSIDAD DE CANTABRIA

PROGRAMA DE DOCTORADO EN BIOLOGÍA MOLECULAR Y BIOMEDICINA

TESIS DOCTORAL

La panoplia de *Brucella*: búsqueda de efectores del Sistema de Secreción de Tipo IV y caracterización de inhibidores de lisozima

PhD THESIS

The panoply of *Brucella*: search for Type IV Secretion System effectors and characterization of lysozyme inhibitors

Realizada por: Yelina Ortiz Pérez

Dirigida por: Félix J. Sangari García

Matxalen Llosa Blas

Santander 2019

UNIVERSIDAD DE CANTABRIA

ESCUELA DE DOCTORADO DE LA UNIVERSIDAD DE CANTABRIA

DOCTORADO EN BIOLOGÍA MOLECULAR Y BIOMEDICINA

TESIS DOCTORAL

La panoplia de *Brucella*: búsqueda de efectores del Sistema de Secreción de Tipo IV y caracterización de inhibidores de lisozima

PHD THESIS

The panoply of *Brucella*: search for Type IV Secretion System effectors and characterization of lysozyme inhibitors

Realizada por:

Yelina Ortiz Pérez

Dirigida por:

Félix J. Sangari García y Matxalen Llosa Blas

Noviembre 2019

El **Dr. Félix J. Sangari García**, profesor del departamento de Bioquímica y Biología Molecular de la Facultad de Medicina de la Universidad de Cantabria y la **Dra. Matxalen Llosa Blas**, Catedrática de Bioquímica y Biología Molecular de la Facultad de Medicina de la Universidad de Cantabria.

CERTIFICAN:

Que la Graduada Yelina Ortiz Pérez, ha realizado bajo su dirección el presente trabajo de Tesis Doctoral titulado "La panoplia de *Brucella*: búsqueda de efectores del Sistema de Secreción de Tipo IV y caracterización de inhibidores de lisozima" ("The panoply of *Brucella*: search for Type IV Secretion System effectors and characterization of lysozyme inhibitors").

Consideramos que este trabajo se encuentra terminado y reúne los requisitos necesarios para su presentación como Memoria de Doctorado, al objeto de poder optar al grado de Doctor en Biología Molecular y Biomedicina de la Universidad de Cantabria.

Santander, 19 de noviembre de 2019

Fdo: Félix J. Sangari García

Fdo: Matxalen Llosa Blas

Esta Tesis ha sido realizada en el Instituto de Biomedicina y Biotecnología de Cantabria (IBBTEC) perteneciente a la Universidad de Cantabria (UC) y al Consejo Superior de Investigaciones Científicas (CSIC), en Santander (Cantabria, España).

La financiación para la realización de esta Tesis doctoral ha sido proporcionada por el Ministerio de Ciencia e Innovación (proyecto BFU2011-25658) y por la Universidad de Cantabria (proyectos 55.VP23.64005 y 55.JU07.64661).

La autora de esta Tesis ha disfrutado de una ayuda para contratos predoctorales en el área de la biomedicina, biotecnología y ciencias de la salud (referencia CVE-2015-11148), concedida por la Universidad de Cantabria.

Agradecimientos generales

Hace casi 10 años el profesor Vicente Ortuño nos dijo en un seminario que en la vida teníamos que ser valientes y coger el tren cuando pasase por nuestra estación. Qué no nos quedásemos esperando a que volviese a pasar, porque había veces en las que eso no sucedía. Desde entonces cada vez que he tenido que tomar una decisión esa frase aparecía por mi mente. Y eso fue lo que sucedió hace unos 4 años cuando el tren de la tesis pasó por mi estación. Me subí a él sin saber muy bien que me esperaría. El viaje no fue uno de los más placenteros que he tenido, la verdad sea dicha. Hubo varios problemas mecánicos, mareos, dolores de cabeza y muchas ganas de bajarse en la próxima estación. Sin embargo, al final a pesar de todo se decidió ser valiente, desarrollar mucha paciencia, afrontar los problemas, intentar solucionarlos y continuar el viaje. Y por fin ya suena por megafonía “próxima parada depósito y defensa, final del trayecto”. Sin embargo, este viaje no habría sido posible sin mucha gente.

En primer lugar gracias a mis directores Félix J. Sangari García y Matxalen Llosa Blas por abrirme las puertas de ese tren. Sin vosotros este viaje no habría sido posible. Gracias por darme la oportunidad y haber estado ahí durante todo el viaje. Y especialmente a Matxalen, gracias por ser un claro ejemplo de que las mujeres podemos conseguir todo lo que nos propongamos incluso en un mundillo predominado por hombres.

Gracias a mi grupo de micro por estar ahí y dejarme compartir mesa durante el viaje. En especial gracias a Candela, la melli, por aguantarme durante estos cuatro años, aunque a veces no haya sido nada fácil, paciencia has tenido. Aún recuerdo esos primeros días por medicina donde no sabíamos ni donde estábamos pinadas.

Sin embargo, aún me queda mucha gente por agradecer, porque sin ellos no hubiese habido viaje, o al menos no habría sido lo mismo. En especial a Lorena y Judit, esas dos personillas que conocí en la estación mientras esperábamos las tres subirnos al mismo tren. Ha sido un verdadero placer hacer este viaje con vosotras. He disfrutado de cada una de las miles de aventuras que he vivido con vosotras estos años. Gracias por sacarme de mi zona de confort.

Espero que aunque lleguemos al destino y cada una se embarque en su viaje personal siempre saquemos un huequito para vernos y seguir viviendo cosas juntas, aunque sea en la otra punta del mundo.

Mario, gracias por ser el chico para todo del IBBTEC y ayudarme a resolver la mayoría de los problemas mecánicos. Sin tu ayuda este tren seguiría estropeado. Bueno y gracias también por tus visitas por el labo a darnos algo de charleta.

A todos aquellos que han aguantado mis mareos y dolores de cabeza. Los que aún siguen subidos en el tren y los que ya llegaron a su parada: Laura, Ali, Ester, Fer, Rocio y Lore. Gracias por haber estado ahí en los cafés, las comidas y las cañas, ya sean de celebración como de terapia. Bueno, en general, gracias al grupo de cafes random, sin vosotros todo habría sido más aburrido.

Gracias también a los del vagón de al lado (grupo de Matxalen) por ayudarme con todos los problemas técnicos. En especial a Coral, que aunque ya no esta fue quién me ayudó durante el principio del viaje. Y como no, gracias también Sandra, Victor y tod@s los que han ido pasando por cocina, todos ellos son mis técnicos maravilla del IBBTEC. En especial a mami Mati, por todas tus sabias conversaciones y porque sin ti no sabría nada del mundo de las proteínas.

A todos aquellos del IBBTEC que aunque no haya nombrado han hecho que el viaje fuese más cómodo, gracias.

I would also like to thank Brett Lindenbach. Thank you for the opportunity to join your lab for three months. But specially, thank you Harish Ramanathan for teaching me all I know about Viruses. Thanks to Ann-Sofie, Alrun, Nagore and Ricardo for all the plans that we made. Pero especialmente, gracias a Ariadna, mi hermana mayor durante la estancia. Sin ti esos meses no hubiesen sido lo mismo.

Ademas, aunque este viaje comenzase hace 4 años, hubo otro anterior que me permitió estar en la parada lista para subirme a este tren. Por ello, gracias a todas esas personillas que conocí por Alcalá y aún siguen estando cerca de mí a pesar de la distancia. En especial a Maria y Rocío, por todas vuestras llamadas para apoyarme en todo momento.

Y no puedo dejar de mencionar a aquellos que realmente han hecho que aunque tuviese ganas, no me bajase de este tren. Mi familia, en especial mis padres. En parte por vosotros fui capaz de subirme al tren. Porque me enseñasteis a luchar por todo aquello que quiero y a no rendirme a pesar de las adversidades. Gracias por vuestras lecciones de vida y por aguantarme cuando he estado insoportable. Tenéis una paciencia infinita conmigo.

Gracias también a mis amigos, que a pesar de no entender muchas veces nada de lo que hablaba han estado ahí y han aguantado mis ausencias.

Y como no, gracias a mi vampiro particular. En parte sin ti el viaje habría acabado hace bastante tiempo. No solo me has facilitado llevar a cabo ciertos experimentos, sino que has sido capaz de aguantarme (tarea nada fácil y más en esta última etapa) y animarme a seguir siempre, por mucha distancia que hubiese. Gracias por subirte a este tren a mitad de trayecto, continuar en él hasta el final y querer subirte conmigo a los siguientes trenes que se presenten.

Gracias a mis cuatro estrellas, porque siempre estuvisteis orgullosos de mí y de lo que iba consiguiendo. Ojala estuvieseis aquí para poder verlo.

¡Uy! Ya suena por megafonía que se acerca el final del trayecto, voy a ir preparando todo para bajarme del tren. Hasta siempre.

Yelina

Agradecimiento a colaboradores

Gracias a Dr. Marcos Lopez Hoyos, Dr. David San Segundo Arribas y Dr. David Merino Fernández (Unidad de citometría de flujo, IDIVAL, Santander) por su ayuda en el análisis de la diferenciación celular.

Gracias al Dr. Víctor M. Campa (Servicio de Microscopia, IBBTEC, Santander) por su ayuda con la microscopia de fluorescencia y microscopia confocal.

Gracias al Dr. Charles M. Rice (The Rochefeller University, New York, EEUU) por proporcionarlos los plásmidos de la YFV y HCV.

Gracias al Dr. Brett Lindenbach (Yale University, New Haven, EEUU) por proporcionarnos los plásmidos pTRIP5-DEST y pTRIP6-DEST y los controles.

Gracias al Dr. Pablo Gastaminza (CNB, Madrid) por proporcionarnos la línea Huh 7.5.

Gracias al Dr. José Yuste (Instituto de salud Carlos III, Madrid) por proporcionarnos la línea celular HL-60.

Gracias al Dr. Javier León (IBBTEC, Santander) por proporcionarnos las líneas celulares THP-1, HL-60 y HEK 293T.

A mis padres,

a Gonzalo

“When it comes to life, we spin our own yarn, and where we end up is really, in fact, where we always intended to be”

-Julia Glass

ABBREVIATIONS

ABBREVIATIONS

aa	Amino acid
aBCVs	Autophagic *Brucella*-containing vacuoles
AhpC	Alkyl hydroperoxide reductase C
AhpD	Alkyl hydroperoxide reductase D
Ap	Ampicillin
APCs	Antigen-presenting cells
ATP	Adenosine 5'- triphosphate
ATRA	All-trans retinoic acid
BCVs	*Brucella*-containing vacuoles
bp	Base pair
BSA	Bovine serum albumin
BvfA	*Brucella* virulence factor A
C- type	Chicken or conventional type of lysozyme
CFUs	Colony-forming units
Cm	Chloramphenicol
CyaA assay	CyaA adenylate cyclase protein translocation reporter assay
CβG	Cyclic β-1-2- glucans
DAP	Diaminopimelic acid
DAPI	4,6' -diamino-2 phenyl indole
DCs	Dendritic cells
DENV	Dengue virus
DMEM	Dulbecco's modified eagle medium
DMF	Dimethylformamide
DNA	Deoxyribonucleotide acid
dNTP	Deoxyribonucleotide triphosphate
eBCVs	Endosomal *Brucella*-containing vacuoles
EDTA	Ethylenediaminetetraacetic acid
ENO-1	α-enolase
ER	Endoplasmic reticulum
ExPEC	Extraintestinal pathogenic *Escherichia coli*
FastAP	Thermosensitive alkaline phosphatase
FBS	Fetal bovine serum
GFP	Green fluorescent protein
Gluc	*Gaussia princeps* luciferase
GTP	Guanosine 5' triphosphate
g-type	Goose type of lysozyme
HCV	Hepatitis C virus
HEWL	Hen egg-white lysozyme
HL	Human lysozyme
IM	Inner menbrane
IPTG	Isopropyl-β-D-thiogalactopyranoside
IRF1	Interferon regulatory factor 1

i-type	Invertebrate type of lysozyme
kb	Kilobase
kDa	KiloDalton
Km	Kanamycin monosulphate
LB	Luria-Bertani broth
LDH	Lactate dehydrogenase
LPS	Lipopolysaccharide
LTs	Lytic transglycosylases
MHC-II	Molecules of major histocompatibility complex type II
MliC	Membrane-bound lysozyme inhibitor of c-type lysozyme
MOI	multiplicity of infection
NAG	N-acetyl glucosamine
NAM	N-acetyl muramic acid
NEAA	Non-essential amino acids
NO	Nitric oxide
NorD	Nitric oxide reductase D
Nx	Nalidixic acid
OD	Optical density
OM	Outer membrane
OMP	Outer membrane proteins
OptiMEM	Minimal essential medium
PAMPs	Pattern recognition receptors
PBS	Phosphate-buffered saline
PCR	Polymerase chain reaction
PEI	Polyethylenimide
PG	Peptidoglycan
PliC	Periplasmic lysozyme inhibitor of c-type lysozyme
PMNs	Polymorphonuclear cells
PMSF	Phenylmethylsulfonyl fluoride
rBCVs	Replicative *Brucella*-containing vacuoles
RNA	Ribonucleic acid
ROIs	Reactive oxygen intermediates
ROS	Reactive oxygen species
rpm	Revolution per minute
RPMI	Roswell park memorial institute culture medium
RT	Room temperature
SDS	Sodium dodecyl (lauryl) sulfate
SDS-PAGE	SDS-polyacrylamide gel electrophoresis
Sp	Spectomycin
T4SS	Type IV secretion system
TBE	Tris-borate-EDTA buffer
TE	Tris-EDTA buffer
TEM1 assay	TEM1 β-lactamase protein translocation reporter assay
TEMED	N, N, N' N'- tetramethylenediamine

TIR	Toll/interleukin-1 receptor
TLRs	Toll-like receptors
TPA	12-O-tetra-decanoylphorbol-13-acetate
TPR	Peptide repeats-containing protein
TSA	Trypticase soy agar
TSB	Trypticase soy broth
UPR	Unfolded protein response
VRCs	Viral replication compartments
WT	Wild-type
YFV	Yellow fever virus

INDEX OF FIGURES AND TABLES

List of figures

Introduction

Experimental procedures

Results

Discussion

List of tables

Introduction

Experimental procedures

Results

INDEX

INDEX

INTRODUCTION

1. INTRODUCTION

1.1 *Brucella* spp.

The organisms belonging to the genus *Brucella* are members of the order Rhizobiales of the α-proteobacteria class. They are small (0.5-0.7 μm in diameter and 0.6-1.5 μm in length) facultative intracellular Gram-negative, non-motile, non-sporing coccobacillus. Although they are aerobic microorganisms some strains require supplementary CO_2 to grow, especially on primary isolation. Most strains of *Brucella* show a strong urease activity, although it can differ between species and biovars (Alton et al., 1988). In addition to *Brucella* urease activity and CO_2 dependence, there are other characteristics used for *Brucella* identification such as oxidative activity, presence of different amino acids and carbohydrates, H_2S production, lysis by *Brucella*-specific bacteriophages, erythritol and dye-sensitivity, agglutination with monospecific sera and host preference (Alton et al., 1988). The *Brucella* genome is organized in two circular chromosomes and lacks any native plasmids. The chromosome I is composed of approximately 2.1 Mbp and contains most of the essential genes, while the chromosome II is smaller, approximately 1.2 Mbp (Jumas-Bilak et al., 1998; Michaux-Charachon et al., 1997; Paulsen et al., 2002).

Brucella organisms are the causative agents of brucellosis, also known as Malta fever, Mediterranean fever or undulant fever. Brucellosis is a zoonotic disease that can affect several animal species (cattle, dogs, sheep, goats, pigs, etc.), as well as humans. In fact, more than 500,000 cases of human brucellosis are diagnosed annually (Pappas et al., 2006). The symptoms of the disease are rather unspecific and similar to those of the flu, including fever, chills or loss of appetite. This fact, together with the scarce diagnostic methods present in some of the underdeveloped countries where brucellosis is more prevalent, makes brucellosis an underdiagnosed disease. Actually, some authors calculate the actual number of infections to be 10 or more times higher. Thus, the real number of brucellosis could be close to five millions of infected humans per year (Godfroid et al., 2013; Hull and Schumaker, 2018).

The *Brucella* genus comprises currently more than ten species. The six classic species are *B. abortus*, *B. melitensis, B. suis, B. neotomae, B. canis* and *B. ovis.* More recently, the genus has been extended including *B. pinnipedialis* and *B. ceti* from seals and cetaceans, respectively (Foster et al., 2007), *B. inopinata* isolated from a human breast implant (Scholz et al., 2010), *B. microti* isolated from soil and the common vole *Microtus arvalis* (Scholz et al., 2008a, 2008b), *B. papionis* isolated from baboons (Whatmore et al., 2014), and *B. vulpis* isolated from mandibular lymph nodes of red foxes (Scholz et al., 2016). Additionally, other bacteria in the genus are being considered as new *Brucella* species, which could increase further the number of species in the genus (Al Dahouk et al., 2017; Eisenberg et al., 2017).

The genus *Brucella* is very homogeneous, with over 90% identity on the basis of DNA-DNA hybridization assays within the classical species, and this results in relatively minor genetic variation between species, that sometimes results in striking differences. As an example, only 253 single nucleotide polymorphisms (SNPs) separate *B. canis* from its nearest *B. suis* neighbor (Foster et al., 2009), but their host specificity differs widely; while *B. canis* is almost entirely restricted to the Canidae family, *B. suis* has a wide host range that includes pigs, dogs, rodents, hares, horses, reindeer, musk oxen, wild carnivores and humans. Similarly, there are only 39 SNPs consistently different between the vaccine strain *B. abortus* S19 and strains *B. abortus* 9-941 and 2308, two well-known virulent isolates (Crasta et al., 2008). The regulation of the *virB* region, that codes for the crucial Type IV Secretion System (T4SS) of *Brucella*, one of the most important virulence factors of the genus, also differs markedly among the different members of the family (Rouot et al., 2003). However, all the components of the secretion apparatus and the effectors for the T4SS described so far are conserved along the genus, and most of the virulence factors are present and play the same role in all the species and isolates. Thus, the results obtained in one species are usually extrapolated directly into other species.

Most of the human infections are caused by just four species: *B. melitensis, B. suis, B. abortus* and *B. canis.* There are two main routes of human infection (Figure 1.1). Firstly, it could happen by direct contact with infected animals, tissues or isolates (professional exposure). Alternatively, it could occur

by consumption of infected, unpasteurized dairy products such as milk and cheese (gastrointestinal exposure) (Atluri et al., 2011). Though human-to human transmission is rare, several cases have been reported of transmission by sexual intercourse (Meltzer et al., 2010), maternal transmission during pregnancy (Vilchez et al., 2015), or by breast milk after birth (Palanduz et al., 2000).

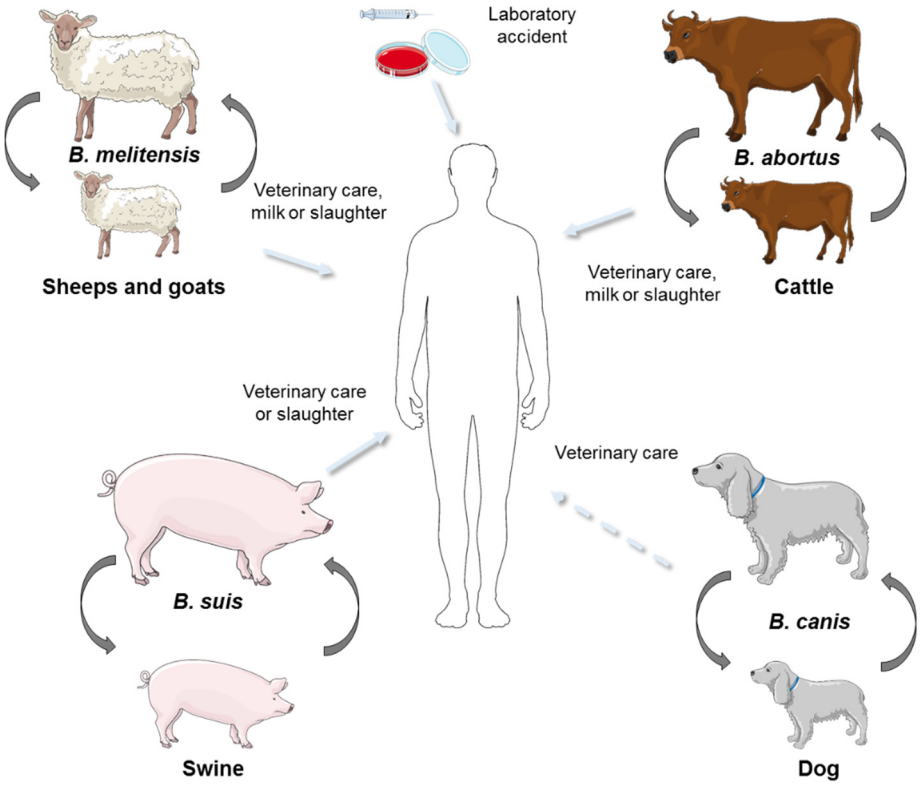

Figure 1.1. More relevant *Brucella* species, their hosts, and main causes of human infection. *Brucella* is transmitted to humans by contact with infected animals or by consumption of infected unpasteurized dairy products, as well as, by laboratory accidents. Infection with *B. melitensis*, *B. abortus* and *B. suis* are the most frequent, while infection with *B. canis* is rarely produced. Based on Alton and Forsyth, 1996.

1.1.1 Clinical and economic importance of *Brucella*

Brucellosis is a disease that continues being a worldwide problem, although in developed countries, the brucellosis incidence has been greatly reduced thanks to control and eradication campaigns in the last years (Figure 1.2). For example, in the case of Spain, human brucellosis decreased from 22.7 cases/100,000 in 1984 to 1.5/100,000 in 2004 (Sánchez Serrano et al., 2005), and the incidence reported by 20 European Union and European Economic Area

countries is around 0.10 cases/100,000 (Stockholm, 2018). However, in some countries where the disease has been controlled or eradicated, brucellosis is appearing again, probably due to increasing population mobility as travelers and immigrants (Ramos et al., 2008).

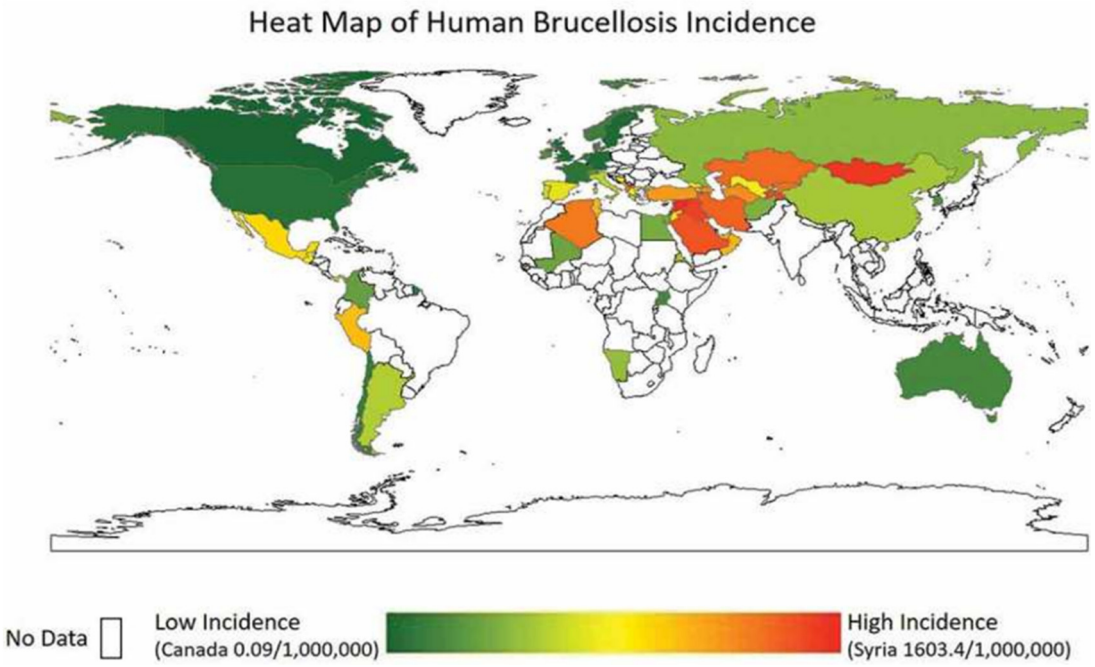

Figure 1.2. Incidence of human brucellosis. Taken from Hull and Schumaker, 2018.

As above mentioned, *Brucella* can infect livestock and humans. In general terms, *Brucella* infection affects the animal reproductive system, where it causes abortion or infertility (Lapaque et al., 2005). However, the development of brucellosis in humans is very different and it can be principally divided in two phases: acute and chronic brucellosis. The acute brucellosis corresponds to the incubation period, where brucellosis is characterized by influenza-like symptoms, especially high, undulating fever. Additionally, other symptoms such as headache, muscular pain, night sweats and fatigue are also frequent (Lulu et al., 1988; Mousa et al., 1988). However, when brucellosis is not properly treated, it derives into chronic brucellosis. In this phase of the infection, *Brucella* is resistant to human immune mechanisms, as well as all treatments used. Consequently, *Brucella* may progress and affect many host organs producing encephalomyelitis,

endocarditis, hepatitis, arthritis and orchitis (de Figueiredo et al., 2015; McDevitt, 1973). Moreover, some spontaneous abortions can be induced in humans by *Brucella*, although with less frequency than in animals (Al-Tawfiq and Memish, 2013).

Brucella is not only important for causing disease in humans, but it causes important economic losses, especially in livestock countries.

Brucellosis in animals has both direct and indirect effects on economy. Among the direct effects, brucellosis triggers economic losses due to productivity decline associated with abortion, reduction in milk production, reduction of weight gain in livestock, the premature death or culling of infected animals and diminution of animal welfare. In addition, other important economic losses are related to business losses, among other factors because infected animals cannot be sold. Indirect effects of brucellosis are mainly associated to an increase in cost related to disease control such as veterinary treatments and infrastructures, vaccination campaigns or control programs (Franc et al., 2018; Peck and Bruce, 2017).

Human brucellosis also causes effects at different levels. In addition to healthcare costs (diagnosis, treatment, and everything required to provide that care), it is necessary to add all indirect costs. At the population level, reduction of livestock production can increase malnutrition and developmental defects in children in some countries and reduce the workforce. Brucellosis also has effects at the individual level, such as loss of productive years due to premature death and loss of workdays. Finally, brucellosis also has intangible costs such as physical pain and emotional suffering (Franc et al., 2018; Peck and Bruce, 2017).

1.1.2 Intracellular life cycle of *Brucella*

Figure 1.3 summarizes the intracellular life cycle of *Brucella*. After invasion, *Brucella* is phagocytized by professional and non-professional phagocytes. Among professional phagocytes, *Brucella* can be phagocytized by macrophages, monocytes, neutrophils and dendritic cells (DCs). *Brucella* can also be phagocytized by other innate immune cells such as B lymphocytes (Goenka et al., 2012). In addition, *Brucella* is also phagocytized by non-

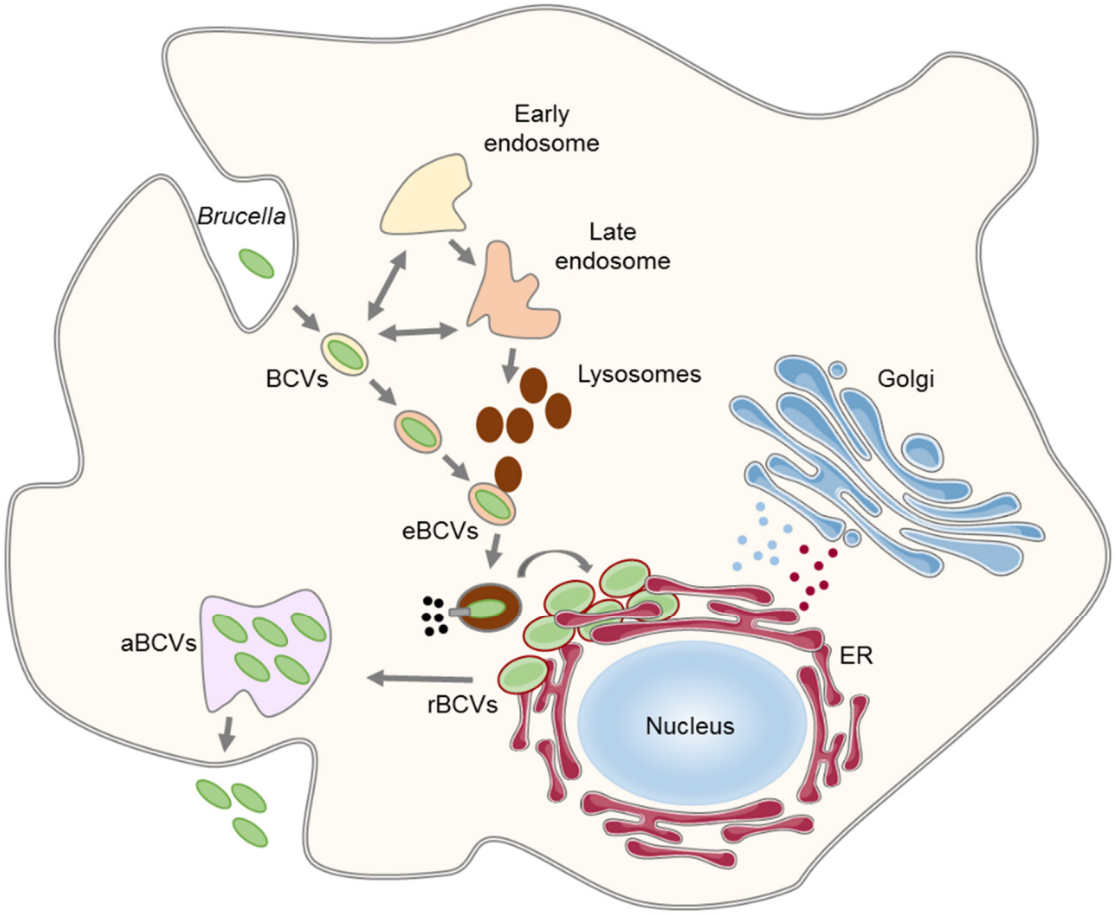

Figure 1.3. *Brucella* intracellular cycle. The Figure depicts the evolution of the BCVs upon interaction with the host to become rBCV, and egression through aBCVs (see text for details). Based on Dehio and Tsolis, 2017.

professional phagocytes like epithelial cells and trophoblasts. However, this bacterium is only able to replicate in some of these cell types. In general terms, after phagocytosis, *Brucella* is contained in membrane-bound compartments called *Brucella*-containing vacuoles (BCVs). These vacuoles interact with the endocytic pathway, including early and late endosomes and lysosomes, to become acidified endosomal BCVs (eBCVs). This acidification of bacterial vacuoles, together with a low nutrient availability, provide signals for expression and function of the T4SS (Boschiroli et al., 2002). The T4SS is a transmembrane channel, which translocates a series of effector proteins, as will be explained in detail later (section 1.1.4.2). In this way, when eBCVs are fused with lysosomes, they begin to lose the endosomal markers acquired during this first step. Then, eBCVs start to interact with the endoplasmic reticulum (ER), acquiring some

specific membrane markers of this intracellular compartment. This converts eBCVs in replicative BCVs (rBCVs). These vacuoles are called rBCVs because within these vacuoles *Brucella* acquires all the characteristics necessary for its replication. Also, there are some evidences of rBCVs interacting with the vesicular traffic between the ER and the Golgi Apparatus, indicating a strong interaction with the host secretory pathway (Celli, 2019; Sedzicki et al., 2018). After replication, rBCVs are captured within autophagosome-like structures in a VirB T4SS-dependent manner. BCVs are then called autophagic BCVs (aBCVs) because they express autophagy host proteins. This process helps *Brucella* to escape from the infected cell and to be released to the extracellular milieu to infect new cells.

1.1.3 Immune response against *Brucella*

The immune system is a host defense system composed by several proteins, types of cells, tissues and organs. The immune system is divided in two major subsystems, known as the innate immune system and the adaptive immune system. These responses are deeply interconnected, being the innate immune system the responsible for the adaptive immune response. The interconnection of these two branches makes the immune system a very efficient machinery for the destruction of many pathogens. Nevertheless, there are some pathogens, as is the case of *Brucella*, that have developed several mechanisms to evade their elimination through the immune system (Galińska and Zagórski, 2013).

1.1.3.1. The innate immune response against *Brucella*

The innate immune system is the first line of defense in the host. This system is composed by anatomical barriers such as the skin and the internal epithelial layers; secretory molecules including, among others, complement proteins and cytokines; and several cellular types. Among the different cell types are included phagocytes such as neutrophils, monocytes, macrophages and DCs; and some innate lymphocyte subsets like natural killer (NK) and γδ T cells. Each of these cell types has a specific function inside the innate immune system. However, they all have the main objective of killing the pathogen. This is the

reason why a coordinated function between them is so necessary. Still, this type of immune response does not induce immunological memory (Chaplin, 2010; Skendros and Boura, 2013; Thakur et al., 2019).

In general terms, the innate immune cells recognize pathogen-associated molecular patterns (PAMPs) such as the lipopolysaccharide (LPS) and the peptidoglycan (PG), through pattern recognition receptors (PRRs) like Toll-like receptors (TLR). After recognition and phagocytosis, innate immune cells use several strategies to kill the pathogens, including bacterial compartmentalization, oxidative and nutrient stress, lysosome-mediate degradation, antimicrobial peptides or autophagy (reviewed in Diacovich and Gorvel, 2010).

There are many intracellular bacteria, such as *Brucella*, which manipulate the host innate immune system to survive inside the host. Among other strategies, bacteria can control the signaling pathways activated by host receptors, escape from the phagosome, prevent phagosome-lysosome fusion or avoid autophagy (Thakur et al., 2019). In particular, *Brucella*, after phagocytosis by macrophages or monocytes, inhibits the activation and the apoptosis of these cells (Barquero-Calvo et al., 2007; Gross et al., 2000; He et al., 2006), promoting bacterial proliferation (Gross et al., 2000; Jimenez de Bagues et al., 2005). Something similar happens inside DCs, where *Brucella* prevents their maturation and activation, allowing its replication inside these cells (Salcedo et al., 2008). Inside neutrophils, *Brucella* resists to the antimicrobial action of these cells and inhibits their degranulation (Barquero-Calvo et al., 2007; Kreutzer et al., 1979; Tejada et al., 1995). Also, the LPS of *Brucella* induces the premature death of neutrophils (Barquero-Calvo et al., 2015), promoting the phagocytosis of these death neutrophils that contain *Brucella* by macrophages (Gutiérrez-Jiménez et al., 2019). In addition, its O-antigen limits the attack of complement proteins, promoting the survival of extracellular *Brucella* (Lapaque et al., 2005). Also, the O-antigen, together with the core and the lipid A, the other components of the LPS, protect bacteria from degradation by antimicrobial cationic peptides (Tejada et al., 1995).

Brucella also secretes some proteins through its T4SS which are capable of modifying the innate immune response, as is the case for BtpA and BtpB, that inhibit the TLR pathway, among other functions (Durward et al., 2012; Salcedo et

al., 2008; Salcedo et al., 2013) (Figure 1.4). The role of T4SS effector proteins will be detailed in section 1.1.4.2.

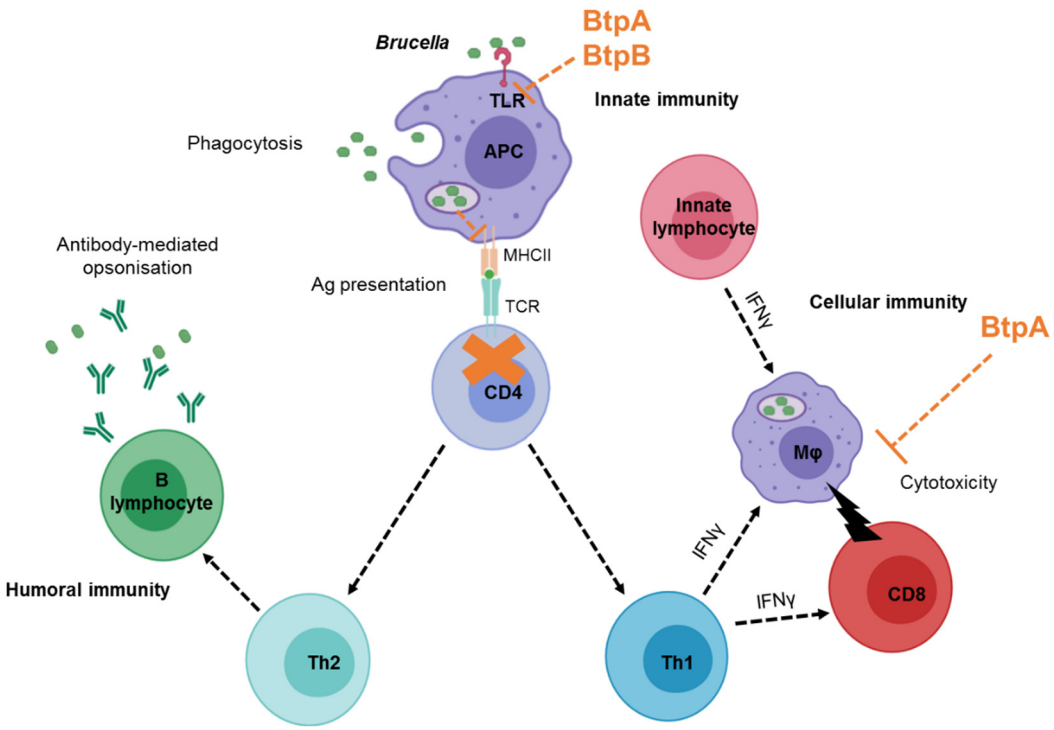

Figure 1.4. Resistance mechanism of *Brucella* to immune response. BtpA, a T4SS effector protein, inhibits the cytotoxicity mediated by lymphocyte $CD8^+$ T cells. Also, BtpA together with BtpB inhibits the TLR pathway response. *Brucella* can also reduce MHCII expression reducing the antigen presentation to $CD4^+$ T cells. Based on Skendros and Boura, 2013.

1.1.3.2. The adaptive immune response against *Brucella*

The adaptive immune response is a specific response where antigen-presenting cells (APCs) present the bacterial peptides, produced during the phagocytosis, to T-cell receptors localized in the surface of $CD4^+$ T cells. Bacterial peptides are presented through the molecules of the major histocompatibility complex type II (MHCII) to $CD4^+$ T cells activating their T-cell receptor. Thus, APCs are able to activate $CD4^+$ T and cytotoxic $CD8^+$ T cells (Figure 1.4). Activated $CD4^+$ T cells secrete pro-inflammatory cytokines and produce the activation of B and $CD8^+$ lymphocytes. All these cells migrate to the infection site where they begin to release cytokines as part of the specific response. At the same time, activated B lymphocytes produce antibodies that facilitate the

detection and destruction of bacteria (Chaplin, 2010; Skendros and Boura, 2013; Thakur et al., 2019).

Many pathogens have developed different mechanisms to avoid adaptive immunity. In the case of *Brucella*, upon phagocytosis by macrophages or DCs that can act as APCs, *Brucella* can downregulate the expression of MHCII reducing the antigen presentation to $CD4^+$ T cells. Thus, *Brucella* can survive inside phagocytic cells and evade the immune system (Velásquez et al., 2017).

1.1.4 Virulence factors of *Brucella*

Although *Brucella* lacks classical virulence factors such as exotoxins, cytolysins, capsule, flagella or fimbria, *Brucella* has many virulence factors to escape of the immune mechanisms in order to survive and replicate in the host, and to establish a persistent infection. Among them, the LPS and the T4SS have special interest in the context of this work.

As previously mentioned, *Brucella* genus is very homogeneous, so most of the virulence factors or mechanisms to survive and replicate inside the host present in a species can be extrapolated to the whole genus.

1.1.4.1. *Brucella* cell envelope and LPS

The *Brucella* cell envelope is schematized in Figure 1.5. As in other Gram-negative bacteria, the cell envelope is composed by the inner and the outer membranes (IM and OM, respectively); in the middle of both bilayers, the periplasmic space contains the PG. *Brucella* cell envelope also contains lipoproteins in its OM that interact with the PG making a more stable OM bilayer (Cloeckaert et al., 2002; Moriyón and López-Goñi, 1998). The most external component of the Gram-negative bacteria cell envelope is the LPS. Here, we will only describe the PG and some peculiarities related to the *Brucella* LPS and the OM.

As mentioned before, *Brucella* cell envelope, as the rest of Gram-negative bacteria, contains PG, a key component of the bacteria cell wall that is located between the IM and the OM. PG protects bacteria from lysis by osmotic pressure and preserves bacterial shape. It is composed of β-linked glycan strands of N-

acetyl muramic acid (NAM) and N-acetyl glucosamine (NAG), cross-linked by short peptide chains (Figure 1.6). Although the sugar composition of this PG is shared between Gram-positive and Gram-negative bacteria, there are some variations in peptide chains. In most Gram-negative bacteria, the peptide structure is L-Ala-D-Glu-mesoDAP-D-Ala-D-Ala while in Gram-positives the third amino acid is generally L-Lys (Vollmer et al., 2008). Due to the importance of this polymer, it is not surprising that its synthesis and degradation is regulated by several proteins, allowing the insertion of new components in the cell envelope and a normal bacterial growth (Typas et al., 2012). One of the most important types of proteins involved in degradation of PG are the N-acetylmuramidases, which can cleave the bond that binds the NAG and NAM, as will be seen later.

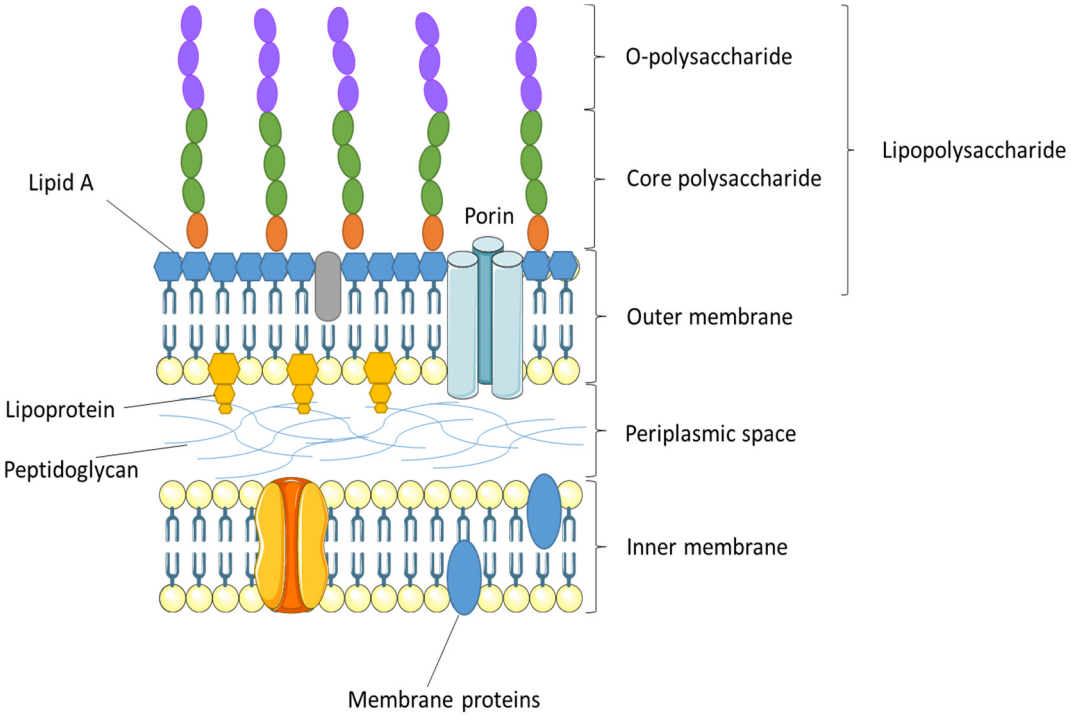

Figure 1.5. Schematic representation of Brucella cell envelope. The cell envelope is comprised of inner and outer membranes. The inner membrane is a bilayer of phospholipids, while the outer membrane contains a phospholipid inner layer and an outer layer with the LPS. LPS has three components: the O-polysaccharide, the core polysaccharide and the lipid A. Finally, *Brucella* cell envelope has a periplasmic space between the inner and the outer membrane which contains peptidoglycan.

Brucella contains a peculiar OM composed of LPS, free lipids, several OM proteins (OMP), including porin proteins, and lipoproteins. It has been demonstrated that some OMPs can interact with the LPS and with the PG,

conferring more stability to the OM (Cloeckaert et al., 2002, 1992; Moriyón and López-Goñi, 1998). The main peculiarity of *Brucella* cell envelope is its LPS, which constitutes one of its most important virulence factors.

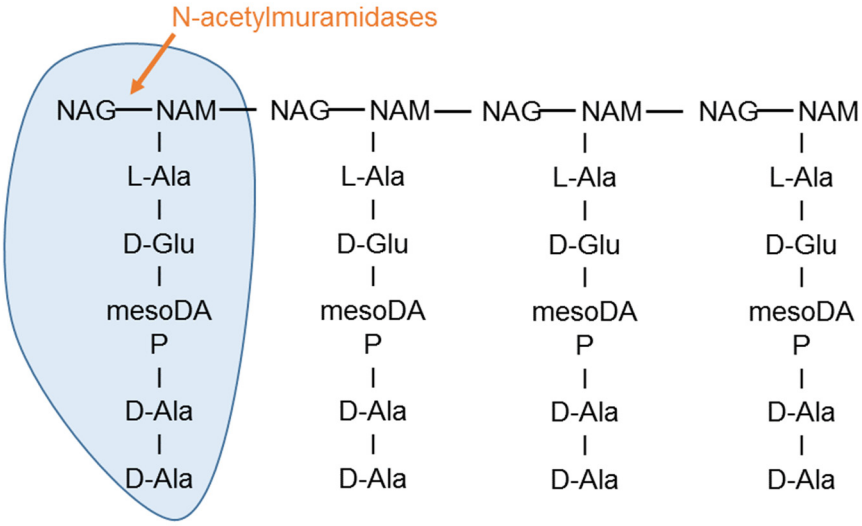

Figure 1.6. Schematic representation of the composition of the typical Gram-negative peptidoglycan.

Brucella LPS, as in other Gram-negative bacteria, is vital for the structural and functional integrity of the OM. It is composed of a large glycolipid that can be divided into three structural domains: the lipid A, the core oligosaccharide and the O-antigen. *Brucella* contains a non-classical or non-endotoxic lipid A, which contains a diaminoglucose backbone instead of glucosamine; and acyl groups are longer than in other Gram-negatives. Moreover, *Brucella* lipid A is only linked to the core by amide bounds, while in other Gram-negative bacteria it is linked by ester and amide bonds (Bertani and Ruiz, 2018; Cardoso et al., 2006; Lapaque et al., 2005). Thus, the composition of this lipid A contains a lower number of negatively charged groups compared with the lipid A of other Gram-negative bacteria sugars (Moriyón and López-Goñi, 1998). This peculiarity prevents binding of the complement, the lysozyme or other cationic peptides to the OM (Martirosyan et al., 2011). In addition, *Brucella* also contains an O-antigen that confers to the bacterium more resistance to the innate immune system, as will be seen later.

1.1.4.2. *Brucella* T4SS and its effector proteins

Brucella encodes a T4SS, named VirB. T4SSs are a family of bacteria secretion systems (Figure 1.7) which stand out for their high plasticity because they are able to translocate proteins, DNA, peptidoglycan and even LPS biosynthesis metabolites (Boudaher and Shaffer, 2019; Gall et al., 2017; Zimmermann et al., 2017). The substrate can be translocated to the extracellular milieu or to another cell, either prokaryotic or eukaryotic. T4SS can participate in several biological functions, such as horizontal DNA transfer through bacterial conjugation or, as in the case of *Brucella*, eukaryotic cell infection (Figure 1.7.B). Through its T4SS, *Brucella* regulates the inflammatory response and manipulates

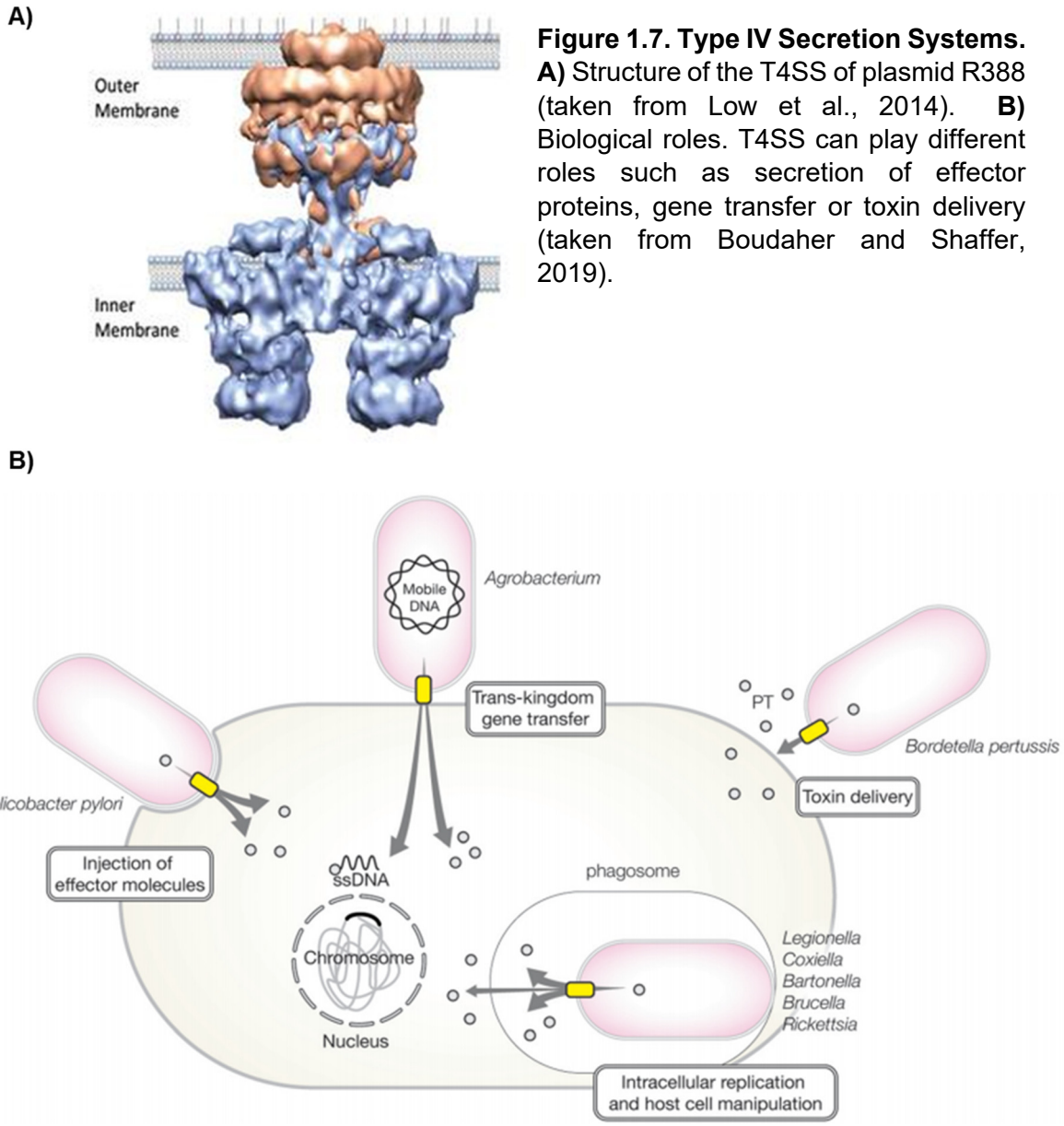

Figure 1.7. Type IV Secretion Systems. A) Structure of the T4SS of plasmid R388 (taken from Low et al., 2014). **B)** Biological roles. T4SS can play different roles such as secretion of effector proteins, gene transfer or toxin delivery (taken from Boudaher and Shaffer, 2019).

the vesicular trafficking in the host, establishing a favorable niche for its replication. It is known that T4SS-deficient strains are attenuated in early stages of infection (Hanna et al., 2011; Sá et al., 2012). Recent studies indicate that *Brucella* T4SS is also necessary in post-replication stages of the intracellular cycle (Smith et al., 2016).

In order to perform its function in the host cell, the T4SS secretes effector proteins into host cells. Thus, it is possible that these effector proteins play important roles during the different stages of the infection, targeting host mechanisms and perpetuating the infection. In this way, the identification of effector proteins secreted by the *Brucella* T4SS and the determination of their target pathway in the host are essential to understand *Brucella* pathogenesis.

- **Effector proteins secreted by *Brucella* T4SS**

The number of substrate proteins translocated by each T4SS varies widely, from a single known protein substrate in the case of the *Helicobacter pylori* T4SS Cag, to the hundreds of effector proteins identified in the intracellular human pathogens *Legionella pneumophila* and *Coxiella burnetti* (Boudaher and Shaffer, 2019; Weber and Faris, 2018). In the case of *Brucella*, since the identification of its T4SS (O'Callaghan et al., 1999), it took almost 10 years to identify the first effector proteins. Since then, scattered new effectors have been found using different methods (Figure 1.8). Until now, 15 effector proteins have been discovered (listed in Table 1.1), most of them with unknown functions or targets in the host cells.

The first reported effector proteins were VceA and VceC, identified using the TEM1 β-lactamase protein translocation reporter assay (TEM1 assay) (de Jong et al., 2008). The authors later showed that VceC interacts with Bip/Grp78, activating the Unfolded Protein Response (UPR) (de Jong et al., 2013). More recently, contradictory results have been reported related to the role of VceC. Some authors found that VceC induces CHOP expression favoring ER stress in placental trophoblast, and thus, inducing cell death and placental inflammation, promoting abortion (Byndloss et al., 2019). Other authors found that VceC inhibits the expression of CHOP protein inhibiting apoptosis mediated by ER stress, and

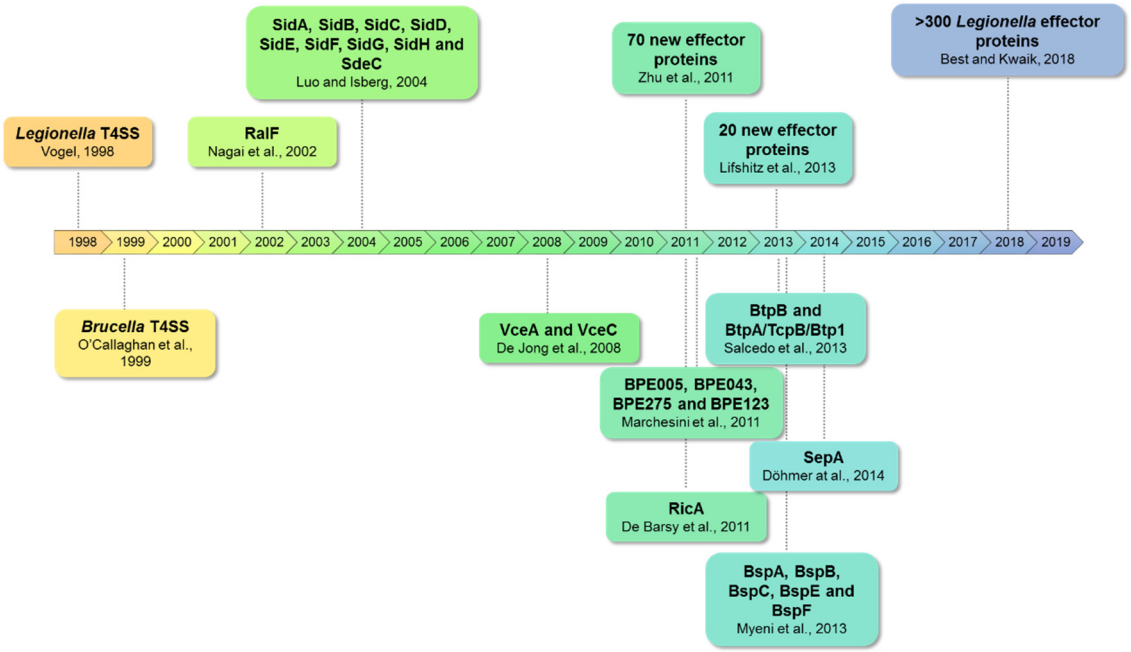

Figure 1.8. Comparison of *Brucella* and *Legionella* effector proteins discovered since the identification of their T4SS. On the top of the timeline the first effector proteins identified in *Legionella* since the discovery of its Dot/Icm T4SS are shown, as well as the total number of effector proteins identified until now. At the bottom of the timeline all effector proteins secreted by *Brucella* T4SS identified since the discovery of its T4SS are shown.

thus, protecting cells from death by apoptosis and favoring intracellular persistence (Zhi et al., 2019). Also, very recently, it has been shown that a *vceA* mutant promotes autophagy and inhibits apoptosis in trophoblasts during *Brucella* infection (Zhang et al., 2019).

Years later, five new effector proteins were reported. BPE005, BPE043, BPE275 and BPE123 were identified using the CyaA adenylate cyclase reporter assay (CyaA assay) (Marchesini et al., 2011). BPE123 was shown to interact with α-enolase (ENO-1), a host cell factor involved in *B. abortus* intracellular replication (Marchesini et al., 2016). Additionally, BPE005 was shown to induce collagen deposition and matrix metalloproteinase 9 down-modulation via transforming growth factor β1 in hepatic stellate cells (Arriola Benitez et al., 2016). Another effector protein, RicA, was shown to interact with Rab2 (de Barsy et al., 2011).

Name	Gene	Target	Function	Method
VceA	*bab1_1652*	Unknown	Inhibit autophagy and induce apoptosis	TEM1
VceC	*bab1_1058*	Bip/Grp78	Activate UPR	TEM1
BPE005	*bab1_2005*	Unknown	Induce collagen deposition and matrix metalloproteinase 9 down-modulation	CyaA
BPE043	*bab1_1043*	Unknown	-	CyaA
BPE275	*bab1_1275*	Unknown	-	CyaA
BPE123	*bab2_0123*	ENO-1	Contribute to intracellular lifestyle of *Brucella*	CyaA
RicA	*bab1_1279*	Rab2	Regulate vesicular trafficking	TEM1
BspA	*bab1_0678*	Unknown	Inhibit the secretory pathway	TEM1 and CyaA
BspB	*bab1_0712*	Unknown	Inhibit the secretory pathway and promote biogenesis of rBCV and bacterial proliferation	TEM1 and CyaA
BspC	*bab1_0847*	Unknown	-	TEM1 and CyaA
BspE	*bab1_1671*	Unknown	-	TEM1 and CyaA
BspF	*bab1_1948*	Unknown	Inhibit the secretory pathway	TEM1 and CyaA
BtpB	*bab1_0756*	Unknown	Inhibit TLR pathways; block energy metabolism	TEM1 and CyaA
BtpA/TcpB/Btp1	*bab1_0279*	MAL	Inhibit TLR pathways and CD8+ T cell killing action; block energy metabolism	TEM1 and CyaA
SepA	*bab1_1492*	Unknown	Inhibit BCV fusion with the lysosome	Immunofluorescence (3xFLAG)

Table 1.1. *Brucella* T4SS effector proteins.

Later on, five more effector proteins were described, BspA, BspB, BspC, BspE and BspF (Myeni et al., 2013). Some of them were shown to inhibit the secretory pathway. BspB was recently shown to remodel the Golgi-associated membrane traffic to promote biogenesis of the rBCV and bacterial proliferation (Miller et al., 2017). BtpA and BtpB were identified together as T4SS effector proteins (Salcedo et al., 2013). BtpA was previously studied by several authors,

who showed that BtpA has a toll interleukin-1-receptor (TIR) domain and is able to interfere with DC maturation (Cirl et al., 2008; Salcedo et al., 2008). It was also reported that its target was the eukaryotic adaptor protein MAL (Radhakrishnan et al., 2009; Sengupta et al., 2010), and that the protein could inhibit *Brucella* killing by $CD8^+$ T cells (Durward et al., 2012). BtpA and BtpB through their TIR domain are able to modulate host inflammatory responses during infection, specifically inhibiting TLR pathway (Salcedo et al., 2013). Finally, the last T4SS effector protein of *Brucella* identified until now is SepA (Döhmer et al., 2014). This protein inhibits the fusion of BCVs with the lysosome.

- **Controversy in the conventional detection methods**

Candidate *Brucella* T4SS effector proteins have been proposed using different methods. VceA and VceC were chosen as candidates due to the presence in their promoter of a conserved region necessary for the activation by VjbR. This conserved region is also present in the VirB promoter (de Jong et al., 2008). RicA was identified as candidate by a high-throughput yeast two-hybrid screen to identify interactions between *Brucella* proteins and human proteins predicted to be associated to phagosomes such as Rab2 (de Barsy et al., 2011). Many other *Brucella* effector proteins were chosen as candidates based on bioinformatic searches or *in silico* screenings. The first bioinformatic search was based on the identification of proteins with eukaryotic domains or protein-protein interaction domains, as well as proteins with domains known to be related to virulence, among others, being good candidates for modulation of host cells functions (Marchesini et al., 2011). Other authors searched for potential horizontally transmitted regions encoding transposases or recombinases adjacent to transfer tRNAs (Döhmer et al., 2014); other criteria used were limited homology in other bacteria genera, GC content, presence of eukaryotic-like motifs, and the presence of features similar to known T4SS effector proteins (Myeni et al., 2013). Finally, BtpA and BtpB were proposed as effector proteins based on the evidence for BtpA role in the host and the presence of the TIR domain in both BtpA and BtpB proteins (Cirl et al., 2008; Salcedo et al., 2008; Salcedo et al., 2013). Thus, depending on the identification method, some putative effector proteins are going to be identified as candidates, while others

will be missed. Therefore, the identification of new *Brucella* effector proteins will depend on the screening method used.

Once the candidate effector proteins have been selected, their translocation through the T4SS must be validated experimentally. Traditionally, there are three methods to detect the secretion of effector proteins from bacteria to eukaryotic cells: CyaA and TEM1 enzymatic translocation assays (Qureshi, 2007; Sory and Cornelis, 1994) and 3xFLAG fusion. However, in the case of *Brucella,* these methods are not 100 % efficient, rendering contradictory results. For instance, SepA (BAB1_1492) translocation was not detected using the CyaA assay (Marchesini et al., 2011), but later it was detected as effector protein secreted by the *Brucella* T4SS using a 3xFLAG construction (Döhmer et al., 2014). Something similar happened with BPE611 (BAB1_1611) and BPE119 (BAB2_0119), not detected as effector proteins by the CyaA assay (Marchesini et al., 2011), but subsequently identified as effector proteins secreted independently of the T4SS by CyaA and TEM1 assays (Myeni et al., 2013). The identification of BAB2_0541 as a secreted protein independently of the *Brucella* T4SS is also controversial, because it was detected by the TEM1 assay but not by the CyaA assay (Myeni et al., 2013). Thus, it is probable that *Brucella* can secrete many other effector proteins, and some of them through its T4SS. Moreover, some of the putative effector proteins which showed negative results for some of the translocation methods used could be real effectors.

Together, everything suggests that the identification of *Brucella* effector proteins secreted by its T4SS is not complete. Therefore, the utilization of a new screening method for the identification of putative effector proteins could provide new candidates not previously studied as putative secreted effector proteins, allowing the identification of new T4SS effector proteins of *Brucella*.

1.1.4.3. Other virulence factors of *Brucella*

- Cyclic β-1-2-glucans (CβG). CβG is a periplasmic homopolysaccharide produced by several bacteria, such as *Brucella*. This glucan is necessary for intracellular survival of *Brucella*. CβG interacts with lipid rafts on macrophage cell membranes, avoiding phagosome-lysosome fusion, so bacteria can survive and travel to the endoplasmic reticulum for its replication (Arellano-Reynoso et al.,

2005). However, its function in the immune response is controversial. Initially, some reports suggested that CβG can promote spleen inflammation due to massive cell recruitment, activate human and mouse dendritic cells, and improve $CD4^+$ and $CD8^+$ T cell response (Martirosyan et al., 2012; Roset et al., 2014). Nevertheless, other report suggests that this compound reduces inflammation because it produces a transient recruitment of neutrophils at the site of infection (Degos et al., 2015). Therefore, CβG can act as an activator or as repressor of the immune response, probably depending on the moment or tissue of infection.

- BvrR/BvrS system. This two component system has an important role in penetration, invasion and intracellular replication, being essential for *Brucella* virulence, among other functions, because it controls the expression of the *Brucella* T4SS, as well as the carbon and nitrogen metabolism (Martínez-Núñez et al., 2010; Sola-Landa et al., 1998; Viadas et al., 2010). Also, it is implicated in cell envelope modulation as it regulates the expression of some OMP and lipid A structure, and thus becoming a necessary system for bacterial homeostasis (Guzman-Verri et al., 2002; Manterola et al., 2005). In addition, it was shown that mutants of the BvrR/BvrS system are more sensitive to cationic peptides (Sola-Landa et al., 1998).

- Superoxide dismutase and catalase. Innate immune cells produce reactive oxygen intermediates (ROIs) for destruction of the ingested bacteria. However, *Brucella* can produce some enzymes such as superoxide dismutase and catalase that counteract ROIs (Gee et al., 2005).

- Urease. This protein is a nickel-containing enzyme that decomposes urea to carbon dioxide and ammonia increasing pH in the medium and thus, allowing *Brucella* survival in acid environment (Głowacka et al., 2018). Moreover, urease can protect *Brucella* during their passage through the stomach (Sangari et al., 2007).

- Cytochrome oxidase. Cytochrome oxidase is an enzyme expressed during intracellular replication allowing adaptation of *Brucella* to the replicative niche inside macrophages, where there is low oxygen availability (Ko and Splitter,

2000). Cytochrome oxidase controls the production of oxidative free radicals and the detoxification of the compartment inside the host (Endley et al., 2001).

- Alkyl hydroperoxide reductase (AhpC, AhpD). The complex composed by AhpC and AhpD plays an important role as an antioxidant in several bacterial species. In the case of *Brucella*, this complex is used to detoxify endogenous H_2O_2 produced during aerobic growth by respiratory metabolism, and it is also important to maintain a chronic infection (Steele et al., 2010).

- Nitric oxide reductase (NorD). Nitric oxide (NO) is produced by infected macrophages via the inducible NO synthase (iNOS), and contributes to mammalian host defense by direct microbicide activity. *Brucella suis* uses NorD to reduce nitrate to dinitrogen gas, allowing the survival of the bacteria in anaerobic denitrifying conditions, or in macrophages producing NO (Loisel-Meyer et al., 2006). This control mechanism could also apply to human infections, despite the low levels of NO that are released by human macrophages, as it happens during *Brucella* infections of human macrophages transfected with iNOS (Gross et al., 2004). A similar process taked place in *Neisseria meningitides,* which during infection of human macrophages show intracellular resistance to NO conferred by the NO reductase (Stevanin et al., 2005).

- *Brucella* virulence factor A (BvfA). It is a small protein specific of *Brucella* genus, essential for *Brucella* virulence in *in vitro* and *in vivo* models. BvfA is expressed after phagosome acidification, being necessary for the correct establishment of the *Brucella* intracellular niche (Lavigne et al., 2005).

- VirJ. VirJ is localized in the bacterial periplasm and is necessary for the intracellular survival, since it is required for the secretion of the *Brucella* effector proteins SepA and BPE123 (Giudice et al., 2016). It is possible that *Brucella* VirJ is interacting with some components of the T4SS to mediate the correct secretion of substrates, as occurs with *Agrobacterium tumefeciens* VirJ (Pantoja et al., 2002).

- EipB, TtpA and MapB. *Brucella* contains several proteins in its cell envelope that play an important role in maintaining the cell envelope homeostasis, such as EipB, TtpA and MapB proteins. EipB and TtpA are

periplasmic proteins that interact with each other to maintain a correct cell envelope integrity, and are necessary for full virulence *in vivo* (Herrou et al., 2019; Lestrate et al., 2003). MapB is a periplasmic protein inserted in the inner membrane necessary for correct cell envelope biogenesis, especially during cellular division. This protein is also implicated in intracellular survival in macrophages and complete virulence of *Brucella* in mouse (Bialer et al., 2019).

1.2 Flaviviridae viruses

Flaviviridae is a family of viruses that infect humans and other mammals. They are Arbovirus (Arthropod-borne virus) and as such, primarily spread through arthropod vectors like ticks and mosquitoes. The family gets its name from the Yellow Fever virus (YFV), the prototypical virus of Flaviviridae; *flavus* is Latin for “yellow”, as jaundice is a very common symptom of yellow fever infection in humans. Currently, there are four genera in this family, but only two of them can produce disease in humans: *flavivirus* and *hepacivirus*. Inside the first genus, it is possible to find viruses with a high impact in human health, such as Dengue virus (DENV), YFV, West Nile virus or Zika virus. The unique virus in the *hepacivirus* genus is the Hepatitis C virus (HCV), also very relevant to human health.

These viruses are small enveloped positive strand RNA particles [(+) RNA]. Their genome is between 10 to 11 kb in size and encodes a single polyprotein. Since Flaviviridae viruses depend on the host cell to complete their life cycle, protein-protein interactions between host cell proteins and virus proteins play a critical role during the infection.

1.2.1 Flaviviridae life cycle

Flaviviridae viruses share a very similar life cycle between them (Figure 1.9). In fact, *Flavivirus* and *Hepacivirus*, the two genera capable to infect human cells, share the principal mechanism of propagation, although some significant differences can be found between both Flaviviridae genera. In general terms, viral particles bind to the host cell surface to be internalized by clathrin-dependent endocytosis, in most of the cases. This is possible because viral

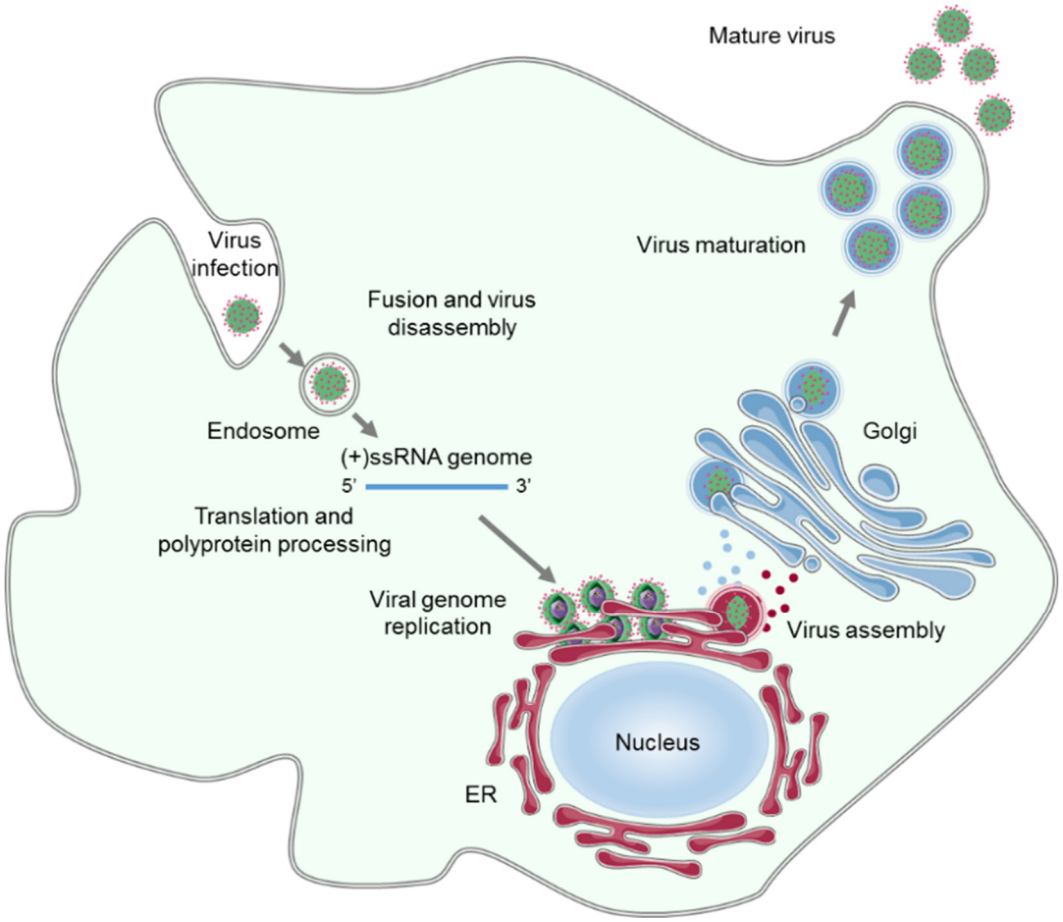

Figure 1.9. Flaviviridae life cycle. The principal stages of Flaviviridae replicative cycle are shown, such as the endocytosis, ER-associated replication, maturation in the Golgi and exocytosis of infective viral particles. Based on Mukhopadhyay et al., 2005.

particles interact with one or several receptor proteins, triggering an endocytosis mediated by receptors. In many *Flavivirus*, including YFV, the attachment to host membranes is mediated by heparin sulfates *in vitro*, acting as receptor or helping to concentrate these viruses around the host cell (Germi et al., 2002). However, other types of cell receptors could be implicated in virus entry to the eukaryotic cells, such as the DC-SIGN and L-SIGN lectines, which are necessary for the attachment of HCV to the membrane (Lozach et al., 2003). After invasion, viral particles interact with endosomes, where their acidification induces the fusion of viral and host membranes. This fusion produces uncoating, which consists on the release of the viral RNA genome into the host cell cytoplasm. All Flaviviridae uncoating could be mediated by the ubiquitination of the viral capsid as happens in DENV (Byk et al., 2016). Then, translation and post-translational processing occur in the ER. During this process, (+) RNA is translated into a single

polyprotein that is guided to the ER membranes by a signal peptide. Then, viral and cellular proteases cleave the polyprotein into several functional individual proteins. The viral polyprotein itself has autocatalytic activity releasing the first viral peptide, a protease. Also, some of the viral proteins induce the remodelation of several ER membranes to form specialized membrane compartments required for viral replication, named viral replication compartments (VRCs). It is in this moment when the viral replication starts. (+) RNA genome works as a template for the synthesis of a negative strand genomic RNA [(-) RNA], generating a double stranded RNA. Thus, the new (-) RNA is used for synthesis of many genomes. These new viral genomes are capped in *flavivirus*, while HCV genome is not capped. After multiple rounds of (+) RNA translation, there are enough structural proteins to encapsulate the RNA. Then, viral genomes are assembled in immature virions that move from the ER to the Golgi acquiring a lipid envelope formed by several copies of the two structural glycoproteins. Afterwards they are activated by furin-mediated cleavage to be released finally from the host cell by exocytosis (Fernandez-Garcia et al., 2009; Gerold et al., 2017).

1.2.2 Comparison between Flaviviridae and *Brucella* intracellular life cycles

As previously mentioned, Flaviviridae viruses completely depend on host proteins for their life cycle. In fact, up to now, several host proteins have been identified which interact with viral proteins in different stages of the viral life cycle. Some receptor proteins necessary for the entry of the virus into the host cell have been identified. For instance, GRP 78 (BIP) protein during DENV infection (Jindadamrongwech et al., 2004), as well as some entry co-factors in HCV infection like serum response factor binding protein 1 (SRFBP1), which is recruited to CD81 during HCV entry (Gerold et al., 2015). RAB5C and RABGEF are involved in *flavivirus* endocytosis, while NDST1 and EXT1 are involved in heparin sulfation (Savidis et al., 2016). Additionally, many host proteins are required during virus translation and replication; some of them have been identified to interact or are associated with some viral proteins, such as NS5 and NS3 (Carpp et al., 2014; Ye et al., 2013). These proteins play very different roles inside the host cell, such as retrograde Golgi-to-ER transport, biosynthesis of

long-chain-fatty-acyl-coenzyme A, and in the UPR. Heat shock protein 70 (Hsp70) was shown to interact with NS5 and NS3 in Japanese Encephalitis virus enhancing the stability of the viral proteins during replication (Ye et al., 2013). However, Hsp70 can play different roles depending on the Flaviviridae viruses. In HCV, Hsp70 is necessary for a correct translation of the virus (Gonzalez et al., 2009). GBF1, a protein implicated in the maintenance of Golgi structure, can interact with viral proteins during DENV infection, being necessary for the correct infection (Carpp et al., 2014). Finally, host proteins are also required for a correct assembly and release of the viruses. Some important eukaryotic proteins for Flaviviridae viruses infection during these stages of the viral life cycle are the endosomal sorting complex required for transport (ESCRT) proteins, since many Flaviviridae viruses interact with several ESCRT proteins (Ariumi et al., 2011; Barouch-Bentov et al., 2016; Tabata et al., 2016). The ESCRT complex is a conserved pathway composed by several heteromeric complexes that are recruited to membrane deformation sites.

Brucella cell cycle occurs in a similar fashion as the Flaviviridae life cycle. However, *Brucella* does not completely depend on host proteins for their life cycle; but it requires the modification, inhibition or overexpression of some host proteins for a correct infective cycle, especially during some critical stages of its intracellular cell cycle. In fact, effector proteins secreted by the *Brucella* T4SS can interact with some host proteins to modify their function (as detailed in section 1.1.4.2), adjusting them to bacterial requirements, allowing the progress of *Brucella*.

Some of these host proteins could be common among Flaviviridae viruses and *Brucella*. For instance, GRP78 is a protein that promotes *Brucella* proliferation by interaction with the *Brucella* effector protein VceC (Zhou et al., 2017). This protein also plays a role during DENV infection, where it works like a receptor protein (Jindadamrongwech et al., 2004). Also, other effector proteins secreted by other bacteria secretion systems interact with proteins of ESCRT complex. This is the case of some effector proteins of *Chlamydia trachomatis*, an intracellular pathogen with a Type III secretion system (Weber and Faris, 2018).

Brucella and Flaviviridae roughly share the same ecological niche: both microorganisms infect the host cell through the endosomal pathway, and both

replicate in the ER (Figure 1.10). Flaviviridae and *Brucella* do not share the same pathway to leave the host cell, they use exocytosis and autophagy pathways respectively; however, there are some evidences that indicate that autophagy promotes viral propagation in host cells and also counteracts stress responses in the host cells induced by viral infection (Arakawa and Morita, 2019; Ke, 2018).

Bacterial effector proteins secreted to the host cell probably play a role manipulating the host cell biology with great specificity and high activity. Thus, these effector proteins could be directly or indirectly affecting host proteins or processes also required for Flaviviridae replication, since as above mentioned, both microorganisms share some intracellular pathways. In this way, an assay measuring viral replication could allow to screen for new effector proteins that interfere with viral replication.

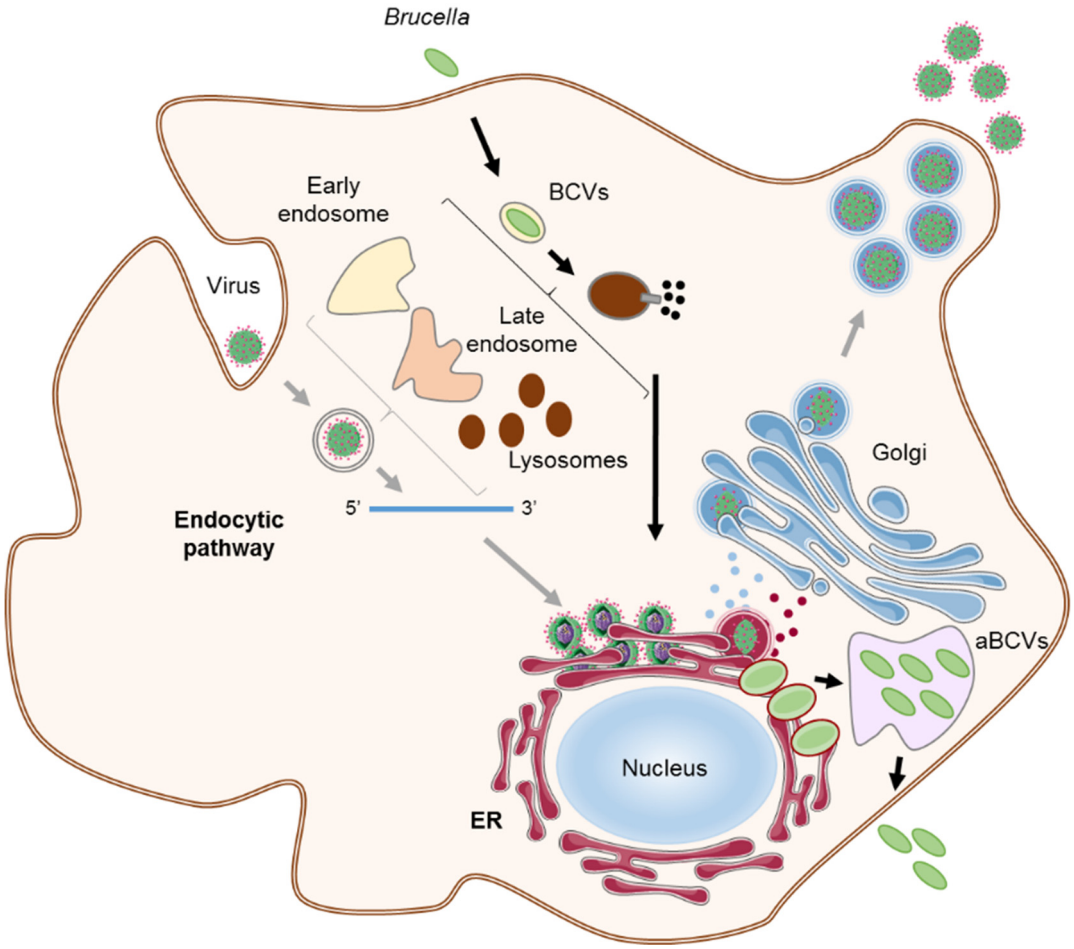

Figure 1.10. Membrane organelles shared among *Brucella* and Flaviviridae intracellular cycles. The intracellular pathway or compartment shared between *Brucella* and Flaviviridae viruses are shown in bold. Gray arrows indicate the virus cycle, while black arrows indicate *Brucella* intracellular cycle.

1.3 Lysozyme and lysozyme inhibitors

Lysozyme is a conserved protein present in insects, amphibious, reptiles, birds, and mammals. One of the most relevant functions of the lysozyme is the role that it plays in defense against infection, that is, its antimicrobial property. Based on their amino acid sequence, biochemical and enzymatic properties, there are three types of lysozyme: chicken or conventional type (c- type), goose type (g-type) and invertebrate type (i-type) (Callewaert and Michiels, 2010) (Figure 1.11). In mammals, lysozyme is one of the antimicrobial proteins produced by phagocytic cells such as neutrophils, macrophages and dendritic cells (Ragland and Criss, 2017). Monocytes also produce lysozyme, although in less amount than polymorphonuclear cells (PMN) (Klüter et al., 2014) like neutrophils. Lysozyme is also found in some body secretions like tears and saliva, and even in blood plasma (Lehrer, 1998) and in many tissues including the intestinal and respiratory tracts (Callewaert and Michiels, 2010). The antibacterial role of lysozyme relies on the hydrolysis of the β-(1-4) glycosidic bond between NAM and NAG in PG (Figure 1.12.A) (Callewaert et al., 2008), therefore destabilizing the bacterial cell envelope and producing the lysis of the bacteria. This is so because, as previously mentioned, the PG is the most abundant polymer in bacterial cell envelope, and its presence is essential to maintain the integrity and prevent the lysis of the bacteria.

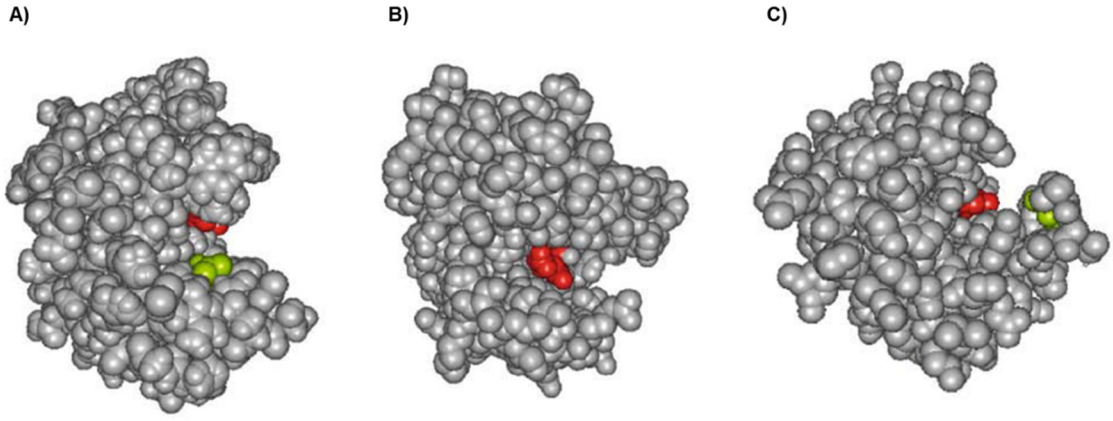

Figure 1.11. Three-dimensional structure of different types of lysozyme. A) c-type, **B)** g-type, and **C)** i-type. Catalytic residues are highlighted: Glu in red and Asp in green. Taken from Callewaert and Michiels, 2010.

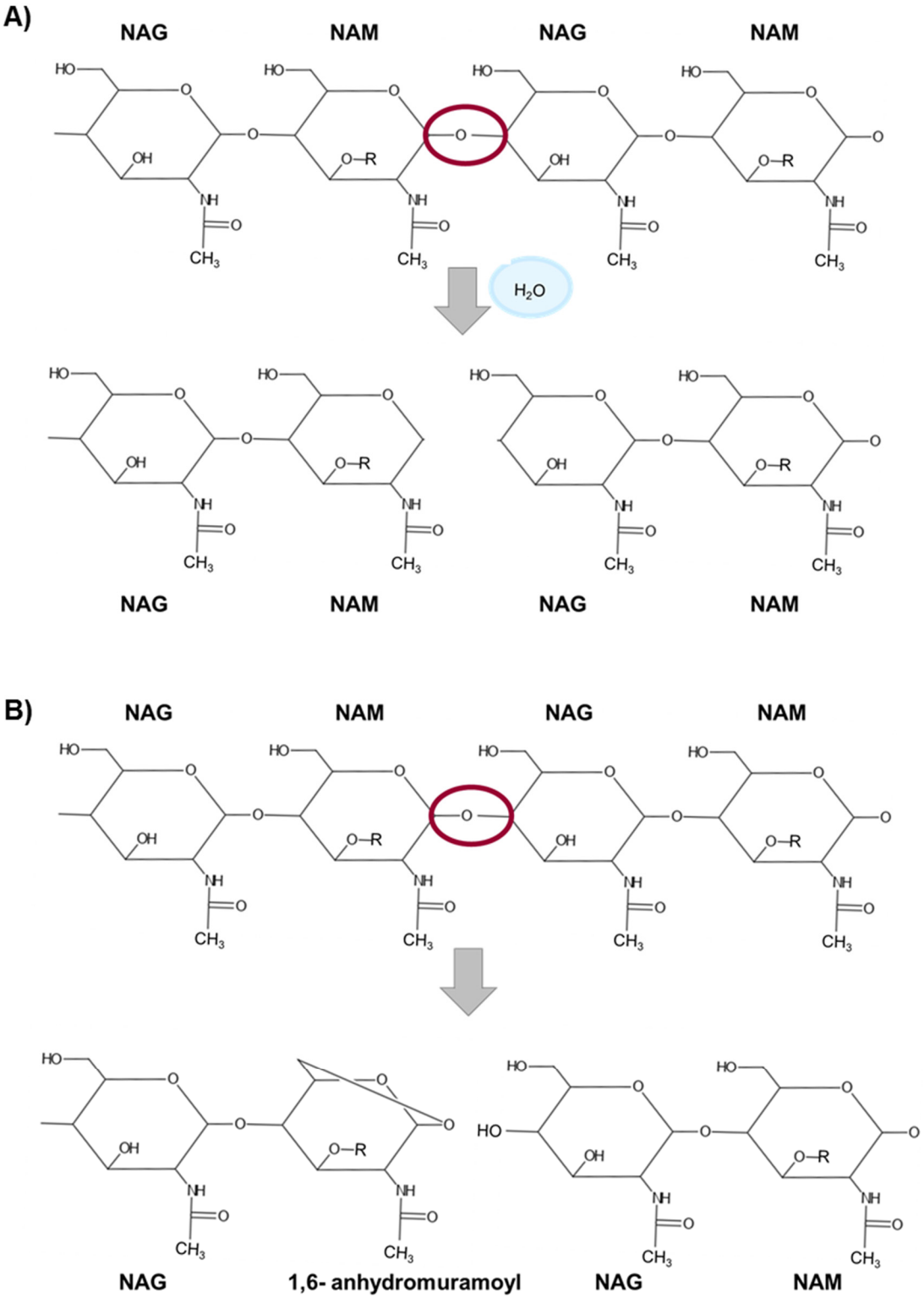

Figure 1.12. Comparison between the reactions catalyzed by lysozyme and lytic transglycosylases. A) Lysozyme hydrolyzes the β-(1-4) glycosidic bond between NAM and NAG in the peptidoglycan. **B) Lytic transglycosylases** catalyze the cleavage between NAG and NAM in the peptidoglycan, resulting in the formation of 1,6-anhydromuramoyl residues.

In many Gram-negative bacteria, lysozyme cannot access the PG layer because the LPS and the OM act as a barrier. Therefore, the innate immune cells produce other accessory antimicrobial proteins, such as lactoferrin, which permeabilize the outer membrane of some bacteria (Ellison et al., 1988). To counteract this last defense, bacteria have developed other mechanisms to avoid lysozyme activity, such as PG modifications or the production of lysozyme inhibitor proteins, which will be detailed later (section 1.3.2).

Bacteria can also produce lysozyme-like proteins called lytic transglycosylases (LTs). These enzymes degrade PG with the same substrate specificity as the lysozyme (Scheurwater et al., 2008). However, the reaction catalyzed by LTs is different to lysozyme reaction (figure 1.12.B), since it is a non-hydrolytic reaction (Höltje et al., 1975). LTs degrade PG in order to allow cell growth and division, but are also required for the assembly of macromolecular transport systems, such as the T4SS (Koraimann, 2003).

1.3.1 Role of lysozyme in the immune response

Lysozyme can either enhance or damp the immune response, in part due to the origin and the localization of that lysozyme. As already mentioned, several cells in the organism produce lysozyme. Some of them are cells of the innate immune system. Usually, the activity of lysozyme present inside these cells is going to potentiate a pro-inflammatory response. At the infection site, neutrophils are the first line of defense against bacteria and they are also the most abundant leukocytes in human blood (Ley et al., 2018). Neutrophils, during internalization of pathogens for intracellular killing, produce reactive oxygen species (ROS) and release several antimicrobial products, many of them cationic peptides such as lysozyme, lactoferrin, defensins, etc (Nathan and Shiloh, 2000).

Neutrophils are not the only innate immune cell type that produce lysozyme; monocytes/macrophages and dendritic cells also secrete lysozyme. In fact, all these phagocytic cells have similar activities against bacteria. In general terms, phagocytic cells can deliver lysozyme extracellularly, but they can also deliver lysozyme to the phagosome that contains internalized bacteria. In this way, bacterial degradation by phagosomal lysozyme releases PAMPs stimulating a robust pro-inflammatory response and activating the inflammasome (Ragland

and Criss, 2017). Indeed, it has been demonstrated that those bacteria that are more sensitive to lysozyme activity are more susceptible to be degraded inside macrophages (Rae et al., 2011). Something similar occurs in human neutrophils infected with *Neisseria gonorrhoeae.* In this bacterium, the susceptibility to lysozyme activity increases the release of neutrophil granule contents extracellularly and into bacteria-containing phagosomes, meaning that neutrophils are more activated (Ragland et al., 2017). Also, sometimes bacterial degradation by lysozyme in phagocytes can produce an over-inflammatory response, as is the case of macrophages infected by *Staphylococcus aureus* without O-acetylation in its PG (Shimada et al., 2010). In contrast, the activity of extracellular lysozyme, produced by epithelial cells and some phagocytic cells, produces soluble PG. Then, the complement molecules will bind to this soluble PG, instead of the PG on bacterial cell surface or to insoluble PG fragments, decreasing anaphylotoxins production and consequently, restricting phagocyte activation and recruitment (Ragland and Criss, 2017).

Therefore, depending on each circumstance lysozyme will regulate the immune system in one way or another. Nevertheless, it is more frequent that lysozyme has a pro-inflammatory activity helping to remove bacterial infection. Therefore, microorganisms have developed several resistance mechanisms against lysozyme. As mentioned earlier, *Brucella* is able to survive the killing action of these phagocytic cells; however, how *Brucella* resists to this killing action, and more specifically how *Brucella* resists to the lysozyme killing action, once the OM shield is compromised, remains still unknown.

1.3.2 Lysozyme resistance mechanisms

In general, bacteria have developed several mechanisms to avoid lysozyme activity and survive and replicate inside the host. Gram-negative bacteria are more insensitive to lysozyme than Gram-positive bacteria because they contain an OM that makes them naturally impermeable to lysozyme. Moreover, in Extraintestinal pathogenic *Escherichia coli* (ExPEC), its O-specific polysaccharide inhibits the hydrolytic action of lysozyme (Bao et al., 2018). In *Brucella,* it is unknown if its O-antigen is able to inhibit the lysozyme action.

However, it is known that the presence of the O-antigen contributes to polycation resistance, such as lysozyme or lactoferrin (Tejada et al., 1995).

Additionally, bacteria have acquired many PG modifications to protect them against lysozyme and other PG degrading enzymes, which also have direct implications on several processes such as host immune response and antibiotic resistance. These PG modifications can be in PG sugars (N-deacetylation of NAG, N-deacetylation of NAM, N-Glycosylation of NAM, O-Acetylation of NAM, O-Acetylation of NAG or O-Deacetylation) or chemical modifications in the peptide structure providing antibiotic resistance, to combat bacterial competition or to act as innate immune modulators (Yadav et al., 2018).

Other bacterial strategy against lysozyme action, more recently identified, is the production of lysozyme inhibitors, proteins that are block the active site of lysozyme to interfere with its activity degrading peptidoglycan (Callewaert et al., 2012). In fact, bacterial inhibitors of the three types of lysozyme have been described, but here only c-type lysozyme inhibitors will be discussed. There are two traditional c-type lysozyme inhibitor families in Gram-negative bacteria: the Ivy family, that includes Ivy (inhibitor of vertebrate lysozyme) and Ivy-like proteins, and the MliC/PliC family, that includes membrane-bound lysozyme inhibitor of c-type lysozyme (MliC) and periplasmic-bound lysozyme inhibitor of c-type lysozyme (PliC) proteins (Zielke et al., 2018). In the case of *B. abortus*, the structure of the interaction between lysozyme and *B. abortus* PliC (also called BAB1_0466) was reported, suggesting that this protein could be a lysozyme inhibitor of the MliC family present in *Brucella* (Um et al., 2013) (Figure 1.13.). However, its inhibitory activity has yet to be proven.

Recently, adhesion complex proteins (ACPs) have been identified as new type of lysozyme inhibitor proteins present in Gram-negative bacteria such as *Neisseria* and *Dichelobacter* (Humbert et al., 2019, 2017). These proteins are structurally similar to MliC/PliC proteins, but the action mode of both proteins is different. ACP proteins have a sequence inserted at the position where MliC/PliC proteins have the binding interface with lysozyme (Callewaert et al., 2008; Humbert et al., 2019).

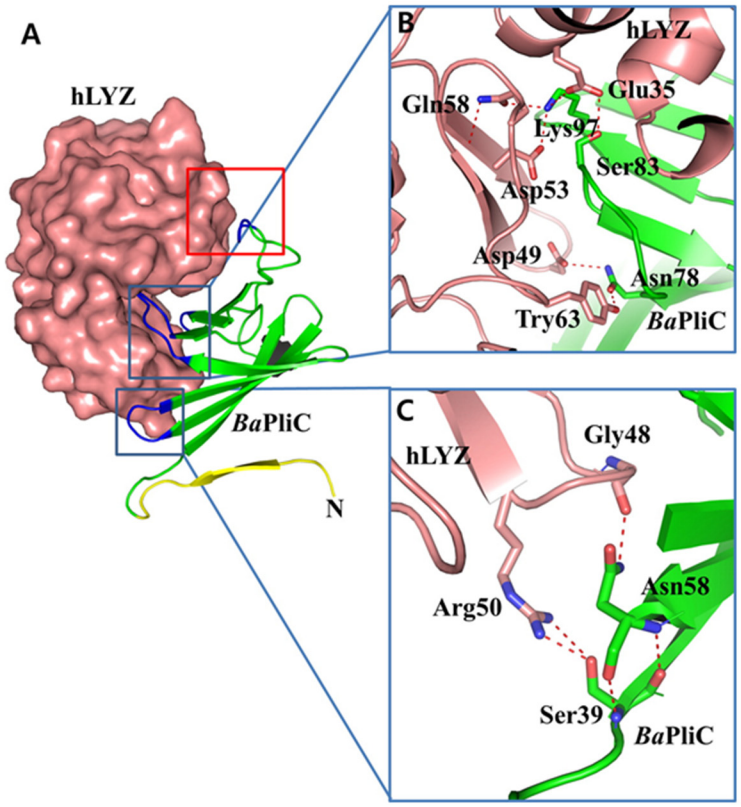

Figure 1.13. Structure of the c-type lysozyme and *B. abortus* PliC complex. A) Active site between lysozyme and PliC. **B)** Interaction between the catalytic residues of lysozyme and the key conserved regions of PliC. **C)** Interactions between lysozyme and the shallow pocket region of PliC. Taken from Um et al., 2013.

The possible role of lysozyme inhibitors in virulence is controversial. For example, in the case of *Salmonella enterica Serovar Enteritidis,* it was shown that incubation with lysozyme and lactoferrin (a membrane permeabilizer) increased the sensitivity of *S. enterica* Enteritidis *pliC* mutant to lysozyme (Callewaert et al., 2008). However, the deletion of *mliC* in *Pseudomonas aeruginosa* has been shown to produce no effect in relation to lysozyme resistance, when the bacteria were treated with lysozyme and colistin (another permeabilizer) (Torrens et al., 2017). One possibility for this discrepancy about the function of lysozyme inhibitor proteins in virulence could be due to the presence of more than one lysozyme inhibitor protein. In this sense, there are some results in *N. gonorrhoeae* where the effect on defense against human sources of lysozyme of one lysozyme inhibitor was only observed when this protein and other lysozyme inhibitor were

mutated (Ragland et al., 2017). However, the effect of this protein in virulence in a mouse model can be observed using only the single mutant (Zielke et al., 2018).

The fact that bacteria have evolved different mechanisms to cope with the lysozyme activity of the host suggests that lysozyme constitutes an old and important mechanism of defense. Consequently, *Brucella* must have developed some resistance mechanism against lysozyme. Direct binding of lysozyme to *Brucella* LPS can occur, similarly to what has been described for LPS of other bacteria (Ohno and Morrison, 1989; Tejada et al., 1995). But, the low permeability of the cell envelope of *Brucella* to polycations (due to the lipid A charge, see section 1.1.4.1) confers the bacteria an intrinsic capacity to resist the action of a number of cationic peptides, including lysozyme, lactoferrin, bactenecin and defensins, among others (Tejada et al., 1995). Therefore, *Brucella* is resistant to lysozyme action. However, when its OM is destabilized, as in the absence of MapB protein, *Brucella* is more sensitive to lysozyme action (Bialer et al., 2019). However, the sensitivity is not complete, suggesting that maybe other factors could be contributing to this resistance.

AIMS AND SCOPE

2. AIMS AND SCOPE

Throughout evolution, *Brucella* has acquired many strategies to thrive both inside and outside the host. Specifically, this bacterium has developed some mechanisms to face the adversities found inside the host. These mechanisms can be compared to weapons, which could have a defensive character, such as responding to the immune system of the host; or they can have an offensive character, actively intervening in the destruction and/or manipulation of the normal function of the cell. In both cases, they have a common objective, the survival and progression of the bacterium. This thesis work has the general goal of getting more insight into the panoply of *Brucella* to survive inside the host, using *B. abortus* as a model. In particular, we centered our study on two mechanisms which presumably favor its intracellular survival and persistent infection: the translocation of effector proteins to subvert the host cell, and the inhibition of the host lysozyme activity.

2.1 Search for new *B. abortus* T4SS effector proteins

As explained in the introduction, it is probable that not all *Brucella* effector proteins have already been described. Some of them could have the potential of interfering with the replication of Flaviviridae viruses, since both microorganisms exploit the same niche. Therefore, a new screening method searching for interference with viral replication will probably result in the identification of a new set of *Brucella* effector proteins. Thus, the objectives that we propose were:

1) Construction of a library of putative T4SS effector proteins.
2) Establishment of a Viral Interference Assay.
3) Library screening.

2.2 Characterization of putative lysozyme inhibitors of *B. abortus*

The existence of a *B. abortus* protein (BAB1_0466) which harbors a MliC domain and is crystalized bound to lysozyme, was a strong suggestion that it

might be a lysozyme inhibitor, although its enzymatic activity remained to be shown. In addition, previous studies in our laboratory led to the re- annotation of BAB1_0102, which was then identified as a putative lysozyme inhibitor. Our goal was to study these two proteins at different levels:

1) *In silico* analysis of BAB1_0102 and BAB1_0466 proteins.
2) *In vitro* activity as lysozyme inhibitors.
3) Determination of BAB1_0466 contribution to *B. abortus* survival upon lysozyme treatment.
4) Determination of BAB1_0466 role in *B. abortus* survival inside different human innate immune cell types.

Overall, with this thesis work we wanted to elucidate new mechanisms contributing to *Brucella* virulence. The newly identified *B. abortus* effector proteins could serve as tools to identify cellular pathways required for Flaviviridae life cycle. Both translocated effectors and lysozyme inhibitors could represent novel targets for antivirulence strategies.

EXPERIMENTAL PROCEDURES

3. EXPERIMENTAL PROCEDURES

3.1 Bacterial strains

Strain	Genotype	Use	Reference
DH5α	Nx^R *F- endA1 hsdR17 supE44 thi-1 recA1 gyrA96 relA1 Δ(argF-lacZYA) U 169 Φ80dlac ΔM15*	Maintenance of plasmids	(Grant et al., 1990)
MDS42	Reduced genome of MG1655. *ΔfhuACDB, ΔendA.* Deletion of 699 additional genes	Maintenance of effector protein lentiviral plasmids	(Pósfai et al., 2006)
C41	*F- dcm ompT hsdS (r_B- m_B-) gal λ (DE3)*	Overexpression strain	(Miroux and Walker, 1996)
Mach1-$T1^R$	*F- φ80(lacZ)ΔM15 ΔlacX74 hsdR(rK- mK+) ΔrecA1398 endA1 tonA*	Maintenance of pDONR223 constructions	(Invitrogen)
SF100 2873	*F- lacX74 galE galK thi rpsL (strA) phoA (PvuII) ompT* with pMALc-VirB1-BS	Maintenance and overexpression of VirB1 protein	(Zahrl et al., 2005)
β2163	*F− RP4-2-Tc::Mu_dapA::(ermpir)* (Km^R Em^R)	Conjugation donor	(Demarre et al., 2005)

Table 3.1. *Escherichia coli* strains used in this work.

Strain	Genotype	Reference
2308	Wild-type 2308	Laboratory strain
Δ0466	2308 deletion of *bab1_0466*	Constructed by Esther González
Δ0466Δ0102	*2*308 deletion of *bab1_0466* and *bab1_0102* genes	Constructed by Esther González
Δ0466 pIN62	*2*308 deletion of *bab1_0466* containing pIN62 plasmid	Constructed for this thesis
2308 pIN62	2308 containing pIN62 plasmid	Constructed for this thesis
ΔmapB	2308 deletion of *mapB g*ene	Constructed for this thesis
ΔmapBΔ0466	2308 deletion of *mapB* and *bab1_0466* genes	Constructed for this thesis
ΔmapBΔ0466Δ0102	*2*308 deletion of *mapB, bab1_0466* and *bab1_0102* genes	Constructed for this thesis
ΔmapBΔ0466::Δ0466	2308 deletion of *mapB* and *bab1_0466* genes and complemented with pBBR1::*bab1_0466*	Constructed for this thesis
Δ0466*::Δ0466*	2308 deletion of *bab1_0466* gene and complemented with pBBR1::*bab1_0466*	Constructed by Esther González

Table 3.2. *Brucella abortus* strains used in this work.

3.2 Bacterial plasmids

3.2.1 Plasmids used in this work

Plasmid	Antibiotic resistance	Description	Reference
EX-NEG-LV103	Ap^R	Lentiviral vector with *EGFP* expression	GeneCopoeia
Jc1-5AB-2xYPet	Ap^R	HCV cDNA plasmid expressing 2xYpet fluorescent protein	(Horwitz et al., 2013)
pBBR1-MCS	Cm^R	Broad host range vector from *Bordetella bronchiseptica*	(Kovach et al., 1994)
pCMV-VSV-G	Ap^R	*vsv-g* gene encoding enveloped lentiviral protein	Didier Trono (Commercial Addgene)
pDONR223	Sp^R	Gateway Cloning Vector	(Rual et al., 2004)
pDS132	Cm^R	Suicide plasmid	(Philippe et al., 2004)
pET29C	Km^R	Expression vector	Novagen
pIN62	Cm^R	pBBR1 plasmid expressing DsRed	(Vergunst et al., 2010)
pMalc-VirB1_BS	Ap^R	Vector for cytoplasmic expression of VirB1_BS protein (VirB1 aa 2–238) fused to MalE	(Zahrl et al., 2005)
pQE30-SagA	Ap^R	Vector for expression of SagA protein from *B. abortus* fused to 6xHis tag	(Giudice et al., 2013)
psPAX2	Ap^R	*gag* and *pol* genes encoding packaging lentiviral proteins	Robert A. Weinberg

Table 3.3. Plasmids used in this work.

Plasmid	Antibiotic resistance	Description	Reference
pTRIP5-Dest	Cm^R, Ap^R	Lentivirus-based, Gateway-compatible destination Vector enconding IRFP670	Brett Lindenbach
pTRIP5::GFP	Ap^R	Expression of *GFP* and IRFP670	Brett Lindenbach
pTRIP5::IRF1	Ap^R	Expression of *IRF1* and IRFP670	Brett Lindenbach
pTRIP5::Gluc	Ap^R	Expression of *gluc* and IRFP670	Brett Lindenbach
pTRIP6-Dest	Cm^R, Ap^R	Lentivirus-based, Gateway-compatible destination Vector encoding m-Cherry	Brett Lindenbach
pTRIP6::GFP	Ap^R	Expression of *GFP* and m-Cherry	Brett Lindenbach
pTRIP6::IRF1	Ap^R	Expression of *IRF1* and m-Cherry	Brett Lindenbach
YF17D (5'C25Venus2AUbi)	Cm^R	YFV cDNA plasmid expressing Venus fluorescent protein	(Yi et al., 2011)

Table 3.3. Plasmids used in this work (continued).

3.2.2 Plasmids constructed for this work

Tables 3.4 to 3.6 list the plasmids constructed for this work. Tables 3.5 and 3.6 list the two series of constructions required to generate a library of putative *B. abortus* effectors using the Gateway technology.

		Construction [1]		
Plasmid	**Description**	**Vector**	**Insert**	**Primers (5'-3')**
pFJS280	pBBR1::bab1_0466	pBBR1	PCR on genomic DNA from *B. abortus* 2308	**F**: AAGCTTGGAAGAGCCGCAATAAACAC **R**: CTGCAGCTCTTCCCCCGACAAGAAAT *Hind*III-*Pst*1
pFJS283	pET29C::bab1_0466	pET29C	PCR on genomic DNA from *B. abortus* 2308	**F:** CATATGAAAATGTGGACCCTTGCG **R:** CTCGAGCTGTTCTACGCAGCTTATAGG *Nde*I- *Xho*I
pYOP155	pET29C::bab1_0102	pET29C	PCR on genomic DNA from *B. abortus* 2308	**F:** ACGTCATATGACTGCATCTGCCCTTCTG **R:** ACGTCTCGAGTTCTTCGGCGGTGTCTGCG *Nde*I- *Xho*I
pYOP156[2]	pDS132::ΔmapB	pDS132	PCR on genomic DNA from *B. abortus* 2308	**F1:** ACGTTCTAGATCTCCGAGCAGATGCGCGTCG **R1:** GCCGTAATGGCCGCTCATAGCCTGCGGCTGGTCATCAGC **F2:** TATGAGCGGCCATTACGGC **R2:** ACGTGAGCTCTGATCCTTCAGGCTGACGACA *Xba*I-*Sac*I

Table 3.4. Plasmid constructed for this work.
(1) First column lists the vector plasmids; second column lists the *B. abortus* gene and the insertion site; and third column indicates the primers used for PCR amplification of the desired fragment and restriction enzymes used for cloning. **(2)** Construction of this plasmid is detailed in section 3.5.3.

	Construction (1)		
Plasmid	**Vector**	**Insert**	**Primers (5'-3')**
pDONR223::bab1_0011	pDONR223	*bab1_0011*	GGGACAACTTTGTACAAAAAAGTTGGCGGCCGCACCTTGCTTGAATCCCTTCGGCA GGGACAACTTTGTACAAGAAAGTTGGGTAATTAATTAATCAGGCCGGTGAGAAAAT
pDONR223::bab1_0061	pDONR223	*bab1_0061*	GGGACAACTTTGTACAAAAAAGTTGGCGGCCGCACCATGAGCACCTATCTTCCCGA GGGACAACTTTGTACAAGAAAGTTGGGTAATTAATTAATCAATCGTCATTCGTTGCAT
pDONR223::bab1_0063	pDONR223	*bab1_0063*	GGGACAACTTTGTACAAAAAAGTTGGCGGCCGCACCATGGCATTCGAGGACATCAAGG GGGACAACTTTGTACAAGAAAGTTGGGTAATTAATTAATCAGGAATCGAAATCTTGT
pDONR223::bab1_0070	pDONR223	*bab1_0070*	GGGACAACTTTGTACAAAAAAGTTGGCGGCCGCACCATGCGAAAAAATAAACAGC GGGACAACTTTGTACAAGAAAGTTGGGTAATTAATTAATCAGATTGCAGCAAGCGCGT
pDONR223::bab1_0101	pDONR223	*bab1_1101*	GGGACAACTTTGTACAAAAAAGTTGGCGGCCGCACCATGAAATTTTTGCCCGTGCT GGGACAACTTTGTACAAGAAAGTTGGGTAATTAATTAATTATGGGACGAGATAGTGCTTG
pDONR223::bab1_0121	pDONR223	*bab1_0121*	GGGACAACTTTGTACAAAAAAGTTGGCGGCCGCACCATGTCTCTGCCTGATACCATCG GGGACAACTTTGTACAAGAAAGTTGGGTAATTAATTAATTATTCACCGCGACGCTTCT
pDONR223::bab1_0143	pDONR223	*bab*1_0143	GGGACAACTTTGTACAAAAAAGTTGGCGGCCGCACCATGAGCGCACACGACCTGAAGC GGGACAACTTTGTACAAGAAAGTTGGGTAATTAATTAACTATGCTGCGGCCTGTGGCG
pDONR223::bab1_0151	pDONR223	*bab1_0151*	GGGACAACTTTGTACAAAAAAGTTGGCGGCCGCACCATGCTGGCAAAACGAATCGTC GGGACAACTTTGTACAAGAAAGTTGGGTAATTAATTAATCAGGAATTCGCCAGCGGT
pDONR223::bab1_0158	pDONR223	*bab1_0158*	GGGACAACTTTGTACAAAAAAGTTGGCGGCCGCACCTTGCCCAGAACGCGGCTTT GGGACAACTTTGTACAAGAAAGTTGGGTAATTAATTAATCAAGCCGGAAAATTTGGGA
pDONR223::bab1_0175	pDONR223	*bab1_0175*	GGGACAACTTTGTACAAAAAAGTTGGCGGCCGCACCATGAGAATGCTGGAAAAGGGC GGGACAACTTTGTACAAGAAAGTTGGGTAATTAATTAATCATTCTGCCGGAGCCGATACC
pDONR223::bab1_0187	pDONR223	*bab1_0187*	GGGACAACTTTGTACAAAAAAGTTGGCGGCCGCACCATGAAGAGATTTGGCTATTC GGGACAACTTTGTACAAGAAAGTTGGGTAATTAATTAATCACAGATAAGGCGAATAGC

Table 3.5. Plasmids containing selected candidate effector proteins constructed for this work.
(1) First column lists the vector plasmids; second column lists the *B. abortus* gene inserted between the attP1 and attP2 recombination sites; and third column indicates the primers used for PCR amplification of the desired fragment.

	Construction (1)		
Plasmid	**Vector**	**Insert**	**Primers (5'-3')**
pDONR223::bab1_0227	pDONR223	*bab1_0227*	GGGACAACTTTGTACAAAAAAGTTGGCGGCCGCACCTTGAGGGCTGAAACGATGAA GGGACAACTTTGTACAAGAAAGTTGGGTAATTAATTAATTATTTTACTTTTTCAAGCGT
pDONR223::bab1_0271	pDONR223	*bab1_0271*	GGGACAACTTTGTACAAAAAAGTTGGCGGCCGCACCGTGAATAATAAAAAAATATT GGGACAACTTTGTACAAGAAAGTTGGGTAATTAATTAATCAAAGGAAAATATCCAAAGG
pDONR223::bab1_0279	pDONR223	*bab1_0279*	GGGACAACTTTGTACAAAAAAGTTGGCGGCCGCACCATGAGTTCGTACTCTTCTAAT GGGACAACTTTGTACAAGAAAGTTGGGTAATTAATTAATCAGATAAGGGAATGCAGTT
pDONR223::bab1_0296	pDONR223	*bab1_0296*	GGGACAACTTTGTACAAAAAAGTTGGCGGCCGCACCATGAACGCTCACACAAACATAA GGGACAACTTTGTACAAGAAAGTTGGGTAATTAATTAATCAAAGCTCCAAGCATCTAATT
pDONR223::bab1_0322	pDONR223	*bab1_0322*	GGGACAACTTTGTACAAAAAAGTTGGCGGCCGCACCATGACTTTGAACCGTACCATCC GGGACAACTTTGTACAAGAAAGTTGGGTAATTAATTAATCATTTCTTGTCTGCCGCCT
pDONR223::bab1_0343	pDONR223	*bab1_0343*	GGGACAACTTTGTACAAAAAAGTTGGCGGCCGCACCATGTTGGGCAGAATGGCAGGT GGGACAACTTTGTACAAGAAAGTTGGGTAATTAATTAATCAGGTCCGCCCCGGTATTGT
pDONR223::bab1_0353	pDONR223	*bab1_0353*	GGGACAACTTTGTACAAAAAAGTTGGCGGCCGCACCTTGGAGCCGCTTCAGCCAAA GGGACAACTTTGTACAAGAAAGTTGGGTAATTAATTAATCAGACGTCACCGGGTTT
pDONR223::bab1_0365	pDONR223	*bab1_0365*	GGGACAACTTTGTACAAAAAAGTTGGCGGCCGCACCATGGCGCTTCTAACCCTGAG GGGACAACTTTGTACAAGAAAGTTGGGTAATTAATTAACTATCGAAAGACCCCGCTTC
pDONR223::bab1_0368	pDONR223	*bab1_0368*	GGGACAACTTTGTACAAAAAAGTTGGCGGCCGCACCATGAAAAATTATCGTGCAAT GGGACAACTTTGTACAAGAAAGTTGGGTAATTAATTAATTACTTGGTCAATGCCTGAA
pDONR223::bab1_0401	pDONR223	*bab1_0401*	GGGACAACTTTGTACAAAAAAGTTGGCGGCCGCACCATGAATCAGCCTTTCCGCAC GGGACAACTTTGTACAAGAAAGTTGGGTAATTAATTAATCAATGCAGCCGGGCTGCGC
pDONR223::bab1_0421	pDONR223	bab1_0421	GGGACAACTTTGTACAAAAAAGTTGGCGGCCGCACCTTGCGCGAATTTTCGCGCGA GGGACAACTTTGTACAAGAAAGTTGGGTAATTAATTAATCACGAAAACGTTTTCCTAA

Table 3.5. Plasmids containing selected candidate effector proteins constructed for this work (continued).

	Construction [1]		
Plasmid	**Vector**	**Insert**	**Primers (5'-3')**
pDONR223::bab1_0445	pDONR223	*bab1_0445*	GGGACAACTTTGTACAAAAAAGTTGGCGGCCGCACCTTGGCCGCCCGACCCGCTCGCCA GGGACAACTTTGTACAAGAAAGTTGGGTAATTAATTAATCAGATCGGCGCGAACGCAGT
pDONR223::bab1_0453	pDONR223	*bab1_0453*	GGGACAACTTTGTACAAAAAAGTTGGCGGCCGCACCATGCATTATCTGATCGGATT GGGACAACTTTGTACAAGAAAGTTGGGTAATTAATTAATTACGGGGCTTCCTGAATATC
pDONR223::bab1_0491	pDONR223	*bab1_0491*	GGGACAACTTTGTACAAAAAAGTTGGCGGCCGCACCATGATCCAGCGCCTCGCCGC GGGACAACTTTGTACAAGAAAGTTGGGTAATTAATTAATCAGGGGAGGGCGTCGAAGC
pDONR223::bab1_0492	pDONR223	*bab1_0492*	GGGACAACTTTGTACAAAAAAGTTGGCGGCCGCACCGTGGATAAGATTGTTGCCGCA GGGACAACTTTGTACAAGAAAGTTGGGTAATTAATTAATTACAGCCCCGCCGCAGCCA
pDONR223::bab1_0544	pDONR223	*bab1_0544*	GGGACAACTTTGTACAAAAAAGTTGGCGGCCGCACCATGGATATACCAGTTTACT GGGACAACTTTGTACAAGAAAGTTGGGTAATTAATTAACTAAATGTGGTTGGAATGAT
pDONR223::bab1_0608	pDONR223	*bab1_0608*	GGGACAACTTTGTACAAAAAAGTTGGCGGCCGCACCGTGAGGCACGGCATTACGGCT GGGACAACTTTGTACAAGAAAGTTGGGTAATTAATTAATCACGCGCCCGGATCAGCCA
pDONR223::bab1_0640	pDONR223	*bab1_0640*	GGGACAACTTTGTACAAAAAAGTTGGCGGCCGCACCATGGCGAGCACCGACGCGTATG GGGACAACTTTGTACAAGAAAGTTGGGTAATTAATTAACTAAGCAGCGTGGGCCCGGG
pDONR223::bab1_0653	pDONR223	*bab1_0653*	GGGACAACTTTGTACAAAAAAGTTGGCGGCCGCACCATGCAAAGCAACTCCGGTGAAGA GGGACAACTTTGTACAAGAAAGTTGGGTAATTAATTAATTAGCTTATGCCAATATAGCGC
pDONR223::bab1_0663	pDONR223	*bab1_0663*	GGGACAACTTTGTACAAAAAAGTTGGCGGCCGCACCATGGAGTATGAGGACGAAATGCC GGGACAACTTTGTACAAGAAAGTTGGGTAATTAATTAATCAGCCAGCCTGTTTTTTTGCG
pDONR223::bab1_0678	pDONR223	*bab1_0678*	GGGACAACTTTGTACAAAAAAGTTGGCGGCCGCACCATGTTGTTCCAACGCAGATA GGGACAACTTTGTACAAGAAAGTTGGGTAATTAATTAATCATGCCTTCTGCAACTCC
pDONR223::bab1_0712	pDONR223	*bab1_0712*	GGGACAACTTTGTACAAAAAAGTTGGCGGCCGCACCATGCGCCCCGTTCTTTTCCT GGGACAACTTTGTACAAGAAAGTTGGGTAATTAATTAATTATGTTTGGGGGCGGCGAA
pDONR223::bab1_0729	pDONR223	*bab1_0729*	GGGACAACTTTGTACAAAAAAGTTGGCGGCCGCACCATGTCTCTCCGTTTTTCGACTT GGGACAACTTTGTACAAGAAAGTTGGGTAATTAATTAATTAACCGGCGTATTTCAGG

Table 3.5. Plasmids containing selected candidate effector proteins constructed for this work (continued).

	Construction [1]		
Plasmid	**Vector**	**Insert**	**Primers(5'-3')**
pDONR223::bab1_0740	pDONR223	*bab1_0740*	GGGACAACTTTGTACAAAAAAGTTGGCGGCCGCACCATGTCGGTGATCGGTGATGT GGGACAACTTTGTACAAGAAAGTTGGGTAATTAATTAATCAGAATTTGTCTAGCAGGT
pDONR223::bab1_0745	pDONR223	*bab1_0745*	GGGACAACTTTGTACAAAAAAGTTGGCGGCCGCACCATGAAATTCACTTCAAATCGA GGGACAACTTTGTACAAGAAAGTTGGGTAATTAATTAATCATATTCCAAAATATTCCT
pDONR223::bab1_0752	pDONR223	*bab1_0752*	GGGACAACTTTGTACAAAAAAGTTGGCGGCCGCACCGTGAATTCGACTAGTAAAGGC GGGACAACTTTGTACAAGAAAGTTGGGTAATTAATTAATCATAGGCGTCCAGACATTCG
pDONR223::bab1_0756	pDONR223	*bab1_0756*	GGGACAACTTTGTACAAAAAAGTTGGCGGCCGCACCATGTACAATTTATTTGTTTCGGGC GGGACAACTTTGTACAAGAAAGTTGGGTAATTAATTAACTAGGTGATGAGGGCGACGC
pDONR223::bab1_0817	pDONR223	*bab1_0817*	GGGACAACTTTGTACAAAAAAGTTGGCGGCCGCACCATGAACGAAGAATACAAAA GGGACAACTTTGTACAAGAAAGTTGGGTAATTAATTAATCAAATTGGTCGGGCGTAGT
pDONR223::bab1_0847	pDONR223	*bab1_0847*	GGGACAACTTTGTACAAAAAAGTTGGCGGCCGCACCATGAAATCGACCAAGATCAT GGGACAACTTTGTACAAGAAAGTTGGGTAATTAATTAATTACTTGCGCACGATTTCTA
pDONR223::bab1_0891	pDONR223	*bab1_0891*	GGGACAACTTTGTACAAAAAAGTTGGCGGCCGCACCATGCGTAGTCGCAGTTTTTC GGGACAACTTTGTACAAGAAAGTTGGGTAATTAATTAATCAGTAACTGCCTTTTACAG
pDONR223::bab1_0917	pDONR223	*bab1_0917*	GGGACAACTTTGTACAAAAAAGTTGGCGGCCGCACCATGACAAGAAGTGAAGGTTTG GGGACAACTTTGTACAAGAAAGTTGGGTAATTAATTAATCAAGCCTCTTCGGACTTGC
pDONR223::bab1_0919	pDONR223	*bab1_0919*	GGGACAACTTTGTACAAAAAAGTTGGCGGCCGCACCATGTGGGTTCGCAGTGCCAG GGGACAACTTTGTACAAGAAAGTTGGGTAATTAATTAATTACATATTCCAGTTTTCAAGC
pDONR223::bab1_0920	pDONR223	*bab1_0920*	GGGACAACTTTGTACAAAAAAGTTGGCGGCCGCACCATGAAGAAATTTCTTACGCA GGGACAACTTTGTACAAGAAAGTTGGGTAATTAATTAATCAGTTTCCGGGGGTCCA
pDONR223::bab1_0939	pDONR223	*bab1_0939*	GGGACAACTTTGTACAAAAAAGTTGGCGGCCGCACCATGGTCGCGGCAGGCGGAA GGGACAACTTTGTACAAGAAAGTTGGGTAATTAATTAATCAATGCGCTCCCCTTGC
pDONR223::bab1_0946	pDONR223	*bab1_0946*	GGGACAACTTTGTACAAAAAAGTTGGCGGCCGCACCATGCCAGAAGTCATTTTCAACG GGGACAACTTTGTACAAGAAAGTTGGGTAATTAATTAACTAGCGAAGACGCTTCGGGC

Table 3.5. Plasmids containing selected candidate effector proteins constructed for this work (continued).

	Construction (1)		
Plasmid	**Vector**	**Insert**	**Primers(5'-3')**
pDONR223::bab1_0955	pDONR223	*bab1_0955*	GGGACAACTTTGTACAAAAAAGTTGGCGGCCGCACCTTGACGACATTTGCCGAACT GGGACAACTTTGTACAAGAAAGTTGGGTAATTAATTAATCACACGCCGGTTGGAATCA
pDONR223::bab1_1016	pDONR223	*bab1_1016*	GGGACAACTTTGTACAAAAAAGTTGGCGGCCGCACCGTGACTTCTCCCCGCAATTG GGGACAACTTTGTACAAGAAAGTTGGGTAATTAATTAACTAAACGGCCACTTCAAAGC
pDONR223::bab1_1035	pDONR223	*bab1_1035*	GGGACAACTTTGTACAAAAAAGTTGGCGGCCGCACCATGGCGATTATTTTTACAAA GGGACAACTTTGTACAAGAAAGTTGGGTAATTAATTAATTACGGGGCAGGCGCATGGGC
pDONR223::bab1_1048	pDONR223	*bab1_1048*	GGGACAACTTTGTACAAAAAAGTTGGCGGCCGCACCATGAATTTCAAGAAACGGGT GGGACAACTTTGTACAAGAAAGTTGGGTAATTAATTAATCAATGGCCCGTCTGGCGCA
pDONR223::bab1_1058	pDONR223	*bab1_1058*	GGGACAACTTTGTACAAAAAAGTTGGCGGCCGCACCATGAAGGAATGGCTCAGCGG GGGACAACTTTGTACAAGAAAGTTGGGTAATTAATTAACTAATTGCGGGTTTCTCCCTTG
pDONR223::bab1_1089	pDONR223	*bab1_1089*	GGGACAACTTTGTACAAAAAAGTTGGCGGCCGCACCATGAAATCATCCCGCAAT GGGACAACTTTGTACAAGAAAGTTGGGTAATTAATTAATTACAGGCCTTTTTTCTTCGC
pDONR223::bab1_1099	pDONR223	*bab1_1099*	GGGACAACTTTGTACAAAAAAGTTGGCGGCCGCACCGTGGTGCTTGCATGGAGCCA GGGACAACTTTGTACAAGAAAGTTGGGTAATTAATTAATCACCCCATCACGCCTTG
pDONR223::bab1_1117	pDONR223	*bab1_1117*	GGGACAACTTTGTACAAAAAAGTTGGCGGCCGCACCATGGCTTATAAAGACCCAGA GGGACAACTTTGTACAAGAAAGTTGGGTAATTAATTAATCAGATGTCGGCGGCGATA
pDONR223::bab1_1118	pDONR223	*bab1_1118*	GGGACAACTTTGTACAAAAAAGTTGGCGGCCGCACCATGTCTTTCATTCGCTCGGC GGGACAACTTTGTACAAGAAAGTTGGGTAATTAATTAATTACTTCGTGTCAGCTTCGATG
pDONR223::bab1_1185	pDONR223	*bab1_1185*	GGGACAACTTTGTACAAAAAAGTTGGCGGCCGCACCATGCGAAAATATACTTCGTT GGGACAACTTTGTACAAGAAAGTTGGGTAATTAATTAATTAGCGGGCAGCAGCCTTGC
pDONR223::bab1_1193	pDONR223	*bab1_1193*	GGGACAACTTTGTACAAAAAAGTTGGCGGCCGCACCGTGCGTACCGCATTCAGTAAAGT GGGACAACTTTGTACAAGAAAGTTGGGTAATTAATTAATCAGTTCGAGTTCGCTACCG

Table 3.5. Plasmids containing selected candidate effector proteins constructed for this work (continued).

	Construction [1]		
Plasmid	**Vector**	**Insert**	**Primers(5'-3')**
pDONR223::bab1_1199	pDONR223	*bab1_1199*	GGGACAACTTTGTACAAAAAAGTTGGCGGCCGCACCTTGTTTTACGGATTTTCCAAG GGGACAACTTTGTACAAGAAAGTTGGGTAATTAATTAATCAGGAATGAGGCAGAAGCA
pDONR223::bab1_1275	pDONR223	*bab1_1275*	GGGACAACTTTGTACAAAAAAGTTGGCGGCCGCACCATGAGCATTCCCCAGCCGGA GGGACAACTTTGTACAAGAAAGTTGGGTAATTAATTAACTATCGCCTCAAAACGGCATCAT
pDONR223::bab1_1278	pDONR223	*bab1_1278*	GGGACAACTTTGTACAAAAAAGTTGGCGGCCGCACCATGACAAAACAAATCTTCAT GGGACAACTTTGTACAAGAAAGTTGGGTAATTAATTAATTAGTGAATGCTGCCGACCA
pDONR223::bab1_1279	pDONR223	*bab1_1279*	GGGACAACTTTGTACAAAAAAGTTGGCGGCCGCACCATGCCGATCTATGCATATAA GGGACAACTTTGTACAAGAAAGTTGGGTAATTAATTAATCAGGCAGGCTCCATGCCGC
pDONR223::bab1_1322	pDONR223	*bab1_1322*	GGGACAACTTTGTACAAAAAAGTTGGCGGCCGCACCATGAGCGAGAGCATTTTTGA GGGACAACTTTGTACAAGAAAGTTGGGTAATTAATTAATCAGCCACAAGACGACGCCT
pDONR223::bab1_1344	pDONR223	*bab1_1344*	GGGACAACTTTGTACAAAAAAGTTGGCGGCCGCACCATGCGTACTTCAAAATGGGTCG GGGACAACTTTGTACAAGAAAGTTGGGTAATTAATTAATTATTTCTGCGCGATTGCGC
pDONR223::bab1_1354	pDONR223	*bab1_1354*	GGGACAACTTTGTACAAAAAAGTTGGCGGCCGCACCATGGAAAGCATAATTGGGGATCT GGGACAACTTTGTACAAGAAAGTTGGGTAATTAATTAATTACTCCCCCGGCGATACCTG
pDONR223::bab1_1374	pDONR223	*bab1_1374*	GGGACAACTTTGTACAAAAAAGTTGGCGGCCGCACCATGCACTTCTTCGCGGTGAT GGGACAACTTTGTACAAGAAAGTTGGGTAATTAATTAATTAAAATGGATTTTTAGCTTTC
pDONR223::bab1_1386	pDONR223	*bab1_1386*	GGGACAACTTTGTACAAAAAAGTTGGCGGCCGCACCATGAAAACCGCGCGCTTC GGGACAACTTTGTACAAGAAAGTTGGGTAATTAATTAATCATGGCTCACGCTGCCGGT
pDONR223::bab1_1396	pDONR223	*bab1_1396*	GGGACAACTTTGTACAAAAAAGTTGGCGGCCGCACCATGAATTTCCGGCGCCAAAGC GGGACAACTTTGTACAAGAAAGTTGGGTAATTAATTAATTATTGGAATGGAGAATTGCAG
pDONR223::bab1_1426	pDONR223	*bab1_1426*	GGGACAACTTTGTACAAAAAAGTTGGCGGCCGCACCGTGAGCACGTCCGCACGCCT GGGACAACTTTGTACAAGAAAGTTGGGTAATTAATTAATCAAAAACCTGGAGCCACCG
pDONR223::bab1_1464	pDONR223	*bab1_1464*	GGGACAACTTTGTACAAAAAAGTTGGCGGCCGCACCTTATTGCGGCTGACGCTCTT GGGACAACTTTGTACAAGAAAGTTGGGTAATTAATTAAGTGCGTTTTGCGTGTTTAAA

Table 3.5. Plasmids containing selected candidate effector proteins constructed for this work (continued).

	Construction (1)		
Plasmid	**Vector**	**Insert**	**Primers(5'-3')**
pDONR223::bab1_1488	pDONR223	*bab1_1488*	GGGACAACTTTGTACAAAAAAGTTGGCGGCCGCACCATGGAAACGAAAAGCTCTCT GGGACAACTTTGTACAAGAAAGTTGGGTAATTAATTAATTACTTTTTCAGTGACGGCG
pDONR223::bab1_1492	pDONR223	*bab1_1492*	GGGACAACTTTGTACAAAAAAGTTGGCGGCCGCACCATGATGCCCGTGATTAGACTT GGGACAACTTTGTACAAGAAAGTTGGGTAATTAATTAATTAGGCGGACGCCGGGCCAG
pDONR223::bab1_1501	pDONR223	*bab1_1501*	GGGACAACTTTGTACAAAAAAGTTGGCGGCCGCACCATGCTTCGCCAGGAGATTTC GGGACAACTTTGTACAAGAAAGTTGGGTAATTAATTAATCATTGCAGCAGCGATTTTAC
pDONR223::bab1_1502	pDONR223	*bab1_1502*	GGGACAACTTTGTACAAAAAAGTTGGCGGCCGCACCATGACTGAAACGACCCCGAA GGGACAACTTTGTACAAGAAAGTTGGGTAATTAATTAATCAGGCAGCCTGTTCGCGCT
pDONR223::bab1_1526	pDONR223	*bab1_1526*	GGGACAACTTTGTACAAAAAAGTTGGCGGCCGCACCATGTCAGCACTGATTTCGCCA GGGACAACTTTGTACAAGAAAGTTGGGTAATTAATTAATCACCCCTTGAAGATCAAGG
pDONR223::bab1_1527	pDONR223	*bab1_1527*	GGGACAACTTTGTACAAAAAAGTTGGCGGCCGCACCATGAGTTTTGCGTTGTCCGC GGGACAACTTTGTACAAGAAAGTTGGGTAATTAATTAATTATTTGCAGGCACGGTAGC
pDONR223::bab1_1543	pDONR223	*bab1_1543*	GGGACAACTTTGTACAAAAAAGTTGGCGGCCGCACCATGACCAGCGGACAGAACC GGGACAACTTTGTACAAGAAAGTTGGGTAATTAATTAATCAGGAATTATCTTTGGATTTTG
pDONR223::bab1_1591	pDONR223	*bab1_1591*	GGGACAACTTTGTACAAAAAAGTTGGCGGCCGCACCATGAGAGTGTGGGATGCAGT GGGACAACTTTGTACAAGAAAGTTGGGTAATTAATTAATTAACGCTCCAGAACCTGCT
pDONR223::bab1_1611	pDONR223	*bab1_1611*	GGGACAACTTTGTACAAAAAAGTTGGCGGCCGCACCATGCTTGGCGTTCTCGTGGC GGGACAACTTTGTACAAGAAAGTTGGGTAATTAATTAACTATTGCATGTCGCGGATGC
pDONR223::bab1_1615	pDONR223	*bab1_1615*	GGGACAACTTTGTACAAAAAAGTTGGCGGCCGCACCATGAAGCCACGTGAAAGCCT GGGACAACTTTGTACAAGAAAGTTGGGTAATTAATTAATCAGCCGATCATGGCGCGGC
pDONR223::bab1_1640	pDONR223	*bab1_1640*	GGGACAACTTTGTACAAAAAAGTTGGCGGCCGCACCATGCATAAATCTATTATTTCC GGGACAACTTTGTACAAGAAAGTTGGGTAATTAATTAACTACTTGGTTGCCAGCAATT
pDONR223::bab1_1652	pDONR223	*bab1_1652*	GGGACAACTTTGTACAAAAAAGTTGGCGGCCGCACCATGAAAATCATCATCACGGC GGGACAACTTTGTACAAGAAAGTTGGGTAATTAATTAACTAGTTCTTGGGCGCGTGGC

Table 3.5. Plasmids containing selected candidate effector proteins constructed for this work (continued).

Plasmid	Construction (1)		
	Vector	Insert	Primers(5'-3')
pDONR223::bab1_1671	pDONR223	*bab1_1671*	GGGACAACTTTGTACAAAAAAGTTGGCGGCCGCACCATGACGTTATCGACGCGTAT GGGACAACTTTGTACAAGAAAGTTGGGTAATTAATTAATCAGGCAGCAACTTGCGATG
pDONR223::bab1_1685	pDONR223	*bab1_1685*	GGGACAACTTTGTACAAAAAAGTTGGCGGCCGCACCGTGCTTAAATCTAGTGATTC GGGACAACTTTGTACAAGAAAGTTGGGTAATTAATTAATCAGAAGAAGCGCATACTGG
pDONR223::bab1_1703	pDONR223	*bab1_1703*	GGGACAACTTTGTACAAAAAAGTTGGCGGCCGCACCATGAATCCGAACTATCGCAA GGGACAACTTTGTACAAGAAAGTTGGGTAATTAATTAATTATTGCGGCTGCGGTTTC
pDONR223::bab1_1705	pDONR223	*bab1_1705*	GGGACAACTTTGTACAAAAAAGTTGGCGGCCGCACCATGAGGAAACCAATGAGAAAAGTG GGGACAACTTTGTACAAGAAAGTTGGGTAATTAATTAATCAGCACTTGGCGCGACTGC
pDONR223::bab1_1720	pDONR223	*bab1_1720*	GGGACAACTTTGTACAAAAAAGTTGGCGGCCGCACCATGAAGCGCAAATTTCTTCTCG GGGACAACTTTGTACAAGAAAGTTGGGTAATTAATTAATCAGCGTATGCGCAGATTATT
pDONR223::bab1_1725	pDONR223	*bab1_1725*	GGGACAACTTTGTACAAAAAAGTTGGCGGCCGCACCATGAGCGATATGAGGGAAAGTCT GGGACAACTTTGTACAAGAAAGTTGGGTAATTAATTAATTACTCCGGCTTGTCGGTAC
pDONR223::bab1_1726	pDONR223	*bab1_1726*	GGGACAACTTTGTACAAAAAAGTTGGCGGCCGCACCATGGCTCTTGCCCGCAACC GGGACAACTTTGTACAAGAAAGTTGGGTAATTAATTAATTATCGTTCTGTCAGTTTCA
pDONR223::bab1_1730	pDONR223	*bab1_1730*	GGGACAACTTTGTACAAAAAAGTTGGCGGCCGCACCATGAATCAGAATGTCCCAGCCT GGGACAACTTTGTACAAGAAAGTTGGGTAATTAATTAACTACCCCACAATGGCGAAGGA
pDONR223::bab1_1738	pDONR223	*bab1_1738*	GGGACAACTTTGTACAAAAAAGTTGGCGGCCGCACCATGGCACCCGATACGATCC GGGACAACTTTGTACAAGAAAGTTGGGTAATTAATTAACTATCGATCCAGAACGGCGC
pDONR223::bab1_1751	pDONR223	*bab1_1751*	GGGACAACTTTGTACAAAAAAGTTGGCGGCCGCACCATGGGCAGTTTCGATGAGG GGGACAACTTTGTACAAGAAAGTTGGGTAATTAATTAATTATCGGAACAGGGCTTCG
pDONR223::bab1_1754	pDONR223	*bab1_1754*	GGGACAACTTTGTACAAAAAAGTTGGCGGCCGCACCATGGCTATAGAGTCCCATCTTGC GGGACAACTTTGTACAAGAAAGTTGGGTAATTAATTAACTAGTGACGTGTTACTTGAG
pDONR223::bab1_1773	pDONR223	*bab1_1773*	GGGACAACTTTGTACAAAAAAGTTGGCGGCCGCACCATGCCAGCATGGACACAGTAC GGGACAACTTTGTACAAGAAAGTTGGGTAATTAATTAACTATTCGCTGATGATCTTCACG

Table 3.5. Plasmids containing selected candidate effector proteins constructed for this work (continued).

	Construction [1]		
Plasmid	**Vector**	**Insert**	**Primers(5'-3')**
pDONR223::bab1_1828	pDONR223	*bab1_1828*	GGGACAACTTTGTACAAAAAAGTTGGCGGCCGCACCATGACGCATCACACGCTGA GGGACAACTTTGTACAAGAAAGTTGGGTAATTAATTAATCAAAGTTTGATCAGATGATCG
pDONR223::bab1_1839	pDONR223	*bab1_1839*	GGGACAACTTTGTACAAAAAAGTTGGCGGCCGCACCATGGGTGAGCGCCAGCAGGC GGGACAACTTTGTACAAGAAAGTTGGGTAATTAATTAATTATACCTGGCTTTGCATGA
pDONR223::bab1_1843	pDONR223	*bab1_1843*	GGGACAACTTTGTACAAAAAAGTTGGCGGCCGCACCATGGGTGTTGGAAGTCTTCTCG GGGACAACTTTGTACAAGAAAGTTGGGTAATTAATTAATCAAGCGCGTTTGACGATGC
pDONR223::bab1_1864	pDONR223	*bab1_1864*	GGGACAACTTTGTACAAAAAAGTTGGCGGCCGCACCATGGCATCAAAGACTACCTT GGGACAACTTTGTACAAGAAAGTTGGGTAATTAATTAATCACCGATCTACAAGCGGC
pDONR223::bab1_1865	pDONR223	*bab1_1865*	GGGACAACTTTGTACAAAAAAGTTGGCGGCCGCACCATGACTGACCTGATTCACATACA GGGACAACTTTGTACAAGAAAGTTGGGTAATTAATTAATCAGCGAAAGCGGCCCAA
pDONR223::bab1_1866	pDONR223	*bab1_1866*	GGGACAACTTTGTACAAAAAAGTTGGCGGCCGCACCATGAAGGAATTGGGGCCGAA GGGACAACTTTGTACAAGAAAGTTGGGTAATTAATTAATCAGCTCTTGGCCGATCCGT
pDONR223::bab1_1941	pDONR223	*bab1_1941*	GGGACAACTTTGTACAAAAAAGTTGGCGGCCGCACCATGGTGCCAGGTCTTGCTAT GGGACAACTTTGTACAAGAAAGTTGGGTAATTAATTAATCATTTCAGGCTATTCTCCCGA
pDONR223::bab1_1948	pDONR223	*bab1_1948*	GGGACAACTTTGTACAAAAAAGTTGGCGGCCGCACCATGGCTGCAAAACCTTTGCTT GGGACAACTTTGTACAAGAAAGTTGGGTAATTAATTAATTATTTATGCTCGGTGAAACTGC
pDONR223::bab1_1985	pDONR223	*bab1_1985*	GGGACAACTTTGTACAAAAAAGTTGGCGGCCGCACCATGACGGATCATAGCAACGA GGGACAACTTTGTACAAGAAAGTTGGGTAATTAATTAATCAGTCGAATTTCAGCAGGC
pDONR223::bab1_2005	pDONR223	*bab1_2005*	GGGACAACTTTGTACAAAAAAGTTGGCGGCCGCACCATGGCGCTAGACGACGATATT GGGACAACTTTGTACAAGAAAGTTGGGTAATTAATTAATCAGTCGCGGTTTGCAAGCC
pDONR223::bab1_2011	pDONR223	*bab1_2011*	GGGACAACTTTGTACAAAAAAGTTGGCGGCCGCACCTTGTTGCAATGGTGTTTTTCT GGGACAACTTTGTACAAGAAAGTTGGGTAATTAATTAATCAAAAACAATTATCACGTGC
pDONR223::bab1_2021	pDONR223	*bab1_2021*	GGGACAACTTTGTACAAAAAAGTTGGCGGCCGCACCATGTCTAACGCGACATTAAA GGGACAACTTTGTACAAGAAAGTTGGGTAATTAATTAACTATTGTACACCCGAGAAT

Table 3.5. Plasmids containing selected candidate effector proteins constructed for this work (continued).

	Construction [1]		
Plasmid	**Vector**	**Insert**	**Primers(5'-3')**
pDONR223::bab1_2079	pDONR223	*bab1_2079*	GGGACAACTTTGTACAAAAAAGTTGGCGGCCGCACCTTGGCATTCTTCCTTGCCA GGGACAACTTTGTACAAGAAAGTTGGGTAATTAATTAATCAGAAAAGCGCCTTCAGC
pDONR223::bab1_2089	pDONR223	*bab1_2089*	GGGACAACTTTGTACAAAAAAGTTGGCGGCCGCACCATGCAAGAGGATCGCAACAT GGGACAACTTTGTACAAGAAAGTTGGGTAATTAATTAACTAATCAAAAGAAACCTTGCCGCG
pDONR223::bab1_2145	pDONR223	*bab1_2145*	GGGACAACTTTGTACAAAAAAGTTGGCGGCCGCACCATGCCGTCCCAGCATACCGTT GGGACAACTTTGTACAAGAAAGTTGGGTAATTAATTAATCAGGGTTTACGCGCCTC
pDONR223::bab1_2152	pDONR223	*bab1_2152*	GGGACAACTTTGTACAAAAAAGTTGGCGGCCGCACCATGATGGGCTTTCCGTTCGG GGGACAACTTTGTACAAGAAAGTTGGGTAATTAATTAATCATTGCGCCCTCTTCAG
pDONR223::bab1_2164	pDONR223	*bab1_2164*	GGGACAACTTTGTACAAAAAAGTTGGCGGCCGCACCATGATGGTCCGCGTCAGG GGGACAACTTTGTACAAGAAAGTTGGGTAATTAATTAACTAATCCAGATTCGATGCGCT
pDONR223::bab1_2178	pDONR223	*bab1_2178*	GGGACAACTTTGTACAAAAAAGTTGGCGGCCGCACCATGTCGAACAAGAAGAAGCCG GGGACAACTTTGTACAAGAAAGTTGGGTAATTAATTAATCAGACCCGGTTGGGCAGCA
pDONR223::bab2_0056	pDONR223	*bab2_0056*	GGGACAACTTTGTACAAAAAAGTTGGCGGCCGCACCATGCGTGAAGCTCTGACAAG GGGACAACTTTGTACAAGAAAGTTGGGTAATTAATTAACTATTTTCTGGGGGCTTTTCC
pDONR223::bab2_0074	pDONR223	*bab2_0074*	GGGACAACTTTGTACAAAAAAGTTGGCGGCCGCACCATGACCGGTTTCGACATCA GGGACAACTTTGTACAAGAAAGTTGGGTAATTAATTAATCAGTCGCGCCCGGTGGGCG
pDONR223::bab2_0099	pDONR223	*bab2_0099*	GGGACAACTTTGTACAAAAAAGTTGGCGGCCGCACCATGGACGGTGAAGACAAGCG GGGACAACTTTGTACAAGAAAGTTGGGTAATTAATTAACTACAGGCGCAGCAACCGCCCGAA
pDONR223::bab2_0119	pDONR223	*bab2_0119*	GGGACAACTTTGTACAAAAAAGTTGGCGGCCGCACCATGAAGAGCTTGCAGTTTTCAA GGGACAACTTTGTACAAGAAAGTTGGGTAATTAATTAATTATCGATATGCCCGAGGTA
pDONR223::bab2_0123	pDONR223	*bab2_0123*	GGGACAACTTTGTACAAAAAAGTTGGCGGCCGCACCATGAGCTTGTTGCTGGCTAACG GGGACAACTTTGTACAAGAAAGTTGGGTAATTAATTAATCATGCCTGTCCCGCCAGTT
pDONR223::bab2_0130	pDONR223	*bab2_0130*	GGGACAACTTTGTACAAAAAAGTTGGCGGCCGCACCATGAAGAAGCCACTGAGCAAG GGGACAACTTTGTACAAGAAAGTTGGGTAATTAATTAATCACCGCCGCATATCGATGA

Table 3.5. Plasmids containing selected candidate effector proteins constructed for this work (continued).

	Construction (1)		
Plasmid	**Vector**	**Insert**	**Primers(5'-3')**
pDONR223::bab2_0145	pDONR223	*bab2_0145*	GGGACAACTTTGTACAAAAAAGTTGGCGGCCGCACCATGCGCCTTGGCGTCATTGC GGGACAACTTTGTACAAGAAAGTTGGGTAATTAATTAATTATTTATCTCCTTCCTGAT
pDONR223::bab2_0147	pDONR223	*bab2_0147*	GGGACAACTTTGTACAAAAAAGTTGGCGGCCGCACCTTGCAGGAAATTCAAACTATTAAGG GGGACAACTTTGTACAAGAAAGTTGGGTAATTAATTAATTAAGCCTGAACCGGTATGG
pDONR223::bab2_0155	pDONR223	*bab2_0155*	GGGACAACTTTGTACAAAAAAGTTGGCGGCCGCACCATGATTATGGCGCATAAAAT GGGACAACTTTGTACAAGAAAGTTGGGTAATTAATTAATCATTGCACCGTATTCCCGG
pDONR223::bab2_0159	pDONR223	*bab2_0159*	GGGACAACTTTGTACAAAAAAGTTGGCGGCCGCACCGTGGTTCCAGCGGTTCTGTT GGGACAACTTTGTACAAGAAAGTTGGGTAATTAATTAACTATTGTATAGGTTGGTTCA
pDONR223::bab2_0160	pDONR223	*bab2_0160*	GGGACAACTTTGTACAAAAAAGTTGGCGGCCGCACCATGCTTGCAGCTTGCGGGAA GGGACAACTTTGTACAAGAAAGTTGGGTAATTAATTAATTATCTTGGCCGCGCACA
pDONR223::bab2_0203	pDONR223	*bab2_0203*	GGGACAACTTTGTACAAAAAAGTTGGCGGCCGCACCGTGGATAAGGCCCTGTCGT GGGACAACTTTGTACAAGAAAGTTGGGTAATTAATTAATCAAAGATCAGGCAATTTTTCCGG
pDONR223::bab2_0208	pDONR223	*bab2_0208*	GGGACAACTTTGTACAAAAAAGTTGGCGGCCGCACCATGAAACATGAAGATGGCGT GGGACAACTTTGTACAAGAAAGTTGGGTAATTAATTAATCATTTCGCTTTCTCCAATGC
pDONR223::bab2_0246	pDONR223	*bab2_0246*	GGGACAACTTTGTACAAAAAAGTTGGCGGCCGCACCATGGCCGAAGCCGAGGCAAC GGGACAACTTTGTACAAGAAAGTTGGGTAATTAATTAATCAGGCCCGGCAGTTCTCAA
pDONR223::bab2_0252	pDONR223	*bab2_0252*	GGGACAACTTTGTACAAAAAAGTTGGCGGCCGCACCATGAATCCAAATATCAAGAAG GGGACAACTTTGTACAAGAAAGTTGGGTAATTAATTAATCACTGCCCTACTGCCCTAT
pDONR223::bab2_0271	pDONR223	*bab2_0271*	GGGACAACTTTGTACAAAAAAGTTGGCGGCCGCACCATGCTGCAATTGGCGATGCG GGGACAACTTTGTACAAGAAAGTTGGGTAATTAATTAATTAACCCCGCGTGCGGGCCA
pDONR223::bab2_0402	pDONR223	*bab2_0402*	GGGACAACTTTGTACAAAAAAGTTGGCGGCCGCACCTTGCTCAAAGGTCCAGCCTT GGGACAACTTTGTACAAGAAAGTTGGGTAATTAATTAATCAGCGGCCTTGCAGTCGCC
pDONR223::bab2_0407	pDONR223	*bab2_0407*	GGGACAACTTTGTACAAAAAAGTTGGCGGCCGCACCTTGGAAAGTATCGAGCGCGC GGGACAACTTTGTACAAGAAAGTTGGGTAATTAATTAATTATTTGTCAGCCGTAGTCACC

Table 3.5. Plasmids containing selected candidate effector proteins constructed for this work (continued).

Plasmid	Construction (1)		
	Vector	Insert	Primers(5'-3')
pDONR223::bab2_0413	pDONR223	*bab2_0413*	GGGACAACTTTGTACAAAAAAGTTGGCGGCCGCACCATGCAGGATTTGAGCCAGAC GGGACAACTTTGTACAAGAAAGTTGGGTAATTAATTAATTATTTGTTCTTTTCGAGCAG
pDONR223::bab2_0481	pDONR223	*bab2_0481*	GGGACAACTTTGTACAAAAAAGTTGGCGGCCGCACCATGAAAAAGCTCCTTGCACA GGGACAACTTTGTACAAGAAAGTTGGGTAATTAATTAATCAATCCACCACCGAAACG
pDONR223::bab2_0516	pDONR223	*bab2_0516*	GGGACAACTTTGTACAAAAAAGTTGGCGGCCGCACCTTGGCCCTATCGGCTTTC GGGACAACTTTGTACAAGAAAGTTGGGTAATTAATTAATTATAAGAGTTTGCGGCAAGC
pDONR223::bab2_0541	pDONR223	*bab2_0541*	GGGACAACTTTGTACAAAAAAGTTGGCGGCCGCACCGTGGTACGAAATGATTTGAACTG GGGACAACTTTGTACAAGAAAGTTGGGTAATTAATTAATCACCGTCCTGAAGAAAGCC
pDONR223::bab2_0634	pDONR223	*bab2_0634*	GGGACAACTTTGTACAAAAAAGTTGGCGGCCGCACCATGAGCACGCTAGAGGCCAA GGGACAACTTTGTACAAGAAAGTTGGGTAATTAATTAATCAAGCGGCGTCGCCGTATT
pDONR223::bab2_0653	pDONR223	*bab2_0653*	GGGACAACTTTGTACAAAAAAGTTGGCGGCCGCACCATGCTCAAAAGTTTGAAAAA GGGACAACTTTGTACAAGAAAGTTGGGTAATTAATTAATCAGTAGGGCGAATAGCACTG
pDONR223::bab2_0665	pDONR223	*bab2_0665*	GGGACAACTTTGTACAAAAAAGTTGGCGGCCGCACCATGTCCAGCACGAAGACAATC GGGACAACTTTGTACAAGAAAGTTGGGTAATTAATTAATTATTTGGCAGCGCCTTTT
pDONR223::bab2_0681	pDONR223	*bab2_0681*	GGGACAACTTTGTACAAAAAAGTTGGCGGCCGCACCATGACGCGTCGTCGCTACGA GGGACAACTTTGTACAAGAAAGTTGGGTAATTAATTAATTACGGAACGTCCCATGCCACCAT
pDONR223::bab2_0691	pDONR223	*bab2_0691*	GGGACAACTTTGTACAAAAAAGTTGGCGGCCGCACCATGACCTTTAAACCGGAAAAG GGGACAACTTTGTACAAGAAAGTTGGGTAATTAATTAATCACTTAACGGGGATCGC
pDONR223::bab2_0692	pDONR223	*bab2_0692*	GGGACAACTTTGTACAAAAAAGTTGGCGGCCGCACCATGAAAATTGCAGTTATC GGGACAACTTTGTACAAGAAAGTTGGGTAATTAATTAATTAAAGGTCATTGGAGCCT
pDONR223::bab2_0711	pDONR223	*bab2_0711*	GGGACAACTTTGTACAAAAAAGTTGGCGGCCGCACCATGGCTGTTCTGGGGGCCGC GGGACAACTTTGTACAAGAAAGTTGGGTAATTAATTAACTACATGTTTGATGATCTGC
pDONR223::bab2_0738	pDONR223	*bab2_0738*	GGGACAACTTTGTACAAAAAAGTTGGCGGCCGCACCATGACGATGGACGGCAGAAT GGGACAACTTTGTACAAGAAAGTTGGGTAATTAATTAATCAGTTCTCCTCCTTCGCTG

Table 3.5. Plasmids containing selected candidate effector proteins constructed for this work (continued).

	Construction (1)		
Plasmid	**Vector**	**Insert**	**Primers(5'-3')**
pDONR223::bab2_0773	pDONR223	*bab2_0773*	GGGACAACTTTGTACAAAAAAGTTGGCGGCCGCACCATGAGCCTGCTTTGTGTCAT GGGACAACTTTGTACAAGAAAGTTGGGTAATTAATTAACTATTTCGCACCAAGATCGACA
pDONR223::bab2_0862	pDONR223	*bab2_0862*	GGGACAACTTTGTACAAAAAAGTTGGCGGCCGCACCATGATTAAGGCTCTCTTCAA GGGACAACTTTGTACAAGAAAGTTGGGTAATTAATTAATCAGAAAACTTTCTTGAGTT
pDONR223::bab2_0865	pDONR223	*bab2_0865*	GGGACAACTTTGTACAAAAAAGTTGGCGGCCGCACCGTGTGTTGGCACAAATTCGC GGGACAACTTTGTACAAGAAAGTTGGGTAATTAATTAATTATGTGTGGTGAAAGCCGG
pDONR223::bab2_0941	pDONR223	*bab2_0941*	GGGACAACTTTGTACAAAAAAGTTGGCGGCCGCACCATGGCCATGATAGATCGCGG GGGACAACTTTGTACAAGAAAGTTGGGTAATTAATTAATCAGTCCTCGCCTTCGGCAA
pDONR223::bab2_1021	pDONR223	*bab2_1021*	GGGACAACTTTGTACAAAAAAGTTGGCGGCCGCACCATGCTTGATCTCGTTTCCCA GGGACAACTTTGTACAAGAAAGTTGGGTAATTAATTAATCAAAGAAAAGGTGAGCCGA
pDONR223::bab2_1084	pDONR223	*bab2_1084*	GGGACAACTTTGTACAAAAAAGTTGGCGGCCGCACCATGATCCGCATTATCGTCATC GGGACAACTTTGTACAAGAAAGTTGGGTAATTAATTAATTATTCACTTTGAGCGGCAG
pDONR223::bab2_1085	pDONR223	*bab2_1085*	GGGACAACTTTGTACAAAAAAGTTGGCGGCCGCACCATGACTGAGACAAGCTCCGA GGGACAACTTTGTACAAGAAAGTTGGGTAATTAATTAATCATCGGGCGTGACCGAGCC
pDONR223::bab2_1100	pDONR223	*bab2_1100*	GGGACAACTTTGTACAAAAAAGTTGGCGGCCGCACCATGGCCGTGGCGCTCCTCAT GGGACAACTTTGTACAAGAAAGTTGGGTAATTAATTAATTACAAAAGCCCGCCGCGGC
pDONR223::bab2_1104	pDONR223	*bab2_1104*	GGGACAACTTTGTACAAAAAAGTTGGCGGCCGCACCATGAGCGCGCTTTCCATC GGGACAACTTTGTACAAGAAAGTTGGGTAATTAATTAATCATTTCACCGCAGCCTTCA
pDONR223::Gluc	pDONR223	*gluc*	GGGACAACTTTGTACAAAAAAGTTGGCGGCCGCACCATGGGAGTCAAAGTTCTGTT GGGACAACTTTGTACAAGAAAGTTGGGTAATTAATTAATCAGTCACCACCGGCCCCCT

Table 3.5. Plasmids containing selected candidate effector proteins constructed for this work (continued).

		Construction [1]	
Plasmid	**Description**	**Vector**	**Insert**
pYOP001	pTRIP5::bab1_0847	pTRIP5	*bab1_0847*
pYOP002	pTRIP5::bab2_0123	pTRIP5	*bab2_0123*
pYOP003	pTRIP5::bab1_1279	pTRIP5	*bab1_1279*
pYOP004	pTRIP5::bab1_0712	pTRIP5	*bab1_0712*
pYOP005	pTRIP5::bab1_1492	pTRIP5	*bab1_1492*
pYOP006	pTRIP5::bab1_0279	pTRIP5	*bab1_0279*
pYOP007	pTRIP5::bab1_0756	pTRIP5	*bab1_0756*
pYOP008	pTRIP5::bab1_1948	pTRIP5	*bab1_1948*
pYOP009	pTRIP5::bab1_2005	pTRIP5	*bab1_2005*
pYOP010	pTRIP5::bab1_1652	pTRIP5	*bab1_1652*
pYOP011	pTRIP5::bab1_0678	pTRIP5	*bab1_0678*
pYOP012	pTRIP5::bab1_1058	pTRIP5	*bab1_1058*
pYOP013	pTRIP5::bab1_1275	pTRIP5	*bab1_1275*
pYOP014	pTRIP5::bab1_1671	pTRIP5	*bab1_1671*
pYOP015	pTRIP6::bab2_0203	pTRIP6	*bab2_0203*
pYOP017	pTRIP6::bab1_1591	pTRIP6	*bab1_1591*
pYOP018	pTRIP6::bab1_0322	pTRIP6	*bab1_0322*
pYOP019	pTRIP6::bab1_1099	pTRIP6	*bab1_1099*
pYOP020	pTRIP6::bab2_0271	pTRIP6	*bab2_0271*
pYOP021	pTRIP6::bab1_1866	pTRIP6	*bab1_1866*
pYOP022	pTRIP6::bab1_0740	pTRIP6	*bab1_0740*
pYOP023	pTRIP6::bab1_1640	pTRIP6	*bab1_1640*

Table 3.6. Lentiviral plasmids containing selected candidate effector proteins constructed for this work.
(1) First column lists the vector plasmids; second column lists the *B. abortus* gene inserted between attR1 and attR2 recombination site.

		Construction [1]	
Plasmid	**Description**	**Vector**	**Insert**
pYOP024	pTRIP6::bab1_0368	pTRIP6	*bab1_0368*
pYOP025	pTRIP5::bab1_1611	pTRIP5	*bab1_1611*
pYOP026	pTRIP6::bab1_1754	pTRIP6	*bab1_1754*
pYOP027	pTRIP6::bab1_1685	pTRIP6	*bab1_1685*
pYOP028	pTRIP6::bab1_1705	pTRIP6	*bab1_1705*
pYOP029	pTRIP6::bab1_1354	pTRIP6	*bab1_1354*
pYOP030	pTRIP6::bab1_1374	pTRIP6	*bab1_1374*
pYOP031	pTRIP6::bab1_1828	pTRIP6	*bab1_1828*
pYOP032	pTRIP5::bab1_1864	pTRIP5	*bab1_1864*
pYOP033	pTRIP5::bab2_0119	pTRIP5	*bab2_0119*
pYOP034	pTRIP6::bab2_0865	pTRIP6	*bab2_0865*
pYOP035	pTRIP6::bab2_1021	pTRIP6	*bab2_1021*
pYOP036	pTRIP6::bab1_0939	pTRIP6	*bab1_0939*
pYOP037	pTRIP6::bab1_1526	pTRIP6	*bab1_1526*
pYOP038	pTRIP6::bab1_0663	pTRIP6	*bab1_0663*
pYOP039	pTRIP6::bab1_1725	pTRIP6	*bab1_1725*
pYOP040	pTRIP6::bab1_0063	pTRIP6	*bab1_0063*
pYOP041	pTRIP6::bab1_1386	pTRIP6	*bab1_1386*
pYOP042	pTRIP5::bab1_1865	pTRIP5	*bab1_1865*
pYOP043	pTRIP6::bab1_1985	pTRIP6	*bab1_1985*
pYOP044	pTRIP6::bab1_2164	pTRIP6	*bab1_2164*
pYOP045	pTRIP5::bab2_0159	pTRIP5	*bab2_0159*
pYOP046	pTRIP6::bab1_0121	pTRIP6	*bab1_0121*

Table 3.6. Lentiviral plasmids containing selected candidate effector proteins constructed for this work (continued).

		Construction (1)	
Plasmid	**Description**	**Vector**	**Insert**
pYOP047	pTRIP6::bab1_0401	pTRIP6	*bab1_0401*
pYOP049	pTRIP6::bab1_0919	pTRIP6	*bab1_0919*
pYOP050	pTRIP6::bab1_1193	pTRIP6	*bab1_1193*
pYOP051	pTRIP6::bab1_1941	pTRIP6	*bab1_1941*
pYOP052	pTRIP6::bab1_2152	pTRIP6	*bab1_2152*
pYOP053	pTRIP6::bab1_2178	pTRIP6	*bab1_2178*
pYOP054	pTRIP6::bab2_0516	pTRIP6	*bab2_0516*
pYOP055	pTRIP6::bab2_0738	pTRIP6	*bab2_0738*
pYOP056	pTRIP6::bab2_0941	pTRIP6	*bab2_0941*
pYOP057	pTRIP6::bab1_0653	pTRIP6	*bab1_0653*
pYOP058	pTRIP6::bab1_0891	pTRIP6	*bab1_0891*
pYOP059	pTRIP6::bab1_1199	pTRIP6	*bab1_1199*
pYOP060	pTRIP6::bab1_1464	pTRIP6	*bab1_1464*
pYOP061	pTRIP6::bab1_1501	pTRIP6	*bab1_1501*
pYOP062	pTRIP6::bab1_1720	pTRIP6	*bab1_1720*
pYOP063	pTRIP6::bab1_1730	pTRIP6	*bab1_1720*
pYOP064	pTRIP6::bab1_1843	pTRIP6	*bab1_1843*
pYOP065	pTRIP6::bab1_2145	pTRIP6	*bab1_2145*
pYOP066	pTRIP6::bab2_0208	pTRIP6	*bab2_0208*
pYOP067	pTRIP6::bab1_0175	pTRIP6	*bab1_0175*
pYOP068	pTRIP6::bab1_0946	pTRIP6	*bab1_0946*
pYOP069	pTRIP6::bab1_1016	pTRIP6	*bab1_1016*
pYOP070	pTRIP6::bab1_1117	pTRIP6	*bab1_1117*

Table 3.6. Lentiviral plasmids containing selected candidate effector proteins constructed for this work (continued).

		Construction [1]	
Plasmid	**Description**	**Vector**	**Insert**
pYOP071	pTRIP6::bab1_1118	pTRIP6	*bab1_1118*
pYOP072	pTRIP6::bab1_1502	pTRIP6	*bab1_1502*
pYOP073	pTRIP6::bab1_1773	pTRIP6	*bab1_1773*
pYOP074	pTRIP6::bab2_0246	pTRIP6	*bab2_0246*
pYOP075	pTRIP6::bab2_0252	pTRIP6	*bab2_0252*
pYOP076	pTRIP6::bab2_0481	pTRIP6	*bab2_0481*
pYOP077	pTRIP6::bab2_0681	pTRIP6	bab2*_068*
pYOP078	pTRIP6::bab2_0773	pTRIP6	*bab2_0773*
pYOP079	pTRIP6::bab1_0343	pTRIP6	*bab1_0343*
pYOP080	pTRIP6::bab1_0752	pTRIP6	*bab1_0752*
pYOP081	pTRIP6::bab2_0160	pTRIP6	*bab2_0160*
pYOP082	pTRIP6::bab1_0745	pTRIP6	*bab1_0745*
pYOP083	pTRIP6::bab1_1035	pTRIP6	*bab1_1035*
pYOP084	pTRIP6::bab1_1615	pTRIP6	*bab1_1615*
pYOP085	pTRIP6::bab2_0074	pTRIP6	*bab2_0074*
pYOP086	pTRIP5::bab1_0227	pTRIP5	*bab1_0227*
pYOP087	pTRIP5::bab2_0541	pTRIP5	*bab2_0541*
pYOP088	pTRIP6::bab1_0445	pTRIP6	*bab1_0445*
pYOP089	pTRIP6::bab1_0920	pTRIP6	*bab1_0920*
pYOP090	pTRIP6::bab1_0955	pTRIP6	*bab1_0955*
pYOP091	pTRIP6::bab1_1089	pTRIP6	*bab1_1089*
pYOP092	pTRIP6::bab1_0158	pTRIP6	*bab1_0158*
pYOP093	pTRIP6::bab1_1703	pTRIP6	*bab1_1703*

Table 3.6. Lentiviral plasmids containing selected candidate effector proteins constructed for this work (continued).

		Construction [1]	
Plasmid	**Description**	**Vector**	**Insert**
pYOP094	pTRIP6::bab2_0692	pTRIP6	*bab2_0692*
pYOP095	pTRIP6::bab1_0271	pTRIP6	*bab1_0271*
pYOP096	pTRIP6::bab1_0151	pTRIP6	*bab1_0151*
pYOP097	pTRIP6::bab1_0296	pTRIP6	*bab1_0296*
pYOP098	pTRIP6::bab1_0453	pTRIP6	*bab1_0453*
pYOP099	pTRIP6::bab1_0608	pTRIP6	*bab1_0608*
pYOP100	pTRIP6::bab1_1048	pTRIP6	*bab1_1048*
pYOP101	pTRIP6::bab1_1278	pTRIP6	*bab1_1278*
pYOP102	pTRIP6::bab1_1396	pTRIP6	*bab1_1396*
pYOP103	pTRIP6::bab1_1543	pTRIP6	*bab1_1543*
pYOP104	pTRIP6::bab1_1726	pTRIP6	*bab1_1726*
pYOP105	pTRIP6::bab1_1738	pTRIP6	*bab1_1738*
pYOP106	pTRIP6::bab1_1751	pTRIP6	*bab1_1751*
pYOP107	pTRIP6::bab1_1839	pTRIP6	*bab1_1839*
pYOP108	pTRIP6::bab1_2011	pTRIP6	*bab1_2011*
pYOP109	pTRIP6::bab1_2079	pTRIP6	*bab1_2079*
pYOP110	pTRIP6::bab2_0056	pTRIP6	*bab2_0056*
pYOP111	pTRIP6::bab2_0130	pTRIP6	*bab2_0130*
pYOP112	pTRIP6::bab2_0145	pTRIP6	*bab2_0145*
pYOP113	pTRIP6::bab2_0147	pTRIP6	*bab2_0147*
pYOP114	pTRIP6::bab2_0155	pTRIP6	*bab2_0155*
pYOP115	pTRIP6::bab2_0402	pTRIP6	*bab2_0402*
pYOP116	pTRIP6::bab2_0407	pTRIP6	*bab2_0407*

Table 3.6. Lentiviral plasmids containing selected candidate effector proteins constructed for this work (continued).

		Construction [1]	
Plasmid	**Description**	**Vector**	**Insert**
pYOP117	pTRIP6::bab2_0634	pTRIP6	*bab2_0634*
pYOP118	pTRIP6::bab2_0653	pTRIP6	*bab2_0653*
pYOP119	pTRIP6::bab2_0665	pTRIP6	*bab2_0665*
pYOP120	pTRIP6::bab2_0691	pTRIP6	*bab2_0691*
pYOP121	pTRIP6::bab2_1084	pTRIP6	*bab2_1084*
pYOP122	pTRIP6::bab2_1085	pTRIP6	*bab2_1085*
pYOP123	pTRIP6::bab2_1100	pTRIP6	*bab2_1100*
pYOP124	pTRIP6::bab2_1104	pTRIP6	*bab2_1104*
pYOP125	pTRIP6::bab1_0492	pTRIP6	*bab1_0492*
pYOP126	pTRIP6::bab1_0544	pTRIP6	*bab1_0544*
pYOP127	pTRIP6::bab1_0817	pTRIP6	*bab1_0817*
pYOP128	pTRIP6::bab1_1322	pTRIP6	*bab1_1322*
pYOP129	pTRIP6::bab1_1426	pTRIP6	*bab1_1426*
pYOP130	pTRIP6::bab1_1488	pTRIP6	*bab1_1488*
pYOP131	pTRIP6::bab1_2021	pTRIP6	*bab1_2021*
pYOP132	pTRIP6::bab1_1527	pTRIP6	*bab1_1527*
pYOP133	pTRIP6::bab1_0101	pTRIP6	*bab1_0101*
pYOP134	pTRIP6::bab1_0070	pTRIP6	*bab1_0070*
pYOP135	pTRIP6::bab1_0729	pTRIP6	*bab1_0729*
pYOP136	pTRIP6::bab1_0917	pTRIP6	*bab1_0917*
pYOP137	pTRIP6::bab1_2089	pTRIP6	*bab1_2089*
pYOP138	pTRIP6::bab1_0011	pTRIP6	*bab1_0011*
pYOP139	pTRIP6::bab1_0061	pTRIP6	*bab1_0061*

Table 3.6. Lentiviral plasmids containing selected candidate effector proteins constructed for this work (continued).

		Construction (1)	
Plasmid	**Description**	**Vector**	**Insert**
pYOP140	pTRIP6::bab1_0353	pTRIP6	*bab1_0353*
pYOP141	pTRIP6::bab1_0365	pTRIP6	*bab1_0365*
pYOP142	pTRIP6::bab1_0421	pTRIP6	*bab1_0421*
pYOP143	pTRIP6::bab1_0187	pTRIP6	*bab1_0187*
pYOP144	pTRIP6::bab1_0491	pTRIP6	*bab1_0491*
pYOP145	pTRIP6::bab1_1185	pTRIP6	*bab1_1185*
pYOP146	pTRIP6::bab2_0862	pTRIP6	*bab2_0862*
pYOP147	pTRIP6::bab2_0099	pTRIP6	*bab2_0099*
pYOP148	pTRIP6::bab1_0143	pTRIP6	*bab1_0143*
pYOP149	pTRIP6::bab1_0640	pTRIP6	*bab1_0640*
pYOP150	pTRIP6::bab1_1344	pTRIP6	*bab1_1344*
pYOP151	pTRIP6::bab1_0264	pTRIP6	*bab1_0264*
pYOP152	pTRIP6::bab2_0711	pTRIP6	*bab2_0711*
pYOP154	pTRIP6::bab2_0413	pTRIP6	*bab2_0413*
pYOP157	pTRIP6::Gluc	pTRIP6	*Gluc*

Table 3.6. Lentiviral plasmids containing selected candidate effector proteins constructed for this work (continued).

3.3 *B*ioinformatic analysis

To compare protein sequences, the Multiple Sequence Comparison by Log-Expectation (MUSCLE) tool was used (https://www.ebi.ac.uk/Tools/msa/muscle/)

To determine protein signal sequences, LipoP 1.0 Server (http://www.cbs.dtu.dk/services/LipoP/) and SignalP-5.0 server (http://www.cbs.dtu.dk/services/SignalP-5.0/) were used.

For envelope localization, the subCELlular LOcalization predictor (CELLO) was used (http://cello.life.nctu.edu.tw/cgi/main.cgi).

To determine identity and predict putative protein structures, PHYRE^2 server was used (http://www.sbg.bio.ic.ac.uk/phyre2/html/page.cgi?id=index). This program allowed the identification of structural analogues of our proteins of interest.

For prediction of putative *Brucella* T4SS effector proteins Bastion4, T4EffPred and T4SEpre servers were used:

- https://sate.cirad.fr/
- http://bastion4.erc.monash.edu/server.jsp
- http://bioinfo.tmmu.edu.cn/T4EffPred/prediction.html
- https://biocomputer.bio.cuhk.edu.hk/T4DB/T4SEpre.php

For analysis of effector protein candidates Venn diagram was used (http://bioinformatics.psb.ugent.be/webtools/Venn/).

3.4 Molecular Biology Techniques

3.4.1 Standard cloning procedures

DNA extraction and purification

Total DNA from *B. abortus* was extracted using Guanidine Thiocyanate protocol as describe in Sangari and Agüero, 1994.

For plasmid DNA isolation, GeneJET Plasmid Miniprep Kit (Thermo Scientific) was used.

DNA samples from PCR reactions or restriction enzyme digestions were cleaned using GeneJET PCR Purification Kit (Thermo Scientific).

DNA purification from agarose gels was performed using GeneJET Gel Extraction Kit (Thermo Scientific).

All kits were used following the manufacturer's recommendations.

DNA concentration was determined using a Nano-Drop Spectrophotometer ND-100 (Thermo Scientific).

PCR amplification

For the amplification of DNA fragments subsequently used for cloning, Phusion High-Fidelity DNA Polymerase (Thermo Scientific) was used. PCR reactions were set up to a final volume of 50 µl. A 2720 Thermal Cycler (Applied Biosystems) thermocycler was used with the following program: 30 seconds of denaturation at 98 ˚C; 25 cycles of amplification, including steps of denaturalization for 10 seconds at 98 ˚C, annealing for 20 seconds at appropriate annealing temperature (depending on the primers) and elongation for 15 seconds/kb to be amplified at 72 ˚C; and a last step of 7 min of final elongation at 72 ˚C.

For colony analysis, Taq polymerase was used. PCR reactions were set up to a final volume of 25 µl. A 2720 Thermal Cycler (Applied Biosystems) thermocycler was used with the following program: 5 min of denaturation at 94 ˚C; 25 cycles of amplification, including steps of denaturalization for 30 seconds at 94 ˚C, annealing for 30 seconds at appropriate annealing temperature (depending on the primers) and elongation for 30 seconds/kb to be amplified at 72 ˚C; and a last step of 7 min of final elongation at 72 ˚C. After completion of the reaction, the samples were maintained at 4 ˚C for short-term or at -20 ˚C for long-term conservation.

After completation of the reactions, samples were maintained at 4 ˚C for short-term or at -20 ˚C for long-term conservation.

Restriction enzyme digestion

FastDigest restriction enzymes were purchased from Thermo Scientific. Reactions were usually performed in 20 µl for 5-30 min at 37 ˚C, following the manufacturer's indications. Enzyme inactivation was carried out during 10 min at 65 or 80 ˚C, as indicated for each enzyme.

DNA dephosphorylation

Dephosphorylation of vector DNA was performed to increase the cloning efficiency by decreasing vector religation. After enzymatic digestion, DNA

samples were supplemented with 1 U of FastAP Thermosensitive Alkaline Phosphatase (Thermo Scientific), in the same reaction buffer, and incubated for 10 min at 37 ˚C. Heat inactivation was performed by incubation at 65˚C during 15 min.

DNA ligation

Insert fragments were obtained either by restriction digestion or PCR amplification with primers incorporating the adequate restriction sites for ligation into the same sites of the vector. A molar ratio of 5:1 (insert/vector) was used. Ligation reaction was performed using 1 U of T4 DNA ligase (Thermo Scientific) with 0.5-10 ng of DNA in a final volume of 20 µl. It was incubated overnight at 22 ˚C. For each ligation, the same reaction without insert DNA was used as negative control, adding water to reach the final volume. The DNA ligase was inactivated by incubation at 65 ˚C during 10 min.

DNA sequencing

DNA sequences of all cloned PCR fragments were determined. Samples were sent to STAB vida DNA Sequencing Service (Caparica, Portugal).

3.4.2 Cloning by Gateway Technology

The gateway Technology is a universal cloning method based on the site-specific recombination properties of bacteriophage lambda (Landy, 1989). To obtain the desired constructs, two recombination reactions were necessary, as explained in Figure 3.1. The desired insert was PCR amplified using specific primers containing the attB region (Table 3.5). Then, these PCR products together with donor vector containing attP sites were used to make the first Gateway reaction, called BP reaction, with the Gateway™ BP Clonase™ II Enzyme mix (Invitrogen™) following manufacturer's recommendations. Briefly, 75 ng of each PCR product were mixed with 150 ng of pDONR223 vector and completed until 8 µl with TE buffer, pH 8.0. Then, 2 µl of BP Clonase™ II Enzyme mix was added, and reactions were incubated at 25 ˚C overnight. Finally, 1 µl of Proteinase K solution was added and incubated at 37 ˚C for 10 min. Thus, entry clones containing attL sites were obtained and checked by sequencing as mentioned before.

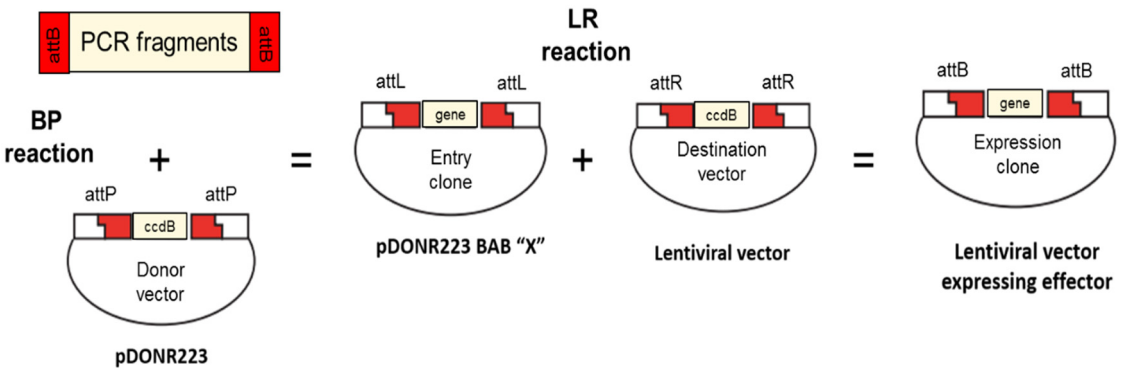

Figure 3.1. Cloning by Gateway Technology. Two reactions are necessary. The BP reaction whereby PCR fragment is interted in a pDONR223 vector and the LR reaction, whereby the gene of interest is transferred from the entry clone to the lentiviral vector, generating a lentiviral vector that contains the gene of interest.

The plasmids constructed in this way were confirmed by restriction analysis, and the DNA sequence of the insert was determined by DNA sequencing.

Then, the second Gateway reaction, called LR reaction, was performed. 75 ng of each entry clone were mixed with 150 ng of pTRIP5-DEST or pTRIP6-DEST, destination vector with attR sites. We used one or the other, depending on the lasers that contain the Flow cytometrer used, but they have the same effectiveness. Plasmid mixes were completed until 8 µl with TE buffer, pH 8.0. Then, 2 µl of LR Clonase™ II Enzyme mix was added, and reactions were incubated at 25 ˚C overnight. Finally, 1 µl of Proteinase K solution was added and incubated at 37 ˚C for 10 min. Thus, expression clones containing attB sites were obtained (Table 3.6).

3.4.3 DNA electrophoresis in agarose gels

DNA was analyzed by agarose gel electrophoresis. Agarose was dissolved in TBE (Tri-HCl 45 mM, boric acid 45 mM, EDTA 0.5 mM, pH 8.2) to a final concentration of 0.8-2 % (w/v), depending on the size of the DNA fragments to be resolved. GreenSage Premium (nzytech) was used as staining solution following manufacturer's recommendations. Loading buffer [bromophenol blue 0.25 % (w/v), sucrose 40 % (w/v) in TBE] was added to DNA samples in a 1:6 ratio. GeneRuler™ 1 kb DNA Ladder (Thermo Scientific) was used as

molecular weight marker. A horizontal BioRad electrophoretic system was used (with constant voltage between 80-120 V). Agarose DNA gels were visualized with a Gel Doc 2000 UV system, and images were analyzed with Quantity One software (BioRad).

3.4.4 Protein overproduction and cellular lysates

E. coli C41 cells harboring pFJS283 plasmid (2 L) were cultivated at 37 ˚C to an OD_{600} of 0.5. Overexpression of BAB1_0466 was induced by addition of 1 mM IPTG and cultured overnight at 37 ˚C with shaking. Then, cells were harvested by centrifugation in an Avanti J-30I centrifuge (Beckman Coulter) using JA-10 rotor at 4 000 rpm for 15 min 4 ˚C and the pellet was stored at -80 ˚C until the purification could be performed.

To lyse the cells, the pellet was thawed in ice and resuspended in 25 ml of lysis buffer (Tris 100 mM pH 7.5, NaCl 500 mM and PMSF 0.001%). Then, cells were lysed by 3 cycles of sonication (1 min at 80% of energy and 1 min of break to avoid sample overheating). The lysates were ultracentifuged at 40 000 rpm for 15 min at 4 ˚C in a Sorvall WX Ultra Series Centrifuge (Thermo Scientific) with T-865 rotor.

To confirm the overexpression, a sample was taken before and after induction of both the supernatant and the pellet obtained after ultracentrifugation. These samples were observed by protein electrophoresis in denaturant conditions.

Purification of BAB1_0102, SagA and VirB1 were carried out with essentially the same protocol, with the following modifications. *bab1_0102* was overexpressed using 0.5 mM IPTG at 37 ˚C for 10 h, while *sagA* was overexpressed using 1 mM IPTG at 37 ˚C for 4 h. *virB1* overexpression and lysis was induced as described by Zahrl et al. (2005): 0.3 mM IPTG at 30 ˚C for 1.5 h.

3.4.5 Protein electrophoresis

SDS-polyacrylamide gels (acrylamide:bisacrylamide 37.5:1) were used for the visualization of proteins. The concentration of polyacrylamide used for

detection was 10-15 % depending on the size of the proteins of interest. Electrophoresis was carried out using a Mini-PROTEAN II system (BioRad) in 6.1 cm x 0.75 mm gels. Samples were mixed with 2X loading buffer [Tris-HCl 50 mM pH 6.8, SDS 2 % (w/v), glycerol 10 % (v/v), bromophenol blue 0.1 % (w/v), β-mercaptoethanol 100 mM]. Samples were then incubated at 95 ºC for 5 min before loading the gel. Precision Plus Protein Dual Color Standards (BioRad) or PageRuler™ Plus Prestained Protein Ladder (Thermo Scientific) were used as molecular weight markers. The electrophoresis was performed at 180 V for 1 h in 1X SDS-PAGE buffer [Tris 25 mM, glycine 192 mM, SDS 1 % (w/v), pH 8.4]. After the run, gels were stained by incubation in staining solution [Coomassie blue R250 0.1 % (w/v), methanol 40% (v/v), glacial acetic acid 10% (v/v)] for 30 min at room temperature. Destaining was performed by incubation in destain solution [methanol: glacial acetic acid: MiliQ® wáter 1:1:8 (v/v/v)] at room temperature.

3.4.6 Protein purification

For protein purification from cell lysates, different affinity columns were used:

- Interaction with nickel: a nickel resin column, called HisTrap HP (GE Healthcare), of 1 ml bed volume was used for purification of proteins tagged with 6 histidine residues. Columns were equilibrated and washed with buffer A (Tris 100 mM pH 7.5, NaCl 500 mM, PMSF 0.001% and Imidazol 20 mM), while Imidazol concentration in buffer B (used for elution) was 500 mM.
- Interaction with amylose: an amylose resin column, called MBPTrap HP (GE Healthcare), of 1 ml bed volume was used for purification of proteins tagged with maltose binding proteins (MBP). In this case, buffer A contained Tris 100 mM pH 7.5, NaCl 200 mM, PMSF 0.001%, while buffer B also contained maltose 10 mM.

A peristaltic pump, called minipuls 3 (Gilson), was used to load proteins in the column, using the flow rate determined by the manufacturer for each case. The column was first washed with 5 ml of filtered Mili-Q® water, and then, it was

balanced with 5 ml of buffer A. Then, samples were loaded and the flow through was collected. The column was washed with 5 ml of buffer A before connect to a Fast Protein Liquid Chromatography (FPLC) type ÄKTA (GE Healthcare). Using this system, protein was eluted by a buffer B gradient using the next program: initial wash with 1 ml of buffer A, 0 to 100% gradient of buffer B in 15 fractions, wash with 5 ml of buffer B, and a final wash with 5 ml of buffer A.

All buffers were filtered using a bottle top vacuum filtration system, 0.22 µm (VWR) to remove suspension particles that could damage the column matrix.

Fractions were analyzed by protein electrophoresis. Those containing the purified protein were pooled and stored in each elution buffer at 4 ˚C.

3.4.7 Determination of protein concentration

Total protein concentration was determined with Nano-Drop Spectrophotometer ND-100 (Thermo Scientific) measuring absorbance at 280 nm. In purified protein samples, the protein extinction coefficient of each protein was used to determine the concentration with more accuracy.

3.4.8 Lysozyme activity assay

The activity of purified proteins as lysozyme inhibitors was tested by a turbidimetric method (Ibrahim et al., 1996). The assay relies on the decrease in turbidity of a *Micrococcus lysodeikticus* suspension in 50 mM potassium phosphate buffer. Suspensions of lyophilized cells in a hypotonic buffer are lysed by the addition of lysozyme to the medium, changing the absorbance of the suspension according to the activity of the enzyme. Briefly, solutions of Hen Egg-White Lysozyme, HEWL (Sigma: L6876) and Human Lysozyme, HL (Sigma: L1667) were used at different concentrations alone or mixed with purified His-tagged fusion proteins BAB1_0102 or BAB1_0466. Then, these solutions were added to 1 ml of *M. lysodeikticus* (Sigma M3770-5G) suspension adjusted to an OD_{600} = 0.7-0.9. The change in absorbance at 600 nm was monitored during 2 h approximately using a spectrometer Ultrospec 10 (Amersham Biosciences).

This assay was also used to determine lysozyme activity of purified VirB1 and SagA proteins tagged with N-terminal MalE and C-terminal 6xHis fusions, respectively.

3.5 Microbiological techniques

3.5.1 Growth conditions and selection media

E. coli

LB Broth (LENNOX) (10 g tryptone, 5 g sodium chloride and 5 g yeast extract) or LB agar (LENNOX) (10 g tryptone, 5 g sodium chloride, 5 g yeast extract and 15 g bacteriological agar) (Conda) were used for bacterial growth for liquid culture or solid culture, respectively. Cultures were incubated at 37 ˚C, with shaking at 120 rpm in the case of liquid growth.

Selective media included antibiotics at the following concentrations: ampicillin (Ap), 100 µg/ml; chloramphenicol (Cm), 50 µg/ml; kanamycin monosulphate (Km), 25 µg/ml; nalidixic acid (Nx), 20 µg/ml and spectinomycin (Sp), 100 µg/ml. For the growth of *E. coli* β2163, which is auxotrophic for diaminopimelic acid (DAP), 0.3 mM DAP was added to both liquid and solid cultures.

B. abortus

Trypticase soy broth (TSB: 15 g pancreatic digest of casein, 5 g papaic digest of soya bean and 5 g sodium chloride) or Trypticase soy agar (TSA: 15 g pancreatic digest of casein, 5 g papaic digest of soya bean, 5 g sodium chloride and 15 g bacteriological agar) (Conda) were used for bacterial growth for liquid culture or solid culture, respectively. *B. abortus* cultures were grown at 37 ˚C under a 5% CO2 atmosphere.

All the bacterial strains were stored in 10 % Skimmed Milk at both -20 ˚C and -80 ˚C. Usually, 10 ml of liquid early stationary phase cultures were centrifuged and resuspended in 10 % Skimmed Milk. Skimmed Milk was prepared by resuspending 10 g of Skimmed Milk Powder in a total volume of 100 ml of

MiliQ® water and autoclaved during only 5 min to avoid caramelization of the milk. Batches of 10 ml of 10 % Skimmed Milk were kept at -20 ˚C until needed.

All experiments with live *B. abortus* were performed in a Biosafety Level3 facility at Institute of Biomedicine and Biotechnology of Cantabria (IBBTEC).

3.5.2 Bacterial transformation

Electroporation

E. coli strains were usually transformed by electroporation.

Transformation efficiency is a linear function of the DNA concentration and cell concentration (Dower et al., 1988). For preparation of electrocompetent cells, bacteria were grown in 250 or 500 ml of LB broth to OD600= 0.5-0.6, and kept in ice for 10 min. The cells were then concentrated by centrifugation at 4 000 rpm and 4 ˚C, and the pelleted cells were washed with one volume ice-cold MilliQ® water and centrifuged again as previously mentioned. This step was repeated by using half volume of ice-cold MilliQ® water. Subsequently, the bacterial cells were washed and concentrated with 1/50 volume of ice-cold glycerol 10 %. Finally, cells were resuspended in 1/400 volume of 10 % glycerol and aliquoted in 50 µl samples. Aliquots were frozen on a bath of dry ice and ethanol and kept at -80 ˚C until needed. Aliquots were mixed with <10 ng of DNA in a 0.2 cm electroporation cuvette (Thermo Scientific) and subjected to an electric pulse (2.5 kV/cm, 25 µF and 200 Ω) in MicroPulser TM (BioRad). 1 ml LB was immediately added to the electroporated cells, and the suspension transferred to 10 ml plastic tubes, which were incubated with shaking at 37 ˚C to allow antibiotic-resistance gene expression. After incubation, cells were plated on antibiotic containing media to select for transformants.

Conjugation

Conjugation was the method of choice for the introduction of plasmids in *B. abortus*. With this technique, we avoid electroporation of *B. abortus*, and the aerosols generated during the process. This method requires a donor bacterium that provides mobilization functions, a plasmid containing an appropriate origin of transfer (*oriT*), and a counterselection marker to eliminate the donor cells.

Donor cell cultures, generally the *E. coli* β2163 strain, which contains the mobilizable functions of plasmid RP4 and is auxotroph for DAP, carrying the plasmid of interet, were grown overnight at 37 ˚C in LB 0.3 mM DAP with shaking in the presence of the appropriate antibiotics for their selection. Additionally, receptor *B. abortus* cells were grown as previously was described. Equal volumes of donor and recipient cells were mixed and washed twice by centrifugation and resuspension in 1 ml TSB to remove antibiotics. After the second centrifugation step, the cell mixture was resuspended in 20 µl of TSB and placed over 0.22 µm pore size cellulose acetate filter of 25 mm of diameter (Sartorius Stedim). This filter was laid over TSA plates pre-incubated at the mating temperature. The plate was incubated for 1.5 h at 37 ˚C. The filters were then removed and introduced in a tube with 1 ml of TSB, and cells were resuspended by vortexing. Serial dilutions of this mixture were plated in TSA with the appropriate antibiotic, but without DAP, to counterselect the donor cells. In this way, only *B. abortus* cells that had incorporated the plasmid could grow.

3.5.3 Mutant constructions

mapB mutants were generated using the same PCR primers described by Bialer et al., (2019), but changing the restriction enzyme recognition sites (Table 3.4). These primers were used to amplify the flanking regions of *mapB* (*bab1_0046*). The central primers contain overlapping regions, and this allows the fusion of both fragments by means of a second PCR reaction that uses only the external primers. Primers mapB_F1_XbaI and mapB_R1 amplify a region of 335 bp upstream *mapB*, and primers mapB_F2 and mapB_R2_SacI a region of 401 bp downstream *mapB*. The resulting PCR fragments were purified and subjected to the second PCR reaction using mapB_F1_XbaI and mapB_R2_SacI. After digestion with the corresponding restriction enzymes, the resulting fragment was ligated to the pDS132 mobilizable suicide vector, previously digested with the same restriction enzymes, obtaining pDS132::Δ*map*. This plasmid was transformed into *E. coli* β2163 and then conjugated with *B. abortus* 2308 wild type, *Δ0466* or *Δ0466Δ0102* mutant strains. The first crossover was selected growing the conjugation mix in TSA plates supplemented with chloramphenicol because those bacteria that have integrated the plasmid are

Cm^R. This intermediate was then resolved by the induction of the second crossover. Positive colonies for the first crossover (Cm^R) were grown on TSA supplemented with sucrose, which counterselects those bacteria expressing *sacB*. Bacteria able to grow on these plates should be chloramphenicol sensitive, because of the loss of the chloramphenicol resistance gene together with the *sacB* gene. As a result of this second crossover, the *B. abortus* 2308 mutant with the correspondent deletion of the *mapB* gene should be obtained. This deletion was confirmed by PCR. The mutants obtained were named *B. abortus* 2308 *ΔmapB, Δ0466ΔmapB* and *Δ0466ΔmapBΔ0102*.

3.5.4 Lysozyme treatment assays

B. abortus 2308 wild type, *Δ0466* and *Δ0466* complemented with BAB1_0466 ($1x10^6$ bacteria) were suspended in 1 ml TSB and incubated for 3 h at 37 ˚C in the presence of lysozyme (1 mg/ml) or MiliQ® water (control: 0 mg/ml lysozyme). Bacterial suspensions were plated in tryptic soy agar (TSA) for determination of CFUs.

We also used the same strains to determine whether sensitivity to lysozyme increases when bacteria are grown with lysozyme (1 mg/ml) and glycine (0.3 M). For that, bacterial suspensions at an OD_{600} of 0.8 were mixed with glycine alone or with glycine and lysozyme in TSB. Then, OD was measured at different times for 3 or 4 h.

B. abortus 2308 wild type, *ΔmapB*, *ΔmapBΔ0466*, *ΔmapBΔ0466* complemented with BAB1_0466 and *ΔmapBΔ0466Δ0102* were suspended at an OD_{600} of 0.8-0.9 in buffer 50 mM Tris-HCl pH 8.0 and mixed with 2 or 20 µg/ml lysozyme at RT. The OD of the suspension was measured at different times for 90 min.

3.6 Cellular biology techniques

3.6.1 Cell culture and maintenance

The cell lines used in this work are listed in Table 3.7.

Most cell lines were grown in either DMEM or RPMI-1640 (LONZA) supplemented with 10 % fetal bovine serum (FBS) (LONZA). HL-60 cells were also maintained with 100 units of penicillin and 100 µg/ml of streptomycin. Huh 7.5 and HEK293T cells were cultivated with 1xNEAA (Gibco™).

All cell lines were grown at 37 ˚C in a humidified 5 % CO_2 atmosphere and splitted every 2-3 days. In the case of HL-60 cells, they were always maintained at a density between $1x10^5$- $1x10^6$ cells/ml, while THP-1 cells were maintained between $2x10^5$- $1x10^6$ cells/ml.

Cell line	Description	Culture medium	Origin/Reference
HEK293T	Human embryonic kidney (SV40 T antigen constitutive expression)	DMEM 10% FBS	Laboratory collection (Graham et al., 1977)
HL-60	Human promyelocytic leukemia cells	RPMI 10% FBS	José Yuste (Collins et al., 1977)
HL-60	Human promyelocytic leukemia cells	RPMI 10% FBS	Javier León (Collins et al., 1977)
Huh 7.5	Human hepatoma cell line	DMEM 10% FBS 1xNEAA	Javier Gastaminza (Blight et al., 2002)
J774	Murine macrophages	DMEM 10% FBS	ATTC (Ralph et al., 1975)
THP-1	Human monocytes	RPMI 10% FBS	Javier León (Tsuchiya et al., 1980)

Table 3.7. Cell lines used in this work.

Viability of the cell lines was routinely assessed by trypan blue exclusion, which is based on the principle that live cells possess intact cell membranes that exclude certain dyes, such as trypan blue, whereas dead cells do not. Briefly,

50 µl of a 1:1 dilution of the cell suspension was made with a 0.4% Trypan Blue solution. After careful mixing, a sample was applied to a hemocytometer chamber, and total cell number and viability were recorded, according to the manufacturer's instructions.

3.6.2 Neutrophil purification

Neutrophils were purified from heparinized blood obtained from healthy volunteers, using the EasySep™ Direct Human Neutrophil Isolation Kit (StemCell technologies) following manufacturer's recommendations. Briefly, 15 ml of venous blood was drawn and mixed with EDTA to a final concentration of 1 mM. Next, 750 µl of a proprietary mixture of antibodies that binds to all the blood cellular types except neutrophils, and 750 µl of magnetic spheres was added to remove the antibodies bound to the different cells. After 5 min of incubation, 30 ml of PBS containing 1 mM EDTA was added. The sample was mixed and incubated into the magnetized support. The enriched cell suspension was collected. The process was repeated adding only the magnetic spheres. At the end of the protocol, a concentrated population of neutrophils was obtained. The purity of the neutrophils was > 95% as determined by flow cytometry using Pacific Blue™ anti-human CD66b (BioLegend) and PE anti-human CD16 (BioLegend), and viability was >90% as determined by the trypan blue exclusion test.

3.6.3 HL-60 and THP-1 cells differentiation

HL-60 cells were differentiated into granulocyte-like cells by incubating $1x10^5$ cells/ml with 1µM all-trans retinoic acid (ATRA) or with 70 mM N,N-dimethylformamide (DMF) for 5 days (Manda□Handzlik et al., 2018). Cell differentiation was initially assessed by evaluating CD11b and CD15 expression using MACSQuant® VYB Flow Cytometer, and data were analyzed with MACSQuantify software (MACS Miltenyi Biotec). However, a more exhaustive analysis was also carried out by the Flow Cytometry facilities of the Instituto de Investigación Sanitaria Valdecilla (IDIVAL). Differentiation to granulocytes was also assessed morphologically by May-Grünwald-Giemsa staining and observation under the microscope. After differentiation, viability of the cells was determined using trypan blue.

THP-1 cells were differentiated into macrophage-like cells by the use of 12-O-tetra-decanoylphorbol-13-acetate (TPA) as previously described (Tsuchiya et al., 1982). Briefly, 3.5 x10^5 THP-1 cells were seeded per well in 24-well plates and cultured for 24 h in complete RPMI containing 50 ng/ml TPA. After differentiation, non-differentiated cells corresponding to suspended cells were removed just by changing the medium.

3.6.4 Infection of mammalian cells with *B. abortus*

Infection of whole blood

Human whole blood infections were made as previously described with some modifications (Mora-Cartín et al., 2016). Briefly, aliquots of 350 µl of fresh human heparinized blood were mixed with 550 µl of PBS supplemented with 0.2 mM $CaCl_2$, 5 mM $MgCl_2$ and 10% of human serum (supplemented PBS). Then, whole blood cells were infected with approximately 5 x10^7 bacteria under mild agitation at 37 ˚C for 120 min, in triplicate. After incubation, samples were centrifuged at 500 g for 3 min, supernatants were removed, and cells were lysed by adding 1 ml of cold sterile Mili-Q® water. Lysates were serially diluted and plated in TSA for determination of CFUs.

For this experiment at least 3 independent donors were used.

Infection of murine macrophages

24 h before infection, confluent monolayers of J774 murine macrophages were trypsinized and 1.5 x 10^5 cells/well were seeded in 24-well plates. Just before infection, the medium was changed to DMEM without FBS, and macrophages were infected at a MOI of 100 with the different *B. abortus* strains, in triplicate wells. Plates were centrifuged for 5 min at RT at 200 x g to sincronize infection, and then incubated for 20 min at 37 ˚C. Wells were then washed 3 times with sterile PBS (time=0), and incubated in DMEM with 10 % FBS and 80 µg/ml gentamicin for 1 h to kill extracellular bacteria. Afterwards, the medium was changed to DMEM with 10 % FBS and 10 µg/ml gentamicin until completion of the experiment. The number of intracellular viable bacteria was determined at different time points post-infection. In each time point, cells were washed twice

with sterile PBS and treated for 15 min at 4 ˚C with 1 ml of cold sterile Mili-Q® water. Lysates were serially diluted and plated in TSA for determination of CFUs.

Infection of differentiated HL-60, purified neutrophils and THP-1 cells

Differentiated HL-60, purified neutrophils and THP-1 cells were infected as previously described (Barquero-Calvo et al., 2007). Briefly, 10^6 cells were diluted in 0.5ml PBS supplemented with 0.2 mM $CaCl_2$, 5 mM $MgCl_2$ and 10% of human serum. The cells were then infected with *B. abortus* strains at a MOI ranging from 5 to 50, in triplicate if enough cells were obtained, or at least in duplicate. The mixture was then incubated for 20 min at 37 ˚C under mild rotation. After this time, cells were centrifuged at 500 x g to remove non-ingested bacteria, that remained in the supernatant (time = 0). In order to kill the remaining extracellular bacteria, infected cells were suspended in 0.5 ml of supplemented PBS in the presence of 10 µg/ml of gentamicin for 30 min at RT. Cells were centrifuged at 500 x g for 5 min and the pellets were resuspended in 0.5 ml of supplemented PBS without gentamicin and incubated during 45 or 90 min at 37 ˚C under mild rotation. After these time points, cells were again centrifuged at 500 x g for 5 min at RT and the cell pellets were lysed with 1 ml of cold sterile Mili-Q® water for 15 min at 4 ˚C. To determine the number of surviving bacteria serial dilutions were plated in TSA plates.

For experiments using purified neutrophils at least 3 independent donors were used.

Infection of differentiated THP-1 cells

After differentiation into macrophage-like cells, THP-1 cells were infected with *B. abortus* strains in triplicate at MOI of 200 in RPMI medium without FBS and antibiotics. Inferction was synchronized by centrifugation at 200 x g for 5 min in RT and then incubated for 20 min at 37 ˚C. After infection (time=0) wells were washed twice with sterile PBS and incubated in RPMI with 10% FBS and 80 µg/ml gentamicin for 30 min to kill extracellular bacteria. At this time, medium was changed to RPMI with 10 % FBS and cells were incubated for 90 min. After that, cells were washed once with sterile PBS and treated for 15 min at 4 ˚C with 1 ml

of cold sterile Mili-Q® water. Lysates were serially diluted and plated in TSA for determination of CFUs.

3.6.5 Flow cytometry analysis

Flow cytometry was used to determine the percentage of viral replication during viral interference assay, as well as to determine hematopoietic populations during HL-60 differentiation or neutrophil purification.

For the Viral Interference Assay, after fixing the infected cells, they were analyzed using a MACSQuant® VYB Flow cytometer (Miltenyi Biotec) using the channels: FSC, SSC, Y2 and B1.

To quantitate the results, firstly the viable cell population was delimited. A window was established in a FSC x SSC graph excluding the clumped and dead cells. Next, the cell population containing lentivirus was determined by selecting the cells that express red fluorescence, corresponding with the expression of m-Cherry or iRFP670 proteins (lentivirus region). Once this population was selected, 10,000 cells were analyzed. When there were not enough cells, 100 µl sample were analyzed. The percentage of cells expressing green fluorescence (encoded in the Flaviviridae genome) inside lentivirus region was determined (yellow population in Figure 4.3). The percentage of cells in the co-infection region is taken as the percentage of replication of each Flaviviridae in the presence of each putative effector protein.

For hematopoietic cell determination the same flow cytometer was used but using the FSC, SSC, Y1, V1 and B1 channels. In this case 10^6 cells were resuspended in 100 µl of PBS and 0.5-5 µl of antibody were used depending on the manufacturer's recommendations for each antibody used (table 3.8).

HL-60 cells were also analyzed in the Flow Cytometry service of IDIVAL, following their standard protocols, to compare with out results.

3.6.6 LDH cytotoxicity assay

Cytotoxicity caused by the expression of the bacterial effector proteins on Huh 7.5 cells was determined using Pierce™ LDH cytotoxicity assay kit (Thermo

Scientific™). Lactate dehydrogenase (LDH) is a cytosolic enzyme that is release to the extracellular medium when the cellular membrane is damaged. The amount of LDH can be measured, because this enzyme catalyzes the conversion of lactate to pyruvate via NAD^+ reduction to NADH. Then, diaphorase use NADH to reduce a tetrazolium salt (INT) to a red formazan product that can be measured at 490 nm. In this way, the level of formazan formation is directly proportional to the amount of LDH released into the medium, which is indicative of cytotoxicity (Decker and Lohmann-Matthes, 1988). Briefly, Huh 7.5 cells at 50 % of confluency were transduced with lentiviral particles expressing *B. abortus* putative effector proteins or g*luc* as a control. After six hours of incubation, $1x10^3$ cells were seeded per well in 96-well plates, and effector genes expression was induced with 3 µg/ml doxycycline. Three wells per effector protein and day were seeded. Cytotoxicity was measured by assaying LDH activity in the supernatant as indicated by the manufacturer's instructions, from day 1 post-transduction to day 6 post-transduction.

Antibody	Immunogen	Type	Origin (reference)
FITC anti-mouse/human CD11b	C57BL/10 splenocytes	Monoclonal	BioLegend ® (101205)
Pacific Blue™ anti-human CD66b	-	Monoclonal	BioLegend ® (305111)
PE anti-human CD16	Human PMN cells	Monoclonal	BioLegend ® (302007)
Anti-human CD15 (MCS-1)	White blood cells	Monoclonal	Immunostep (15CFB-100T)

Table 3.8. Antibodies used for characterization of hematopoietic cells.

3.6.7 Fluorescence microscopy

Fluorescence microscopy was used to visualize bacterial infection using red fluorescence bacteria, to monitor virus transfection and infection, as well as

to check the correct induction of effector proteins. A Nikon Eclipse Ti microscopy was used for these purposes. We used the following filters (excitation and emission spectra): 450-490 nm and 520 nm for GFP, Venus and Ypet positive cells and 510-560 nm and 590 nm for DsRed.

Confocal fluorescence microscopy was used to check bacterial phagocytosis by HL-60 cells and human neutrophils. Infected cells with bacteria expressing DsRed were fixed with ice-cold 100% methanol and then mounted using Duolink® mounting medium (Sigma). For visualization, a Leica TCS SPE upright spectral confocal microscope was used. Lasers of 405 nm and 532 nm were used to visuzlize DAPI and DsRed fluorescence, respectively. Also, 15-25 Z-stages were taken depending on the sample. All images were analyzed by ImageJ image processing program.

3.7 Production of viral particles and Viral Interference Assay

3.7.1 YFV and HCV *in vitro* transcription

YF17D (5'C25Venus2AUbi) is a monocistronic Yellow Fever reporter virus (kindly provided by Charles M. Rice, The Rockefeller University) encoding the Venus fluorescent protein. *In vitro* transcripts were generated as described in Lindenbach and Rice (1997). Briefly, 20 µg of plasmid DNA were linearized with *Xho*I (Thermo Scientific) and purified using a GeneJET PCR Purification kit (Thermo Scientific). Then, RNA was transcribed from 1 µg of the purified template by using mMESSAGE mMACHINE™ SP6 Transcription kit (Invitrogen) following manufacturer's recommendations and supplementing the reaction with 1 µl of GTP 20 mM, as YF17D transcripts are longer (around 12 Kb) than the size recommended in the kit. Reaction mixtures were incubated at 37 ˚C for 2 h, followed by a 15 min digestion with 2 U of TURBO DNase (Invitrogen). RNA was purified by using a Speedtools total RNA extraction kit (Biotools) following manufacturer's recommendations. RNA was quantified by absorbance at 260 nm, diluted to 100 ng/µl and stored at -80 ˚C.

Jc1-5AB-2xYPet is a monocistronic Jc1 HCV genome (kindly provided by Charles M. Rice, The Rockefeller University) encoding two Venus-YFP (Ypet)

proteins. *In vitro* transcripts were generated as previously described with some modifications (Lindenbach et al., 2005). Briefly, 30 µg of plasmid DNA were linearized with *Xba*I (Thermo Scientific) and purified using a GeneJET PCR Purification kit (Thermo Scientific). Then, linearized DNA was treated with 0.5 U/µg of Mung Bean Nuclease (New England Biolabs) at 22 ˚C for 15 min and purified again with GeneJET PCR Purification kit (Thermo Scientific). RNA was transcribed from 1 µg of the purified template by using MEGAscript T7 Transcription kit (Invitrogen) following manufacturer's recommendations. RNA purification, quantification and storage were as for the YFV samples.

3.7.2 Flaviviridae and lentivirus production

Infective particles of Flaviviridae viruses or lentivirus were generated using the following transfection reagents and protocols:

Lentivirus expressing IRFP670

TransIT-LT1 Transfection Reagent (Mirusbio) was used for transfection of HEK293T cells to obtain lentiviral particles expressing IRFP670 fluorescent protein. The day before transfection, cells were seeded at 60 % of confluence in 100 mm TC-treated cell culture dishes, (VWR, 734-2321). Approximately 1 h before transfection, the cell culture medium was changed to DMEM plus 2 % FBS because higher concentrations of serum difficult the transfection process. During this incubation time, the DNA mixes necessary for lentiviral particle production were prepared. Each DNA mix contains three different plasmids: (i) 1,250 ng of pCMV-VSV-G, the envelope plasmid encoding the *vsv-g* gene; (ii) 5,600 ng of psPAX2, the packaging plasmid encoding the HIV *gas*, *pol*, *rev* and *tat* genes; and (iii) 6,200 ng of the lentiviral vector containing putative *B. abortus* effector proteins to be assayed. Each DNA mix was diluted in 1.4 ml of Opti-MEM medium (Invitrogen), vortexed and incubated for 5 min at RT. Then, 50 µl of TransIT-LT1 Transfection Reagent tempered at RT was added to the DNA solution, mixed by flicking the tube without vortexing and incubated for 20 min at RT. After this time, the mixture was added in a dropwise manner to the plate. The supernatants were collected at 48 and 72 h after transfection. They were centrifuged for 10 min at 1000 xg and filtered through 0.22 µm pore size sterile syringe filters (Merk

Millipore). Next, 8 µg/ml of polybrene ® (Merk millipore) was added. Polybrene ® neutralizes charge repulsion between virions and sialic acid on cell surface and improves lentiviral infection. Finally, aliquots of 1 ml were prepared and kept at -80 ˚C until their use.

Lentivirus expressing m-Cherry

PEI reagent (1 µg/µl pH: 7, Polysciences, Inc.) was used for transfection of HEK293T cells to obtain lentiviral particles expressing m-Cherry fluorescent protein. The day before transfection, cells were seeded at 40-60 % of confluence in TC-treated 100 mm cell culture dishes (VWR-734-2321). 1 h before transfection, the cell culture medium was also changed to DMEM plus 2 % FBS. During this incubation time, DNA mixes were prepared as above. After the incubation step of 5 min at RT in Opti-MEM medium (Invitrogen), 35 µg PEI were added to the DNA dilution, mixed by vortexing again and incubated for at least 20 min at RT. The mixture was then added in a dropwise manner to the plate. Supernatant was collected at 48 and 72 h after transfection, and centrifuged, filtered, and stored as describe above.

Flaviviridae

Lipofectamine™ 3000 Reagent (Invitrogen) was used for transfection of Huh 7.5 cells to obtain infective YFV or HCV viral particles. The day before transfection, cells were seeded to have at 70-90 % of confluence at the time of transfection in six-well plates. One day later cells were transfected by mixing 125 µl Opti-MEM medium (Invitrogen) with 5 µl Lipofectamine 3000 reagent in one tube, and 125 µl Opti-MEM medium, 5 µl P3000 reagent and 3 µg YFV RNA or HCV RNA in a different tube. Both tubes were then mixed and incubated for 20 min at RT. After the incubation time, the mix was added to the cells that were incubated for 2-3 days, until fluorescence was detected. Then, supernatants were collected, processed as above, and freezed at – 80 ˚C. In the case of YFV infective particles, once they were generated by lipofectamine transfection, supernatants were used to reinfect cell monolayers to amplify the virus. To avoid losing the fluorescence gene the viruses were only used for one amplification round.

3.7.3 Viral Interference Assay

The viral interference assay is based on of the observation of the change of replication of a virus expressing a fluorescent marker, when a putative effector is co-expressed in the same cell. Viral particles expressing fluorescent proteins in the host cell, as well as the collection of lentiviruses encoding the putative effectors, were used to coinfect Huh 7.5 cells. To set up the assay, 60 % confluence Huh 7.5 cells were seeded in 6-well plates, with DMEM 10 % FBS medium, and incubated at 37 ˚C in 5 % CO_2. This way, we obtained cells at an 80 % confluency at the time of transduction, the next day. Culture media was then removed from the plates and 2 ml of media containing lentivirus (coding for either controls or putative effector proteins) were added to the different wells. Plates were centrifuged at 1100 x g at 30 ˚C for 90 min, to facilitate cells and lentiviral particles interaction. At the end of the run, plates were incubated at 37 ˚C in a 5% CO_2 incubator for 5 h. After this step, media was removed and cells were washed with sterile PBS and dissociated using 1 ml of AccuMax (Labclinics) diluted 1:1 with PBS at RT for 10-15 min. Cells were then resuspended with 8 ml of complete DMEM supplemented with 3 µg/ml Doxycycline (ThermoFisher). 1 ml aliquots of infected cells were deposited into 4 separate wells in 12-well plates (making quadruplicates) and cells were incubated at 37 ˚C. After 48 h, the medium was removed and replenished with 1 ml of complete medium containing doxycycline at the same concentration. This process was repeated every two days until the moment of infection with the flaviviruses. In the case of YFV infection, cells were infected at day 6 after transduction with the lentivirus. Virus stocks were diluted 1:3 with DMEM containing 2% FBS and 3 µg/ml of doxycycline and then 1 ml of this dilution was added to each well. Cells were incubated for at least 24 h. In the case of HCV infection, cells were infected after 4 days of transduction with the lentivirus. Virus stocks were diluted 1:3 with DMEM containing 10 % FBS and 3 µg/ml of doxycycline. Then, 1 ml of this dilution was added to each well. In this case infected cells were incubated for at least 72 h. After the infection period, cells were washed with PBS and dissociated as before but using only 300 µl of AccuMax. The resuspended cells were fixed with paraformaldehyde at a final concentration of 1 % to be analysed by flow cytometry (see section 3.6.5).

3.8 Ethics

Human fresh blood samples were collected from healthy volunteer donors. All blood donors involved were informed about the study. Extractions and infection protocols for those samples have been approved by the Research Project Ethics Committee of the University of Cantabria.

3.9 Statistical analysis

Experimental values presented in this work represent the mean ± the standard error of the mean (SEM) or ± standard deviation (SD). A two tailed student's t-test was performed, and significance was determined as a p-value less than 0.05 (*), 0.01 (**) or 0.001 (***).

RESULTS

4. RESULTS

4.1 Search for new *B. abortus* T4SS effector proteins

4.1.1 Construction of a library of putative T4SS effector proteins

Brucella is an intracellular pathogen whose survival during infection depend on the expression of its T4SS. To date, 15 T4SS effector proteins have been identified (Ke et al., 2015). However, as explained in the Introduction, there is some controversy around the identification of these proteins which suggests that there are other T4SS effector proteins not identified until now.

Since it is not viable to analyze all *Brucella* proteins, we decided to reduce the number of candidates using several T4SS effector protein prediction softwares: S4TE (Meyer et al., 2013; Sankarasubramanian et al., 2016), T4SEpre (Wang et al., 2014), Bastion4 (Wang et al., 2017) and T3EffPred (Zou et al., 2013). Table 4.1 shows the number of candidates predicted by each method, and the number of actual T4SS effectors validated experimentally in each case. We also used all candidates identified in previous papers where some effector proteins secreted by *Brucella* T4SS had been described, because maybe using other approach some other effector proteins could be identified. These are listed under “Other methods” in Table 4.1. Candidates in this category were selected on the basis of: i) the presence of a conserved region in the promoter necessary for the activation by VjbR (de Jong et al., 2008); ii) the occurrence of eukaryotic domains, protein-protein interaction domains and proteins with domains known to be related to virulence (Marchesini et al., 2011); iii) the existence of potential horizontally transmitted regions encoding transposases or recombinases adjacent to transfer tRNAs (Döhmer et al., 2014); or iv) the limited homology in other bacteria genera, the GC content, the presence of eukariotic-like motifs or the existence of features similar to known T4SS effector proteins (Myeni et al., 2013). In total, we have crossed all data obtained generating a list with 256 unique candidates (Table 4.1).

Prediction method	Number of candidates	Number of T4SS effector proteins	Obtained from
S4TE	78	5	Sankarasubramanian et al., 2016
Bastion4	33	7	http://bastion4.erc.monash.edu/server.jsp
T4EffPred	35*	7	http://bioinfo.tmmu.edu.cn/T4EffPred/prediction.html
T4SEpre	53	5	https://biocomputer.bio.cuhk.edu.hk/T4DB/T4SEpre.php
Other methods	144	15	de Jong et al.,2008; Marchesini et al.,2011; Myeni et al.,2013; de Barsy et al.,2011; Döhmer et at.,2014
TOTAL unique candidates	**256**		

Table 4.1. Summary of putative effector proteins secreted by *B. abortus* T4SS.
*not all *Brucella* proteins could be analyzed. The software stopped working.

In this way, we confirmed that there is not any software able to predict all identified T4SS effector proteins of *Brucella*. All effector proteins only appear in the group classified as other methods, because this group includes all candidates studied during the identification of some T4SS effector protein, as mentioned before. Figure 4.1 displays graphically the candidate effectors predicted by each method. Although there are some candidates that are common among some of the different methods, many others do not. There are only two candidates predicted by all methods, that correspond with two known effector proteins secreted by the T4SS (BAB1_1043 and BAB1_1275). With respect to the other 13 known effector proteins, four are included in four groups, other three are included in two groups, and there are six *Brucella* T4SS effector proteins that are only included in Other methods, meaning they are not detected by any recent bioinformatic software. In summary, no predictive method is 100 % effective for *Brucella* T4SS effector proteins, because neither of them can identify all identified effector proteins of *Brucella*.

Since there was not one method more efficient than other, in order to select the most likely candidates for the generation of a library of putative effectors, we decided to prioritize the 256 candidates following several criteria (Table 4.2):

- First, we selected the 15 identified effector proteins secreted by *Brucella* T4SS.
- We added proteins that had been identified as secreted, but not through its T4SS (Marchesini et al., 2011; Myeni et al., 2013).
- Following, the first complete prediction of the complete *Brucella* genome was obtained using S4TE servidor (Sankarasubramanian et al., 2016). Thus, we started to select many putative effector proteins according to this software, including proteins that contain a signal peptide to localize to mitochondria or nucleous, proteins containing eukaryotic domains, as well as several hypothetical proteins and known function proteins predicted by this method.

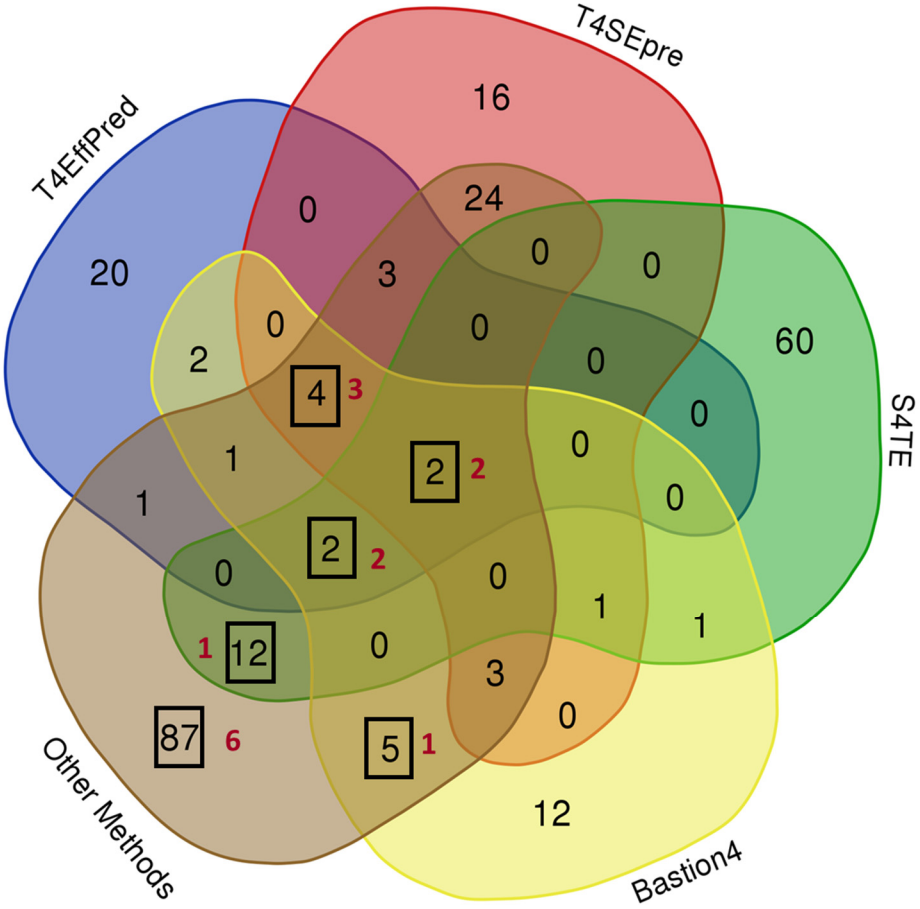

Figure 4.1. Putative *Brucella* T4SS effector proteins predicted by different methods. The number of putative T4SS effector proteins predicted by each method is represented in the corresponding section of the Venn diagram. Numbers boxed indicate those groups where some validated effector protein secreted by *Brucella* T4SS is included. The number of effectors validated experimentally in each group is indicated in red.

- In addition, the putative effector proteins predicted by several methods were selected, especially those predicted by more than 2 methods.
- We also selected putative effector proteins classified as hypothetical proteins.
- Finally, the rest of the proteins that cannot be included in previus criteria were classified as other proteins.

Once we selected our pool of effector proteins candidates, we decided to use the Gateway technology to clone the ORFs. As explained in Experimental Procedures (section 3.4.2), this system is based on a site-specific recombination reaction, which allows for easy re-cloning in different vectors. Altogether, we have cloned the 151 genes listed in Table 4.3 by Gateway technology in the pDONR223 plasmid, as described in Experimental Procedures. In a second step, the inserts were transferred to a lentivial plasmid under the control of the pTet promoter, a strong promoter inducible with doxycycline.

From the selected candidates, one of the known effector proteins (*bab1_1043* gene) was impossible to clone, probably because it was a very big gene, more than 4,000 bp. Also, genes encoding 13 putative effector proteins predicted by several methods have not been cloned until now and can be very good candidates. This is because the list is being updated continuously, so we did not have time to clone them yet. Some of them could be added to this library in the future.

Criteria of selection	Predicted proteins	Cloned genes
Effector proteins secreted by T4SS	15	14
Effector proteins independently secreted by T4SS	7	7
S4TE	73	58
Predicted by several methods	39	26
Hypothetical proteins	74	40
Other proteins	48	6
Total	**256**	**151**

Table 4.2. Putative *Brucella* effector proteins selected by different criteria, and the number of genes cloned in each category.

Gene	size (bp)	Prediction method	Selection criterion
bab1_0011	324	T4EffPred	Hypothetical proteins
bab1_0061	192	T4EffPred	Hypothetical proteins
bab1_0063	188	Bastion4, other methods	Predicted by several methods
bab1_0070	549	Other methods	Hypothetical proteins
bab1_0101	470	Other methods	Hypothetical proteins
bab1_0121	1,880	S4TE	S4TE
bab1_0143	2,804	S4TE	S4TE
bab1_0151	324	Other methods	Hypothetical proteins
bab1_0158	440	T4EffPred, T4SEpre and other methods	Predicted by several methods
bab1_0175	662	S4TE	S4TE
bab1_0187	389	Other methods	Hypothetical proteins
bab1_0227	740	Other methods	Effector proteins independently secreted by T4SS
bab1_0264	480	Bastion4, T4EffPred	Predicted by several methods
bab1_0271	560	T4EffPred, T4SEpre and other methods	Predicted by several methods
bab1_0279	390	Bastion4 and other methods	Effector proteins secreted by T4SS
bab1_0296	389	Other methods	Hypothetical proteins
bab1_0322	1,193	S4TE and other methods	S4TE
bab1_0343	455	T4SEpre and other methods	Predicted by several methods
bab1_0353	234	T4EffPred	Hypothetical proteins
bab1_0365	216	T4EffPred	Hypothetical proteins
bab1_0368	521	Other methods	Other proteins
bab1_0401	1,184	S4TE	S4TE
bab1_0421	234	T4EffPred	Hypothetical proteins
bab1_0445	545	T4SEpre and other methods	Predicted by several methods
bab1_0453	252	Other methods	Hypothetical proteins
bab1_0491	596	Other methods	Hypothetical proteins

Table 4.3. Putative effector protein genes cloned. Gene name, size, prediction method or methods and criterion of selection are indicated.

Gene	size (bp)	Prediction method	Selection criterion
bab1_0492	962	T4SEpre and other methods	Predicted by several methods
bab1_0544	1,178	T4SEpre and other methods	Predicted by several methods
bab1_0608	449	Bastion4 and other methods	Predicted by several methods
bab1_0640	2,351	S4TE	S4TE
bab1_0653	773	S4TE	S4TE
bab1_0663	674	Other methods	Hypothetical proteins
bab1_0678	573	Other methods and S4TE	Effector proteins secreted by T4SS
bab1_0712	564	Other methods	Effector proteins secreted by T4SS
bab1_0729	525	Other methods	Hypothetical proteins
bab1_0740	590	S4TE and other methods	S4TE
bab1_0745	419	Bastion4, other methods, T4EffPred and T4SEpre	Predicted by several methods
bab1_0752	1,307	Bastion4, other methods and T4SEpre	Predicted by several methods
bab1_0756	834	Other methods	Effector proteins secreted by T4SS
bab1_0817	470	T4SEpre and other methods	Predicted by several methods
bab1_0847	414	Other methods	Effector proteins secreted by T4SS
bab1_0891	803	S4TE	S4TE
bab1_0917	1,439	S4TE	S4TE
bab1_0919	503	S4TE	S4TE
bab1_0920	485	T4SEpre and other methods	Predicted by several methods
bab1_0930	2,768	S4TE	S4TE
bab1_0939	266	S4TE and other methods	S4TE
bab1_0946	674	S4TE	S4TE
bab1_0955	1,523	T4SEpre and other methods	Predicted by several methods
bab1_1016	818	S4TE	S4TE
bab1_1035	752	T4EffPred, T4SEpre and other methods	Predicted by several methods
bab1_1048	621	Other methods	Hypothetical proteins

Table 4.3. Putative effector protein genes cloned (continued).

Gene	size (bp)	Prediction method	Selection criterion
bab1_1058	1,257	Bastion4, other methods, T4EffPred and T4SEpre	Effector proteins secreted by T4SS
bab1_1089	899	T4SEpre and other methods	Predicted by several methods
bab1_1099	947	S4TE and other methods	S4TE
bab1_1117	506	S4TE	S4TE
bab1_1118	590	S4TE	S4TE
bab1_1185	422	Other methods	Hypothetical proteins
bab1_1193	1,418	S4TE	S4TE
bab1_1199	806	S4TE	S4TE
bab1_1275	762	Bastion4, other methods, S4TE, T4EffPred and	S4TE
bab1_1278	606	Other methods	Hypothetical proteins
bab1_1279	528	Bastion4, other methods, T4EffPred and T4SEpre	Effector proteins secreted by T4SS
bab1_1322	521	T4SEpre and other methods	Predicted by several methods
bab1_1344	2,537	S4TE	S4TE
bab1_1354	662	S4TE	S4TE
bab1_1374	1,295	S4TE	S4TE
bab1_1386	626	Other methods	Hypothetical proteins
bab1_1396	516	Other methods	Hypothetical proteins
bab1_1426	401	T4SEpre and other methods	Predicted by several methods
bab1_1464	404	Other methods	Other proteins
bab1_1488	1,178	T4SEpre	Other proteins
bab1_1492	573	Other methods	Effector proteins secreted by T4SS
bab1_1501	452	S4TE	S4TE
bab1_1502	1,223	S4TE	S4TE
bab1_1527	986	Other methods	Hypothetical proteins
bab1_1543	321	Other methods	Hypothetical proteins
bab1_1591	1,196	S4TE	S4TE

Table 4.3. Putative effector protein genes cloned (continued).

Gene	size (bp)	Prediction method	Selection criterion
bab1_1611	935	Other methods	Effector proteins independently secreted by T4SS
bab1_1615	392	T4SEpre and other methods	Predicted by several methods
bab1_1640	1,550	S4TE and other methods	S4TE
bab1_1652	318	Bastion4, other methods, T4EffPred and T4SEpre	Effector proteins secreted by T4SS
bab1_1671	795	Other Methods	Effector proteins secreted by T4SS
bab1_1685	1,226	S4TE and other methods	S4TE
bab1_1703	2,009	T4SEpre and other methods	Predicted by several methods
bab1_1705	1,466	S4TE and other methods	S4TE
bab1_1720	1,088	S4TE	S4TE
bab1_1725	1,049	S4TE	S4TE
bab1_1726	1,032	Other methods	Hypothetical proteins
bab1_1730	692	S4TE	S4TE
bab1_1738	273	Other methods	Hypothetical proteins
bab1_1751	192	Other methods	Hypothetical proteins
bab1_1754	179	S4TE and other methods	S4TE
bab1_1773	1,481	S4TE	S4TE
bab1_1828	641	S4TE	S4TE
bab1_1839	358	Other methods	Hypothetical proteins
bab1_1843	254	S4TE	S4TE
bab1_1864	1,439	Other methods	Effector proteins independently secreted by T4SS
bab1_1865	674	Other methods	Effector proteins independently secreted by T4SS
bab1_1866	1,955	Other methods	Other proteins
bab1_1941	791	S4TE	S4TE
bab1_1948	1,287	Other Methods	Effector proteins secreted by T4SS
bab1_1985	2,660	S4TE	S4TE
bab1_2005	462	Bastion4, other methods, S4TE and T4EffPred	Effector proteins secreted by T4SS

Table 4.3. Putative effector protein genes cloned (continued).

Gene	size (bp)	Prediction method	Selection criterion
bab1_2011	460	Other methods	Hypothetical proteins
bab1_2021	1,160	Bastion4, other methods and T4SEpre	Predicted by several methods
bab1_2079	1,000	Bastion4 and other methods	Predicted by several methods
bab1_2089	437	S4TE	S4TE
bab1_2145	722	S4TE	S4TE
bab1_2152	500	S4TE	S4TE
bab1_2164	602	S4TE	S4TE
bab1_2178	1,004	S4TE	S4TE
bab2_0056	1,230	Other methods	Hypothetical proteins
bab2_0074	986	T4SEpre and other methods	Predicted by several methods
bab2_0099	1,718	S4TE	S4TE
bab2_0119	521	Other methods	Effector proteins independently secreted by T4SS
bab2_0123	462	Bastion4, other methods, S4TE and T4EffPred	Effector proteins secreted by T4SS
bab2_0130	590	Other methods	Hypothetical proteins
bab2_0145	1,350	Other methods	Hypothetical proteins
bab2_0147	210	Other methods	Hypothetical proteins
bab2_0155	630	Other methods	Hypothetical proteins
bab2_0159	494	Other methods	Effector proteins independently secreted by T4SS
bab2_0160	416	T4SEpre and other methods	Predicted by several methods
bab2_0203	881	S4TE and other methods	S4TE
bab2_0208	743	S4TE	S4TE
bab2_0246	1,139	S4TE	S4TE
bab2_0252	773	S4TE	S4TE
bab2_0271	887	S4TE and other methods	S4TE
bab2_0402	570	Other methods	Hypothetical proteins
bab2_0407	1,100	Other methods	Hypothetical proteins

Table 4.3. Putative effector protein genes cloned (continued).

Gene	size (bp)	Prediction method	Selection criterion
bab2_0413	2,741	S4TE and Bastion4	S4TE
bab2_0481	866	S4TE	S4TE
bab2_0516	236	S4TE	S4TE
bab2_0541	458	Other methods	Effector proteins independently secreted by T4SS
bab2_0634	530	Other methods	Hypothetical proteins
bab2_0653	570	Other methods	Hypothetical proteins
bab2_0665	700	T4EffPred and other methods	Predicted by several methods
bab2_0681	362	S4TE	S4TE
bab2_0691	620	Other methods	Hypothetical proteins
bab2_0692	1,499	T4SEpre and other methods	Predicted by several methods
bab2_0711	695	Other methods	Other proteins
bab2_0738	2,918	S4TE	S4TE
bab2_0773	944	S4TE	S4TE
bab2_0862	344	Other methods	Other proteins
bab2_0865	914	S4TE	S4TE
bab2_0941	695	S4TE	S4TE
bab2_1021	1,460	S4TE	S4TE
bab2_1084	600	Other methods	Hypothetical proteins
bab2_1085	540	Other methods	Hypothetical proteins
bab2_1100	540	Other methods	Hypothetical proteins
bab2_1104	750	Other methods	Hypothetical proteins

Table 4.3. Putative effector protein genes cloned (continued).

4.1.2 Establishment of a Viral Interference Assay

In order to test if the selected putative effector proteins have any role in *B. abortus* infection, a Viral Interference Assay was designed, as depicted in Figure 4.2. To this purpose, a short stay was carried out in the laboratory of Dr. Brett Lindenbach at Yale University (New Haven, EEUU). This laboratory has set up a system to measure Flaviviridae replication with a fluorescent reporter, which can be used to measure factors interfering with its replication, in a similar way that was made for interferon-stimulated genes (Schoggins et al., 2011). Thus, we adapted this reporter assay to the screening of our library of candidate effector proteins in search for interference with viral replication, as reasoned in Introduction, section 1.2.2.

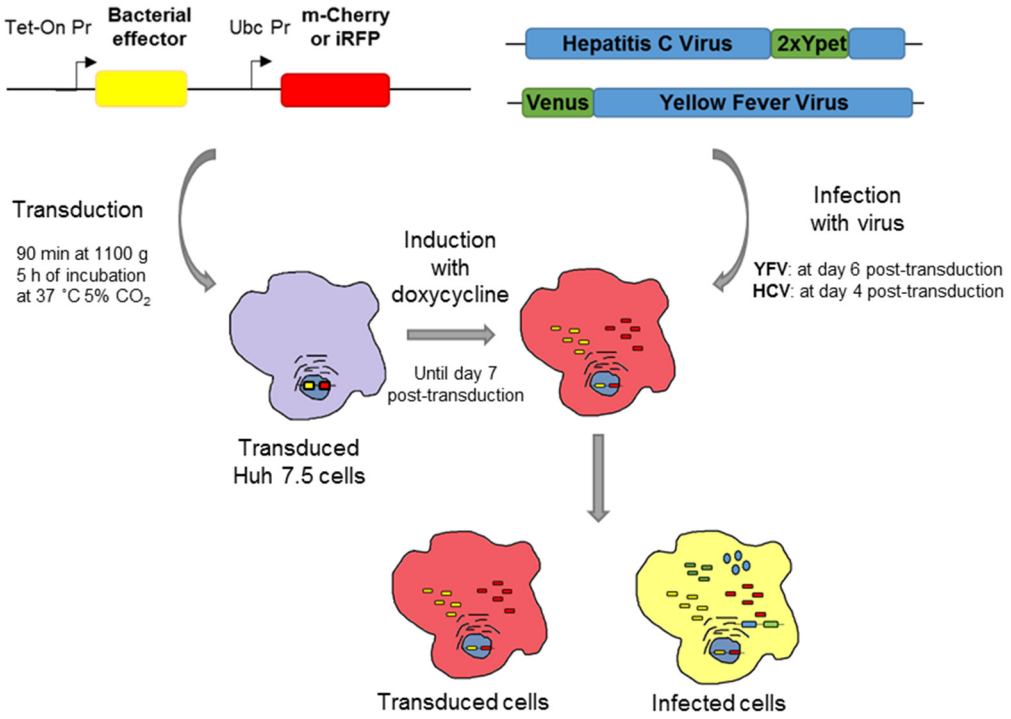

Figure 4.2. Schematic representation of viral interference assay.

The Viral Interference Assay consists in the co-infection of human cells with the Flaviviridae viruses that express a green fluorescence protein, and lentiviral particles that express constitutively a red fluorescence protein plus each putative effector protein under a doxycycline inducible promoter. As depicted in Figure 4.2, first, cells are infected with lentiviral particles and the expression of each putative effector protein is promoted by the addition of doxycycline in the

medium. Thus, these cells express the effector protein and the red fluorescence protein, becoming red cells. Then, four or six days after lentiviral infection these cells are co-infected with the Flaviviridae HCV or YFV, as indicated, which express a green fluorescent protein. These viruses will infect the eukaryotic cells and replicate. The expression of the *Brucella* candidate effector protein may prevent or facilitate the virus replication or have no effect. In this way, depending on the effect that putative effector proteins cause in virus infection and replication, different results can be expected in the flow cytometry analysis, as shown in Figure 4.3.

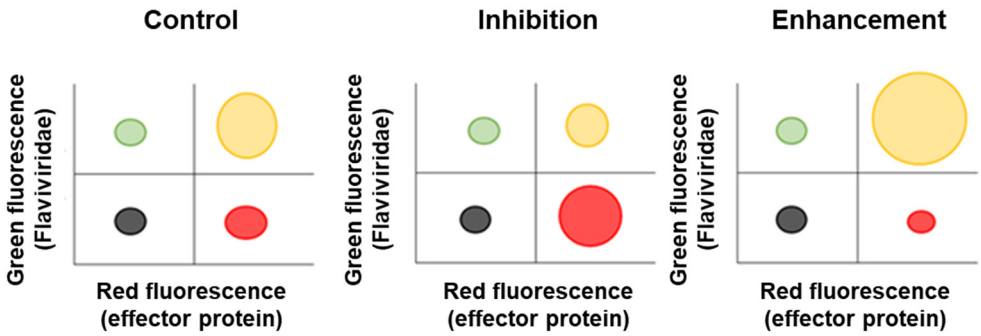

Figure 4.3. Schematic representation of the expected flow cytometry results in the viral interference assay. In the left panel, the standard coinfection population (yellow) can be observed. The middle and right panels represent the expected outcome if the expressed effector has a negative or positive effect on the Flaviviridae replication, respectively, as inferred from the size of the yellow population relative to the total of red cells.

To obtain the lentivirus expressing each putative effector protein, a collection of plasmids was constructed by the gateway technology as detailed in Experimental Procedures section 3.4.2.

In order to set up the assay, in a first step, only the genes for the 14 effector proteins secreted by *Brucella* T4SS and the 7 effector proteins secreted independently from *Brucella* T4SS were assayed. The corresponding genes were transferred from pDONR223 vector to pTRIP5-DEST vector by Gateway technology. As controls, lentiviral plasmids encoding Gluc, IRF1 and GFP were used. The controls used in this assay have been previously reported in a similar assay (Schoggins et al., 2011). Briefly, a plasmid containing a luciferase gene from *Gaussia princeps* (*gluc*) was used as a negative control. The expression of

the luciferase gene does not produce any effect during Flaviviridae infection. Also, a plasmid containing the interferon regulatory factor 1 gene (*irf1*) was used as positive inhibition control. And finally, a plasmid expressing GFP protein with the same inducible promoter that the putative effector proteins and the controls was used as induction control.

The generated lentiviral plasmids, including the corresponding control plasmids, were transfected to HEK293T cells using auxiliary plasmids necessary for the obtaining of the lentiviral particles (see Experimental Procedures section 3.7.2). Supernatants containing these lentiviral particles were used to transduce Huh 7.5 cells. After 6 h of incubation, each well containing transduced cells was divided into four wells per virus and treated with doxycycline to induce the expression of genes that codify for *Brucella* proteins and control proteins. Then, four and six days post-transduction, these cells were co-infected with HCV and YFV, respectively. After the time necessary for each virus life cycle, 3 days for HCV and 1 day for YFV, cells were analyzed by flow cytometry, and the results were converted to % viral replication as explained in Experimental Procedures section 3.6.5.

The results for the YFV interference assay are shown in Figure 4.4. Several effector proteins significantly decrease the replication of YFV. Especially, there were two effector proteins secreted by *Brucella* T4SS, BAB1_0279 (BtpA) and BAB1_0756 (BtpB), that dramatically decrease the replication of YFV, even below the level of replication observed with the inhibition control IRF1.

We suspected that these two proteins induce a high cytotoxicity, since a third population can be seen in the flow cytometry analysis, which is absent in the Gluc control (see Figure 4.5.A). If we remove this population, the decrement of the YFV replication is not so pronounced, but it is still evident (Figure 4.5.A). To confirm this cytotoxicity, we performed a LDH release assay. This assay is based in the release of LDH by the cells upon membrane damage, since LDH is a cytosolic enzyme. Huh 7.5 cells were transduced with lentivirus containing *B. abortus* effector genes and *gluc* control gene, and their cytotoxicity was measured in the presence of doxycycline, that induces the expression of these genes. This assay confirms the high cytotoxicity of BAB1_0279 and BAB1_0756 *B. abortus* proteins previously observed by flow cytometry (Figure 4.5.B).

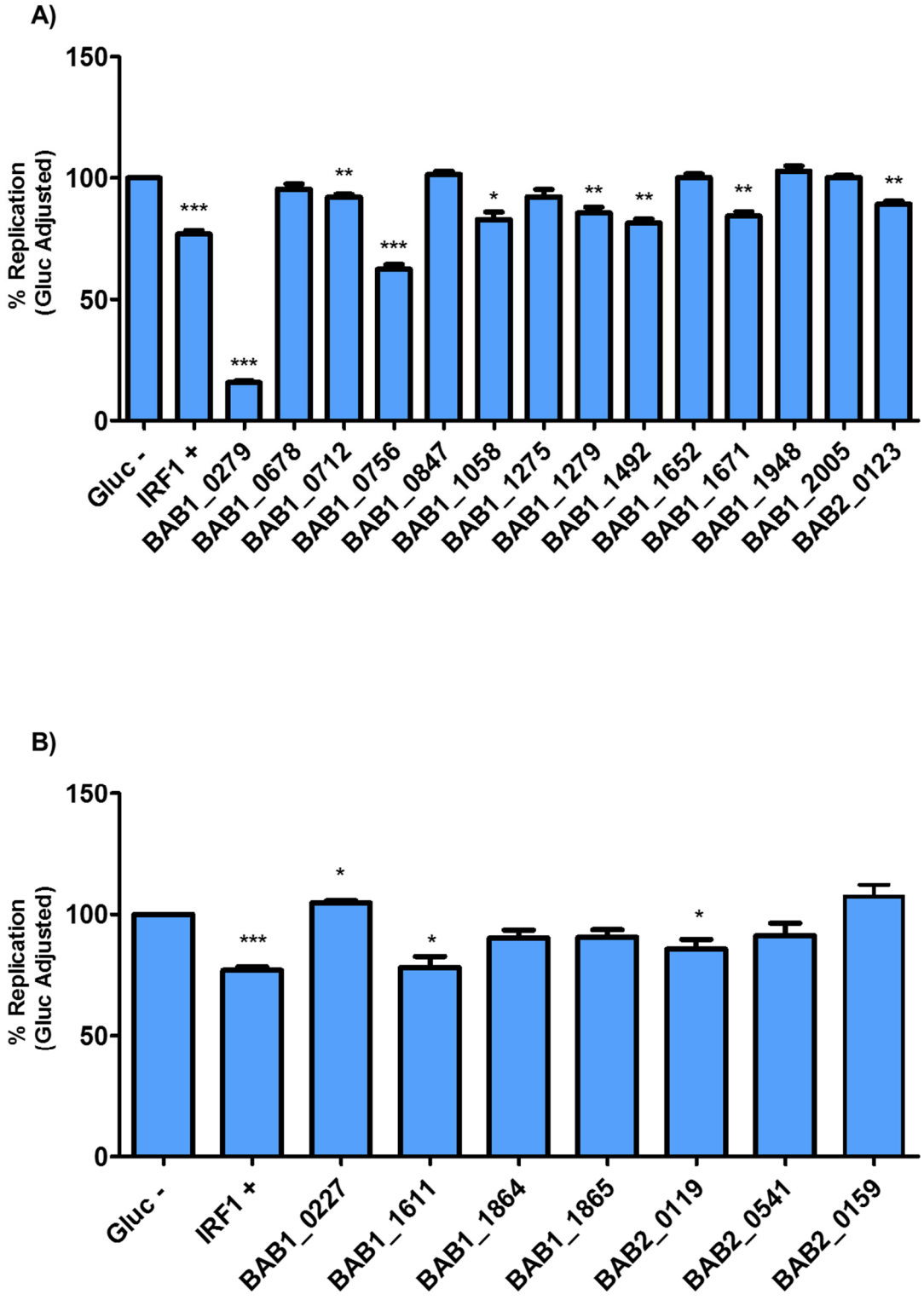

Figure 4.4. YFV interference assay. Huh 7.5 cells were co-infected with YFV infective particles and lentivirus expressing **(A)** effector proteins secreted by *Brucella* T4SS or **(B)** effector proteins secreted independently of *Brucella* T4SS. Percent of YFV replication was normalized to Gluc (control). IRF1= inhibition control. The values represent the mean ± SEM of quadruplicate wells. Two tailed *t*-test = *p<0.05, **p<0.005 and ***p<0.001.

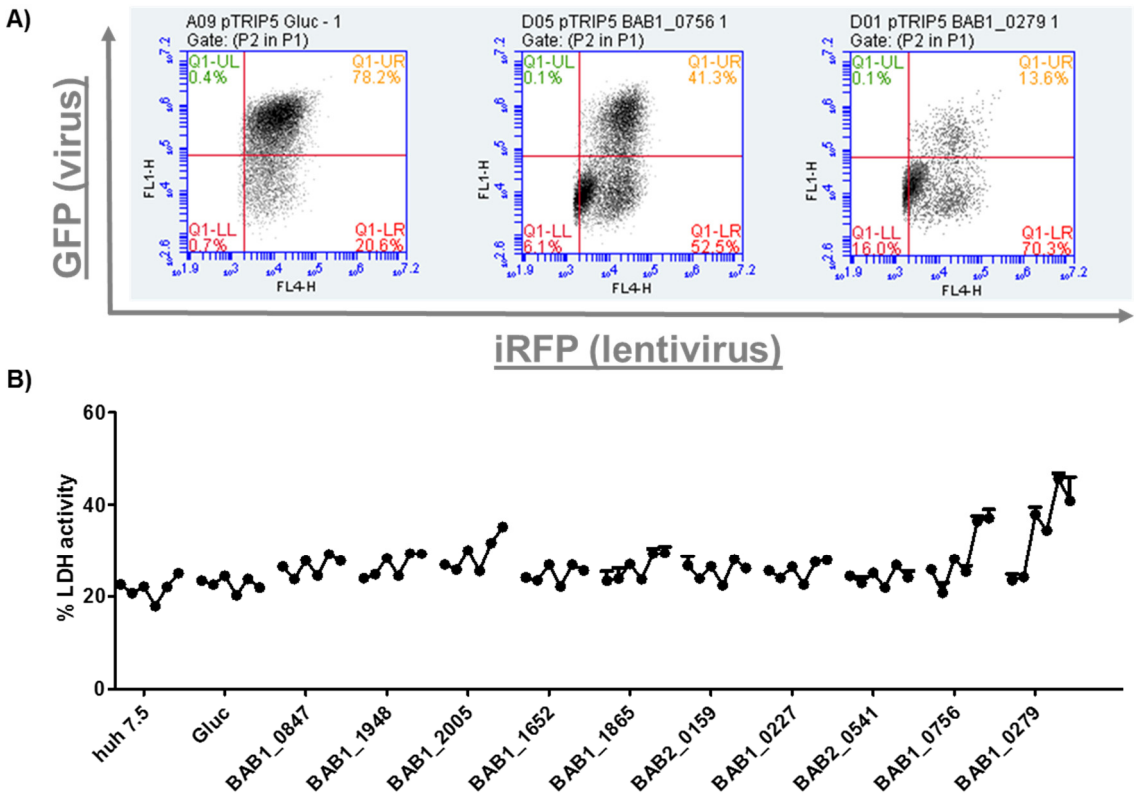

Figure 4.5. Determination of the cytotoxicity of BAB1_0756 and BAB1_0279 effector proteins. **A)** Representative flow cytometry plots of Gluc (control), BAB1_0756 and BAB1_0279 effector proteins. **B)** LDH cytotoxicity assay of some *B. abortus* effector proteins. LDH activity is measured by lactate dehydrogenase release by Huh 7.5 cells transduced with different *B. abortus* effector proteins. The dots represent time points from day 1 to day 6 post-transduction. The values represent the mean ± SEM of triplicate wells.

Figure 4.6 shows the results of the HCV interference assay. In this case, unexpectedly, all effector proteins tested significantly decrease HCV replication. We found two effector proteins that decrease HCV replication below 50 %, BAB1_1611 and BAB1_1492. These two effector proteins also decrease YFV replication (Figure 4.4). Conversely, BAB1_0279 effector protein does not inhibit replication as much as during YFV infection.

In view of these results, we considered that YFV was a better candidate than HCV for the Viral Interference Assay, because we obtained more reasonable results that with HCV. Also, we decided that flow cytometry analysis could be enough to detect effector cytotoxicity.

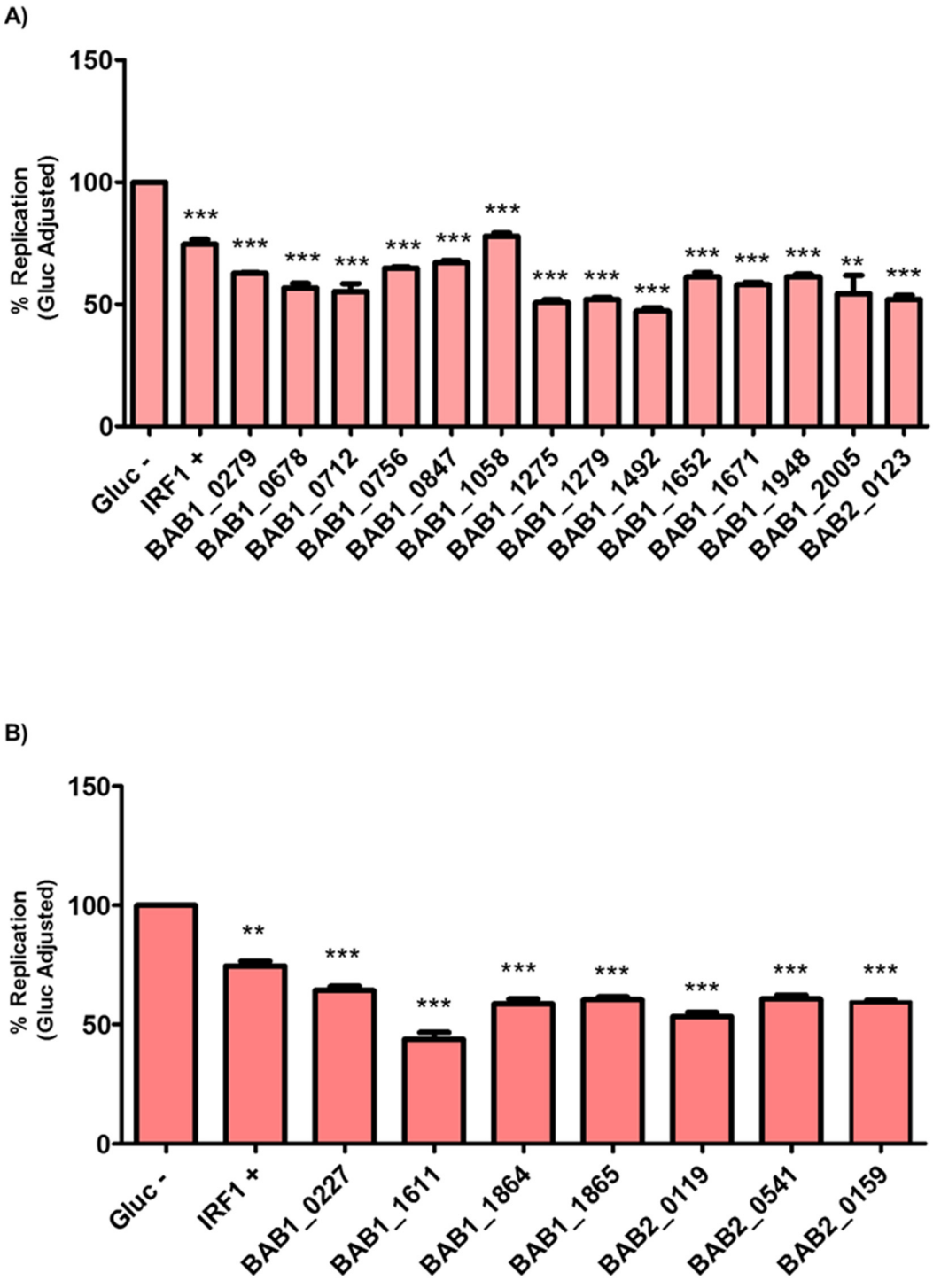

Figure 4.6. HCV interference assay. Huh 7.5 cells were co-infected with HCV infective particles and lentivirus expressing **(A)** effector proteins secreted by *Brucella* T4SS or **(B)** effector proteins secreted by *Brucella* independently of its T4SS. Percent of HCV replication was normalized to Gluc (control). IRF1= inhibition control. The values represent the mean ± SEM of quadruplicate wells. Two tailed *t*-test = *p<0.05, **p<0.005 and ***p<0.001.

4.1.3 Library screening

Once we had set up the assay, we decided to extend our analysis to the rest of effector protein candidates selected in section 4.1.1. We transferred the remaining 130 *B. abortus* putative effector genes and *gluc* control cloned in pDONR223 vector to pTRIP6-DEST vector, which expresses the m-Cherry fluorescent protein instead of IRFP670 fluorescent protein expressed by pTRIP5-DEST vector. We selected pTRIP6-DEST instead of pTRIP5-DEST because the flow cytometer that we have in the IBBTEC detect m-Cherry fluorescence better than IRFP670 fluorescence. These constructions and pTRIP6::IRF1 and pTRIP6::GFP controls were used to generate lentiviral particles for the YFV Interference Assay. The amount of lentivirus obtained in the supernatant was enough to obtain routinely more than 60 % of the cells transduced.

Once back in our laboratory, we had to generate infective viral particles of YFV and HCV. An *in vitro* transcription was made for each viral genome, as explained in Experimental Procedures section 3.7.1. Then, the viral RNA obtained was used to transfect Huh 7.5 cells (Experimental Procedures section 3.7.2). We tested several conditions, but we only obtained infective viral particles for YFV when transfecting 3 µg of YFV RNA with Lipofectamine™ 3000 reagent (Figure 4.7). Since the number of viral particles obtained per transfection was not very abundant, we decided to use supernatants containing YFV viral particles to amplify virus production during only one infection round. In this way, we obtained enough infective particles to make the viral interference assay. For HCV, although several conditions were tested, it was impossible to obtain infective particles, even using 3 µg RNA for transfection (Figure 4.7). Since, in any case, our previous results recommended the use of YFV, we continued the Viral Interference Assay with YFV.

Once we obtained both the lentiviral particles, which contain our selected putative effector proteins, as well as the infective YFV particles, we carried out the Viral Interference Assay for each effector protein. Figure 4.8 shows a summary of the results obtained here and during the standatization (section 4.1.2). The graph highlights in color those effector proteins showing levels of

replication above or below the standard deviation of the assay. In the case of those effector proteins that increase YFV replication, we were more restrictive. Consequently, we only selected those effector proteins that increase the replication more than 24 %. There are eight putative effector proteins that favor the replication of YFV. Other seven putative effector proteins decrease the replication of YFV to levels lower than those obtained with IRF1 protein (inhibitory control), apart from the two effector proteins determined in the previous assay, which are also shown in the graph for comparison.

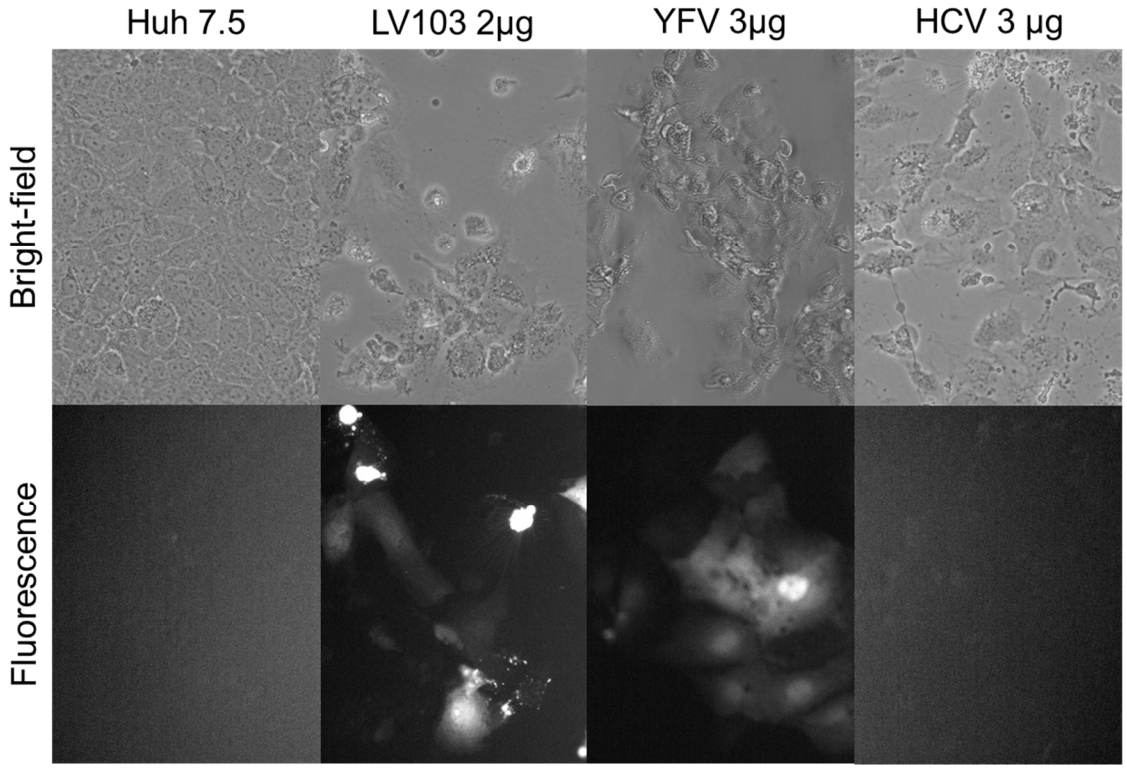

Figure 4.7. YFV and HCV transfections. YFV and HCV genome RNAs were transfected into Huh 7.5 cells. LV103 plasmid was used as positive transfection control. Transfection was tested by fluorescence microscopy. The bright-field images correspond with the visualization of Huh 7.5 cells and fluorescence images indicate the transfection.

Table 4.4 list the putative effector proteins selected for their interference with viral replication. Among proteins that favor the YFV replication, there are four proteins predicted by several methods (BAB2_0074, BAB2_0271, BAB1_0608 and BAB1_0740). Also, there is one unknown function protein (BAB1_1199) and three known proteins (BAB2_0773, BAB1_1344 and BAB2_0246). On the other hand, among proteins that inhibit the YFV replication, there are two proteins

predicted by several methods (BAB1_0817 and BAB1_1322). Four hypothetical proteins (BAB1_1185, BAB1_1386, BAB1_1396 and BAB2_0634). One known protein (BAB1_1730), and finally the two effector proteins secreted by *Brucella* T4SS (BAB1_0279 and BAB1_0756). These two proteins, known as BspA and BspB, are the only known effector proteins secreted dependently or independently of the *Brucella* T4SS that affect YFV replication.

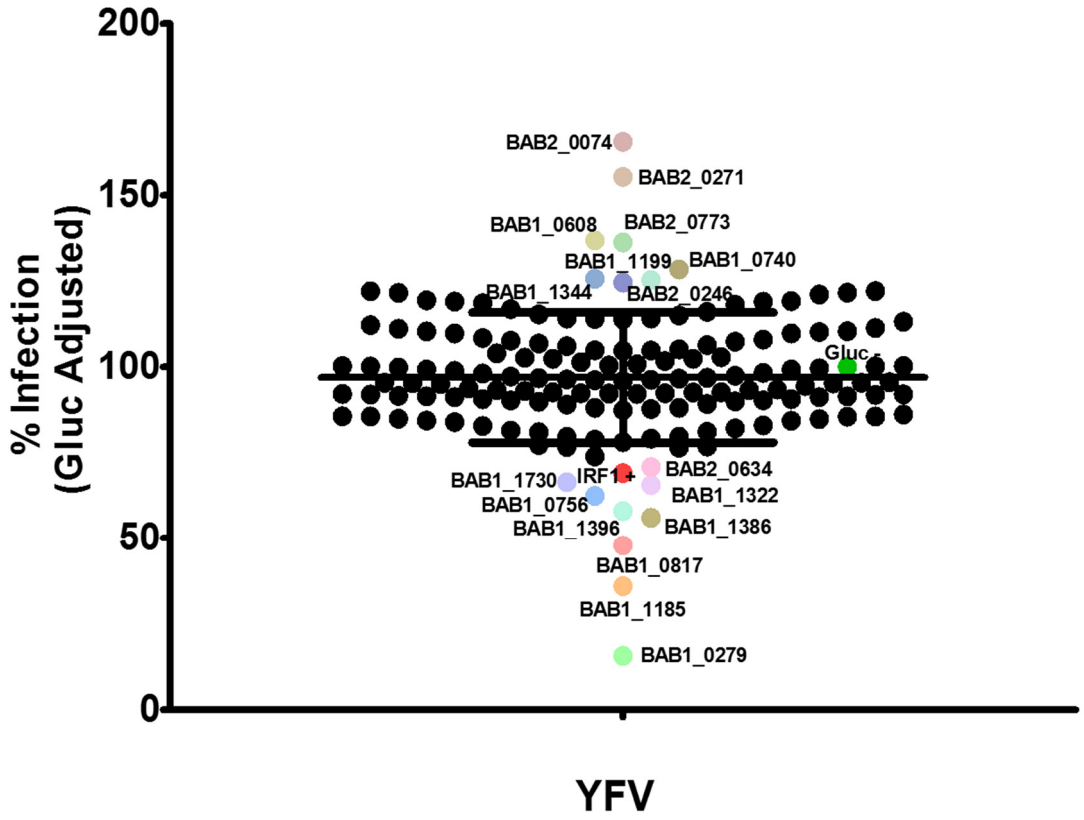

Figure 4.8. Screening of the library of putative effector proteins with the YFV interference assay. Replication levels were normalized to the Gluc control. Selected putative effector proteins are indicated in different colors. The black lines indicate the population mean ± SD. IRF1= inhibition control. The values represent the mean of quadruplicate wells. The graph was created with GraphPad Prism 5.0.

It should be noted that most *Brucella* proteins that negatively affect YFV replication present cytotoxicity, according to the new population observed by flow cytometry, that is absent in the plot of the Gluc control (Figure 4.9), similar to the population previously observed in the flow cytometry analysis of cytotoxic *B. abortus* effector proteins BAB1_0279 and BAB1_0756 (Figure 4.5).

Putative effector protein	Difference to Gluc control (%)	Effect in YFV infection	Principal protein characteristics
BAB1_0279	84,33	↓	Effector protein secreted by T4SS; contain a TIR-domain
BAB1_1185	64,08	↓	Secretory protein associate with *Brucella* cytotoxicity
BAB1_0817	52,17	↓	Essential protein for *Brucella* growth
BAB1_1386	44	↓	High identity with CbiM of other *Brucella* strains
BAB1_1396	42,06	↓	High identity with Ba14K family protein of *B. suis*; putative function in pathogenesis
BAB1_0756	37,57	↓	Effector protein secreted by T4SS; contain a TIR-domain
BAB1_1322	34,43	↓	TerB region
BAB1_1730	33,61	↓	Bacterial regulatory protein of the GntR family
BAB2_0634	29,16	↓	-
BAB2_0074	65,61	↑	Band 7 protein: stomatin; HflC region; putative membrane protein
BAB2_0271	55,4	↑	TPR protein
BAB1_0608	36,86	↑	High identity with an ATPase of *B. melitensis*
BAB2_0773	36,29	↑	Secretion protein HlyD
BAB1_0740	28,42	↑	-
BAB1_1344	25,68	↑	Essential protein for *Brucella* growth; SecD/SecF/SecDF membrane protein related with intracellular protein transport
BAB2_0246	25,36	↑	ATP/GTP- binding site motif A (P-loop): cobalamin synthesis proteins/P47K
BAB1_1199	24,6	↑	Contain unknown function DUF218 domain

Table 4.4. *B. abortus* putative candidate effector proteins.

Taken together, all the results about this part of the thesis indicate that no single method for prediction of bacterial effector proteins secreted by T4SS is totally effective for the prediction of *Brucella* effector proteins. We have constructed a library of candidate effectors using a combination of the different prediction methods, and we have set up a new screening assay based on interference with Flaviviridae replication. Also, flow cytometry analysis allowed us to determine cell toxicity generated by *B. abortus* proteins. As a result of our screening, we found eight putative *B. abortus* effector proteins that upregulate YFV replication: BAB2_0074, BAB2_0271, BAB1_0608, BAB1_0740, BAB1_1199, BAB2_0773, BAB1_1344 and BAB2_0246. Whereas other seven putative *B. abortus* effector proteins downregulate YFV replication: BAB1_0817, BAB1_1322, BAB1_1730, BAB1_1185, BAB1_1386, BAB1_1396 and BAB2_0634. Our screening assay also determined that the known effectors, BAB1_0279 and BAB1_0756 downregulate YFV replication.

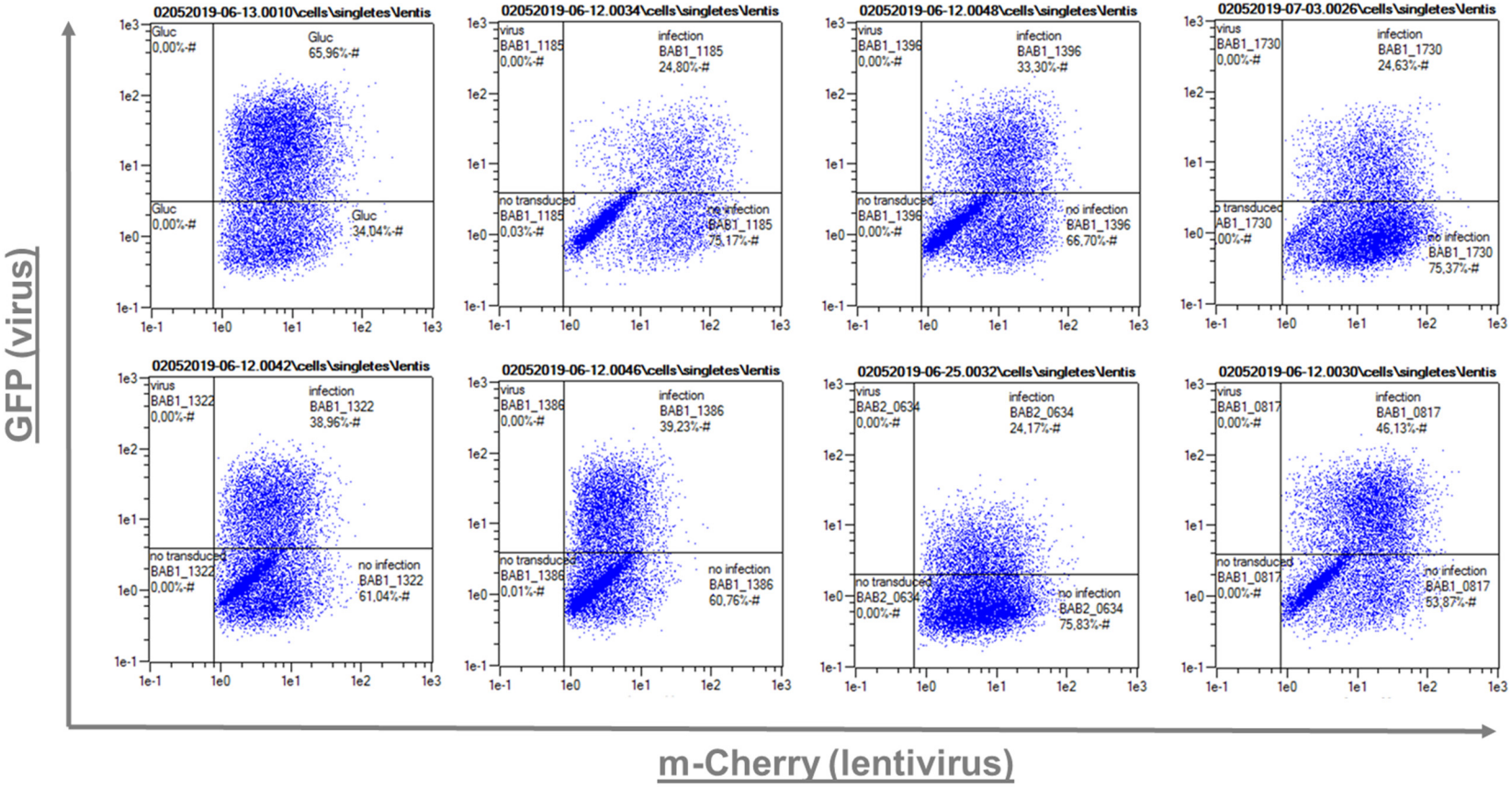

Figure 4.9. Flow cytometry plots of *B. abortus* proteins that downregulate YFV replication in the YFV interference assay. A third population corresponding with dead cells is observed in all plots except in BAB2_0634 protein and in the negative control, Gluc.

4.2 Characterization of putative lysozyme inhibitors of *B. abortus*

4.2.1 *In silico* analysis of BAB1_0102 and BAB1_0466.

As previously mentioned, the structure of *B. abortus* protein BAB1_0466 bound to lysozyme (Figure 1.13) suggested that it could act as a lysozyme inhibitor. In addition, our group had predicted the presence of a putative second lysozyme inhibitor in *B. abortus* 2308, after re-annotation of *bab1_0102* gene. In a first analysis of the proteins, a tridimensional prediction of both BAB1_0102 and BAB1_0466 was modelled and compared with the databases using the PHYRE^2 server (Kelley et al., 2015). This analysis shows that the re-annotated BAB1_0102 protein has a 25 % identity with the lysozyme inhibitor PliC from *Salmonella typhimurium* and with MliC from *P. aeruginosa*. However, while BAB1_0466 also presents a 25% identity with PliC from *S. typhimurium,* it presents a much higher identity (46 %) with MliC protein from *P. aeruginosa*. Moreover, the BAB1_0102 and BAB1_0466 modelled structures were predicted to have a 99.9% confidence with the PliC and MliC-type structure, respectively, with more than a 68% of coverage. Thus, the structures predicted were very similar for both proteins (Figure 4.10.A).

Like other MliC/PliC inhibitors, BAB1_0102 and BAB1_0466 are also predicted to have a signal peptide, as determined using the LipoP 1.0 and SignalP-5.0 servers. Additionally, using Blastp, both proteins are predicted to contain the MliC superfamily domain (Figure 4.10.B). Regarding the location of the proteins, and using the CELLO server, BAB1_0466 is predicted to have a periplasmic localization, while BAB1_0102 would be a cytoplasmic protein.

Regarding the conservation of specific residues known to be important for the structure and function of lysozyme inhibitors, it is known that Ser89 and Lys103 residues of *P. aeruginosa* MliC are necessary for the interaction with the active site of lysozyme and therefore, for MliC inhibitory function (Yum et al., 2009). These residues are also conserved in other characterized PliC/MliC proteins such as PliC protein of *S. typhimurium* (Figure 4.10.C) and are also present in BAB1_0466. However, BAB1_0102 contains aspartic acid and

A)

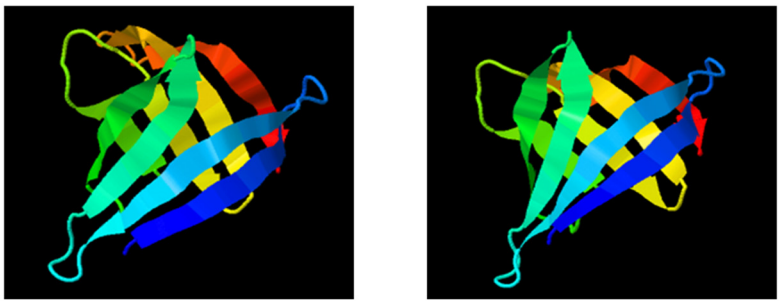

B)

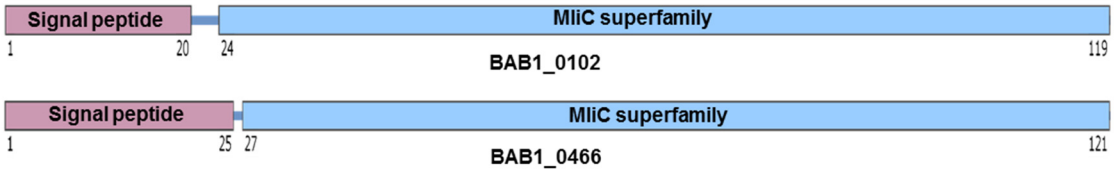

C)

```
BAB1_0102_reannotated      MTASALLAVALMPV--SAHAQADEEQP---------------PIERVDYICERSVVVPVT
P._aeruginosa_MliC         MKKALWLLLAAVPVVLVACGGSDDDKQTAQVDYLALPGDAKLDTRSVDYKCENGRKFTVQ
S._typhimurium_PliC        MMKRKLIPFTLFLAALSASTTSIAASQ---------------EISKSIYTCNDNQVMEVI
                           *     : .: . .   *   :   .                      * *: .  . *

BAB1_0102_reannotated      YIRSNGAPAAAVLEVEGKMVALQW--HGDLKKYVAIDEQDSYRWADRGGQATLSHLEADH
P._aeruginosa_MliC         YLNKGDNSLAVVPVSDNSTLVFSNVISASGAKYAA----GQYIWWTKGEEATLY---GDW
S._typhimurium_PliC        YVNTEAGNAYAIISQVNEMIPMRLMKMASGANYEAIDKNYTYKLYTKGKTAELV------
                           *:..      .:    .. : :     ..  :* *      *    .*  * *

BAB1_0102_reannotated      TAKEVTLLSACRADTAEE
P._aeruginosa_MliC         KGGEPTDGVACKER----
S._typhimurium_PliC        EGDDKPVLSNCSLAN---
                            . : .    *

S._typhimurium_PliC        MMKR---KLIPFTLFLAALSASTTSIAASQ------------EISKSIYTCNDNQVMEVI
BAB1_0466                  --MKMW-TLAKMSVAAAALSFAASAASASEIT-IKLPDSVKVSTNSILYKC-GAKDLSVT
P._aeruginosa_MliC         MKKALWLLLAAVPVVLVACGGSDDDKQTAQVDYLALPGDAKLDTRSVDYKCENGRKFTVQ
                                   *  ..:  .* . :     :::           .  .  *.* . . : *

S._typhimurium_PliC        YVNTEAGNAYAIISQVNE-MIPMRLMKMASGANYEAIDKNYTYKLYTKGKTAEL---VEG
BAB1_0466                  YYN-AGDISLAKLELEDE-TVVASNVISGSGAKYAG----SVYIWWTKGKTASLYNLIDN
P._aeruginosa_MliC         YLN-KGDNSLAVVPVSDNSTLVFSNVISASGAKYAA----GQYIWWTKGEEATLYGDWKG
                           * *  .. : * :   ::  :    :  .***:* .      *  :***: * *    ..

S._typhimurium_PliC        DDKPVLSNCSLAN
BAB1_0466                  PEEDKPISCVEQ-
P._aeruginosa_MliC         GEPTDGVACKER-
                           :      *
```

Figure 4.10. *In silico* analysis of BAB1_0102 and BAB1_0466. **A)** Predicted structure of BAB1_0102 and BAB1_0466 using the PHYRE^2 server. **B)** Schematic representation of BAB1_0102 and BAB1_0466 proteins. MliC superfamily: Membrane-bound inhibitor of C-type lysozyme domain. **C)** MUSCLE alignment of BAB1_0102 (top) and BAB1_0466 (bottom) with *P. aeruginosa* MliC and *S. typhimurium* PliC proteins. Asterisks (*) denote fully conserved amino acids. Colons (:) denote amino acids with strongly similar properties. Periods (.) denote amino acids with weakly similar properties. The serine (S) and lysine (K) residues implicated in lysozyme inhibition are in black boxes.

sequence position. Considering this *in silico* analysis, we hypothesized that BAB1_0466 could be a lysozyme inhibitor protein, while the re-annotated BAB1_0102 could have or not a similar function.

4.2.2 *In vitro* activity as lysozyme inhibitors

Having these two proteins as candidates, the next step was to determine if they could inhibit the activity of lysozyme. In order to test their putative activity, we cloned the genes that codified for these proteins in a pET29C overexpression vector (Figure 4.11.A). This vector inserts a 6xHis tag at the C-terminus of the proteins, allowing the purification of the fusion proteins using a His-Trap HP column. These vectors were then used to overexpress BAB1_0102 and BAB1_0466 in 2 l of LB medium as mentioned in Experimental Procedures section 3.4.4. The cleared lysate was used to purify each protein using a His-Trap HP column. After purification, the aliquots obtained were analysed by electrophoresis in SDS-PAGE gels. Some of them presented high amount of purified protein as we can see in Figure 4.11.B. Also, the expected protein size for each protein corresponds to the observed in the gel, around 14 kDa for both fusion proteins. With these results, we decided to select the aliquot with more amount of each protein for subsequent analysis: aliquot 34 for BAB1_0466, with 1.16 mg/ml pure protein, and aliquot 40 for BAB1_0102, with 1.64 mg/ml.

Once we obtained enough purified protein, we tested if these proteins could inhibit the lysis of *M. lysodeikticus* produced by lysozyme. *M. lysodeikticus* is a Gram-positive bacterium that is intrinsically sensitive to lysozyme. Suspension of *M. lysodeikticus* cells in hypotonic buffer were treated with BSA or lysozyme at 2 µg/ml. For this experiment, both Human (HL) and Hen-Egg White (HEWL) lysozyme were used. As expected, no lysis was observed in the BSA treated control, while the lysozyme treated samples experienced a rapid lysis under these conditions. Then, increasing amounts of the purified proteins were assayed in parallel. The putative inhibitors were mixed with the lysozyme solution before addition to the *M. lysodeikticus* suspension. As we can see in Figure 4.12, 1 µg/ml of BAB1_0466 was enough to change significantly the lysis curve produced by both types of lysozyme, while 2 µg/ml achieved a complete inhibition of the activity. Considering the molecular weight of lysozyme (HL: 16.5 kDa and

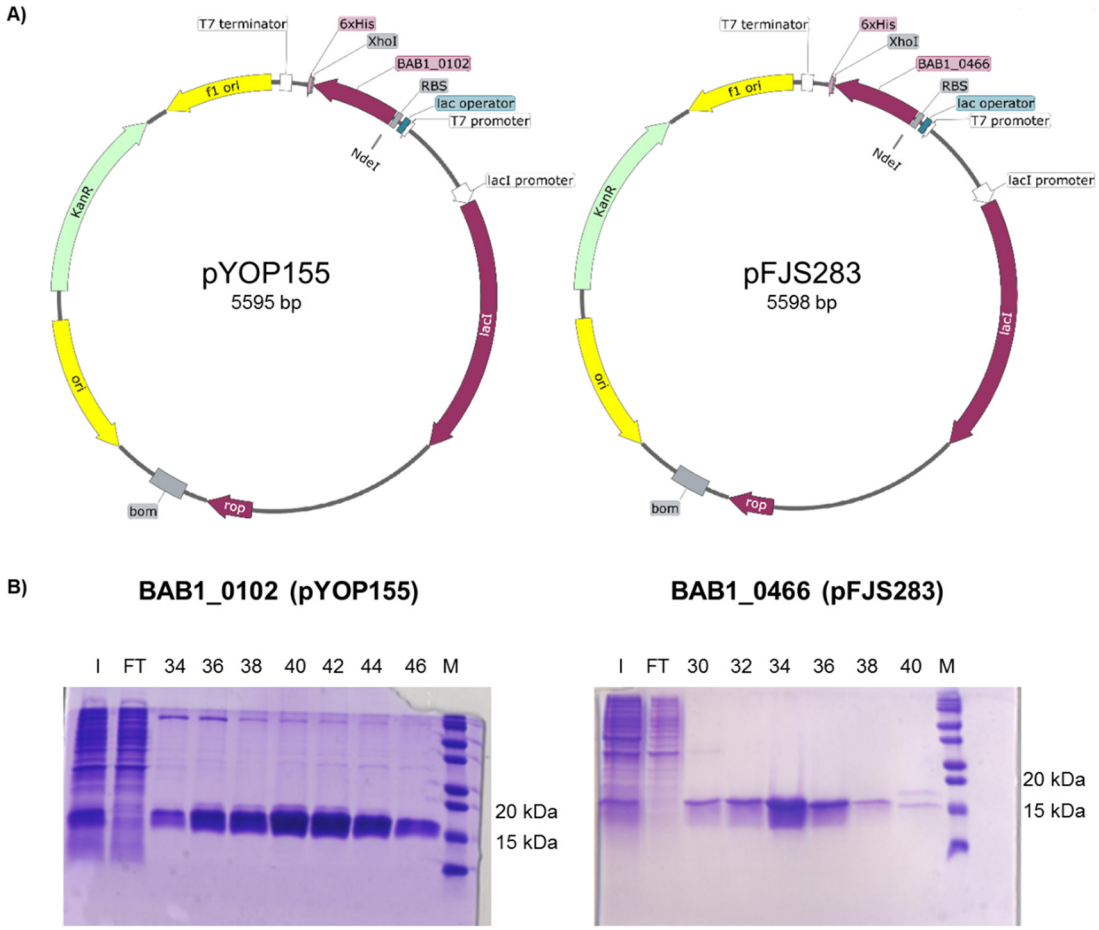

Figure 4.11. Overexpression and purification of BAB1_0102 and BAB1_0466. **A)** Plasmids constructed for the overexpression of BAB1_0102 and BAB1_0466. The 6xHis tag, the enzyme restriction sites used, and the antibiotic resistance gene are shown. **B)** SDS-PAGE gels obtained after BAB1_0102 and BAB1_0466 overexpression and purification through a His-Trap HP column. The numbers refer to the aliquots eluted from the column. I, input. FT, flowthrough.M, molecular weight marker. Kda are indicated to the right.

HEWL: 14.3 kDa) and BAB1_0466 (13.7 kDa), equimolar amounts of both proteins result in complete inhibition. However, we did not see any inhibitory effect of BAB1_0102 protein when we tested its activity using HEWL and HL (Figure 4.12). Thus, with these results we can conclude that BAB1_0466 inhibits c-type lysozyme activity in a concentration-dependent manner, while the re-annotated BAB1_0102 protein does not have this inhibitory activity.

Interestingly, BAB1_0466 inhibits HL differently than it does with HEWL. As we can observe in Figure 4.12, 1 µg/ml of BAB1_0466 is able to keep blocked the lysozyme activity of HL after 30 minutes of the assay, while the same

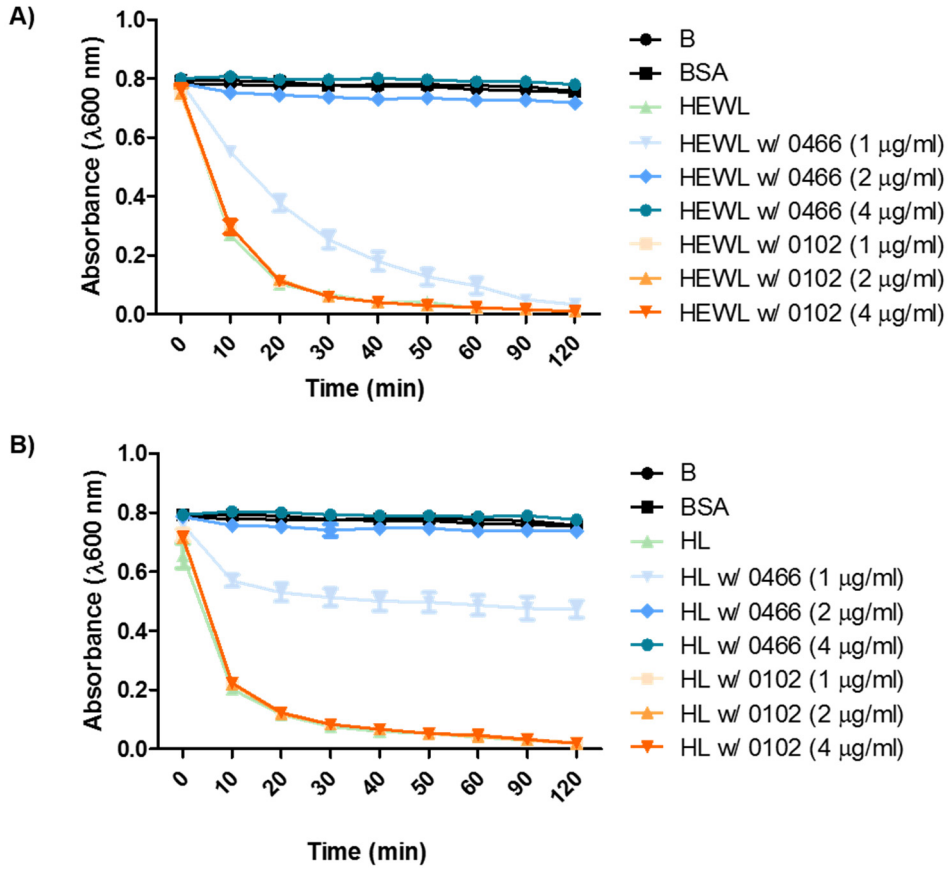

Figure 4.12. *In vitro* assay for determination of lysozyme inhibitor activity of BAB1_0466 and BAB1_0102. *M. lysodeikticus* was treated with 2 µl/ml of BSA, 2 µl/ml of **A)** HEWL or **B)** HL lysozyme alone or 2 µl/ml of lysozyme with increasing concentrations of BAB1_0102 and BAB1_0466. Absorbance at λ600 nm was measured at different time points. n=3 biological replicates. All values are represented as the mean ± SEM.

concentration of inhibitor cannot prevent the total clearance of the *M. lysodeikticus* suspension at the end of the assay.

Although we have not observed any inhibitory effect of BAB1_0102 on lysozyme activity, we cannot discard that it does not have some inhibitory effect on other bacterial proteins with lysozyme-like activity. That is also a possibility for BAB1_0466. To test this hypothesis, we searched for the presence of putative LTs, also named muramidases, in the *B. abortus* genome. We found seven proteins that contain SLT transglycosylase or glycosyl hydrolase domains, potentially responsible for lytic activity (Table 4.5). Two of them, SagA and VirB1, had previously been described to have lysozyme-like activity (Giudice et al., 2013; Zahrl et al., 2005), so we decided to check if either BAB1_0466 and

BAB1_0102 had some inhibitory effect on these proteins. We obtained the published overexpressing constructs, and proceded to induce overexpression using the same conditions reported by the authors. SagA was purified using a His-Trap HP column, while VirB1 was purified using a MBP-Trap column (Figure 4.13.A). As we can see in panel A, in both cases we were able to purify the protein, SagA was overproduced in higher amounts than VirB1. The size of the purified proteins agrees with the published sequence (SagA-6xHis: 24.25 kDa; MalE-VirB1: 68 kDa). We selected those fractions with an almost electrophoretically pure protein (28-30). The selected fractions were used to assay their activity as lysozyme-like proteins in the *M. lysodeikticus* lysis assay. In the case of SagA, we were able to reproduce its lytic activity, as had been previously published. However, we did not see any inhibitory effect of neither BAB1_0466 nor BAB1_0102 on SagA activity when we used the same concentration of both proteins (Figure 4.13.B).

Gene	Protein name	Domain	Reference
bab2_0068	VirB1	SLT transglycosylase	Zahrl et al., 2005
bab1_1002	SagA	Glycosyl hydrolase 108	Giudice et al., 2013
bab1_1531	BAB1_1531	SLT transglycosylase	
bab1_1461	BAB1_1461	SLT transglycosylase	
bab1_0064	BAB1_0064	SLT transglycosylase	
bab2_1100	BAB2_1100	SLT transglycosylase	
bab1_1227	BAB1_1227	SLT transglycosylase	

Table 4.5. Putative lytic transglycosylases of *B. abortus* 2308

In the case of VirB1, we could not detect its lytic activity (Figure 4.13.C). Despite several attempts to purify enough protein to carry out the assay, we could only obtain 0.5 µM of purified VirB1 protein. In these conditions it was not possible to detect the activity. In their original publication Zarhrl et al. (2005) used between 3 and 6 µM of VirB1 to observe VirB1 activity, with a different assay that has higher sensitivity than our assay. As this was a rather collateral study, we did not pursue any further.

Therefore, as a summary of these experiments, we have observed that BAB1_0466 inhibits the lytic activity of HEWL and HL, but it does not inhibit the

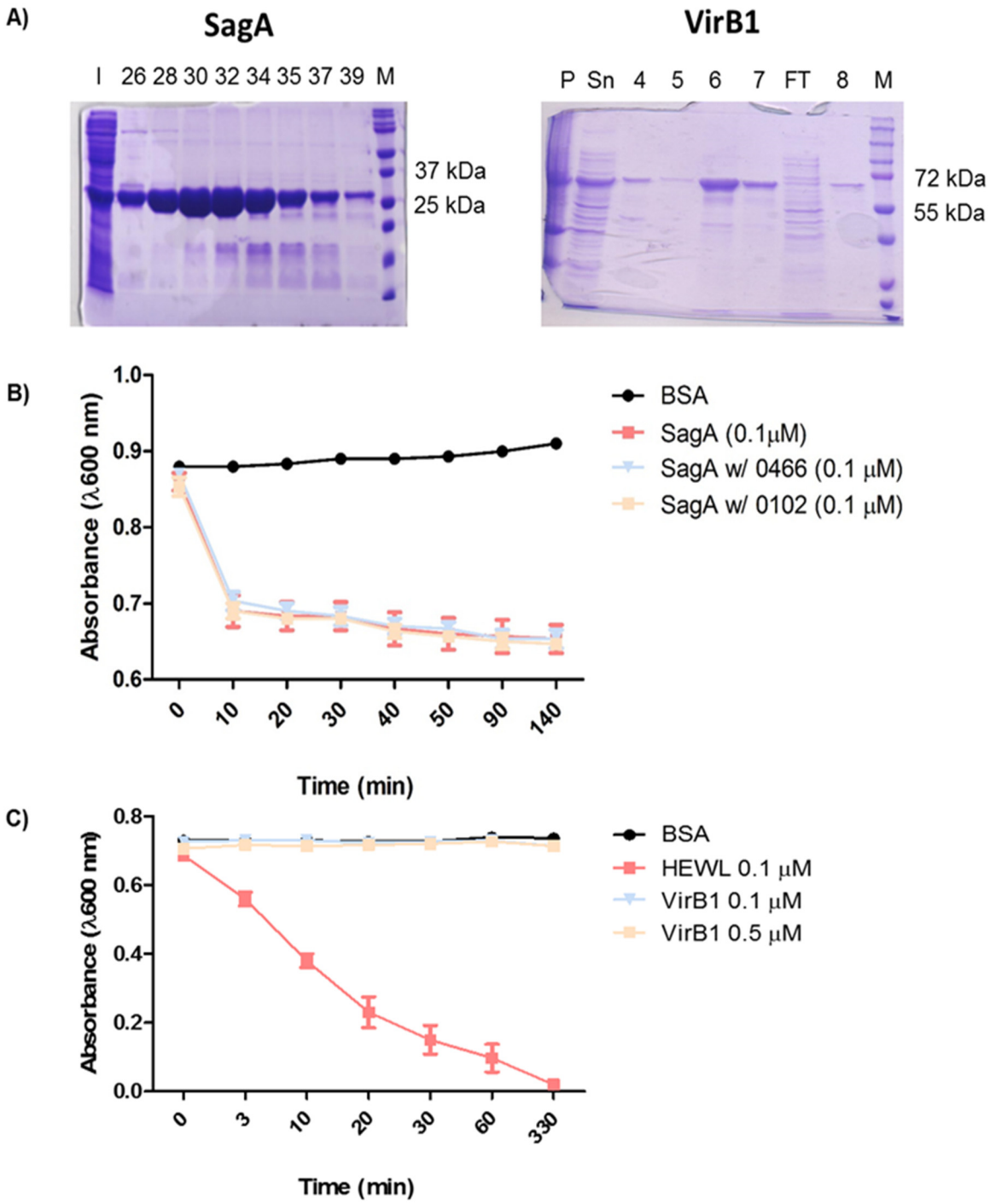

Figure 4.13. Testing the activity of VirB1 and SagA and their inhibition by BAB1_0102 and BAB1_0466. A) SDS-PAGE gels obtained after SagA and VirB1 overexpression and purification through His-Trap HP and MBP-Trap HP columns, respectively. Gel lanes are labelled as in figure 4.12. P, precipitate. Sb, supernatant. **B-C)** *In vitro* assay for determination of protein activity as lysozyme-like and lysozyme inhibitor proteins. **B)** *M. lysodeikticus* was treated with 0.1 μM of BSA, 0.1 μM of SagA alone or 0.1 μM of SagA with 0.1 μM of BAB1_0102 and BAB1_0466 proteins. **C)** *M. lysodeikticus* was exposed to 0.1 μM of BSA, 0.1 μM of HEWL or increasing concentrations of VirB1 protein. Absorbance at λ600 nm was measured at different time points**.** n=3 biological replicates. All values are represented as the mean ± SEM.

sustained over time with HL than with HEWL, a fact that could imply a higher affinity to the human enzyme. On the other hand, our results showed that the re-annotated BAB1_0102 protein does not have inhibitory effect on lysozyme or SagA, at least in the tested conditions. For these reasons, we decided to focus in the characterization of BAB1_0466.

4.2.3 Determination of BAB1_0466 contribution to *B. abortus* survival upon lysozyme treatment

Once stablished that BAB1_0466 possess lysozyme inhibitor activity *in vitro*, we wanted to check if this activity affects *Brucella* resistance to the deletereous action of lysozyme. Lysozyme is found in abundance in the blood, in secretions, including tears, urine, saliva, and milk, at mucosal surfaces (where it can reach concentrations as high as 1 mg/ml), and in professional phagocytes, including macrophages, neutrophils, and dendritic cells, so *Brucella* species certainly have to cope with lysozyme to establish an infection. In order to test a putative role of BAB1_0466 in *Brucella* resistance to lysozyme, we used a deletion mutant in *bab1_0466* (*B. abortus* 2308Δ0466) and the corresponding complemented strain (*B. abortus* 2308Δ0466::0466), previously constructed in our laboratory. We know that *Brucella* peptidoglycan is sensitive to lysozyme, but also that the OM of *Brucella* is highly impermeable to polycations such as lysozyme, and also to lactoferrin, as well as other cationic peptides (Tejada et al., 1995). Confirming this data, when the survival of *B. abortus* was tested upon exposure to lysozyme (Figure 4.14.A), we did not observe any decrease in the survival of neither the WT, nor the mutant strain. The high concentration of lysozyme used in the assay represents the highest concentration reached at mucosal surfaces.

As there are several other components that could be affecting the stability of the *Brucella* envelope *in vivo*, we also tested the activity of lysozyme combined with glycine. When present in high concentration, glycine is incorporated into the nucleotide-activated peptidoglycan precursors, and the amount of incorporated glycine is equivalent to the decrease in the amount of alanine. The overall effect of this substitution is a fragilized peptidoglycan (Hammes et al., 1973; Ralston et al., 1961). First, we checked that growth in 0.3 M glycine does not induce lysis of

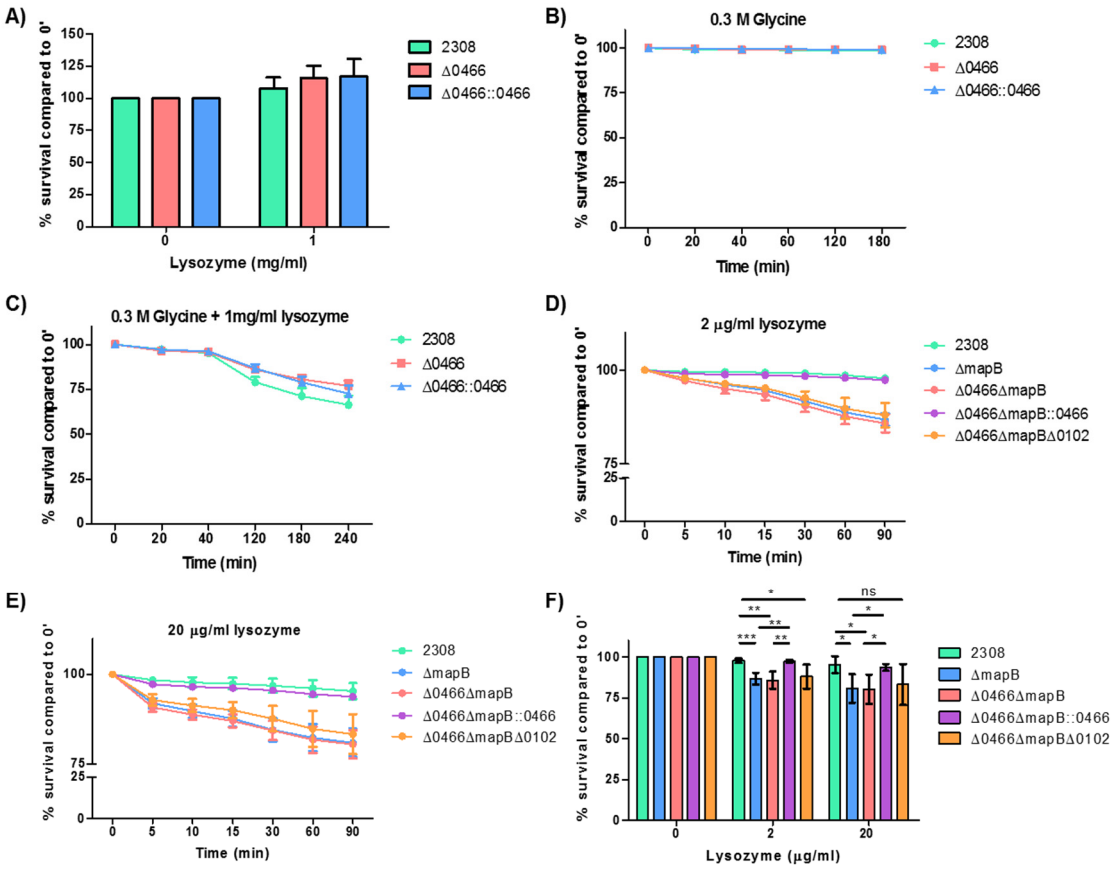

Figure 4.14. BAB1_0466 plays a role in *B. abortus* defense from lysozyme when the OM is damaged. **A)** *B. abortus* WT, Δ*0466* and Δ*0466::0466* strains were exposed to 0 or 1 mg/ml lysozyme for 3 h in TSB. The percentage of *Brucella* survival was determined by dividing the CFU/ml at 3h by the CFU/ml at 0 h and normalized to 0 mg/ml of lysozyme (100%). n=3 biological replicates. **B)** The same *B. abortus* strains were exposed to 0.3 M glycine and absorbance at λ600 nm was measured for 3 h. The percentage of survival was determined by dividing the OD at each time point by the OD at 0 min and normalized to time 0 (100%). n=1 biological replicate. **C)** The same *B. abortus* strains were exposed to 0.3 M glycine and 1 mg/ml of lysozyme. Absorbance at λ600 nm was measured for 4 h. The percentage of survival was determined as in B. n=3 biological replicates. **D-F)** The WT, Δ*mapB*, Δ*mapB*Δ*0466*, Δ*mapB*Δ*0466::0466* and Δ*mapB*Δ*0466*Δ*0102* strains were exposed to **D)** 2 µg/ml or **E)** 20 µg/ml of lysozyme for 90 min. The percentage of survival was determined by dividing the OD at each time point by the OD at 0 min and normalized to time 0 (100%). **F)** t-test for data at time 90 min obtained in D and E was calculated. n=5 biological replicate. Two tailed *t*-test = *p<0.05, **p<0.005 and ***p<0.001. All values are represented as the mean ± SEM.

B. abortus per se (Figure 4.14.B). However, when *B. abortus* strains were grown in the presence of 1 mg/ml of lysozyme and 0.3 M of glycine, we can observe how bacterial lysis increases when compared with the same strains treated with glycine alone (Figure 4.14. B-C). However, the lysis seems to be taken place to

the same extent in the presence of the lysozyme inhibitor, since no significant difference was observed in the survival of strains 2308Δ0466 and 2308 (Figure 4.14.C).

MapB is a *B. suis* protein orthologous to TamB, that together with TamA, a protein belonging to the Omp85 family, form a complex that has been proposed to participate in the translocation of autotransporter proteins across the OM. A mutant defective in MapB *(*Δ*mapB*) shows an accumulation in the cell periplasm of an autotransporter adhesin of the OM, and a markedly reduced resistance to both lysozyme and the cationic lipopeptide polymyxin B (Bialer et al., 2019). In order to test if this background could be useful to determine the role of BAB1_0466, we introduced the Δ*mapB* mutation in the same way that Bialer et al. (2019) in *B. suis*, in *B. abortus* 2308, *B. abortus* 2308Δ*0466*, *B. abortus* 2308Δ*0466*Δ*mapB::0466* and *B. abortus* 2308Δ*0466*Δ*0102*. The strains were then treated with 2 or 20 µg/ml of lysozyme. The results obtained show that 2308Δ*mapB* is sensitive to lysozyme, extending to *B. abortus* the observation of Bialer et al in *B. suis*. The decrease in viability was similar for the Δ*0466*Δ*mapB* double mutant, even at very early times of treatment (Figure 4.14.D-E). After 90 min of treatment with lysozyme, Δ*mapB* and Δ*0466*Δ*mapB* mutants showed a very similar survival (Figure 4.14.F). However, the complemented strain Δ*0466*Δ*mapB::0466* showed a survival level similar to that of the WT strain 2308, and significantly different to those of the *Δ0466*Δ*mapB* or *Δ0466*Δ*mapB*Δ*0102* strains (Figure 4.14.F).

In summary, we have confirmed that *B. abortus* is highly resistant to lysozyme activity. The lysozyme inhibitor BAB1_0466 could be playing a role by inhibiting the activity of lysozyme when the OM is damaged.

4.2.4 Determination of BAB1_0466 role in *B. abortus* survival inside different human innate immune cell types

We have seen that BAB1_0466 can inhibit the activity of lysozyme in vitro, and that it also could play a role in protecting the bacteria from lysozyme activity when the OM is compromised. The next step is to test if it plays a role in the survival of *B. abortus* during infection. *Brucella* is an intracellular pathogen whose initial niche are innate immune cells. These immune cells are large producers of

lysozyme, as well as other compounds that destabilize bacteria OM or are bactericidal (Ragland and Criss, 2017).

Macrophages are one of the cell types where *Brucella* can replicate during infection, and probably the most used cellular model for these bacteria. Macrophages produce lysozyme, as well as other components that facilitate the destruction of the bacteria. In fact, after infection of macrophages, roughly more 90% of the *Brucella* are killed in the first 8-10 hours. However, those bacteria which survive this initial phase, can adapt and replicate, presenting a typical V-shaped replication curve. So, as a first, approach, we tested the effect of BAB1_0466 in infection of the mouse macrophage J774 cell line. Infection of J774 cells with the different strains assayed resulted in phagocytosis of the bacteria, as we observed using bacteria which produce the fluorescent protein DsRed (Figure 4.15.A), with few bacteria located outside the cells after antibiotic treatment. When the viable number of bacteria inside the cells at different post-infection times was checked, we could not observe any significant differences between 2308 WT, 2308Δ*0466* and 2308Δ*0466::0466* (Figure 4.15.B). This result confirmed that BAB1_0466 protein does not play a role during mouse macrophage infection.

However, we have to consider that we used a mouse cell line, and also that macrophages are only one of the different immune cell types that *Brucella* can infect, that also produce lysozyme. So, we decided to carry out a different experiment, to check if BAB1_0466 could be playing some role during the bacteremia phase in human infection. To do so, we performed whole human blood infections, a rather crude assay, in which we have a number of different cell types, as well as complement, which could potentially affect *Brucella* survival. We used peripheral blood from healthy human volunteers with no history of brucellosis. In this model of infection, we checked survival of the different strains at two hours post-infection, and the results are shown in Figure 4.16. We can observe a significant decrease of the 2308Δ*0466* mutant compared to 2308 WT. Furthermore, complementation of the mutant with BAB1_0466 results in a recovery of the survival percentage. Although the complement strain does not reach the same level as the 2308 WT strain, there is no significant difference between them. This result indicate that there are some factors in the blood that

can differentially kill *Brucella* in the absence of the lysozyme inhibitor BAB1_0466.

In the blood we can find several cell types, such as leukocytes, platelets or erythrocytes, and plasma, which contains a number of compounds like albumin, immunoglobulins, complement, or secreted lysozyme. The most obvious candidates to check for a putative role in killing *Brucella* are the leukocytes of the innate immune system, such as neutrophils and monocytes, that phagocyte *Brucella* and also produce high amounts of lysozyme. Thus, the next step was to determine the innate immune cells that were involved in the

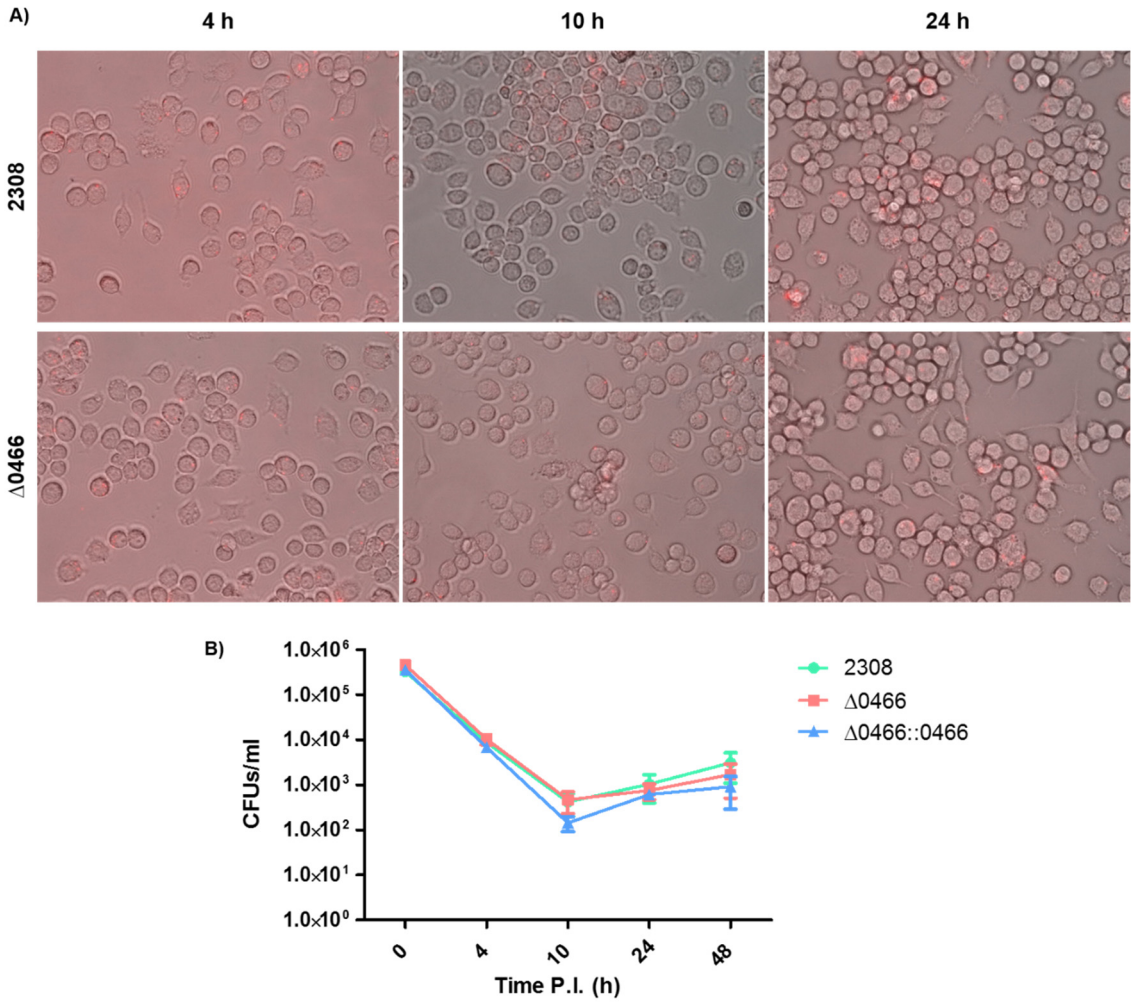

Figure 4.15. BAB1_0466 does not play a role during infection of mouse macrophages. **A)** J774 mouse macrophages monolayers infected with either 2308 WT or 2308Δ*0466* harboring the plasmid pBBR1::DsRed which encodes DsRed, observed by fluorescence microscopy, at different time points. **B)** J774 mouse macrophages monolayers were infected with 2308 WT, 2308Δ*0466* and 2308Δ*0466::0466* at a MOI of 100. At indicated time points, CFU/ml were determined. n= 2 biological replicates. All values are represented as the mean ± SEM.

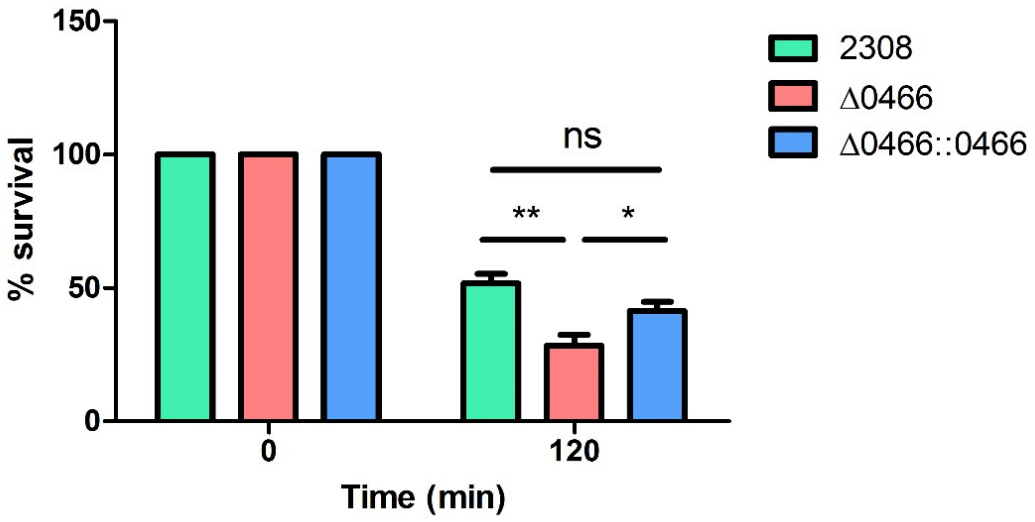

Figure 4.16. BAB1_0466 protein plays a role in *B. abortus* survival in human blood. Human whole blood was infected with 2308 WT, 2308Δ*0466* and 2308Δ*0466::0466* strains. CFUs were determined in blood lysates at the time of infection and 120 minutes after. Percent of *Brucella* survival was determined by dividing CFU/ml at each time point by CFU/ml at 0 min and normalized to time 0 (100 %). n=3 biological replicates. Two tailed *t*-test = *p<0.05 and **p<0.01. ns, not significant. All values are represented as the mean ± SEM.

enhanced killing of *Brucella* in the absence of BAB1_0466. For that purpose, we used different innate immune cell lines as outlined in Figure 4.17.

Among the innate immune cells, neutrophils are the first line of defense after *Brucella* invasion, and are the cells with higher lysozyme content. *Brucella* is known to resist the killing action of these cells (Barquero-Calvo et al., 2013), so it is tempting to hypothesize that the presence of a lysozyme inhibitor could play an important part of this resistance. In order to have a stable and reliable source of neutrophils, we decided to use HL-60, a promyeloblast stable cell line that can be differentiated to neutrophils after treatment with reagents, such as DMF and ATRA (Manda-Handzlik et al., 2018), as outlined in Figure 4.17. Initially, we used HL-60 cells kindly provided by the laboratory of Javier León (IBBTEC). HL-60 cultures were treated with DMF for 5 days to obtain neutrophil-like cells. After infection of differentiated HL-60 cells, we could observed that after 90 minutes of infection, the 2308Δ*0466* mutant presented a statistically significant reduction in survival when compared with 2308 WT *Brucella* (Figure 4.18). However, analysis of these cells by flow cytometry shows that the initial

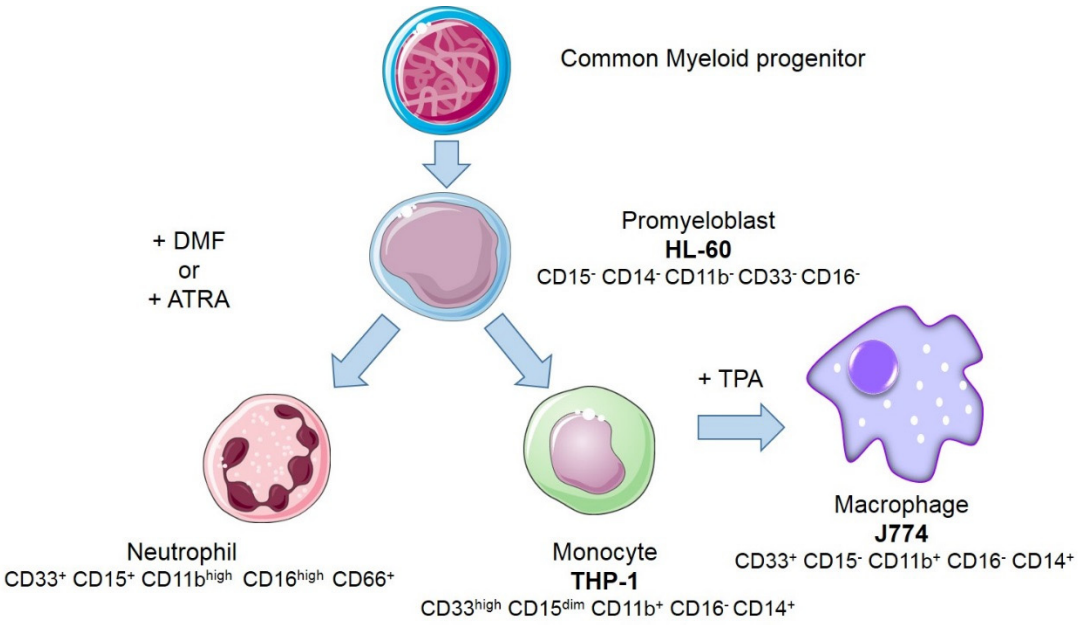

Figure 4.17. Schematic representation of the differentiation of myeloblastic cells. Common myeloid progenitor cells give origin to promyeloblast cells, which can proceed to differentiate into neutrophils or circulating monocytes. The monocytes can further differentiate into other cell types (only macrophages are shown here). HL-60 cells can be differentiated to neutrophil-like cells or monocyte/macrophages-like cells depending on the treatment. Cells treated with DMF or ATRA differentiate to neutrophil-like cells. However, HL-60 cells can also autodifferentiate to monocyte-like cells. The cell type can be determined by different membrane markers as indicated in the figure. There are available stable cell lines for monocytes, such as THP-1, and for macrophages, such as J774 (murine), but not for neutrophils. THP-1 cells can be differentiated to macrophages by treating the cells with TPA.

undifferentiated cell culture was highly heterogeneous (Table 4.6). Undifferentiated HL-60 cells should be negative for CD15, CD14, CD16, CD11b and CD33 antibodies (Figure 4.17). However, our initial population was highly heterogeneous: $CD15^+$ (100%), $CD16^-$, $CD14^+$, $CD11b^{lo}$ (3.45%), $CD33^+$ (75%) and $CD33^-$ (25%). And after treatment with DMF, instead of having a more or less homogeneous neutrophil-like population, HL-60 cells were differentiated to three different populations, neither of them with neutrophil-like markers (Table 4.6). According to the different markers present in each population, we had a 36.19 % of cells with specific markers of monocytes/macrophages; a 18.25 % of cells in an immature stage of monocytic differentiation, such as promonocyte-like cells; and the remaining 38.53 % of cells was very heterogeneous, so it was difficult to classify in a specific group. This implies that this cell line has probably suffered some level of predifferentiation during culture and storage in the laboratory, or

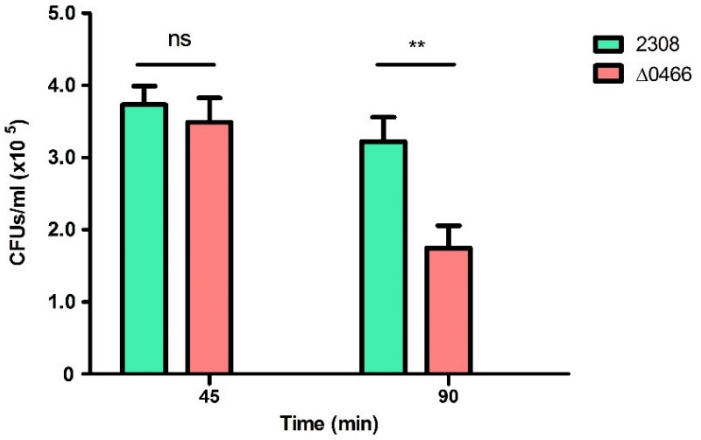

Figure 4.18. The lack of BAB1_0466 affects *B. abortus* survival in DMF-differentiated HL-60 cells. HL-60 cells (suerce: Javier León lab, IBBTEC) differentiated with DMF were infected with 2308 WT and 2308Δ*0466* strains at a MOI of 50. At indicated time points, CFU/ml were determined. n=4 biological replicates. Two tailed *t*-test = **p<0.01. ns, not significantAll values are represented as the mean ± SEM.

even some level of contamination. But it was interesting that some of the pupulations found in this mix showed a clear phenotype in mutant 2308Δ0466, so we did not discard these results.

We then tested a different batch of HL-60 cells, obtained from Jose Yuste's laboratory, which works specifically with HL-60 differentiation to neutrophil-like cells, and had published results with original cells. In this case, with his advice, we also changed the compound to promote the differentiation used previously for ATRA. This batch of HL-60 cells, previous to differentiation, were also heterogeneous (Table 4.6), and in agreement with our previous results. However, after differentiation with ATRA for 5 days, we obtained a homogeneous population consisting in a 96.16 % of neutrophil-like cells, something that was not observed in HL-60 cells from Javier León differenciated with ATRA (Table 4.6). Morevover, the cellular morphology when stained with Giemsa was consistent with neutrophils. So we carried out the phagocytosis assay with the neutrophil-like cells. First, we determined that neutrophil-like cells were phagocytizing either 2308 WT or 2308Δ0466 mutant expressing a fluorescent marker (Figure 4.19.A). Next, we determined *B. abortus* survival during neutrophil-like cells infection at MOI 50. As we can see in Figure 4.19.B, there are not significant differences in bacterial survival between 2308 WT and 2308Δ*0466*. Since *Brucella* LPS induces the premature death of neutrophils when there are many bacteria inside the same

cell (Barquero-Calvo et al., 2015), we decided to decrease the MOI. Thus, we repeated the experiment using a MOI of 5, but once again, we did not detect any significant difference between Δ*0466* mutant and WT (Figure 4.19.C).

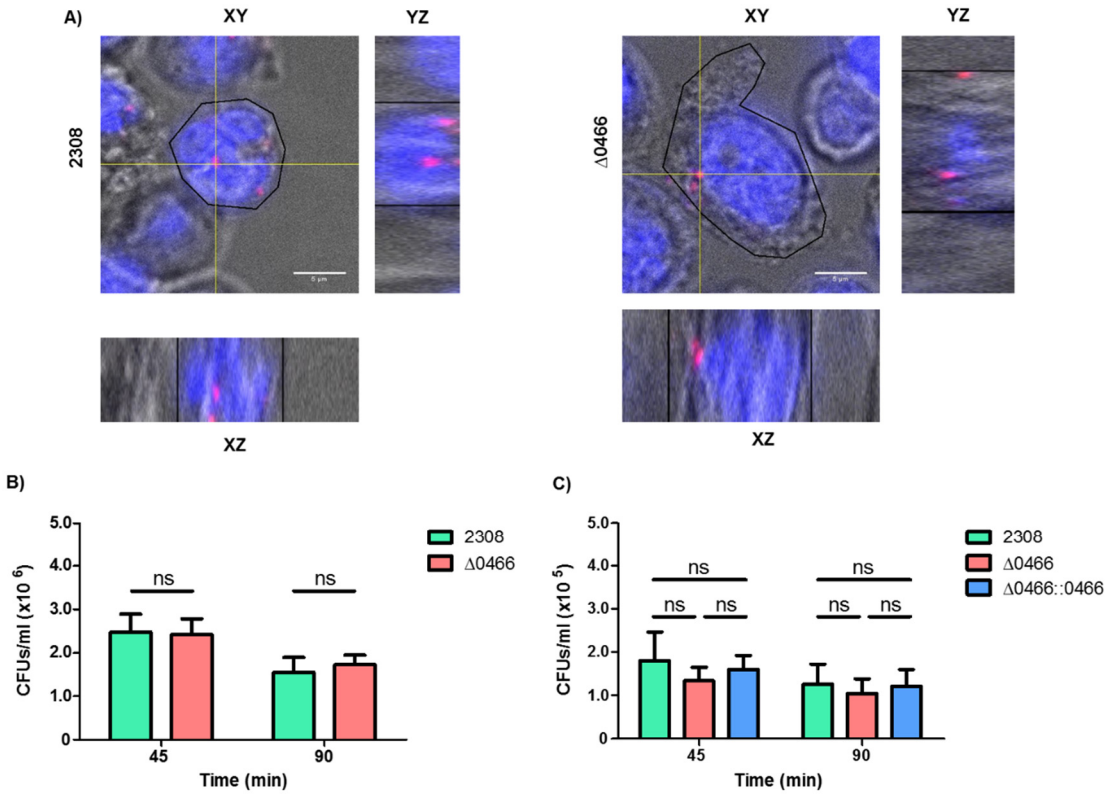

Figure 4.19. BAB1_0466 does not play a role in *B. abortus* survival during infection of neutrophil-like cells. **A)** Determination of neutrophil-like cells phagocytosis of 2308 WT and 2308Δ*0466* strains encoding DsRed by confocal microscopy. The orthogonal view of the cell was determined. Scale bar, 5 μm **B)** HL-60 cells (source: Jose Yuste lab) differentiated with ATRA were infected with 2308 WT and 2308Δ*0466* strains at a MOI of 50. At indicated time points, CFU/ml were determined. n=2 biological replicates. **C)** Same HL-60 cells differentiated with ATRA were infected with 2308 WT, 2308Δ*0466* and 2308Δ*0466::0466* strains at a MOI of 5. At indicated time points, CFU/ml were determined. n=3 biological replicates. Two tailed *t*-test = *p<0.05. ns, not significant. All values are represented as the mean ± SEM.

Due to inconsistencies with differenciated cell lines, we decided to carry out another assay using purified neutrophils from human whole blood samples. In other to maximize the integrity and function of the neutrophils, we used a purification kit that isolates functional, highly purified neutrophils directly from human whole blood by immunomagnetic negative selection. As the antibodies do not bind the neutrophil population, they are not activated. We also aimed to carry out the experiment in the first hour after extraction. With these precautions, we

consistently obtained preparations with more than 90 % of purity of neutrophils. The phagocytosis assay was repeated with the purified human neutrophils, and the results are shown in Figure 4.20. Again, neutrophils were phagocytizing 2308 WT and 2308Δ0466 strains, but the survival assay did not show any significant difference between groups. There was a slight, non-significant decrease in survival in the case of the 2308Δ0466 mutant strain when compared with the WT control, and it is also noteworthy that the complemented strain did not show the same level of survival as the other strains, but again, with no significant differences between groups (Figure 4.20.B).

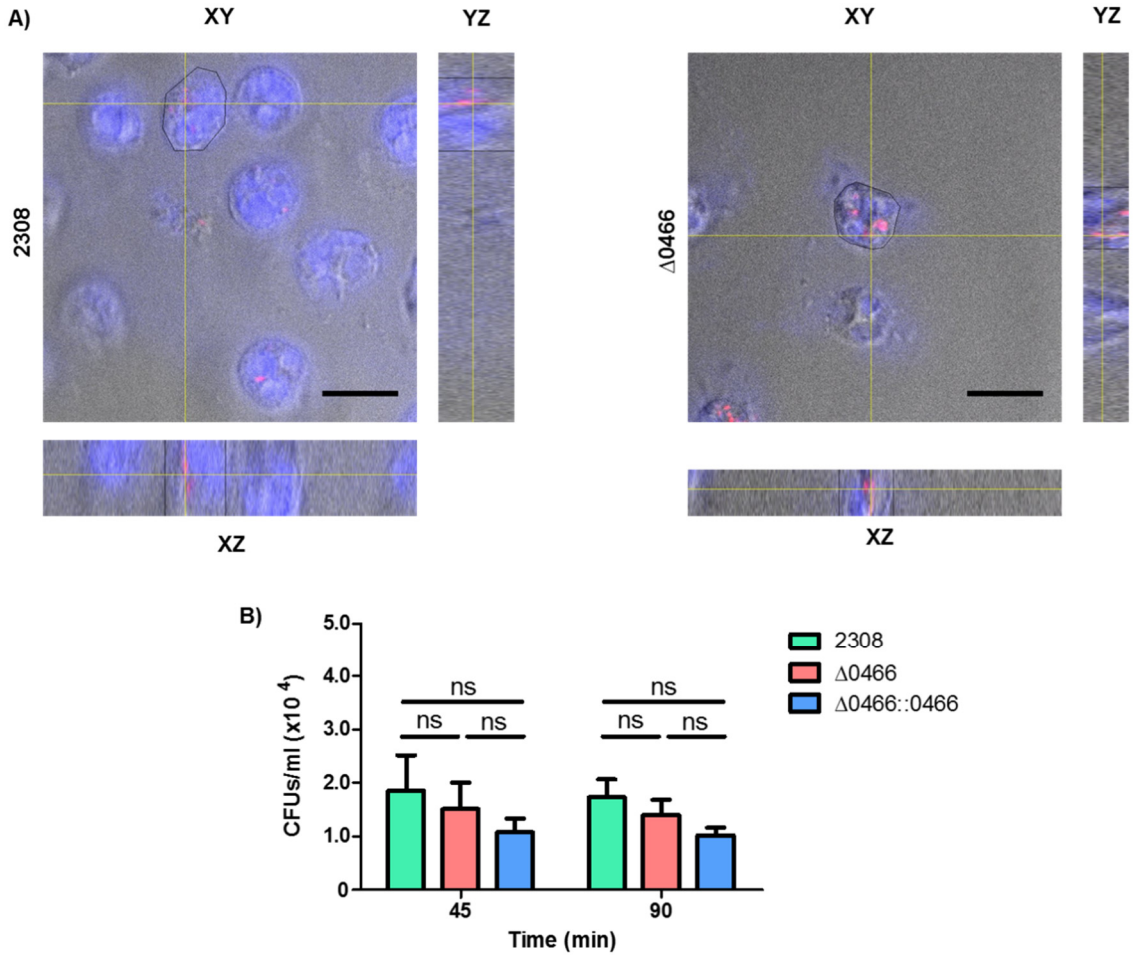

Figure 4.20. BAB1_0466 does not play a role in *B. abortus* survival during infection of purified human neutrophils. A) Determination of neutrophil phagocytosis of 2308 WT and 2308Δ*0466* strains expressing d*sRed* by confocal microscopy. The orthogonal view of the cell was determined. Scale bar, 5 μm. **B)** Human neutrophils were infected with the 2308 WT, 2308Δ*0466* and 2308Δ*0466::0466* strains at a MOI of 5. At indicated time points, CFU/ml were determined. n=3 biological replicates. Two tailed *t*-test = *p<0.05. ns, not significant. All values are represented as the mean ± SEM.

Cell line	Source	Treatment	Percentage (%)	Markers (%)					Phenotype
				CD15	CD16	CD14	CD11	CD33	
HL-60	Javier León laboratory	None	100	100	0	0	3.36	75	Heterogeneous
		70 µM DMF	36.19	14.40	0	36.19	100	99.84	Monocyte/Macrophage
			18.25	84.08	0	0	94.03	97.94	Promonocyte
			38.53	75.13	0	75.13	15.04	82.01	Heterogeneous
		1 µM ATRA	100	47.74	-	19.69	-	-	Heterogeneous
HL-60	Jose Yuste laboratory	None	100	92.60	0	0.36	3.45	100	Heterogeneous
		1 µM ATRA	96.16	96.16	100	9.14	100	100	Neutrophils

Table 4.6. Flow cytometry analysis of HL-60 cell lines from different origins before and after differentiation with different protocols.

These findings suggest that the decreased survival observed in the absence of BAB1_0466, both in whole blood and in the pre-differentiated HL-60 batch from Javier León laboratory, is not caused by a different survival inside neutrophils. We focused then in the contribution of monocytes/macrophages, the other populations present in the first HL-60 experiments. For this purpose, we carried out the phagocytosis experiment using a stable human monocytic cell line, THP-1. Using this cell line, we could observe approximately a 50 % reduction in the 2308Δ0466 mutant survival when compared to the 2308 WT (Figure 4.21). However, the different replicates of the experiment showed very high variability, and this difference is not significant. The complementation group, on the other hand was less dispersed, and it showed significant differences in the survival between the 2308Δ0466 mutant and the 2308Δ0466::0466 complemented strain. These results suggest that the presence of BAB1_0466 protein could favor *B. abortus* survival inside monocytes.

Finally, although we had already assayed the effect of BAB1_0466 in murine macrophages, where BAB1_0466 does not seem to play any significant role in *B. abortus* survival, we wanted to determine if BAB1_0466 could be playing a role during human macrophages infection. To do that, we differentiated THP-1

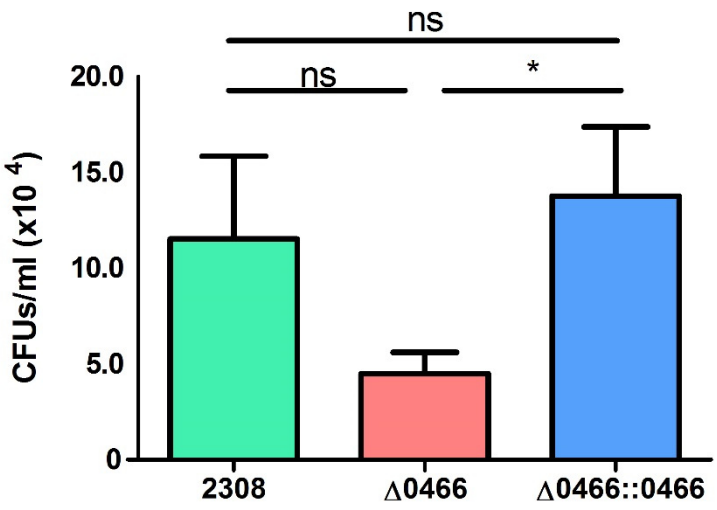

Figure 4.21. BAB1_0466 play a role in *B. abortus* survival during infection of human monocytes. THP1 monocytes were infected with 2308 WT, 2308Δ*0466* and *2308Δ0466::0466* strains at a MOI of 50. After 90 min of infection, CFU/ml were determined. n=3 biological replicates. Two tailed *t*-test = *p<0.05. ns, not significant. All values are represented as the mean ± SEM

monocytes into adherent macrophages using TPA. After differentiation, adherent cells were infected with the 2308 WT, 2308Δ0466 and 2308Δ0466::0466 *Brucella* strains. Results are shown in Figure 4.22, no differences could be observed in any group.

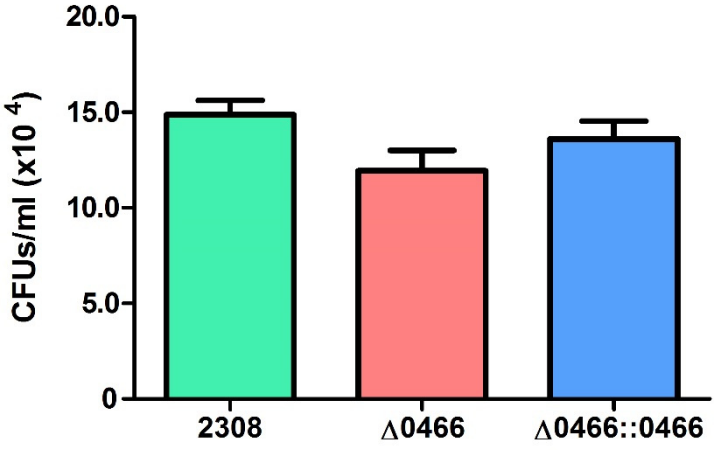

Figure 4.22. BAB1_0466 does not play a role in *B. abortus* survival during infection of human macrophages. THP1 monocytes were differentiated to macrophages using TPA and then infected with 2308 WT, 2308Δ*0466* and 2308Δ*0466::0466* strains at a MOI of 200. After 90 min of infection, CFU/ml were determined. n=1 biological replicate. All values are represented as the mean ± SEM

As a summary, we can conclude that BAB1_0466 contributes to *B. abortus* survival during infection, as was determined by peripheral whole blood assays. Our results indicate that this protein does not contribute to survival inside neither neutrophils nor macrophages. It is likely that this protein is playing a role during human monocyte infection, as indicate by the infection of HL-60 cells differentiated to monocyte/macrophage cells and infection of THP-1 cells.

Taken together, the results from this part of the thesis indicate that *B. abortus* expresses at least one lysozyme inhibitor that inhibits the activity of lysozyme *in vitro* and contributes to *B. abortus* defense against lysozyme activity when its OM is damaged. In addition, BAB1_0466 protein can play a role during *B. abortus* infection protecting the bacteria from the lytic action of lysozyme secreted by innate immune cells, especially during human monocyte infection.

DISCUSSION

5. DISCUSSION

5.1 Search for new *B. abortus* T4SS effector proteins

The first part of this Thesis work had the objective of finding new *Brucella* effector proteins through their interaction with Flaviviridae replication. For this purpose, we established a new screening method and tested selected putative effector proteins. Our main accomplishments are:

1) The generation of a pool of candidate effectors after thorough analysis of the existing prediction methods for effector proteins secreted by T4SS.
2) The setting up of a new screening method for effectors based on their interference with Flaviviridae replication.
3) The screening of the library with this method and, detection of some putative *B. abortus* effector proteins which alter the normal replication of YFV, becoming candidates for future research.

5.1.1 Analysis of T4SS effector protein prediction methods and generation of a list of *B. abortus* candidate effector proteins

T4SS secretes effector proteins into the host cell, where they play several roles promoting intracellular bacterial survival. They can mimic the function of host proteins, subvert functions in the cytoplasm of infected eukaryotic cells, and play vital roles in host-pathogen interactions (Xiong et al., 2018). The characterization of effectors, their host targets and functions, has contributed to our understanding of bacterial pathogenicity, and newly discovered effectors continue to provide insight into the complex interplay between bacteria and host.

Several experimental approaches have been developed to identify novel effector proteins secreted by bacterial T4SS, such as fusion protein reporter assays (Voth et al., 2012). However, these experimental approaches are time-consuming and expensive process, especially if the entire set of proteins in the complete genome of a bacterial pathogen wants to be analyzed. Therefore, it is essential to limit the number of proteins requiring experimental validation.

We revised several published software methods for the prediction of T4SS effector proteins (Meyer et al., 2013; Wang et al., 2017, Wang et al., 2014; Zou et al., 2013). We saw that neither of them is 100 % effective because none can predict the fifteen *Brucella* effector proteins described so far. Also, each of them predicted a set of putative effector proteins very different from the others, as can be seen in the Venn diagram in Figure 4.1. This is not surprising, because these methods use different sets of protein characteristics as features for their prediction (Figure 5.1). In addition, the methods used to validate effectors do not work for all of them (see section 4.1.1). These methodological limitations suggested that many Brucella T4SS effector proteins might still remain unknown.

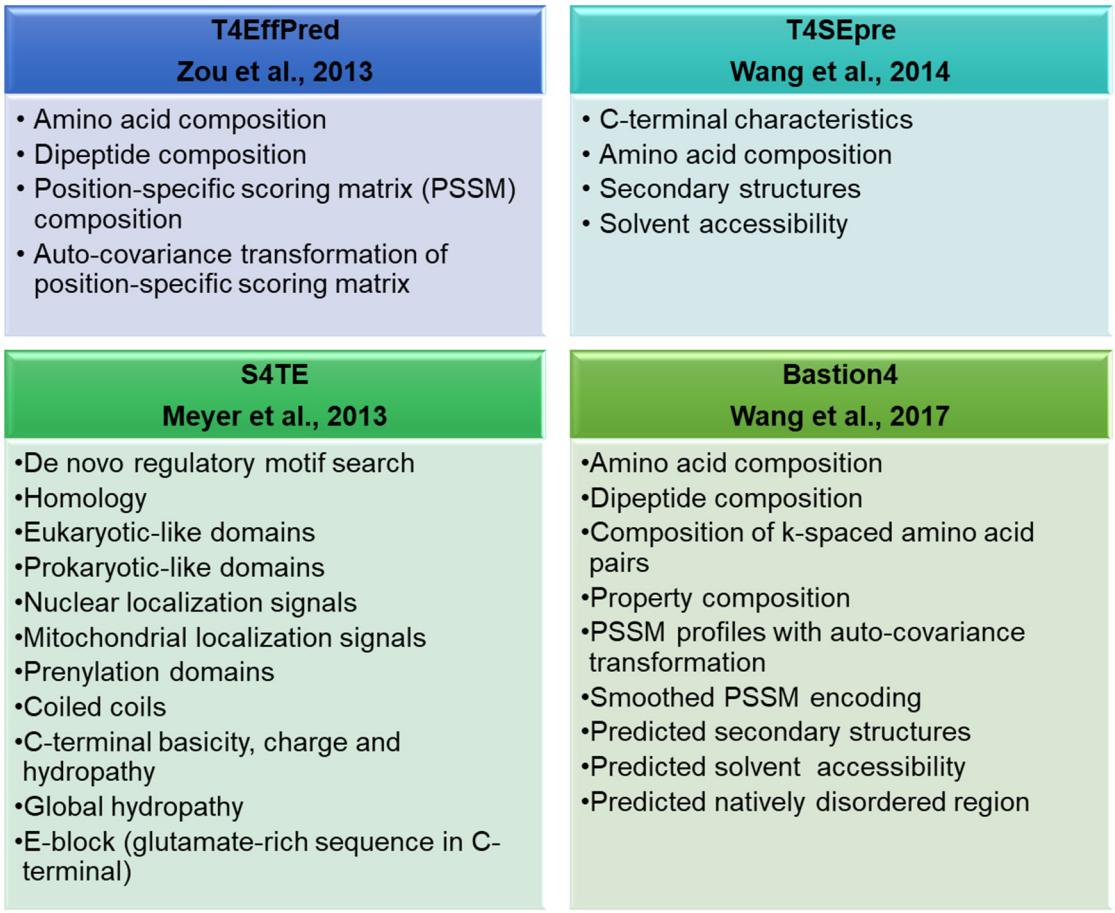

Figure 5.1. Comparison of the methods for prediction of T4SS effector proteins used in this work. The reference is indicated below the name of the method. The boxes detail the main protein features on which each method is based.

In order to select a reduced number of *Brucella* proteins for their study as putative effector proteins, we pooled all the candidates predicted by the four methods shown in Figure 5.1, and, we extended our list of candidates with other *Brucella* proteins predicted in the bibliography as putative effectors. Thus, our set of candidates was reduced from more than 3300 proteins in the *B. abortus* genome to a list of 256 proteins. These proteins were classified following several criteria, and 151 of them were selected for further study.

This library was continuously updated with new predictive methods. The generation of improved softwares for the prediction of effector proteins secreted by T4SS is a trendy topic. In fact, several methods are developed each year. The most recent are PredT4SE-stack (Xiong et al., 2018), S4TE 2.0 (Noroy et al., 2019) and OPT4e (Esna Ashari et al., 2019). S4TE 2.0 is the second version of S4TE, one of the softwares that we used. This new program is based on fourteen distinctive features and differs mainly, in the incorporation of one module to locate phosphorylation (EPIYA-like) domains. Also, compared with T4SEpre, this software is more sentitive and accurate for the identification of the known T4SS effector proteins of *Coxiella* and *Legionella* (around 10% more sensitive), and it is easir to use. (Noroy et al., 2019). Therefore, it is probable that more proteins will be included in the library in the future, and therefore new candidate proteins will be selected for screening.

5.1.2 Setting up a Viral Interference Assay to screen for new T4SS effectors

From the liste of 151 effector proteins and candidates, we picked a short list of *B. abortus* proteins known to be secreted, dependently or independently of the T4SS, to set up the assay and the initial screening. We co-infected human cells with YFV or HCV infective particles and lentiviral particles expressing our proteins of interest. As expected, heterogeneous levels of YFV infection were observed when cells were expressing different effector proteins, indicating that the assay was working as expected, and some of the *B. abortus* proteins were interfering with viral replication. However, the levels of HCV infection always decreased, independently of the effector protein that is being expressed in the cell. This result was unexpected, and we do not have an explanation for this

generalized inhibition. In view of this result, we considered that YFV is a better candidate than HCV to make the screening with our library of putative effector proteins.

From the YFV interference assay we could observe that BAB1_0279 and BAB1_0756 proteins, that correspond to the characterized BtpA and BtpB *Brucella* effector proteins, respectively, are toxic for the cells. The cytotoxic activity of these effector proteins has been very recently described, and it was associated with the TIR domain that both proteins contain (Coronas-Serna et al., 2019). These effectors also have to modulate energy metabolism in host cells (Coronas-Serna et al., 2019). Interestingly, these proteins also reduce YFV replication more than the rest of effector proteins tested. Additionally, the decrease in viral replication could be due to a defect in viral infection. In this way, BtpB could be reducing YFV infection by its capacity to inhibit endocytosis (Coronas-Serna et al., 2019).

5.1.3 Some putative *B. abortus* effector proteins alter YFV replication

Once the screening method was established, we carried out the viral interference assay for all putative *Brucella* effector proteins selected, co-infecting cells with our set of candidates and YFV infective particles. In this way, we found several *B. abortus* proteins that alter YFV replication (Figure 5.2): eight proteins that upregulate YFV replication, and seven proteins which downregulate YFV replication, plus the two effector proteins previously mentioned, BAB1_0279 and BAB1_0756.

We have found that most of the proteins which interfere negatively with viral replication show cytotoxicity (Fig. 4.9). This is not surprising, considering that effector proteins subvert the host cell metabolism, and we are overexpressing them from a strong promoter. Thus, cytotoxicity could also be a hint that these proteins play a role which alters the normal metabolism of the eukaryotic cell.

There is not much available information about the candidate effectors selected by our screening. Figure 5.3 shows the presence of conserved motifs in

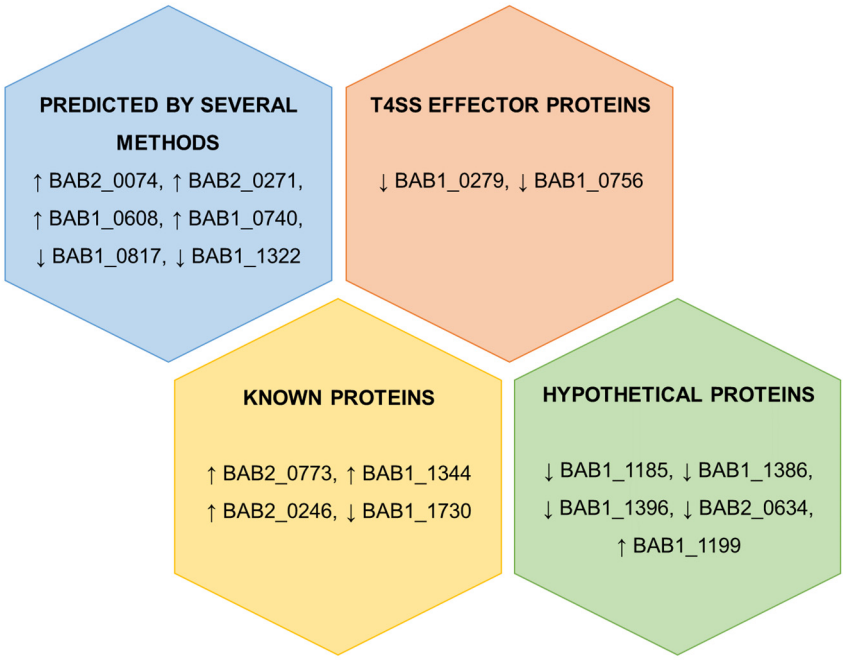

Figure 5.2. *Brucella* proteins that affect YFV replication. The main characteristic why they were selected is shown in each of the hexagons. Arrows indicate if the viral replication is increased or decreased in each case.

many of them. The available information about these *B. abortus* proteins will be detailed next, in the same order shown in Figure 5.3:

- BAB1_1185, was very recently identified as a secreted protein, and, it was also associated with *Brucella* cytotoxicity (Li et al., 2019). We also observed during our screening that the overexpression of this protein killed the cells (see plot in Figure 4.9). This protein is classified as a hypothetical protein in *B. abortus* 2308. However, a Blastp analysis determined that this protein presents a high homology with SgcJ/EcaC family of oxidoreductases of other *Brucella* strains.
- BAB1_0817 is classified as a hypothetical protein, although it has a region characteristic of FlgT-C superfamily. This type of proteins makes up part of the basal body of the flagellum. This protein was determined as essential for *Brucella* growth on rich medium (Sternon et al., 2018).
- BAB1_1386 has 98 % identity with cobalamin biosynthesis protein, CbiM, of other *Brucella* strains.
- BAB1_1396 was predicted to have 99% identity with the strongly immunoreactive BA14K protein of *B. suis* (Chirhart-Gilleland et al., 1998).

This protein was predicted to have a function in *Brucella* pathogenesis, due to the presence of the BA14K domain

- BAB1_1322 is a conserved hypothetical protein that contains a tellurite resistance protein B (TerB) region.
- BAB1_1730 is classified as a bacterial regulatory protein of the GntR family, and it seems that this protein can regulate bacterial transcription through its activity as DNA-binding transcription factor (Haydon and Guest, 1991).
- BAB2_0634 has a DUF983 superfamily domain, a domain with unknown functions.
- BAB2_0074 is a band 7 protein: stomatin and contains an HflC region that functions as regulator of the protease activity of HflC. It is predicted to be a membrane protein.
- BAB2_0271 contain a TPR domain that it is also present in human proteins (Bangs et al., 1998). Also, TPR-containing proteins are involved in a variety of biological processes including immunity and viral replication (Allan and Ratajczak, 2011).
- BAB1_0608 is classified as conserved hypothetical protein with an ALDH superfamily domain. Also, it has a 98 % identity with an ATPase of *B. melitensis.*
- BAB2_0773 is a secretion protein HlyD, a component of the prototypical alpha-haemolysin (HlyA) bacterial type I secretion system (Gentschev et al., 2002).
- There is no available information or relevant homology related to BAB1_0740
- BAB1_1344 is a SecD/SecF/SecDF membrane protein and according to InterPro database its function is related with the intracellular protein transport. This proteins was determined as essential proteins for *Brucella* growth on rich medium (Sternon et al., 2018).
- BAB2_0246 is a known *B. abortus* protein which product is ATP/GTP-binding site motif A (P-loop): cobalamin synthesis proteins /P47K.
- BAB1_1199 is an uncharacterized *Brucella* protein. This protein contain the domain of unknown function DUF218, that it is also found in other

bacteria proteins such as YdcF from *E. coli*, which has been shown to bind S-adenosyL- methionine (Chao et al., 2008).

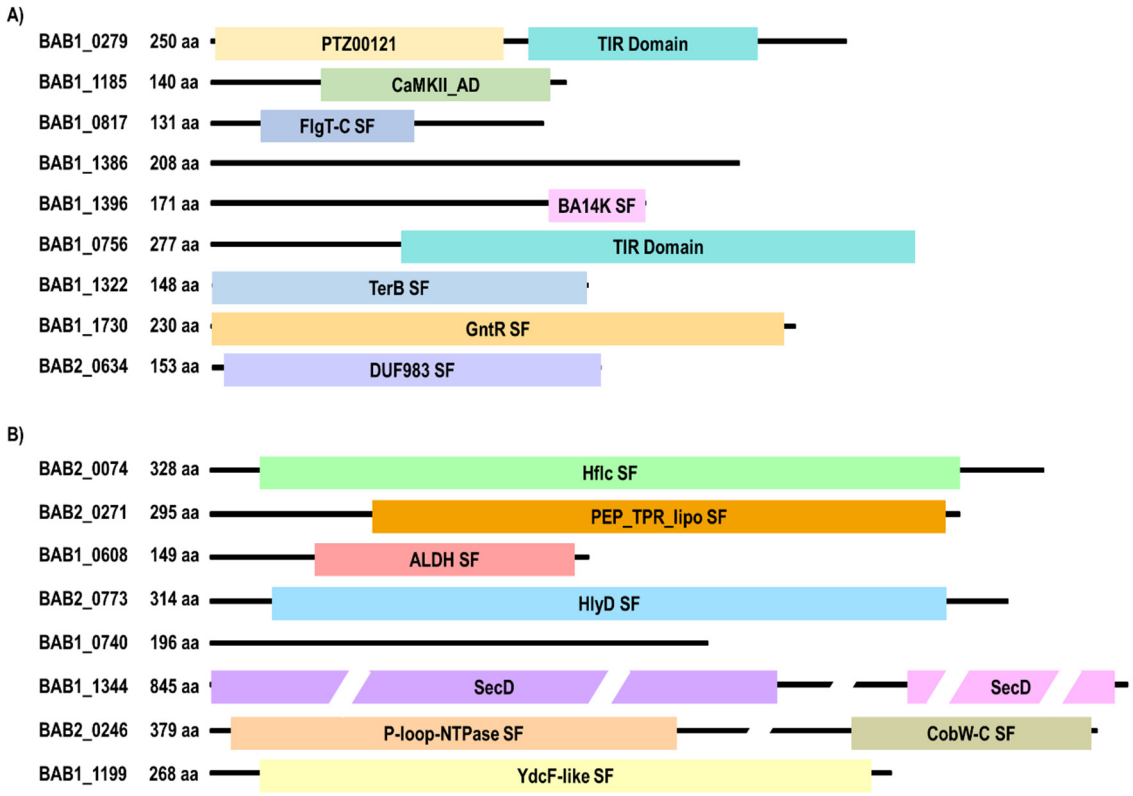

Figure 5.3. Main characteristics of *B. abortus* candidate effector proteins that **(A)** downregulate or **(B)** upregulate YFV replication**.** Colored rectangles represent homologies with known functional domains present in putative effector proteins.

Altogether, these results suggest that there are some putative T4SS effector proteins, according to prediction programs, that interfere with the YFV replication. Although there is not much information about many of them, the strength of the phenotype observed for some of them, together with other features such as the presence of eukaryotic domains, or the fact that they have been predicted as effectors by several different methods, lead us to think that they are good effector candidates. Much caution is needed, though, since these results are preliminary, and more assays are necessary to determine if these proteins are interfering with Flaviviridae viruses replication through their action in the host cell. And of course, it will be required to determine if these proteins are in fact *Brucella* effector proteins secreted by T4SS, testing them with the available translocation assays.

5.2 Characterization of putative lysozyme inhibitors of *Brucella*

In the second part of this Thesis, we have focused on potential lysozyme inhibitor proteins of *B.abortus*, selected on the basis of sequence homology and available structural data. We found that BAB1_0466 protein inhibits the lytic activity of Human and Hen Egg-White lysozyme *in vitro*. Its expression in *B.abortus* restores the resistance of 2308Δ*mapB*Δ*0466* double mutant to lysozyme activity to WT levels. Finally, our results suggest that BAB1_0466 could be playing a role during monocyte infection. Together, these results increase our knowledge of the importance of lysozyme inhibitor proteins during *Brucella* infection, especially when its cell envelope is damaged.

5.2.1 BAB1_0466 protein acts as a lysozyme inhibitor protein, while re-annotated BAB1_0102 protein does not

As previously mentioned, BAB1_0102 protein was re-annotated in our laboratory and identified as a putative lysozyme inhibitor by *in silico* analysis, based on the presence of the MliC superfamily domain. The re-annotation proposed a new transcriptional start site, which resulted in an N-terminal signal peptide, as expected for a lysozyme inhibitor. The MliC domain is necessary for the lysozyme inhibitor activity (Callewaert et al., 2008), because it contains the residues necessary for the interaction with the catalytic residues of lysozyme, the S89 and K103 residues of *P. aeruginosa* MliC (Yum et al., 2009). BAB1_0466, the other putative lysozyme inhibitor identified in *B. abortus*, contains both the MliC domain and the two residues necessary for the interaction with the lysozyme. In fact, Um et al., 2013 crystalized this protein alone and in complex with human lysozyme. BAB1_0102 protein, however, contains the MliC domain, but it does not have the residues necessary for interaction with lysozyme (see Figure 4.10). Consequently, the in vitro assay for the determination of BAB1_0466 and BAB1_0102 proteins as lysozyme inhibitors showed that BAB1_0466 is a functional homolog of MliC/PliC lysozyme inhibitors in *B. abortus*, while BAB1_0102 does not inhibit lysozyme activity. Thus, we conclude that, although BAB1_0102 contains a domain homologous to lysozyme

inhibitors, it is not a member of this protein family, probably due to the lack of the conserved residues required to interact with lysozyme.

We also attempted to test the activity of these proteins as inhibitors of other lysozyme-like proteins encoded by *B. abortus*, such as VirB1 and SagA. While we could not assess their role as inhibitors of VirB1, probably due to the lack of enough purified VirB1 protein, we could observe the lysozyme-like activity of SagA, and neither BAB1_0466 nor re-annotated BAB1_0102 inhibited its activity (Figure 4.13). However, it was recently published that PhiA, the complete BAB1_0102, inhibits SagA activity when both proteins are co-expressed in the same strain (Del Giudice et al., 2019). One possibility for the discrepancy between their results and ours is that the assay that they used is more sensitive than ours, and that is the reason why we cannot see the activity. Another possibility is that the complete BAB1_0102 protein is necessary to allow interaction with SagA. As we can see in Figure 5.4, there are some differences apart from the size between the complete BAB1_0102 (number 1 in Figure 5.4) and our re-annotated protein (numer 4 in Figure 5.4), such as is the presence of a putative signal peptide in our protein, absent in the complete BAB1_0102. When Del Giudice et al. (2019) analyzed the localization of PhiA-3xFLAG, they detected a protein of approximately 20 kDa instead of the expected size for the complete proteins (approximately 28 kDa). So, it is possible that the complete protein undergoes some post-translational processing, or that the transcription initiation site is not the one suggested by these authors. The detected protein is

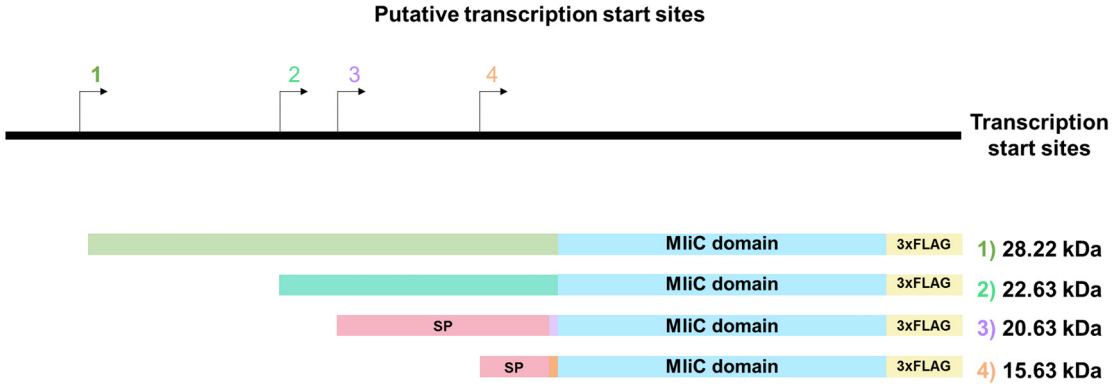

Figure 5.4. Putative transcriptional start sites of *bab1_0102*. *bab1_0102* gene could have four different transcription start sites, generating four different proteins, all of them containing the MliC domain. The expected size of these proteins fused to a C-terminal 3xFLAG tag is indicated to the right. SP, signal peptide

slightly larger than the putative size of our predicted protein with a 3xFLAG tag (16 kDa). This ORF has two other putative transcription initiation sites, which would encode proteins of approximately 23 and 21 kDa with a 3xFLAG tag (see Figure 5.4). Using SignalP-5.0, we searched for signal peptide cleavage sites. Only protein number 3 in Figure 5.4 presents a putative cleavage site that corresponds with the same cleavage site found in our re-annotated BAB1_0102. The presence of this signal peptide in the N-terminus, essential for Sec-dependent transport to the periplasm found in other lysozyme inhibitor proteins (Callewaert et al., 2008). In the future, it will be interesting to determine the correct initial transcriptional site and the BAB1_0102 protein isoform that inhibits SagA activity, as well as to test its activity inhibiting exogenous lysozyme.

5.2.2 BAB1_0466 inhibits lysozyme activity when the *B. abortus* cell envelope is damaged

Since we were able to detect a lysozyme inhibitoy activity only for BAB1_0466 protein, we decided to focus mainly in the study of this protein.

Once we demonstrated its lysozyme inhibitory function *in vitro*, the next step was to know if this protein play a role in the *in vivo* survival of *B. abortus*. As *Brucella* is know to be higly resistant to lysozyme and other cationic peptides such as lactoferrin and polymyxin B (Tejada et al., 1995), it was not unexpected to see that survival of a *B. abortus* mutant strain lacking BAB1_0466 was similar to the WT strain after exposure to lysozyme (Figure 4.14). We attempted to permeabilize the OM using different detergents, and did not see any effect in the sensibilization of *B. abortus* to lysozyme (not shown). It has been described that glycine, an amino acid that is incorporated instead of alanine into the nucleotide-activated peptidoglycan precursors, renders bacteria more sensitive to lysozyme action (Hammes et al., 1973). Growth of *Brucella* in the presence of a high concentration of glycine, and the concomitant increase in the sensitivity to lysozyme has been reported in the literature (Ralston et al., 1961). We confirmed that the tested *B. abortus* strains were more sensitive to lysis by lysozyme when treated with high concentrations of glycine (see Figure 4.14), but there were no significant differences in the survival of the ∆*0466* mutant when compared to the WT.

The role of BAB1_0466 as an inhibitor of lysozyme in *B. abortus* was finally revealed in the absence of MapB, a protein necessary for the integrity of *Brucella* OM (Bialer et al., 2019). A *B. suis* mutant defective in MapB (Δ*mapB*) shows an increased sensitivity to both lysozyme and the cationic lipopeptide polymyxin B. We decided to test if this was also the case in *B. abortus* 2308, so we re-constructed the Δ*mapB* mutation in all tested *B. abortus* strains. The introduction of the mutation renders all these strains more sensitive to the action of lysozyme (Figure 4.14.D-F). We did not detect significant differences between the single *mapB* mutant strain and any of the strains that contain in addition mutation of the putative inhibitors. But the complemented strain 2308Δ*mapB*Δ0466::0466 recovers the level of resistance of the WT strain. This is somehow puzzling, but not completely unexpected. The backbone vector for the complementation is pBBR1-MCS, a medium copy number plasmid that contains the lacZ promoter. Although useful in most instances, the expression levels driven by this plasmid are known to be excesive in some cases, like in the complementation of *virB5* mutants in *Brucella*, for example (Sprynski et al., 2012). As we do not know the basal levels of expression of *bab1_0466*, it is possible that we are expressing higher levels of the inhibitor, compensating not only the effect of the Δ*0466* mutation, but also those of the Δ*mapB* mutation. Thus, it is possible that, if the levels of inhibitor had been similar to WT, we would not have observed any phenotype, as the sensitivity to lysozyme of strains 2308ΔmapB and 2308ΔmapBΔ0466 is not significantly different. The use of a different complementation system, with a lower copy number plasmid, or even a single copy insertion, like those obtained with the miniTn7T-KmR system, would help to clarify this effect. In any case, these results suggest that BAB1_0466 inhibits lysozyme activity when a damaged cell envelope facilitates the access of this protein to the *B. abortus* periplasm, and thus it could play a role in *B. abortus* survival when the outer membrane is compromised, as illustrated in Figure 5.5.

5.2.3 BAB1_0466 plays a role in *B. abortus* survival inside human innate immune cells

When compared with other Gram-negative bacteria, *Brucella* has a more impermeable OM and this characteristic confers higher resistance to a number of

compounds, including lytic lysozyme (Tejada et al., 1995). Phagocytic cells, however, produce a vast array of antimicrobials, including reactive oxygen species, reactive nitrogen species, antimicrobial proteins like proteases, lysozyme or lactoferrin, and antimicrobial peptides, like defensins (Cohn and Wiener, 1963; Hancock and Scott, 2000). All these compounds can help disrupting the OM thus contributing to lysozyme action (Hancock et al., 1981; Hancock and Scott, 2000; Sawyer et al., 1988). It is possible that the combined action of a number of them, as occurs inside innate immune cells, destabilizes

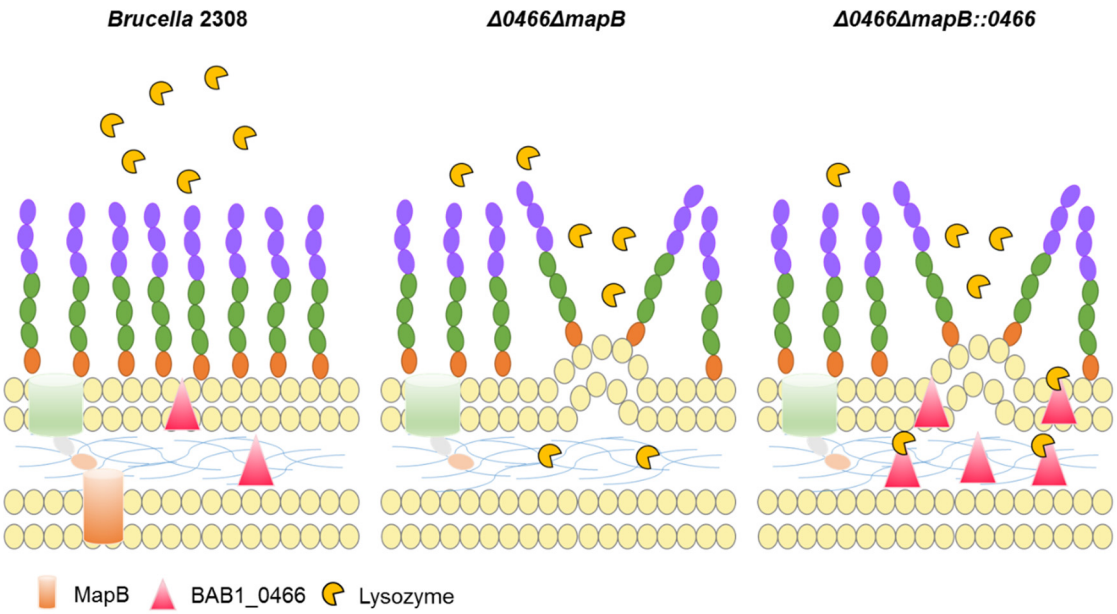

Figure 5.5. Model for BAB1_0466 role in *B. abortus*. In normal situations, *Brucella* produces MapB and BAB1_0466 proteins that protect *Brucella* from lysis by lysozyme. However, when these proteins are absent *Brucella* have an unstable OM that allows lysozyme access to peptidoglycan and lysates it. If BAB1_0466 expression is restored, lysozyme action is inhibit.

the *Brucella* OM, promoting the lysis of the bacteria by lysozyme. In this case, BAB1_0466 could be playing a role in *Brucella* survival inside these cells.

We have confirmed a role of BAB1_0466 in *B. abortus* survival using whole blood. Our attempts to pinpoint the specific cell types involved in this phenotype conclusively discarded neutrophils (purified from fresh blood) and macrophages, both from murine and human origin. Our results suggest that monocytes could be responsible for the differential killing of the mutant strain defective in BAB1_0466, since we observed significant differences between the survival rate of *Δ0466* and

Δ0466::0466 B. abortus strains upon infection of the monocyte cell line THP1 (Figure 4.21).

We cannot rule out in this moment the possibility that BAB1_0466 plays a role in defending *B. abortus* from the phagocytic activity of other cell types, like dendritic cells, or from lysozyme found in the plasma. It would not be surprising if the combined action of several innate immune cells found in the blood as well as factors found in the plasma may be required in order to cause the differences observed in survival between the 2308 WT and the 2308*Δ0466 B. abortus* strains in whole blood. Further experiments will be required to clarify all these pending questions.

One of the first clues that suggested that monocytes could be the cellular type responsible for the phenotype we were studying was the result obtained with a pre-differentiated batch of HL-60 cells. While the result was positive for our interests, a thorough analysis of the cell line concluded that these cells were not differenciating into the expected cell type (neutrophils). This result highlights the necessity to check the cell cultures that we use for our research. Cell lines can be contaminated or, as in our case, differentiated, and these differences compared to the original cells could account for a number of important deviations that could be the difference between obtaining a conclusive result or an artifact.

The other result that gave us a hint on the *in vivo* involvement of BAB1_0466 came from the complementation results obtained in mutant 2308*ΔmapBΔ0466::0466* (Figure 4.14 D-F). As discussed in the previous section, this result suggests that the defensive effect of the inhibitor is manifested only when the bacterial envelope is damaged, allowing acces of the lysozyme to the periplasm. The fact that we observe a decrease in bacterial survival in monocytes and not in other blood cell types could be explained by a specific action of these cells against the bacterial envelope. Figure 5.6 illustrates a possible model for the defensive action of BAB1_0466 during infection. Monocytes could combine an attack of different molecules compromising the integrity of the OM barrier of *Brucella*, and allowing lysozyme to cross; under these circumstances, BAB1_0466 could play a role in vivo neutralizing this periplasmic lysozyme.

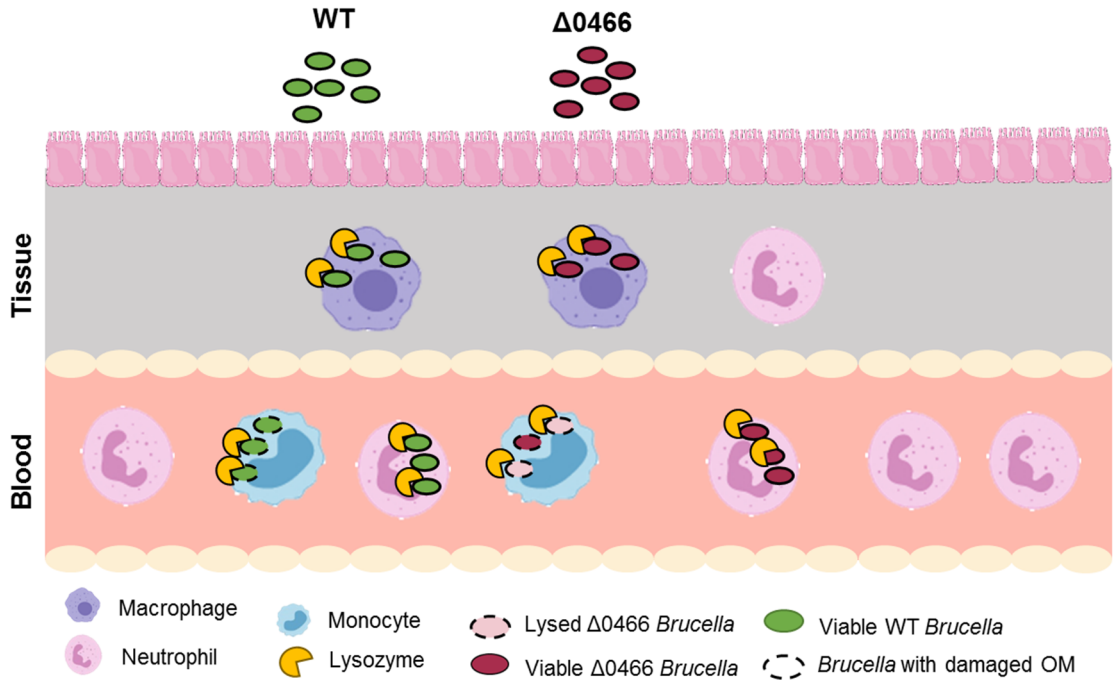

Figure 5.6. Proposed model of action of BAB1_0466 during *B. abortus* infection. When BAB1_0466 is absent, *B. abortus* is more sensitive to lysozyme action in whole blood. Monocytes would be producing lysozyme and other compounds that could permeabilize the *B. abortus* cell envelope, facilitating lysozyme action. In contrast, when BAB1_0466 is present, it inhibits lysozyme activity allowing *B. abortus* survival inside the cells even if the envelope is damaged.

Altogether, our findings support a role for BAB1_0466 in *B. abortus* lysozyme resistance and suggest that this lysozyme inhibitor is a new virulence determinant in *Brucella*. Because lysozyme inhibitors play a role in the survival of pathogenic Gram-negative bacteria in animal hosts, they have been proposed as an attractive novel target for antibacterial drug development, and also for vaccine production (Callewaert et al., 2008; Humbert et al., 2019). Although antibiotic resistance in Brucella is not a current concern, it is always good to expand the range of available treatments, and a new vaccine would certainly be useful. However, we are far from being able to propose the lysozyme inhibitor described in this work as a target for new antibiotics or part of a vaccine strategy, either as an immunogenic component, or as an attenuating mutation. Its contribution to virulence needs to be tested in an animal model to assess the impact of BAB1_0466, and we currently have no data about the antigenic potential of this protein, that would require future work.

CONCLUSIONS

6. CONCLUSIONS

1. None of the existing methods for prediction of bacterial effector proteins is totally effective for the prediction of *Brucella* T4SS effector proteins.
2. We have set up a new effector screening method based on assaying the interference with replication of the YFV. This method could be applied to any library of potential effectors affecting common intracellular routes with the YFV biology.
3. Screening of a library of 151 candidate *B. abortus* effector proteins by this assay showed that YFV replication is upregulated by proteins BAB2_0074, BAB2_0271, BAB1_0608, BAB1_0740, BAB1_1199, BAB2_0773, BAB1_1344 and BAB2_0246; while it is downregulated by BAB1_0817, BAB1_1322, BAB1_1730, BAB1_1185, BAB1_1386, BAB1_1396, BAB2_0634, BAB1_0279 and BAB1_0756.
4. The *B. abortus* genome encodes for two putative lysozyme inhibitors, according to their predicted homology to the MliC domain. BAB1_0466 MliC domain contains the conserved serine and lysine residues necessary for the interaction with lysozyme, while BAB1_0102 MliC domain does not.
5. Purified BAB1_0466 protein inhibits the lytic activity of hen egg-white and human lysozymes, while BAB1_0102 does not inhibit their activity.
6. Purified BAB1_0466 and BAB1_0102 do not inhibit the lytic activity of the lysozyme-like protein, SagA.
7. *B. abortus* is intrinsically resistant to the lytic action of lysozyme, which is only observed upon destabilization of the outer membrane by the absence of MapB protein.
8. In the absence of MapB, BAB1_0466 protein inhibits the lytic activity of lysozyme in vivo.
9. BAB1_0466 is necessary for survival of *B. abortus* during whole blood infection.
10. A *B. abortus bab1_0466* deletion mutant shows reduced survival rates within a human monocyte cell line, while it does not affect survival either within neutrophils purified from blood, or whithin mice or human macrophage cell lines.

BIBLIOGRAPHY

7. BIBLIOGRAPHY

Al Dahouk, S., Köhler, S., Occhialini, A., Jiménez de Bagüés, M.P., Hammerl, J.A., Eisenberg, T., Vergnaud, G., Cloeckaert, A., Zygmunt, M.S., Whatmore, A.M., Melzer, F., Drees, K.P., Foster, J.T., Wattam, A.R., Scholz, H.C., 2017. *Brucella* spp. of amphibians comprise genomically diverse motile strains competent for replication in macrophages and survival in mammalian hosts. Sci. Rep. 7, 44420. https://doi.org/10.1038/srep44420

Allan, R.K., Ratajczak, T., 2011. Versatile TPR domains accommodate different modes of target protein recognition and function. Cell Stress Chaperones 16, 353–367. https://doi.org/10.1007/s12192-010-0248-0

Al-Tawfiq, J.A., Memish, Z.A., 2013. Pregnancy associated brucellosis. Recent Patents Anti-Infect. Drug Disc. 8, 47–50. https://doi.org/10.2174/1574891X11308010009

Alton, G.G. (Commonwealth S. and I.R.O., Jones, L.M., Angus, R.D., Verger, J.M., 1988. Techniques for the brucellosis laboratory. INRA.

Arakawa, M., Morita, E., 2019. Flavivirus Replication Organelle Biogenesis in the Endoplasmic Reticulum: Comparison with Other Single-Stranded Positive-Sense RNA Viruses. Int. J. Mol. Sci. 20, 2336. https://doi.org/10.3390/ijms20092336

Arellano-Reynoso, B., Lapaque, N., Salcedo, S., Briones, G., Ciocchini, A.E., Ugalde, R., Moreno, E., Moriyón, I., Gorvel, J.-P., 2005. Cyclic β-1,2-glucan is a *brucella* virulence factor required for intracellular survival. Nat. Immunol. 6, 618. https://doi.org/10.1038/ni1202

Ariumi, Y., Kuroki, M., Maki, M., Ikeda, M., Dansako, H., Wakita, T., Kato, N., 2011. The ESCRT system is required for hepatitis C virus production. PloS One 6, e14517. https://doi.org/10.1371/journal.pone.0014517

Arriola Benitez, P.C., Rey Serantes, D., Herrmann, C.K., Pesce Viglietti, A.I., Vanzulli, S., Giambartolomei, G.H., Comerci, D.J., Delpino, M.V., 2016. The Effector Protein BPE005 from *Brucella abortus* Induces Collagen

Deposition and Matrix Metalloproteinase 9 Downmodulation via Transforming Growth Factor β1 in Hepatic Stellate Cells. Infect. Immun. 84, 598–606. https://doi.org/10.1128/IAI.01227-15

Atluri, V.L., Xavier, M.N., de Jong, M.F., den Hartigh, A.B., Tsolis, R.M., 2011. Interactions of the human pathogenic *Brucella* species with their hosts. Annu. Rev. Microbiol. 65, 523–541. https://doi.org/10.1146/annurev-micro-090110-102905

Bangs, P., Burke, B., Powers, C., Craig, R., Purohit, A., Doxsey, S., 1998. Functional Analysis of Tpr: Identification of Nuclear Pore Complex Association and Nuclear Localization Domains and a Role in mRNA Export. J. Cell Biol. 143, 1801–1812. https://doi.org/10.1083/jcb.143.7.1801

Bao, Y., Zhang, H., Huang, X., Ma, J., Logue, C.M., Nolan, L.K., Li, G., 2018. O-specific polysaccharide confers lysozyme resistance to extraintestinal pathogenic *Escherichia coli*. Virulence 9, 666–680. https://doi.org/10.1080/21505594.2018.1433979

Barouch-Bentov, R., Neveu, G., Xiao, F., Beer, M., Bekerman, E., Schor, S., Campbell, J., Boonyaratanakornkit, J., Lindenbach, B., Lu, A., Jacob, Y., Einav, S., 2016. Hepatitis C Virus Proteins Interact with the Endosomal Sorting Complex Required for Transport (ESCRT) Machinery via Ubiquitination To Facilitate Viral Envelopment. mBio 7, e01456-16. https://doi.org/10.1128/mBio.01456-16

Barquero-Calvo, E., Chaves-Olarte, E., Weiss, D.S., Guzmán-Verri, C., Chacón-Díaz, C., Rucavado, A., Moriyón, I., Moreno, E., 2007. *Brucella abortus* Uses a Stealthy Strategy to Avoid Activation of the Innate Immune System during the Onset of Infection. PLOS ONE 2, e631. https://doi.org/10.1371/journal.pone.0000631

Barquero-Calvo, E., Martirosyan, A., Ordoñez-Rueda, D., Arce-Gorvel, V., Alfaro-Alarcón, A., Lepidi, H., Malissen, B., Malissen, M., Gorvel, J.-P., Moreno, E., 2013. Neutrophils Exert a Suppressive Effect on Th1 Responses to Intracellular Pathogen *Brucella abortus*. PLOS Pathog. 9, e1003167. https://doi.org/10.1371/journal.ppat.1003167

Barquero-Calvo, E., Mora-Cartín, R., Arce-Gorvel, V., Diego, J.L. de, Chacón-Díaz, C., Chaves-Olarte, E., Guzmán-Verri, C., Buret, A.G., Gorvel, J.-P., Moreno, E., 2015. *Brucella abortus* Induces the Premature Death of Human Neutrophils through the Action of Its Lipopolysaccharide. PLOS Pathog. 11, e1004853. https://doi.org/10.1371/journal.ppat.1004853

Bertani, B., Ruiz, N., 2018. Function and Biogenesis of Lipopolysaccharides. EcoSal Plus 8. https://doi.org/10.1128/ecosalplus.ESP-0001-2018

Bialer, M.G., Ruiz-Ranwez, V., Sycz, G., Estein, S.M., Russo, D.M., Altabe, S., Sieira, R., Zorreguieta, A., 2019. MapB, the *Brucella suis* TamB homologue, is involved in cell envelope biogenesis, cell division and virulence. Sci. Rep. 9. https://doi.org/10.1038/s41598-018-37668-3

Blight, K.J., McKeating, J.A., Rice, C.M., 2002. Highly Permissive Cell Lines for Subgenomic and Genomic Hepatitis C Virus RNA Replication. J. Virol. 76, 13001–13014. https://doi.org/10.1128/JVI.76.24.13001-13014.2002

Boschiroli, M.L., Ouahrani-Bettache, S., Foulongne, V., Michaux-Charachon, S., Bourg, G., Allardet-Servent, A., Cazevieille, C., Liautard, J.P., Ramuz, M., O'Callaghan, D., 2002. The *Brucella suis virB* operon is induced intracellularly in macrophages. Proc. Natl. Acad. Sci. 99, 1544–1549. https://doi.org/10.1073/pnas.032514299

Boudaher, E., Shaffer, C.L., 2019. Inhibiting bacterial secretion systems in the fight against antibiotic resistance. MedChemComm 10, 682–692. https://doi.org/10.1039/C9MD00076C

Byk, L.A., Iglesias, N.G., De Maio, F.A., Gebhard, L.G., Rossi, M., Gamarnik, A.V., 2016. Dengue Virus Genome Uncoating Requires Ubiquitination. mBio 7. https://doi.org/10.1128/mBio.00804-16

Byndloss, M.X., Tsai, A.Y., Walker, G.T., Miller, C.N., Young, B.M., English, B.C., Seyffert, N., Kerrinnes, T., Jong, M.F. de, Atluri, V.L., Winter, M.G., Celli, J., Tsolis, R.M., 2019. *Brucella abortus* Infection of Placental Trophoblasts Triggers Endoplasmic Reticulum Stress-Mediated Cell Death and Fetal Loss via Type IV Secretion System-Dependent Activation of CHOP. mBio 10, e01538-19. https://doi.org/10.1128/mBio.01538-19

Callewaert, L., Aertsen, A., Deckers, D., Vanoirbeek, K.G.A., Vanderkelen, L., Herreweghe, J.M.V., Masschalck, B., Nakimbugwe, D., Robben, J., Michiels, C.W., 2008. A New Family of Lysozyme Inhibitors Contributing to Lysozyme Tolerance in Gram-Negative Bacteria. PLOS Pathog. 4, e1000019. https://doi.org/10.1371/journal.ppat.1000019

Callewaert, L., Michiels, C.W., 2010. Lysozymes in the animal kingdom. J. Biosci. 35, 127–160. https://doi.org/10.1007/s12038-010-0015-5

Callewaert, L., Van Herreweghe, J.M., Vanderkelen, L., Leysen, S., Voet, A., Michiels, C.W., 2012. Guards of the great wall: bacterial lysozyme inhibitors. Trends Microbiol. 20, 501–510. https://doi.org/10.1016/j.tim.2012.06.005

Cardoso, P.G., Macedo, G.C., Azevedo, V., Oliveira, S.C., 2006. *Brucella* spp noncanonical LPS: structure, biosynthesis, and interaction with host immune system. Microb. Cell Factories 5, 13. https://doi.org/10.1186/1475-2859-5-13

Carpp, L.N., Rogers, R.S., Moritz, R.L., Aitchison, J.D., 2014. Quantitative Proteomic Analysis of Host-virus Interactions Reveals a Role for Golgi Brefeldin A Resistance Factor 1 (GBF1) in Dengue Infection. Mol. Cell. Proteomics 13, 2836–2854. https://doi.org/10.1074/mcp.M114.038984

Celli, J., 2019. The Intracellular Life Cycle of *Brucella* spp. Microbiol. Spectr. 7. https://doi.org/10.1128/microbiolspec.BAI-0006-2019

Chao, K.L., Lim, K., Lehmann, C., Doseeva, V., Howard, A.J., Schwarz, F.P., Herzberg, O., 2008. The *Escherichia coli* YdcF binds S-adenosyl-L-methionine and adopts an α/β-fold characteristic of nucleotide-utilizing enzymes. Proteins Struct. Funct. Bioinforma. 72, 506–509. https://doi.org/10.1002/prot.22046

Chaplin, D.D., 2010. Overview of the immune response. J. Allergy Clin. Immunol., 2010 Primer on Allergic and Immunologic Diseases 125, S3–S23. https://doi.org/10.1016/j.jaci.2009.12.980

Chirhart-Gilleland, R.L., Kovach, M.E., Elzer, P.H., Jennings, S.R., Roop, R.M., 1998. Identification and characterization of a 14-kilodalton *Brucella*

abortus protein reactive with antibodies from naturally and experimentally infected hosts and T lymphocytes from experimentally infected BALB/c mice. Infect. Immun. 66, 4000–4003.

Christie, P.J., Whitaker, N., González-Rivera, C., 2014. Mechanism and structure of the bacterial type IV secretion systems. Biochim. Biophys. Acta 1843, 1578–1591. https://doi.org/10.1016/j.bbamcr.2013.12.019

Cirl, C., Wieser, A., Yadav, M., Duerr, S., Schubert, S., Fischer, H., Stappert, D., Wantia, N., Rodriguez, N., Wagner, H., Svanborg, C., Miethke, T., 2008. Subversion of Toll-like receptor signaling by a unique family of bacterial Toll/interleukin-1 receptor domain-containing proteins. Nat. Med. 14, 399–406. https://doi.org/10.1038/nm1734

Cloeckaert, A., Vizcaíno, N., Paquet, J.-Y., Bowden, R.A., Elzer, P.H., 2002. Major outer membrane proteins of *Brucella* spp.: past, present and future. Vet. Microbiol., Brucellosis S.I. 90, 229–247. https://doi.org/10.1016/S0378-1135(02)00211-0

Cloeckaert, A., Zygmunt, M.S., de Wergifosse, P., Dubray, G., Limet, J.N., 1992. Demonstration of peptidoglycan-associated *Brucella* outer-membrane proteins by use of monoclonal antibodies. J. Gen. Microbiol. 138, 1543–1550. https://doi.org/10.1099/00221287-138-7-1543

Cohn, Z.A., Wiener, E., 1963. The Particulate Hydrolases of Macrophages: I. Comparative Enzymology, Isolation, and Properties. J. Exp. Med. 118, 991–1008. https://doi.org/10.1084/jem.118.6.991

Collins, S.J., Gallo, R.C., Gallagher, R.E., 1977. Continuous growth and differentiation of human myeloid leukaemic cells in suspension culture. Nature 270, 347–349. https://doi.org/10.1038/270347a0

Coronas-Serna, J.M., Louche, A., Rodríguez-Escudero, M., Roussin, M., Imbert, P.R.C., Rodríguez-Escudero, I., Molina, M., Gorvel, J.-P., Cid, V.J., Salcedo, S.P., 2019. The TIR-domain containing effectors BtpA and BtpB from *Brucella abortus* block energy metabolism. bioRxiv 703330. https://doi.org/10.1101/703330

Crasta, O.R., Folkerts, O., Fei, Z., Mane, S.P., Evans, C., Martino-Catt, S., Bricker, B., Yu, G., Du, L., Sobral, B.W., 2008. Genome Sequence of *Brucella abortus* Vaccine Strain S19 Compared to Virulent Strains Yields Candidate Virulence Genes. PLOS ONE 3, e2193. https://doi.org/10.1371/journal.pone.0002193

de Barsy, M., Jamet, A., Filopon, D., Nicolas, C., Laloux, G., Rual, J.-F., Muller, A., Twizere, J.-C., Nkengfac, B., Vandenhaute, J., Hill, D.E., Salcedo, S.P., Gorvel, J.-P., Letesson, J.-J., De Bolle, X., 2011. Identification of a *Brucella* spp. secreted effector specifically interacting with human small GTPase Rab2. Cell. Microbiol. 13, 1044–1058. https://doi.org/10.1111/j.1462-5822.2011.01601.x

de Figueiredo, P., Ficht, T.A., Rice-Ficht, A., Rossetti, C.A., Adams, L.G., 2015. Pathogenesis and immunobiology of brucellosis: review of *Brucella*-host interactions. Am. J. Pathol. 185, 1505–1517. https://doi.org/10.1016/j.ajpath.2015.03.003

de Jong, M.F., Starr, T., Winter, M.G., den Hartigh, A.B., Child, R., Knodler, L.A., van Dijl, J.M., Celli, J., Tsolis, R.M., 2013. Sensing of bacterial type IV secretion via the unfolded protein response. mBio 4, e00418-00412. https://doi.org/10.1128/mBio.00418-12

de Jong, M.F., Sun, Y.-H., den Hartigh, A.B., van Dijl, J.M., Tsolis, R.M., 2008. Identification of VceA and VceC, two members of the VjbR regulon that are translocated into macrophages by the *Brucella* type IV secretion system. Mol. Microbiol. 70, 1378–1396. https://doi.org/10.1111/j.1365-2958.2008.06487.x

Decker, T., Lohmann-Matthes, M.-L., 1988. A quick and simple method for the quantitation of lactate dehydrogenase release in measurements of cellular cytotoxicity and tumor necrosis factor (TNF) activity. J. Immunol. Methods 115, 61–69. https://doi.org/10.1016/0022-1759(88)90310-9

Degos, C., Gagnaire, A., Banchereau, R., Moriyón, I., Gorvel, J.-P., 2015. *Brucella* CβG induces a dual pro- and anti-inflammatory response leading to a transient neutrophil recruitment. Virulence 6, 19–28. https://doi.org/10.4161/21505594.2014.979692

Del Giudice, M.G., Romani, A.M., Ugalde, J.E., Czibener, C., 2019. PhiA, a peptidoglycan hydrolase inhibitor of *Brucella* involved in the virulence process. Infect. Immun. https://doi.org/10.1128/IAI.00352-19

Demarre, G., Guérout, A.-M., Matsumoto-Mashimo, C., Rowe-Magnus, D.A., Marlière, P., Mazel, D., 2005. A new family of mobilizable suicide plasmids based on broad host range R388 plasmid (IncW) and RP4 plasmid (IncPα) conjugative machineries and their cognate *Escherichia coli* host strains. Res. Microbiol. 156, 245–255. https://doi.org/10.1016/j.resmic.2004.09.007

Diacovich, L., Gorvel, J.-P., 2010. Bacterial manipulation of innate immunity to promote infection. Nat. Rev. Microbiol. 8, 117–128. https://doi.org/10.1038/nrmicro2295

Döhmer, P.H., Valguarnera, E., Czibener, C., Ugalde, J.E., 2014. Identification of a type IV secretion substrate of *Brucella abortus* that participates in the early stages of intracellular survival. Cell. Microbiol. 16, 396–410. https://doi.org/10.1111/cmi.12224

Dower, W.J., Miller, J.F., Ragsdale, C.W., 1988. High efficiency transformation of *E. coli* by high voltage electroporation. Nucleic Acids Res. 16, 6127–6145. https://doi.org/10.1093/nar/16.13.6127

Durward, M., Radhakrishnan, G., Harms, J., Bareiss, C., Magnani, D., Splitter, G.A., 2012. Active Evasion of CTL Mediated Killing and Low Quality Responding CD8+ T Cells Contribute to Persistence of Brucellosis. PLOS ONE 7, e34925. https://doi.org/10.1371/journal.pone.0034925

Eisenberg, T., Riße, K., Schauerte, N., Geiger, C., Blom, J., Scholz, H.C., 2017. Isolation of a novel 'atypical' *Brucella* strain from a bluespotted ribbontail ray (*Taeniura lymma*). Antonie Van Leeuwenhoek 110, 221–234. https://doi.org/10.1007/s10482-016-0792-4

Ellison, R.T., Giehl, T.J., LaForce, F.M., 1988. Damage of the outer membrane of enteric gram-negative bacteria by lactoferrin and transferrin. Infect. Immun. 56, 2774–2781.

Endley, S., McMurray, D., Ficht, T.A., 2001. Interruption of the *cydB* locus in *Brucella abortus* attenuates intracellular survival and virulence in the mouse model of infection. J. Bacteriol. 183, 2454–2462. https://doi.org/10.1128/JB.183.8.2454-2462.2001

Esna Ashari, Z., Brayton, K.A., Broschat, S.L., 2019. Prediction of T4SS Effector Proteins for *Anaplasma phagocytophilum* Using OPT4e, A New Software Tool. Front. Microbiol. 10. https://doi.org/10.3389/fmicb.2019.01391

Fernandez-Garcia, M.-D., Mazzon, M., Jacobs, M., Amara, A., 2009. Pathogenesis of *flavivirus* infections: using and abusing the host cell. Cell Host Microbe 5, 318–328. https://doi.org/10.1016/j.chom.2009.04.001

Foster, G., Osterman, B.S., Godfroid, J., Jacques, I., Cloeckaert, A., 2007. *Brucella ceti* sp. nov. and *Brucella* pinnipedialis sp. nov. for *Brucella* strains with cetaceans and seals as their preferred hosts. Int. J. Syst. Evol. Microbiol. 57, 2688–2693. https://doi.org/10.1099/ijs.0.65269-0

Foster, J.T., Beckstrom-Sternberg, S.M., Pearson, T., Beckstrom-Sternberg, J.S., Chain, P.S.G., Roberto, F.F., Hnath, J., Brettin, T., Keim, P., 2009. Whole-genome-based phylogeny and divergence of the genus *Brucella*. J. Bacteriol. 191, 2864–2870. https://doi.org/10.1128/JB.01581-08

Franc, K.A., Krecek, R.C., Häsler, B.N., Arenas-Gamboa, A.M., 2018. Brucellosis remains a neglected disease in the developing world: a call for interdisciplinary action. BMC Public Health 18. https://doi.org/10.1186/s12889-017-5016-y

Galińska, E.M., Zagórski, J., 2013. Brucellosis in humans--etiology, diagnostics, clinical forms. Ann. Agric. Environ. Med. AAEM 20, 233–238.

Gall, A., Gaudet, R.G., Gray-Owen, S.D., Salama, N.R., 2017. TIFA Signaling in Gastric Epithelial Cells Initiates the cag Type 4 Secretion System-Dependent Innate Immune Response to Helicobacter pylori Infection. mBio 8. https://doi.org/10.1128/mBio.01168-17

Gee, J.M., Valderas, M.W., Kovach, M.E., Grippe, V.K., Robertson, G.T., Ng, W.-L., Richardson, J.M., Winkler, M.E., Roop, R.M., 2005. The *Brucella abortus* Cu,Zn Superoxide Dismutase Is Required for Optimal Resistance

to Oxidative Killing by Murine Macrophages and Wild-Type Virulence in Experimentally Infected Mice. Infect. Immun. 73, 2873–2880. https://doi.org/10.1128/IAI.73.5.2873-2880.2005

Gentschev, I., Dietrich, G., Goebel, W., 2002. The *E. coli* α-hemolysin secretion system and its use in vaccine development. Trends Microbiol. 10, 39–45. https://doi.org/10.1016/S0966-842X(01)02259-4

Germi, R., Crance, J.-M., Garin, D., Guimet, J., Lortat-Jacob, H., Ruigrok, R.W.H., Zarski, J.-P., Drouet, E., 2002. Heparan Sulfate-Mediated Binding of Infectious Dengue Virus Type 2 and Yellow Fever Virus. Virology 292, 162–168. https://doi.org/10.1006/viro.2001.1232

Gerold, G., Bruening, J., Weigel, B., Pietschmann, T., 2017. Protein Interactions during the *Flavivirus* and *Hepacivirus* Life Cycle. Mol. Cell. Proteomics 16, S75–S91. https://doi.org/10.1074/mcp.R116.065649

Gerold, G., Meissner, F., Bruening, J., Welsch, K., Perin, P.M., Baumert, T.F., Vondran, F.W., Kaderali, L., Marcotrigiano, J., Khan, A.G., Mann, M., Rice, C.M., Pietschmann, T., 2015. Quantitative Proteomics Identifies Serum Response Factor Binding Protein 1 as a Host Factor for Hepatitis C Virus Entry. Cell Rep. 12, 864–878. https://doi.org/10.1016/j.celrep.2015.06.063

Giudice, M.G.D., Döhmer, P.H., Spera, J.M., Laporte, F.T., Marchesini, M.I., Czibener, C., Ugalde, J.E., 2016. VirJ Is a *Brucella* Virulence Factor Involved in the Secretion of Type IV Secreted Substrates. J. Biol. Chem. 291, 12383–12393. https://doi.org/10.1074/jbc.M116.730994

Giudice, M.G.D., Ugalde, J.E., Czibener, C., 2013. A lysozyme-like protein in *Brucella abortus* is involved in the early stages of intracellular replication. Infect. Immun. IAI.01158-12. https://doi.org/10.1128/IAI.01158-12

Głowacka, P., Żakowska, D., Naylor, K., Niemcewicz, M., Bielawska-Drózd, A., 2018. *Brucella* – Virulence Factors, Pathogenesis and Treatment. Pol. J. Microbiol. 67, 151–161. https://doi.org/10.21307/pjm-2018-029

Godfroid, J., Al Dahouk, S., Pappas, G., Roth, F., Matope, G., Muma, J., Marcotty, T., Pfeiffer, D., Skjerve, E., 2013. A “One Health” surveillance and control of brucellosis in developing countries: Moving away from

improvisation. Comp. Immunol. Microbiol. Infect. Dis., Special issue: One Health 36, 241–248. https://doi.org/10.1016/j.cimid.2012.09.001

Goenka, R., Guirnalda, P.D., Black, S.J., Baldwin, C.L., 2012. B Lymphocytes provide an infection niche for intracellular bacterium *Brucella abortus*. J. Infect. Dis. 206, 91–98. https://doi.org/10.1093/infdis/jis310

Gonzalez, O., Fontanes, V., Raychaudhuri, S., Loo, R., Loo, J., Arumugaswami, V., Sun, R., Dasgupta, A., French, S.W., 2009. The heat shock protein inhibitor Quercetin attenuates hepatitis C virus production. Hepatol. Baltim. Md 50, 1756–1764. https://doi.org/10.1002/hep.23232

Graham, F.L., Smiley, J., Russell, W.C., Nairn, R., 1977. Characteristics of a human cell line transformed by DNA from human adenovirus type 5. J. Gen. Virol. 36, 59–74. https://doi.org/10.1099/0022-1317-36-1-59

Grant, S.G., Jessee, J., Bloom, F.R., Hanahan, D., 1990. Differential plasmid rescue from transgenic mouse DNAs into *Escherichia coli* methylation-restriction mutants. Proc. Natl. Acad. Sci. U. S. A. 87, 4645–4649. https://doi.org/10.1073/pnas.87.12.4645

Gross, A., Bertholet, S., Mauel, J., Dornand, J., 2004. Impairment of *Brucella* growth in human macrophagic cells that produce nitric oxide. Microb. Pathog. 36, 75–82. https://doi.org/10.1016/j.micpath.2003.09.003

Gross, A., Terraza, A., Ouahrani-Bettache, S., Liautard, J.P., Dornand, J., 2000. In vitro *Brucella suis* infection prevents the programmed cell death of human monocytic cells. Infect. Immun. 68, 342–351. https://doi.org/10.1128/iai.68.1.342-351.2000

Gutiérrez-Jiménez, C., Mora-Cartín, R., Altamirano-Silva, P., Chacón-Díaz, C., Chaves-Olarte, E., Moreno, E., Barquero-Calvo, E., 2019. Neutrophils as Trojan Horse Vehicles for *Brucella abortus* Macrophage Infection. Front. Immunol. 10. https://doi.org/10.3389/fimmu.2019.01012

Guzman-Verri, C., Manterola, L., Sola-Landa, A., Parra, A., Cloeckaert, A., Garin, J., Gorvel, J.-P., Moriyon, I., Moreno, E., Lopez-Goni, I., 2002. The two-component system BvrR/BvrS essential for *Brucella abortus* virulence regulates the expression of outer membrane proteins with counterparts in

members of the Rhizobiaceae. Proc. Natl. Acad. Sci. U. S. A. 99, 12375–12380. https://doi.org/10.1073/pnas.192439399

Hammes, W., Schleifer, K.H., Kandler, O., 1973. Mode of Action of Glycine on the Biosynthesis of Peptidoglycan. J. Bacteriol. 116, 1029–1053.

Hancock, R.E., Raffle, V.J., Nicas, T.I., 1981. Involvement of the outer membrane in gentamicin and streptomycin uptake and killing in Pseudomonas aeruginosa. Antimicrob. Agents Chemother. 19, 777–785.

Hancock, R.E.W., Scott, M.G., 2000. The role of antimicrobial peptides in animal defenses. Proc. Natl. Acad. Sci. 97, 8856–8861. https://doi.org/10.1073/pnas.97.16.8856

Hanna, N., Jiménez de Bagüés, M.P., Ouahrani-Bettache, S., El Yakhlifi, Z., Köhler, S., Occhialini, A., 2011. The *virB* operon is essential for lethality of *Brucella microti* in the Balb/c murine model of infection. J. Infect. Dis. 203, 1129–1135. https://doi.org/10.1093/infdis/jiq163

Haydon, D.J., Guest, J.R., 1991. A new family of bacterial regulatory proteins. FEMS Microbiol. Lett. 63, 291–295. https://doi.org/10.1016/0378-1097(91)90101-f

He, Y., Reichow, S., Ramamoorthy, S., Ding, X., Lathigra, R., Craig, J.C., Sobral, B.W.S., Schurig, G.G., Sriranganathan, N., Boyle, S.M., 2006. *Brucella melitensis* Triggers Time-Dependent Modulation of Apoptosis and Down-Regulation of Mitochondrion-Associated Gene Expression in Mouse Macrophages. Infect. Immun. 74, 5035–5046. https://doi.org/10.1128/IAI.01998-05

Herrou, J., Willett, J.W., Fiebig, A., Czyż, D.M., Cheng, J.X., Ultee, E., Briegel, A., Bigelow, L., Babnigg, G., Kim, Y., Crosson, S., 2019. *Brucella* Periplasmic Protein EipB Is a Molecular Determinant of Cell Envelope Integrity and Virulence. J. Bacteriol. 201, e00134-19. https://doi.org/10.1128/JB.00134-19

Höltje, J.V., Mirelman, D., Sharon, N., Schwarz, U., 1975. Novel type of murein transglycosylase in *Escherichia coli*. J. Bacteriol. 124, 1067–1076.

Horwitz, J.A., Dorner, M., Friling, T., Donovan, B.M., Vogt, A., Loureiro, J., Oh, T., Rice, C.M., Ploss, A., 2013. Expression of heterologous proteins flanked by NS3-4A cleavage sites within the hepatitis C virus polyprotein. Virology 439, 23–33. https://doi.org/10.1016/j.virol.2013.01.019

Hull, N.C., Schumaker, B.A., 2018. Comparisons of brucellosis between human and veterinary medicine. Infect. Ecol. Epidemiol. 8. https://doi.org/10.1080/20008686.2018.1500846

Humbert, M.V., Awanye, A.M., Lian, L.-Y., Derrick, J.P., Christodoulides, M., 2017. Structure of the *Neisseria* Adhesin Complex Protein (ACP) and its role as a novel lysozyme inhibitor. PLOS Pathog. 13, e1006448. https://doi.org/10.1371/journal.ppat.1006448

Humbert, M.V., Jackson, A., Orr, C.M., Tews, I., Christodoulides, M., 2019. Characterization of two putative *Dichelobacter nodosus* footrot vaccine antigens identifies the first lysozyme inhibitor in the genus. Sci. Rep. 9, 10055. https://doi.org/10.1038/s41598-019-46506-z

Ibrahim, H.R., Higashiguchi, S., Koketsu, M., Juneja, L.R., Kim, M., Yamamoto, T., Sugimoto, Y., Aoki, T., 1996. Partially Unfolded Lysozyme at Neutral pH Agglutinates and Kills Gram-Negative and Gram-Positive Bacteria through Membrane Damage Mechanism. J. Agric. Food Chem. 44, 3799–3806. https://doi.org/10.1021/jf960133x

Jimenez de Bagues, M.-P., Dudal, S., Dornand, J., Gross, A., 2005. Cellular bioterrorism: how *Brucella* corrupts macrophage physiology to promote invasion and proliferation. Clin. Immunol., Renovations for an intracellular life style 114, 227–238. https://doi.org/10.1016/j.clim.2004.07.010

Jindadamrongwech, S., Thepparit, C., Smith, D.R., 2004. Identification of GRP 78 (BiP) as a liver cell expressed receptor element for dengue virus serotype 2. Arch. Virol. 149, 915–927. https://doi.org/10.1007/s00705-003-0263-x

Jumas-Bilak, E., Michaux-Charachon, S., Bourg, G., Ramuz, M., Allardet-Servent, A., 1998. Unconventional Genomic Organization in the Alpha Subgroup of the Proteobacteria. J. Bacteriol. 180, 2749–2755.

Ke, P.-Y., 2018. The Multifaceted Roles of Autophagy in *Flavivirus*-Host Interactions. Int. J. Mol. Sci. 19. https://doi.org/10.3390/ijms19123940

Ke, Y., Wang, Y., Li, W., Chen, Z., 2015. Type IV secretion system of *Brucella* spp. and its effectors. Front. Cell. Infect. Microbiol. 5. https://doi.org/10.3389/fcimb.2015.00072

Kelley, L.A., Mezulis, S., Yates, C.M., Wass, M.N., Sternberg, M.J.E., 2015. The Phyre2 web portal for protein modeling, prediction and analysis. Nat. Protoc. 10, 845–858. https://doi.org/10.1038/nprot.2015.053

Klüter, T., Fitschen-Oestern, S., Lippross, S., Weuster, M., Mentlein, R., Steubesand, N., Neunaber, C., Hildebrand, F., Pufe, T., Tohidnezhad, M., Beyer, A., Seekamp, A., Varoga, D., 2014. The Antimicrobial Peptide Lysozyme Is Induced after Multiple Trauma [WWW Document]. Mediators Inflamm. https://doi.org/10.1155/2014/303106

Ko, J., Splitter, G.A., 2000. Residual virulence of *Brucella abortus* in the absence of the cytochrome bc(1)complex in a murine model in vitro and in vivo. Microb. Pathog. 29, 191–200. https://doi.org/10.1006/mpat.2000.0373

Koraimann, G., 2003. Lytic transglycosylases in macromolecular transport systems of Gram-negative bacteria. Cell. Mol. Life Sci. CMLS 60, 2371–2388. https://doi.org/10.1007/s00018-003-3056-1

Kreutzer, D.L., Dreyfus, L.A., Robertson, D.C., 1979. Interaction of polymorphonuclear leukocytes with smooth and rough strains of *Brucella abortus*. Infect. Immun. 23, 737–742.

Landy, A., 1989. Dynamic, structural, and regulatory aspects of lambda site-specific recombination. Annu. Rev. Biochem. 58, 913–949. https://doi.org/10.1146/annurev.bi.58.070189.004405

Lapaque, N., Moriyon, I., Moreno, E., Gorvel, J.-P., 2005. *Brucella* lipopolysaccharide acts as a virulence factor. Curr. Opin. Microbiol., Host--microbe interactions: bacteria 8, 60–66. https://doi.org/10.1016/j.mib.2004.12.003

Lavigne, J.-P., Patey, G., Sangari, F.J., Bourg, G., Ramuz, M., O'Callaghan, D., Michaux-Charachon, S., 2005. Identification of a New Virulence Factor,

BvfA, in Brucella suis. Infect. Immun. 73, 5524–5529. https://doi.org/10.1128/IAI.73.9.5524-5529.2005

Lehrer, R.I., 1998. Microbicidal Mechanisms, Oxygen-Independent, in: Encyclopedia of Immunology. Elsevier, pp. 1719–1725. https://doi.org/10.1006/rwei.1999.0436

Lestrate, P., Dricot, A., Delrue, R.-M., Lambert, C., Martinelli, V., Bolle, X.D., Letesson, J.-J., Tibor, A., 2003. Attenuated Signature-Tagged Mutagenesis Mutants of Brucella melitensis Identified during the Acute Phase of Infection in Mice. Infect. Immun. 71, 7053–7060. https://doi.org/10.1128/IAI.71.12.7053-7060.2003

Ley, K., Hoffman, H.M., Kubes, P., Cassatella, M.A., Zychlinsky, A., Hedrick, C.C., Catz, S.D., 2018. Neutrophils: New insights and open questions. Sci. Immunol. 3. https://doi.org/10.1126/sciimmunol.aat4579

Li, P., Tian, M., Hu, H., Yin, Y., Guan, X., Ding, C., Wang, S., Yu, S., 2019. Lable-free based comparative proteomic analysis of secretory proteins of rough Brucella mutants. J. Proteomics 195, 66–75. https://doi.org/10.1016/j.jprot.2019.01.008

Lindenbach, B.D., Evans, M.J., Syder, A.J., Wölk, B., Tellinghuisen, T.L., Liu, C.C., Maruyama, T., Hynes, R.O., Burton, D.R., McKeating, J.A., Rice, C.M., 2005. Complete Replication of Hepatitis C Virus in Cell Culture. Science 309, 623–626. https://doi.org/10.1126/science.1114016

Lindenbach, B.D., Rice, C.M., 1997. trans-Complementation of Yellow Fever Virus NS1 Reveals a Role in Early RNA Replication. J VIROL 71, 10.

Loisel-Meyer, S., Jiménez de Bagüés, M.P., Bassères, E., Dornand, J., Köhler, S., Liautard, J.-P., Jubier-Maurin, V., 2006. Requirement of norD for Brucella suis Virulence in a Murine Model of In Vitro and In Vivo Infection. Infect. Immun. 74, 1973–1976. https://doi.org/10.1128/IAI.74.3.1973-1976.2006

Lozach, P.-Y., Lortat-Jacob, H., Lavalette, A.D.L.D., Staropoli, I., Foung, S., Amara, A., Houlès, C., Fieschi, F., Schwartz, O., Virelizier, J.-L., Arenzana-Seisdedos, F., Altmeyer, R., 2003. DC-SIGN and L-SIGN Are

High Affinity Binding Receptors for Hepatitis C Virus Glycoprotein E2. J. Biol. Chem. 278, 20358–20366. https://doi.org/10.1074/jbc.M301284200

Lulu, A.R., Araj, G.F., Khateeb, M.I., Mustafa, M.Y., Yusuf, A.R., Fenech, F.F., 1988. Human brucellosis in Kuwait: a prospective study of 400 cases. Q. J. Med. 66, 39–54. https://doi.org/10.1093/oxfordjournals.qjmed.a068178

Manda-Handzlik, A., Bystrzycka, W., Wachowska, M., Sieczkowska, S., Stelmaszczyk-Emmel, A., Demkow, U., Ciepiela, O., 2018. The influence of agents differentiating HL-60 cells toward granulocyte-like cells on their ability to release neutrophil extracellular traps. Immunol. Cell Biol. 96, 413–425. https://doi.org/10.1111/imcb.12015

Manterola, L., Moriyón, I., Moreno, E., Sola-Landa, A., Weiss, D.S., Koch, M.H.J., Howe, J., Brandenburg, K., López-Goñi, I., 2005. The lipopolysaccharide of Brucella abortus BvrS/BvrR mutants contains lipid A modifications and has higher affinity for bactericidal cationic peptides. J. Bacteriol. 187, 5631–5639. https://doi.org/10.1128/JB.187.16.5631-5639.2005

Marchesini, M.I., Herrmann, C.K., Salcedo, S.P., Gorvel, J.-P., Comerci, D.J., 2011. In search of Brucella abortus type IV secretion substrates: screening and identification of four proteins translocated into host cells through VirB system. Cell. Microbiol. 13, 1261–1274. https://doi.org/10.1111/j.1462-5822.2011.01618.x

Marchesini, M.I., Seijo, M., M, S., Guaimas, F.F., Comerci, D.J., 2016. A T4SS Effector Targets Host Cell Alpha-Enolase Contributing to Brucella abortus Intracellular Lifestyle. Front. Cell. Infect. Microbiol. 6. https://doi.org/10.3389/fcimb.2016.00153

Martínez-Núñez, C., Altamirano-Silva, P., Alvarado-Guillén, F., Moreno, E., Guzmán-Verri, C., Chaves-Olarte, E., 2010. The two-component system BvrR/BvrS regulates the expression of the type IV secretion system VirB in *Brucella abortus*. J. Bacteriol. 192, 5603–5608. https://doi.org/10.1128/JB.00567-10

Martirosyan, A., Moreno, E., Gorvel, J.-P., 2011. An evolutionary strategy for a stealthy intracellular *Brucella* pathogen. Immunol. Rev. 240, 211–234. https://doi.org/10.1111/j.1600-065X.2010.00982.x

Martirosyan, A., Pérez-Gutierrez, C., Banchereau, R., Dutartre, H., Lecine, P., Dullaers, M., Mello, M., Salcedo, S.P., Muller, A., Leserman, L., Levy, Y., Zurawski, G., Zurawski, S., Moreno, E., Moriyón, I., Klechevsky, E., Banchereau, J., Oh, S., Gorvel, J.-P., 2012. *Brucella* β 1,2 Cyclic Glucan Is an Activator of Human and Mouse Dendritic Cells. PLOS Pathog. 8, e1002983. https://doi.org/10.1371/journal.ppat.1002983

McDevitt, D.G., 1973. Symptomatology of chronic brucellosis. Br. J. Ind. Med. 30, 385–389. https://doi.org/10.1136/oem.30.4.385

Meltzer, E., Sidi, Y., Smolen, G., Banai, M., Bardenstein, S., Schwartz, E., 2010. Sexually Transmitted Brucellosis in Humans. Clin. Infect. Dis. 51, e12–e15. https://doi.org/10.1086/653608

Meyer, D.F., Noroy, C., Moumène, A., Raffaele, S., Albina, E., Vachiéry, N., 2013. Searching algorithm for type IV secretion system effectors 1.0: a tool for predicting type IV effectors and exploring their genomic context. Nucleic Acids Res. 41, 9218–9229. https://doi.org/10.1093/nar/gkt718

Michaux-Charachon, S., Bourg, G., Jumas-Bilak, E., Guigue-Talet, P., Allardet-Servent, A., O'Callaghan, D., Ramuz, M., 1997. Genome structure and phylogeny in the genus *Brucella*. J. Bacteriol. 179, 3244–3249. https://doi.org/10.1128/jb.179.10.3244-3249.1997

Miller, C.N., Smith, E.P., Cundiff, J.A., Knodler, L.A., Bailey Blackburn, J., Lupashin, V., Celli, J., 2017. A *Brucella* Type IV Effector Targets the COG Tethering Complex to Remodel Host Secretory Traffic and Promote Intracellular Replication. Cell Host Microbe 22, 317-329.e7. https://doi.org/10.1016/j.chom.2017.07.017

Miroux, B., Walker, J.E., 1996. Over-production of proteins in *Escherichia coli*: mutant hosts that allow synthesis of some membrane proteins and globular proteins at high levels. J. Mol. Biol. 260, 289–298. https://doi.org/10.1006/jmbi.1996.0399

Mora-Cartín, R., Chacón-Díaz, C., Gutiérrez-Jiménez, C., Gurdián-Murillo, S., Lomonte, B., Chaves-Olarte, E., Barquero-Calvo, E., Moreno, E., 2016. N-Formyl-Perosamine Surface Homopolysaccharides Hinder the

Recognition of *Brucella abortus* by Mouse Neutrophils. Infect. Immun. 84, 1712–1721. https://doi.org/10.1128/IAI.00137-16

Moriyón, I., López-Goñi, I., 1998. Structure and properties of the outer membranes of *Brucella abortus* and *Brucella melitensis*. Int. Microbiol. Off. J. Span. Soc. Microbiol. 1, 19–26.

Mousa, A.R., Elhag, K.M., Khogali, M., Marafie, A.A., 1988. The nature of human brucellosis in Kuwait: study of 379 cases. Rev. Infect. Dis. 10, 211–217. https://doi.org/10.1093/clinids/10.1.211

Myeni, S., Child, R., Ng, T.W., Kupko, J.J., Wehrly, T.D., Porcella, S.F., Knodler, L.A., Celli, J., 2013. *Brucella* modulates secretory trafficking via multiple type IV secretion effector proteins. PLoS Pathog. 9, e1003556. https://doi.org/10.1371/journal.ppat.1003556

Nathan, C., Shiloh, M.U., 2000. Reactive oxygen and nitrogen intermediates in the relationship between mammalian hosts and microbial pathogens. Proc. Natl. Acad. Sci. 97, 8841–8848. https://doi.org/10.1073/pnas.97.16.8841

Noroy, C., Lefrançois, T., Meyer, D.F., 2019. Searching algorithm for Type IV effector proteins (S4TE) 2.0: Improved tools for Type IV effector prediction, analysis and comparison in proteobacteria. PLoS Comput. Biol. 15, e1006847. https://doi.org/10.1371/journal.pcbi.1006847

O'Callaghan, D., Cazevieille, C., Allardet-Servent, A., Boschiroli, M.L., Bourg, G., Foulongne, V., Frutos, P., Kulakov, Y., Ramuz, M., 1999. A homologue of the *Agrobacterium tumefaciens* VirB and *Bordetella pertussis* PtI type IV secretion systems is essential for intracellular survival of Brucella suis. Mol. Microbiol. 33, 1210–1220. https://doi.org/10.1046/j.1365-2958.1999.01569.x

Ohno, N., Morrison, D.C., 1989. Lipopolysaccharide interaction with lysozyme. Binding of lipopolysaccharide to lysozyme and inhibition of lysozyme enzymatic activity. J. Biol. Chem. 264, 4434–4441.

Palanduz, A., Palanduz, S., Güler, K., Güler, N., 2000. Brucellosis in a mother and her young infant: probable transmission by breast milk. Int. J. Infect.

Dis. IJID Off. Publ. Int. Soc. Infect. Dis. 4, 55–56. https://doi.org/10.1016/S1201-9712(00)90068-7

Pantoja, M., Chen, L., Chen, Y., Nester, E.W., 2002. *Agrobacterium* type IV secretion is a two-step process in which export substrates associate with the virulence protein VirJ in the periplasm. Mol. Microbiol. 45, 1325–1335. https://doi.org/10.1046/j.1365-2958.2002.03098.x

Pappas, G., Papadimitriou, P., Akritidis, N., Christou, L., Tsianos, E.V., 2006. The new global map of human brucellosis. Lancet Infect. Dis. 6, 91–99. https://doi.org/10.1016/S1473-3099(06)70382-6

Paulsen, I.T., Seshadri, R., Nelson, K.E., Eisen, J.A., Heidelberg, J.F., Read, T.D., Dodson, R.J., Umayam, L., Brinkac, L.M., Beanan, M.J., Daugherty, S.C., Deboy, R.T., Durkin, A.S., Kolonay, J.F., Madupu, R., Nelson, W.C., Ayodeji, B., Kraul, M., Shetty, J., Malek, J., Van Aken, S.E., Riedmuller, S., Tettelin, H., Gill, S.R., White, O., Salzberg, S.L., Hoover, D.L., Lindler, L.E., Halling, S.M., Boyle, S.M., Fraser, C.M., 2002. The *Brucella suis* genome reveals fundamental similarities between animal and plant pathogens and symbionts. Proc. Natl. Acad. Sci. U. S. A. 99, 13148–13153. https://doi.org/10.1073/pnas.192319099

Peck, D., Bruce, M., 2017. The economic efficiency and equity of government policies on brucellosis: comparative insights from Albania and the United States of America. Rev. Sci. Tech. Int. Off. Epizoot. 36, 291–302. https://doi.org/10.20506/rst.36.1.2629

Philippe, N., Alcaraz, J.-P., Coursange, E., Geiselmann, J., Schneider, D., 2004. Improvement of pCVD442, a suicide plasmid for gene allele exchange in bacteria. Plasmid 51, 246–255. https://doi.org/10.1016/j.plasmid.2004.02.003

Pósfai, G., Plunkett, G., Fehér, T., Frisch, D., Keil, G.M., Umenhoffer, K., Kolisnychenko, V., Stahl, B., Sharma, S.S., Arruda, M. de, Burland, V., Harcum, S.W., Blattner, F.R., 2006. Emergent Properties of Reduced-Genome *Escherichia coli*. Science 312, 1044–1046. https://doi.org/10.1126/science.1126439

Qureshi, S.A., 2007. Beta-lactamase: an ideal reporter system for monitoring gene expression in live eukaryotic cells. BioTechniques 42, 91–96. https://doi.org/10.2144/000112292

Radhakrishnan, G.K., Yu, Q., Harms, J.S., Splitter, G.A., 2009. *Brucella* TIR Domain-containing Protein Mimics Properties of the Toll-like Receptor Adaptor Protein TIRAP. J. Biol. Chem. 284, 9892–9898. https://doi.org/10.1074/jbc.M805458200

Rae, C.S., Geissler, A., Adamson, P.C., Portnoy, D.A., 2011. Mutations of the *Listeria monocytogenes* peptidoglycan N-deacetylase and O-acetylase result in enhanced lysozyme sensitivity, bacteriolysis, and hyperinduction of innate immune pathways. Infect. Immun. 79, 3596–3606. https://doi.org/10.1128/IAI.00077-11

Ragland, S.A., Criss, A.K., 2017. From bacterial killing to immune modulation: Recent insights into the functions of lysozyme. PLoS Pathog. 13. https://doi.org/10.1371/journal.ppat.1006512

Ragland, S.A., Schaub, R.E., Hackett, K.T., Dillard, J.P., Criss, A.K., 2017. Two lytic transglycosylases in *Neisseria gonorrhoeae* impart resistance to killing by lysozyme and human neutrophils. Cell. Microbiol. 19, e12662. https://doi.org/10.1111/cmi.12662

Ralph, P., Prichard, J., Cohn, M., 1975. Reticulum cell sarcoma: an effector cell in antibody-dependent cell-mediated immunity. J. Immunol. Baltim. Md 1950 114, 898–905.

Ralston, D.J., Baer, B.S., Elberg, S.S., 1961. Lysis of *Brucellae* by the combined action of glycine and a lysozyme-like agent from rabbit monocytes 82, 12.

Ramos, J.M., Bernal, E., Esguevillas, T., Lopez-Garcia, P., Gaztambide, M.S., Gutierrez, F., 2008. Non-imported brucellosis outbreak from unpasteurized raw milk in Moroccan immigrants in Spain. Epidemiol. Infect. 136, 1552–1555. https://doi.org/10.1017/S0950268807000210

Roset, M.S., Ibañez, A.E., Filho, J.A. de S., Spera, J.M., Minatel, L., Oliveira, S.C., Giambartolomei, G.H., Cassataro, J., Briones, G., 2014. *Brucella* Cyclic β-1,2-Glucan Plays a Critical Role in the Induction of Splenomegaly

in Mice. PLOS ONE 9, e101279. https://doi.org/10.1371/journal.pone.0101279

Rouot, B., Alvarez-Martinez, M.-T., Marius, C., Menanteau, P., Guilloteau, L., Boigegrain, R.-A., Zumbihl, R., O'Callaghan, D., Domke, N., Baron, C., 2003. Production of the Type IV Secretion System Differs among *Brucella* Species as Revealed with VirB5- and VirB8-Specific Antisera. Infect. Immun. 71, 1075–1082. https://doi.org/10.1128/IAI.71.3.1075-1082.2003

Rual, J.-F., Hirozane-Kishikawa, T., Hao, T., Bertin, N., Li, S., Dricot, A., Li, N., Rosenberg, J., Lamesch, P., Vidalain, P.-O., Clingingsmith, T.R., Hartley, J.L., Esposito, D., Cheo, D., Moore, T., Simmons, B., Sequerra, R., Bosak, S., Doucette-Stamm, L., Peuch, C.L., Vandenhaute, J., Cusick, M.E., Albala, J.S., Hill, D.E., Vidal, M., 2004. Human ORFeome Version 1.1: A Platform for Reverse Proteomics. Genome Res. 14, 2128–2135. https://doi.org/10.1101/gr.2973604

Sá, J.C., Silva, T.M.A., Costa, E.A., Silva, A.P.C., Tsolis, R.M., Paixão, T.A., Carvalho Neta, A.V., Santos, R.L., 2012. The *virB*-encoded type IV secretion system is critical for establishment of infection and persistence of *Brucella ovis* infection in mice. Vet. Microbiol. 159, 130–140. https://doi.org/10.1016/j.vetmic.2012.03.029

Salcedo, Suzana Pinto, Chevrier, N., Lacerda, T.L.S., Ben Amara, A., Gerart, S., Gorvel, V.A., de Chastellier, C., Blasco, J.M., Mege, J.-L., Gorvel, J.-P., 2013. Pathogenic *brucellae* replicate in human trophoblasts. J. Infect. Dis. 207, 1075–1083. https://doi.org/10.1093/infdis/jit007

Salcedo, Suzana P., Marchesini, M.I., Degos, C., Terwagne, M., Von Bargen, K., Lepidi, H., Herrmann, C.K., Santos Lacerda, T.L., Imbert, P.R.C., Pierre, P., Alexopoulou, L., Letesson, J.-J., Comerci, D.J., Gorvel, J.-P., 2013. BtpB, a novel *Brucella* TIR-containing effector protein with immune modulatory functions. Front. Cell. Infect. Microbiol. 3. https://doi.org/10.3389/fcimb.2013.00028

Salcedo, S.P., Marchesini, M.I., Lelouard, H., Fugier, E., Jolly, G., Balor, S., Muller, A., Lapaque, N., Demaria, O., Alexopoulou, L., Comerci, D.J., Ugalde, R.A., Pierre, P., Gorvel, J.-P., 2008. *Brucella* Control of Dendritic

Cell Maturation Is Dependent on the TIR-Containing Protein Btp1. PLoS Pathog. 4. https://doi.org/10.1371/journal.ppat.0040021

Sánchez Serrano, L.P., Ordóñez Banegas, P., Díaz García, M.O., Torres Frías, A., 2005. Human and animal incidence of brucellosis declining in Spain. Euro Surveill. Bull. Eur. Sur Mal. Transm. Eur. Commun. Dis. Bull. 10, E050421.4. https://doi.org/10.2807/esw.10.16.02687-en

Sangari, F.J., Agüero, J., 1994. Identification of *Brucella abortus* B19 vaccine strain by the detection of DNA polymorphism at the ery locus. Vaccine 12, 435–438.

Sangari, F.J., Seoane, A., Rodríguez, M.C., Agüero, J., García Lobo, J.M., 2007. Characterization of the urease operon of *Brucella abortus* and assessment of its role in virulence of the bacterium. Infect. Immun. 75, 774–780. https://doi.org/10.1128/IAI.01244-06

Sankarasubramanian, J., Vishnu, U.S., Dinakaran, V., Sridhar, J., Gunasekaran, P., Rajendhran, J., 2016. Computational prediction of secretion systems and secretomes of *Brucella*: identification of novel type IV effectors and their interaction with the host. Mol. Biosyst. 12, 178–190. https://doi.org/10.1039/c5mb00607d

Savidis, G., McDougall, W.M., Meraner, P., Perreira, J.M., Portmann, J.M., Trincucci, G., John, S.P., Aker, A.M., Renzette, N., Robbins, D.R., Guo, Z., Green, S., Kowalik, T.F., Brass, A.L., 2016. Identification of Zika Virus and Dengue Virus Dependency Factors using Functional Genomics. Cell Rep. 16, 232–246. https://doi.org/10.1016/j.celrep.2016.06.028

Sawyer, J.G., Martin, N.L., Hancock, R.E., 1988. Interaction of macrophage cationic proteins with the outer membrane of *Pseudomonas aeruginosa*. Infect. Immun. 56, 693–698.

Scheurwater, E., Reid, C.W., Clarke, A.J., 2008. Lytic transglycosylases: Bacterial space-making autolysins. Int. J. Biochem. Cell Biol. 40, 586–591. https://doi.org/10.1016/j.biocel.2007.03.018

Schoggins, J.W., Wilson, S.J., Panis, M., Murphy, M.Y., Jones, C.T., Bieniasz, P., Rice, C.M., 2011. A diverse range of gene products are effectors of the

type I interferon antiviral response. Nature 472, 481–485. https://doi.org/10.1038/nature09907

Scholz, H.C., Hubalek, Z., Nesvadbova, J., Tomaso, H., Vergnaud, G., Le Flèche, P., Whatmore, A.M., Al Dahouk, S., Krüger, M., Lodri, C., Pfeffer, M., 2008a. Isolation of *Brucella microti* from Soil. Emerg. Infect. Dis. 14, 1316–1317. https://doi.org/10.3201/eid1408.080286

Scholz, H.C., Hubalek, Z., Sedlácek, I., Vergnaud, G., Tomaso, H., Al Dahouk, S., Melzer, F., Kämpfer, P., Neubauer, H., Cloeckaert, A., Maquart, M., Zygmunt, M.S., Whatmore, A.M., Falsen, E., Bahn, P., Göllner, C., Pfeffer, M., Huber, B., Busse, H.-J., Nöckler, K., 2008b. *Brucella microti* sp. nov., isolated from the common vole *Microtus arvalis*. Int. J. Syst. Evol. Microbiol. 58, 375–382. https://doi.org/10.1099/ijs.0.65356-0

Scholz, H.C., Nöckler, K., Göllner, C., Bahn, P., Vergnaud, G., Tomaso, H., Al Dahouk, S., Kämpfer, P., Cloeckaert, A., Maquart, M., Zygmunt, M.S., Whatmore, A.M., Pfeffer, M., Huber, B., Busse, H.-J., De, B.K., 2010. *Brucella inopinata* sp. nov., isolated from a breast implant infection. Int. J. Syst. Evol. Microbiol. 60, 801–808. https://doi.org/10.1099/ijs.0.011148-0

Scholz, H.C., Revilla-Fernández, S., Al Dahouk, S., Hammerl, J.A., Zygmunt, M.S., Cloeckaert, A., Koylass, M., Whatmore, A.M., Blom, J., Vergnaud, G., Witte, A., Aistleitner, K., Hofer, E., 2016. *Brucella vulpis* sp. nov., isolated from mandibular lymph nodes of red foxes (*Vulpes vulpes*). Int. J. Syst. Evol. Microbiol. 66, 2090–2098. https://doi.org/10.1099/ijsem.0.000998

Sedzicki, J., Tschon, T., Low, S.H., Willemart, K., Goldie, K.N., Letesson, J.-J., Stahlberg, H., Dehio, C., 2018. 3D correlative electron microscopy reveals continuity of *Brucella*-containing vacuoles with the endoplasmic reticulum. J. Cell Sci. 131, jcs210799. https://doi.org/10.1242/jcs.210799

Sengupta, D., Koblansky, A., Gaines, J., Brown, T., West, A.P., Zhang, D., Nishikawa, T., Park, S.-G., Roop, R.M., Ghosh, S., 2010. Subversion of innate immune responses by *Brucella* through the targeted degradation of the TLR signaling adapter, MAL. J. Immunol. Baltim. Md 1950 184, 956–964. https://doi.org/10.4049/jimmunol.0902008

Shimada, T., Park, B.G., Wolf, A.J., Brikos, C., Goodridge, H.S., Becker, C.A., Reyes, C.N., Miao, E.A., Aderem, A., Götz, F., Liu, G.Y., Underhill, D.M., 2010. *Staphylococcus aureus* evades lysozyme-based peptidoglycan digestion that links phagocytosis, inflammasome activation, and IL-1beta secretion. Cell Host Microbe 7, 38–49. https://doi.org/10.1016/j.chom.2009.12.008

Skendros, P., Boura, P.G., 2013. Immunity to brucellosis. Rev. Sci. Tech. 32, 137–147. https://doi.org/10.20506/rst.32.1.2190

Smith, E.P., Miller, C.N., Child, R., Cundiff, J.A., Celli, J., 2016. Postreplication Roles of the *Brucella* VirB Type IV Secretion System Uncovered via Conditional Expression of the VirB11 ATPase. mBio 7. https://doi.org/10.1128/mBio.01730-16

Sola-Landa, A., Pizarro-Cerdá, J., Grilló, M.J., Moreno, E., Moriyón, I., Blasco, J.M., Gorvel, J.P., López-Goñi, I., 1998. A two-component regulatory system playing a critical role in plant pathogens and endosymbionts is present in *Brucella abortus* and controls cell invasion and virulence. Mol. Microbiol. 29, 125–138. https://doi.org/10.1046/j.1365-2958.1998.00913.x

Sory, M.P., Cornelis, G.R., 1994. Translocation of a hybrid YopE-adenylate cyclase from *Yersinia enterocolitica* into HeLa cells. Mol. Microbiol. 14, 583–594. https://doi.org/10.1111/j.1365-2958.1994.tb02191.x

Sprynski, N., Felix, C., O'Callaghan, D., Vergunst, A.C., 2012. Restoring virulence to mutants lacking subunits of multiprotein machines: functional complementation of a *Brucella virB5* mutant. FEBS Open Bio 2, 71–75. https://doi.org/10.1016/j.fob.2012.03.003

Steele, K.H., Baumgartner, J.E., Valderas, M.W., Roop, R.M., 2010. Comparative Study of the Roles of AhpC and KatE as Respiratory Antioxidants in *Brucella abortus* 2308. J. Bacteriol. 192, 4912–4922. https://doi.org/10.1128/JB.00231-10

Sternon, J.-F., Godessart, P., Freitas, R.G. de, Henst, M.V. der, Poncin, K., Francis, N., Willemart, K., Christen, M., Christen, B., Letesson, J.-J., Bolle, X.D., 2018. Transposon Sequencing of *Brucella abortus* Uncovers

Essential Genes for Growth *In Vitro* and Inside Macrophages. Infect. Immun. 86, e00312-18. https://doi.org/10.1128/IAI.00312-18

Stevanin, T.M., Moir, J.W.B., Read, R.C., 2005. Nitric oxide detoxification systems enhance survival of *Neisseria meningitidis* in human macrophages and in nasopharyngeal mucosa. Infect. Immun. 73, 3322–3329. https://doi.org/10.1128/IAI.73.6.3322-3329.2005

Stockholm, 2018. Brucellosis - Annual Epidemiological Report for 2016 [WWW Document]. Eur. Cent. Dis. Prev. Control. URL http://ecdc.europa.eu/en/publications-data/brucellosis-annual-epidemiological-report-2016 (accessed 8.23.19).

Tabata, K., Arimoto, M., Arakawa, M., Nara, A., Saito, K., Omori, H., Arai, A., Ishikawa, T., Konishi, E., Suzuki, R., Matsuura, Y., Morita, E., 2016. Unique Requirement for ESCRT Factors in *Flavivirus* Particle Formation on the Endoplasmic Reticulum. Cell Rep. 16, 2339–2347. https://doi.org/10.1016/j.celrep.2016.07.068

Tejada, G.M.D., Pizarro-Cerda, J., Moreno, E., 1995. The Outer Membranes of *Brucella* spp. Are Resistant to Bactericidal Cationic Peptides. INFECT IMMUN 63, 8.

Thakur, A., Mikkelsen, H., Jungersen, G., 2019. Intracellular Pathogens: Host Immunity and Microbial Persistence Strategies [WWW Document]. J. Immunol. Res. https://doi.org/10.1155/2019/1356540

Torrens, G., Pérez-Gallego, M., Moya, B., Munar-Bestard, M., Zamorano, L., Cabot, G., Blázquez, J., Ayala, J.A., Oliver, A., Juan, C., 2017. Targeting the permeability barrier and peptidoglycan recycling pathways to disarm *Pseudomonas aeruginosa* against the innate immune system. PLOS ONE 12, e0181932. https://doi.org/10.1371/journal.pone.0181932

Tsuchiya, S., Kobayashi, Y., Goto, Y., Okumura, H., Nakae, S., Konno, T., Tada, K., 1982. Induction of maturation in cultured human monocytic leukemia cells by a phorbol diester. Cancer Res. 42, 1530–1536.

Tsuchiya, S., Yamabe, M., Yamaguchi, Y., Kobayashi, Y., Konno, T., Tada, K., 1980. Establishment and characterization of a human acute monocytic

leukemia cell line (THP-1). Int. J. Cancer 26, 171–176. https://doi.org/10.1002/ijc.2910260208

Typas, A., Banzhaf, M., Gross, C.A., Vollmer, W., 2012. From the regulation of peptidoglycan synthesis to bacterial growth and morphology. Nat. Rev. Microbiol. 10, 123–136. https://doi.org/10.1038/nrmicro2677

Um, S.-H., Kim, J.-S., Kim, K., Kim, N., Cho, H.-S., Ha, N.-C., 2013. Structural Basis for the Inhibition of Human Lysozyme by PliC from *Brucella abortus*. Biochemistry 52, 9385–9393. https://doi.org/10.1021/bi401241c

Velásquez, L.N., Milillo, M.A., Delpino, M.V., Trotta, A., Fernández, P., Pozner, R.G., Lang, R., Balboa, L., Giambartolomei, G.H., Barrionuevo, P., 2017. *Brucella abortus* down-regulates MHC class II by the IL-6-dependent inhibition of CIITA through the downmodulation of IFN regulatory factor-1 (IRF-1). J. Leukoc. Biol. 101, 759–773. https://doi.org/10.1189/jlb.4A0416-196R

Vergunst, A.C., Meijer, A.H., Renshaw, S.A., O'Callaghan, D., 2010. *Burkholderia cenocepacia* Creates an Intramacrophage Replication Niche in Zebrafish Embryos, Followed by Bacterial Dissemination and Establishment of Systemic Infection. Infect. Immun. 78, 1495–1508. https://doi.org/10.1128/IAI.00743-09

Viadas, C., Rodríguez, M.C., Sangari, F.J., Gorvel, J.-P., García-Lobo, J.M., López-Goñi, I., 2010. Transcriptome Analysis of the *Brucella abortus* BvrR/BvrS Two-Component Regulatory System. PLOS ONE 5, e10216. https://doi.org/10.1371/journal.pone.0010216

Vilchez, G., Espinoza, M., D'Onadio, G., Saona, P., Gotuzzo, E., 2015. Brucellosis in pregnancy: clinical aspects and obstetric outcomes. Int. J. Infect. Dis. IJID Off. Publ. Int. Soc. Infect. Dis. 38, 95–100. https://doi.org/10.1016/j.ijid.2015.06.027

Vollmer, W., Blanot, D., de Pedro, M.A., 2008. Peptidoglycan structure and architecture. FEMS Microbiol. Rev. 32, 149–167. https://doi.org/10.1111/j.1574-6976.2007.00094.x

Voth, D.E., Broederdorf, L.J., Graham, J.G., 2012. Bacterial Type IV secretion systems: versatile virulence machines. Future Microbiol. 7, 241–257. https://doi.org/10.2217/fmb.11.150

Wang, J., Yang, B., An, Y., Marquez-Lago, T., Leier, A., Wilksch, J., Hong, Q., Zhang, Y., Hayashida, M., Akutsu, T., Webb, G.I., Strugnell, R.A., Song, J., Lithgow, T., 2017. Systematic analysis and prediction of type IV secreted effector proteins by machine learning approaches. Brief. Bioinform. https://doi.org/10.1093/bib/bbx164

Wang, Y., Wei, X., Bao, H., Liu, S.-L., 2014. Prediction of bacterial type IV secreted effectors by C-terminal features. BMC Genomics 15, 50. https://doi.org/10.1186/1471-2164-15-50

Weber, M.M., Faris, R., 2018. Subversion of the Endocytic and Secretory Pathways by Bacterial Effector Proteins. Front. Cell Dev. Biol. 6. https://doi.org/10.3389/fcell.2018.00001

Weber, M.M., Faris, R., van Schaik, E.J., McLachlan, J.T., Wright, W.U., Tellez, A., Roman, V.A., Rowin, K., Case, E.D.R., Luo, Z.-Q., Samuel, J.E., 2016. The Type IV Secretion System Effector Protein CirA Stimulates the GTPase Activity of RhoA and Is Required for Virulence in a Mouse Model of *Coxiella burnetii* Infection. Infect. Immun. 84, 2524–2533. https://doi.org/10.1128/IAI.01554-15

Whatmore, A.M., Davison, N., Cloeckaert, A., Al Dahouk, S., Zygmunt, M.S., Brew, S.D., Perrett, L.L., Koylass, M.S., Vergnaud, G., Quance, C., Scholz, H.C., Dick, E.J., Hubbard, G., Schlabritz-Loutsevitch, N.E., 2014. *Brucella papionis* sp. nov., isolated from baboons (*Papio* spp.). Int. J. Syst. Evol. Microbiol. 64, 4120–4128. https://doi.org/10.1099/ijs.0.065482-0

Xiong, Y., Wang, Q., Yang, J., Zhu, X., Wei, D.-Q., 2018. PredT4SE-Stack: Prediction of Bacterial Type IV Secreted Effectors From Protein Sequences Using a Stacked Ensemble Method. Front. Microbiol. 9, 2571. https://doi.org/10.3389/fmicb.2018.02571

Yadav, A.K., Espaillat, A., Cava, F., 2018. Bacterial Strategies to Preserve Cell Wall Integrity Against Environmental Threats. Front. Microbiol. 9. https://doi.org/10.3389/fmicb.2018.02064

Ye, J., Chen, Z., Zhang, B., Miao, H., Zohaib, A., Xu, Q., Chen, H., Cao, S., 2013. Heat Shock Protein 70 Is Associated with Replicase Complex of Japanese Encephalitis Virus and Positively Regulates Viral Genome Replication. PLOS ONE 8, e75188. https://doi.org/10.1371/journal.pone.0075188

Yi, Z., Sperzel, L., Nürnberger, C., Bredenbeek, P.J., Lubick, K.J., Best, S.M., Stoyanov, C.T., Law, L.M.J., Yuan, Z., Rice, C.M., MacDonald, M.R., 2011. Identification and Characterization of the Host Protein DNAJC14 as a Broadly Active *Flavivirus* Replication Modulator. PLoS Pathog. 7, e1001255. https://doi.org/10.1371/journal.ppat.1001255

Yum, S., Kim, M.J., Xu, Y., Jin, X.L., Yoo, H.Y., Park, J.-W., Gong, J.H., Choe, K.-M., Lee, B.L., Ha, N.-C., 2009. Structural basis for the recognition of lysozyme by MliC, a periplasmic lysozyme inhibitor in Gram-negative bacteria. Biochem. Biophys. Res. Commun. 378, 244–248. https://doi.org/10.1016/j.bbrc.2008.11.039

Zahrl, D., Wagner, M., Bischof, K., Bayer, M., Zavecz, B., Beranek, A., Ruckenstuhl, C., Zarfel, G.E., Koraimann, G., 2005. Peptidoglycan degradation by specialized lytic transglycosylases associated with type III and type IV secretion systems. Microbiology 151, 3455–3467. https://doi.org/10.1099/mic.0.28141-0

Zhang, J., Li, M., Li, Z., Shi, J., Zhang, Y., Deng, X., Liu, L., Wang, Z., Qi, Y., Zhang, H., 2019. Deletion of the Type IV Secretion System Effector VceA Promotes Autophagy and Inhibits Apoptosis in *Brucella*-Infected Human Trophoblast Cells. Curr. Microbiol. 76, 510–519. https://doi.org/10.1007/s00284-019-01651-6

Zhi, F., Zhou, D., Bai, F., Li, J., Xiang, C., Zhang, G., Jin, Y., Wang, A., 2019. VceC Mediated IRE1 Pathway and Inhibited CHOP-induced Apoptosis to Support *Brucella* Replication in Goat Trophoblast Cells. Int. J. Mol. Sci. 20. https://doi.org/10.3390/ijms20174104

Zhou, D., Zhi, F.-J., Qi, M.-Z., Bai, F.-R., Zhang, G., Li, J.-M., Liu, H., Chen, H.-T., Lin, P.-F., Tang, K.-Q., Liu, W., Jin, Y.-P., Wang, A.-H., 2017. *Brucella* induces unfolded protein response and inflammatory response via GntR

in alveolar macrophages. Oncotarget 9, 5184–5196. https://doi.org/10.18632/oncotarget.23706

Zhu, W., Banga, S., Tan, Y., Zheng, C., Stephenson, R., Gately, J., Luo, Z.-Q., 2011. Comprehensive Identification of Protein Substrates of the Dot/Icm Type IV Transporter of *Legionella pneumophila*. PLOS ONE 6, e17638. https://doi.org/10.1371/journal.pone.0017638

Zielke, R.A., Van, A.L., Baarda, B.I., Herrera, M.F., Acosta, C.J., Jerse, A.E., Sikora, A.E., 2018. SliC is a surface-displayed lipoprotein that is required for the anti-lysozyme strategy during *Neisseria gonorrhoeae* infection. PLOS Pathog. 14, e1007081. https://doi.org/10.1371/journal.ppat.1007081

Zimmermann, S., Pfannkuch, L., Al-Zeer, M.A., Bartfeld, S., Koch, M., Liu, J., Rechner, C., Soerensen, M., Sokolova, O., Zamyatina, A., Kosma, P., Mäurer, A.P., Glowinski, F., Pleissner, K.-P., Schmid, M., Brinkmann, V., Karlas, A., Naumann, M., Rother, M., Machuy, N., Meyer, T.F., 2017. ALPK1- and TIFA-Dependent Innate Immune Response Triggered by the *Helicobacter pylori* Type IV Secretion System. Cell Rep. 20, 2384–2395. https://doi.org/10.1016/j.celrep.2017.08.039

Zou, L., Nan, C., Hu, F., 2013. Accurate prediction of bacterial type IV secreted effectors using amino acid composition and PSSM profiles. Bioinforma. Oxf. Engl. 29, 3135–3142. https://doi.org/10.1093/bioinformatics/btt554

RESUMEN EN CASTELLANO

8. RESUMEN EN CASTELLANO

8.1 Introducción

Los organismos del género *Brucella* son cocobacilos gram negativos responsables de la brucelosis. Esta enfermedad puede afectar a varias especies animales, así como a humanos. De hecho, la brucelosis es una de las principales zoonosis a nivel mundial, con más de 500.000 casos reportados anualmente (Pappas et al., 2006) y posiblemente infradiagnosticada unas 4-5 veces. La enfermedad en humanos es causada principalmente por 4 especies del género: *B. melitensis, B. suis, B. abortus y B. canis*.

Tras la invasión, *Brucella* es fagocitada por fagocitos profesionales como macrófagos, monocitos, neutrófilos y células dendríticas, y también por muchas células epiteliales, así como por trofoblastos. Sin embargo, *Brucella* no es capaz de replicar en alguna de estas células. En términos generales, tras la fagocitosis *Brucella* es contenida en BCVs que van a interaccionar con la vía endocítica, incluyendo endosomas tempranos y tardíos, y lisosomas, produciendo la acidificación de la vacuola que se convertirá en eBCVs. Esta acidificación, junto con la baja disponibilidad de nutrientes, van a hacer que se exprese el T4SS (Boschiroli et al., 2002). A continuación, las eBCVs en su viaje hasta el ER van a ir perdiendo marcadores endosomales y adquiriendo marcadores específicos del ER formando las rBCVs, donde *Brucella* se replicará. Además, estas vacuolas pueden interaccionar con el tráfico vesicular entre el ER y el Golgi (Celli, 2019; Sedzicki et al., 2018). Tras la replicación, las rBCVs son capturadas dentro de estructuras como autofagosomas de manera dependiente del T4SS, llamándose en este momento aBCVs. Este proceso va a ayudar a *Brucella* a escapar de la célula infectada, liberándose al medio y pudiendo infectar otras células.

Como vemos, el T4SS es un factor de virulencia clave para *Brucella*. Los T4SS son una familia de sistemas de secreción bacterianos con una alta plasticidad, ya que son capaces de translocar tanto proteínas, ADN como peptidoglicano (Christie et al., 2014). En el caso específico de *Brucella* este

sistema de secreción es clave para la infección de células eucariotas. De hecho, el T4SS de *Brucella* es necesario tanto al inicio como al final de su ciclo intracelular (Hanna et al., 2011; Sá et al., 2012; Smith et al., 2016). Además, se sabe que este sistema de secreción es capaz de secretar efectores a las células hospedadoras, pudiendo tener un papel fundamental favoreciendo la infección. En comparación con otros patógenos intracelulares, como *Legionella* o *Coxiella*, donde se han identificado cientos de efectores (Weber et al., 2016; Zhu et al., 2011), en *Brucella* únicamente se han identificado 15 efectores secretados por el T4SS (de Barsy et al., 2011; de Jong et al., 2008; Döhmer et al., 2014; Marchesini et al., 2011; Myeni et al., 2013; Salcedo et al., 2013). Además, mediante la búsqueda de estos efectores secretados a través del T4SS, se identificaron otros 7 efectores secretados a la célula hospedadora de manera independiente de su T4SS (Marchesini et al., 2011; Myeni et al., 2013). Estos efectores fueron propuestos como candidatos a ser proteínas secretadas por el T4SS en base a diversos métodos. Algunos autores estudiaron las proteínas que poseían una región conservada en el promotor para la activación por VjbR, una secuencia también presente en el promotor de VirB (de Jong et al., 2008); mientras que otros determinaron interacciones con proteínas del hospedador necesarias para la bacteria durante la infección (de Barsy et al., 2011), entre otras cosas. Además, la determinación de estos efectores como proteínas secretadas se ha llevado a cabo por varios métodos convencionales como son los ensayos CyaA y TEM1, así como por immunofluorescencia. Sin embargo, estos métodos de selección de candidatos y comprobación de los mismos no han sido demasiado eficientes para la búsqueda de efectores de *Brucella*, ya que no siempre han sido capaces de identificar proteínas secretadas por *Brucella*, ya sea de forma dependiente o independiente de su T4SS. Por ello, es lógico pensar que nuevas estrategias para detectar efectores de *Brucella* pueden identificar nuevas proteínas efectoras.

La familia Flaviviridae está compuesta de virus pequeños con envuelta de cadena positiva de RNA, cuya replicación depende completamente de la célula hospedadora. Estos virus usan maquinaria especializada para fusionar la membrana del virus con las membranas del hospedador a través de la vía endosomal. Tras la internalización, se van a replicar y salir de la célula

hospedadora manipulando varias membranas del hospedador, principalmente ER, Golgi y vesículas autofágicas (Arakawa and Morita, 2019; Fernandez-Garcia et al., 2009; Gerold et al., 2017; Ke, 2018). Esta dependencia por las membranas del hospedador recuerda al ciclo intracelular de muchas bacterias intracelulares como es el caso de *Brucella*. Por lo que se puede pensar que los efectores de *Brucella* que afecten a funciones del huésped para favorecer su supervivencia intracelular, puedan interferir con el ciclo biológico de estos virus, al compartir dianas y nichos.

Uno de los mecanismos más ancestrales de defensa contra las bacterias desarrollado por los organismos eucariotas es la producción de lisozima (Callewaert and Michiels, 2010). En mamíferos, esta proteína es producida por la mayoría de las células fagocíticas del sistema inmune innato, incluyendo neutrófilos, macrófagos, monocitos y células dendríticas (Klüter et al., 2014; Ragland and Criss, 2017), aunque también se puede encontrar en muchas otras secreciones del cuerpo como lágrimas, salivas e incluso en plasma sanguíneo (Lehrer, 1998), así como en muchos tejidos incluyendo el tracto intestinal y respiratorio (Callewaert and Michiels, 2010). La lisozima es capaz de hidrolizar los enlaces β-(1-4) glicosídicos del peptidoglicano (Callewaert et al., 2008), uno de los principales componentes de la pared celular de las bacterias. Sin embargo, las bacterias han sido capaces de desarrollar una serie de mecanismos de resistencia frente a la lisozima. Una de las últimas estrategias identificadas contra la acción de la lisozima es la producción de inhibidores de lisozima. Sin embargo, en el caso de *Brucella*, poco se sabe acerca de cómo es capaz de resistir a la acción de la lisozima. De hecho, es posible que *Brucella* tenga una capacidad intrínseca para resistir a la lisozima gracias a la composición de su membrana celular que le confiere una baja permeabilidad a los péptidos catiónicos como la lisozima o lactoferrina (Tejada et al., 1995). Sin embargo, recientemente se ha visto como cuando se mutan ciertas proteínas esenciales para la estabilidad de la membrana celular de *Brucella*, como MapB, la sensibilidad de estas bacterias a la lisozima aumenta, aunque esta no es total (Bialer et al., 2019). De este modo se puede pensar que podría haber otros me*canis*mos de resistencia implicados en la resistencia de *Brucella* a la lisozima, como son los inhibidores de lisozima.

8.2 Objetivos

Brucella es capaz de sobrevivir y replicar dentro de las células del huésped. Sin embargo, este fenómeno clave para la patogenicidad de *Brucella* no sería posible sin el desarrollo de una serie de mecanismos que permiten a la bacteria enfrentarse a las adversidades con las que se encuentra dentro del hospedador. Esta tesis tiene por tanto el objetivo de estudiar dos mecanismos que podría haber desarrollado *Brucella* para favorecer su supervivencia y con ello la infección: los efectores del T4SS y los inhibidores de lisozima. Para ello nos planteamos los siguientes objetivos detallados:

Búsqueda de nuevos efectores del T4SS de *B. abortus*

1) Construcción de una librería de posibles efectores del T4SS.
2) Establecimiento de un ensayo de interferencia viral.
3) Cribado de la librería.

Caracterización de posibles inhibidores de lisozima de *B. abortus*

1) Análisis *in silico* de BAB1_0102 y BAB1_0466.
2) Actividad *in vitro* como inhibidores de lisozima.
3) Determinación de la contribución de BAB1_0466 a la supervivencia de *B. abortus* durante el tratamiento con lisozima.
4) Determinación del papel de BAB1_0466 en la supervivencia de *B. abortus* dentro de distintos tipos celulares del sistema inmune innato humano.

8.3 Resultados y discusión

8.3.1 Búsqueda de nuevos efectores del T4SS de *B. abortus*

En esta primera parte, se quería llevar a cabo una búsqueda de nuevos efectores de *Brucella* a través de la interacción con la replicación de virus de la familia Flaviviridae. Para ello inicialmente se utilizaron varios software publicados para la predicción de efectores secretados a través del T4SS (Meyer et al., 2013; Wang et al., 2017, 2014; Zou et al., 2013), con el fin de reducir el

número de candidatos. Sin embargo, se vio que ninguno de estos métodos de predicción era totalmente eficaz, ya que ninguno de ellos era capaz de predecir como candidatos a los 15 efectores de *Brucella* secretados a través de su T4SS descritos hasta la fecha. Además, existía mucha heterogeneidad entre los candidatos predichos por cada método. Algo que tampoco resultó especialmente sorprendente, ya que cada uno de ellos analiza conjuntos de características de las proteínas diferentes (Meyer et al., 2013; Wang et al., 2017, 2014; Zou et al., 2013). Además, también se incluyeron proteínas anteriormente descritas en la bibliografía como candidatos. Así se generó una lista de 256 proteínas de *B. abortus* candidatas a ser efectores secretados por su T4SS. De estas 256 proteínas se seleccionaron 151 según varias características: efectores reales secretados por el T4SS; proteínas secretadas independientemente al T4SS; la mayoría de las proteínas predichas por el S4TE software (Sankarasubramanian et al., 2016), así como proteínas predichas como candidatas por varios métodos; proteínas hipotéticas e incluso se incluyeron algunas proteínas con función conocida.

Así, mediante una estancia en la Universidad de Yale, en el laboratorio del Dr. Lindenbach, se puso a punto el ensayo y se probó para los primeros 21 efectores, donde se incluyeron 14 efectores de *Brucella* secretados a través de su T4SS y 7 proteínas de *Brucella* secretadas de forma independiente a su T4SS. Para ello, los genes que codifican para esas proteínas se clonaron mediante una reacción Gateway primero en el vector pDONR223 y finalmente en un vector lentiviral que expresaba una proteína roja constitutivamente, IRF670. Estos vectores lentivirales se utilizaron para generar partículas lentivirales que se usaron para expresar cada candidato en células eucariotas bajo el control de un promotor inducible. Así, las células que se encontraban expresando estas proteínas fueron infectadas con partículas infectivas de YFV y HCV. Mediante este primer ensayo se vio como los niveles de infección de YFV eran más heterogéneos cuando las células expresaban las diferentes proteínas de *B. abortus*; mientras que la expresión de estas proteínas siempre disminuía los niveles de infección de HCV. Sugiriendo que quizás YFV es un mejor candidato para llevar a cabo el cribado de efectores. Por otro lado, se vio que los efectores BAB1_0279 y BAB1_0756, ademas de ser los que presentaban mayor

inhibición sobre la replicacion viral, son tóxicos para las células. Esta actividad citotóxica ha sido también descrita recientemente, y se ha asociado con los dominios TIR presentes en estas proteínas (Coronas-Serna et al., 2019).

Tras este análisis inicial, el ensayo se completó con las restantes 130 proteínas seleccionadas. Para ello, el método de análisis fue adaptado a los medios de los que disponíamos en nuestro laboratorio. Así, los genes que codifican para estas proteínas se clonaron en un vector lentiviral que expresaba constitutivamente m-Cherry. Paralelamente, se intentaron generar partículas virales de YFV y HCV. Sin embargo, mientras que para YFV se obtuvieron bastantes partículas infectivas para llevar a cabo el ensayo, fue imposible generar partículas infectivas de HCV. De este modo, el ensayo únicamente se llevó a cabo con YFV. Tras el análisis global de los 151 candidatos, se encontraron varios candidatos que aumentaban o disminuían los niveles de infección de YFV. Entre las proteínas de *B. abortus* que favorecían la infección de YFV estaban: BAB2_0074, BAB2_0271, BAB1_0608, BAB1_0740, BAB1_1199, BAB2_0773, BAB1_1344 y BAB2_0246. Mientras que BAB1_0817, BAB1_1322, BAB1_1730, BAB1_1185, BAB1_1386, BAB1_1396, BAB2_0634, BAB1_0279 y BAB1_0756 disminuían la infección de YFV, incluso por niveles inferiores al control de inhibición IRF1.

En conjunto, estos resultados sugieren que hay algunas proteínas de *B. abortus* que podrían ser efectores secretados por su T4SS de acuerdo con la predicción de varios programas que son capaces de modificar la infección del YFV. Sin embargo, estos resultados aún son preliminares y más ensayos son necesarios para concluir si estas proteínas están efectivamente haciendo algo en la célula hospedadora que afecta a la replicación de los virus de la familia Flaviviridae, y para determinar si estas proteínas efectivamente son efectores de *Brucella* secretados a través de su T4SS.

8.3.2 Caracterización de posibles inhibidores de lisozima de *B. abortus*

En esta segunda parte, estudiamos el papel de dos posibles inhibidores de lisozima presentes en *B. abortus*, BAB1_0102 y BAB1_0466, previamente identificados en nuestro laboratorio. BAB1_0466 había sido cristalizada unida a

lisozima (Um et al., 2013). Mientras que BAB1_0102 fue re-anotada tras un estudio realizado por nuestro grupo, y esta re-anotación estableció un nuevo inicio de la transcripción y una proteina de menor tamaño, que resultó ser homóloga a otros inhibidores de lisozima. Se realizaron varios análisis *in silico* que determinaron que estas proteínas contenían el dominio MliC de inhibidores de lisozima. El dominio MliC de BAB1_0466 contiene los residuos conservados de lisina y serina necesarios para la interacción con la lisozima, mientras que el dominio MliC de BAB1_0102 no.

Teniendo estos dos candidatos, inicialmente se llevaron a cabo estudios *in vitro* para determinar la actividad de BAB1_0102 y BAB1_0466 como posibles inhibidores de lisozima. De este modo se demostró que BAB1_0466 es un homólogo funcional de los inhibidores de lisozima MliC/PliC en *B. abortus*, aunque todavía se desconoce su localización. Sin embargo, la proteína BAB1_0102 re-anotada no es capaz de inhibir la actividad de la lisozima. Además, se ha intentado ver la actividad de estas proteínas como inhibidores de otras proteínas con actividad tipo lisozima presentes en *B. abortus*, como SagA. Sin embargo, en nuestras condiciones ninguna de estas proteínas es capaz de inhibir la actividad lítica de SagA. Recientemente se ha visto como la proteína completa de BAB1_0102, no la re-anotada, es capaz de inhibir la acción de SagA mediante otros ensayos diferentes (Del Giudice et al., 2019). Estos datos hacen pensar que quizás la proteína completa de BAB1_0102 sea necesaria para obtener una estructura adecuada para la interacción con SagA, o que el ensayo que se ha utilizado aquí no sea suficientemente sensible como para detectar esta actividad.

Tras comprobar la actividad de BAB1_0466 como inhibidor de lisozima se quiso determinar el papel que jugaba esta proteína en la supervivencia de *Brucella* cuando la lisozima estaba presente en el medio. Para ello, inicialmente, se utilizaron cepas de *B. abortus* WT, un mutante 2308*Δ0466*, y este mismo mutante al que se le había insertado un plásmido de expresión que contenía la proteína BAB1_0466. Sin embargo, cuando estas cepas fueron tratadas con lisozima no se vieron diferencias entre el mutante 2308*Δ0466* y el WT. Esto, posiblemente se debiese a que la membrana externa de *Brucella* es bastante impermeable a los péptidos catiónicos como es la lisozima (Tejada et al., 1995).

Por ello, para intentar hacer a *B. abortus* más sensible a la acción de la lisozima, las bacterias se trataron además de con lisozima con glicina (Ralston et al., 1961). Con ello vimos, que, aunque *B. abortus* era más sensible a la acción de la lisozima, seguía sin haber diferencia entre el mutante 2308*Δ0466* y el WT. Finalmente, dado que se había descrito que la ausencia de MapB desestabilizaba la membrana de *Brucella* haciendo a la bacteria más sensible a la acción de la lisozima (Bialer et al., 2019), se quiso comprobar si existía una diferencia en la supervivencia de *B. abortus* entre el mutante 2308*ΔmapB* y el doble mutante 2308*Δ0466ΔmapB*. De este modo, se vio que efectivamente, la ausencia de MapB aumentaba la sensibilidad de *B. abortus* a la acción de la lisozima. Aunque no se pudo ver una diferencia significativa entre el mutante simple en *mapB* y el doble mutante sin inhibidor de lisozima, se vio que cuando se complementaba éste último con BAB1_0466, las bacterias restablecían su supervivencia a niveles similares a los del WT. Podemos concluir que BAB1_0466 inhibe la acción de la lisozima, jugando un papel importante en la supervivencia de *B. abortus* cuando ésta tiene comprometida su envuelta celular.

Finalmente, se quiso determinar el papel que podía jugar esta proteína durante la infección en células humanas. Como se ha dicho las células fagocíticas producen grandes cantidades de péptidos antimicrobianos como defensinas que desestabilizan la membrana externa ayudando a la acción de la lisozima (Hancock et al., 1981; Hancock and Scott, 2000; Sawyer et al., 1988). Inicialmente se llevaron a cabo infecciones con *B. abortus* en macrófagos de ratón, el modelo por excelencia usado en infecciones con *Brucella*. Sin embargo, aunque se pudo observar la curva típica de supervivencia, no se detectó ninguna diferencia en la supervivencia entre el mutante 2308*Δ0466* y el WT. El siguiente paso fue realizar infecciones de sangre completa con *B. abortus*. En este caso se pudo ver que la pérdida de BAB1_0466 reducía significativamente la supervivencia de *B. abortus*. Esto indica que es posible que haya alguna célula fagocítica en la sangre que es capaz de matar más eficientemente a *B. abortus* en ausencia del inhibidor de lisozima BAB1_0466.

Para intentar determinar la población responsable de la disminución de la supervivencia de *B. abortus* se probaron distintos tipos celulares: neutrófilos humanos, monocitos y macrófagos humanos, y únicamente se pudo ver una

diferencia significativa entre el mutante 2308*Δ0466* y el WT en células HL-60 tratadas con DMF, que supuestamente determina su diferenciación hacia neutrófilos. Sin embargo, tras el análisis por citometría de flujo, se vio que estas células en vez de corresponder con una población de neutrófilos, se diferenciaban a tres poblaciones distintas bastante heterogéneas. De hecho, únicamente se pudieron clasificar dos poblaciones, una de ellas poseía un fenotipo como monocitos/macrófagos y la otra de ellas eran células en un estadio anterior de diferenciación, posiblemente promonocitos. La tercera población obtenida era tan heterogénea que no se pudo clasificar en un tipo celular determinado. Tras estos resultados se intentó ver si los monocitos/macrófagos humanos eran los responsables de esta diferencia en la supervivencia del mutante 2308*Δ0466*. Cuando se llevó a cabo el ensayo con células THP-1 se pudo ver una diferencia, aunque no significativa entre la supervivencia del mutante 2308*Δ0466* y el WT, y cuando se complementaba el mutante 2308*Δ0466* con BAB1_0466 si se pudo ver una diferencia significativa entre el mutante 2308*Δ0466*y la cepa de complementación. Lo que nos hace pensar que, como ocurría cuando se usaban los distintos mutantes en 2308*ΔmapB*, BAB1_0466 es capaz de inhibir la acción de la lisozima producida por monocitos cuando esta proteína se está expresando a niveles superiores a los basales.

Estos datos en conjunto sugieren que BAB1_0466 es un inhibidor de lisozima, que desempaña un papel importante en la supervivencia de *Brucella* cuando ésta tiene la OM dañada. Además, todo parece indicar que esta proteína juega un papel importante en la supervivencia de la bacteria durante la infección, especialmente durante la infección de monocitos. Aunque hacen falta más datos que confirmen esta hipótesi, así como determinar el papel que juega esta proteína en la virulencia de la bacteria en infecciones *in vivo.*

8.4 Conclusiones

1. Ninguno de los métodos existentes para la predicción de efectores bacterianos es totalmente efectivo para la predicción de efectores del T4SS de *Brucella*.

2. Hemos establecido un nuevo método de cribado de efectores basado en un ensayo de interferencia con la replicación del YFV. Este método podría ser aplicado a cualquier librería de potenciales efectores que pudiesen estar afectando a rutas intracelulares comunes con las utilizadas por el YFV.
3. El cribado de una librería de 151 efectores candidatos de *B. abortus* por este ensayo mostró que la replicación del YFV se ve incrementada en presencia de las proteínas BAB2_0074, BAB2_0271, BAB1_0608, BAB1_0740, BAB1_1199, BAB2_0773, BAB1_1344 y BAB2_0246; mientras que disminuye en presencia de BAB1_0817, BAB1_1322, BAB1_1730, BAB1_1185, BAB1_1386, BAB1_1396, BAB2_0634, BAB1_0279 y BAB1_0756.
4. El genoma de *B. abortus* codifica dos posibles inhibidores de lisozima, de acuerdo con la predicción de su homología con el dominio MliC. El dominio MliC de BAB1_0466 contiene los residuos conservados de lisina y serina necesarios para la interacción con la lisozima, mientras que el dominio MliC de BAB1_0102 no.
5. La proteína purificada BAB1_0466 inhibe la actividad lítica de las lisozimas de la clara de huevo de gallina y humana, mientras que BAB1_0102 no inhibe su actividad.
6. Las proteínas purificadas BAB1_0466 y BAB1_0102 no inhiben la actividad lítica de la proteína similar a lisozima, SagA.
7. *B. abortus* es intrínsecamente resistente a la acción lítica de la lisozima, únicamente se observa dicha acción tras la desestabilización de la membrana externa por la ausencia de la proteína MapB.
8. En la ausencia de MapB, la proteína BAB1_0466 inhibe la actividad lítica de la lisozima in vivo.
9. BAB1_0466 es necesaria para la supervivencia de *B. abortus* durante la infección de sangre completa.
10. Un mutante por deleción de *bab1_0466* de *B. abortus* muestra unas tasas de supervivencia reducida en una línea celular de monocitos humanos, mientras que su supervivencia no se ve afectada ni en neutrofilos purificados de sangre ni en líneas celulares de macrófagos humanos o de ratón.

PUBLICATIONS

Polymorphisms in *Brucella* Carbonic anhydrase II mediate CO_2 dependence and fitness *in vivo.*

García-Lobo JM[1], Ortiz Y[1], González-Riancho C[1], Seoane A[1], Arellano-Reynoso B[2], and Sangari FJ[1]*

*Corresponding author

1. Instituto de Biomedicina y Biotecnología de Cantabria (IBBTEC), CSIC-Universidad de Cantabria, and Departamento de Biología Molecular, Universidad de Cantabria, 39011 Santander, Spain.

2. Departamento de Microbiología, Facultad de Medicina Veterinaria y Zootecnia, Universidad Nacional Autónoma de México, Circuito Exterior de Ciudad Universitaria, Delegación Coyoacán, Mexico City, C.P. 04510, Mexico.

FJS conceived and coordinated the study, conducted bacteriology work and wrote the manuscript. JMGL analyzed the data and wrote the manuscript. YO, CGR, AS and BAR conducted bacteriology work. All authors interpreted the data, corrected the manuscript, and approved the content for publication.

Keywords. *Brucella*, Carbonic anhydrase, CO_2 requirement, fitness, protein structure

Abstract

Some *Brucella* isolates are known to require an increased concentration of CO_2 for growth, especially in the case of primary cultures obtained directly from infected animals. Moreover, the different *Brucella* species and biovars show a characteristic pattern of CO_2 requirement, and this trait has been included among the routine typing tests used for species and biovar differentiation. By comparing the differences in gene content among different CO_2-dependent and CO_2-independent *Brucella* strains we have confirmed that carbonic anhydrase II (CA II), is the enzyme responsible for this phenotype in all the *Brucella* strains tested. *Brucella* species contain two carbonic anhydrases of the β family, CA I and CA II; genetic polymorphisms exist for both of them in different isolates, but only those putatively affecting the activity of CA II correlate with the CO_2 requirement of the corresponding isolate. Analysis of these polymorphisms does not allow the determination of CA I functionality, while the polymorphisms in CA II consist of small deletions that cause a frameshift that changes the C-terminus of the protein, probably affecting its dimerization status, essential for the activity.

CO_2-independent mutants arise easily *in vitro*, although with a low frequency ranging from 10^{-6} to 10^{-10} depending on the strain. These mutants carry compensatory mutations that produce a full length CA II. At the same time, no change was observed in the sequence coding for CA I. A competitive index assay designed to evaluate the fitness of a CO_2-dependent strain compared to its corresponding CO_2-independent strain revealed that while there is no significant difference when the bacteria are grown in culture plates, growth *in vivo* in a mouse model of infection provides a significant advantage to the CO_2-dependent strain. This could explain why some *Brucella* isolates are CO_2-dependent in primary isolation. The polymorphism described here also allows the *in silico* determination of the CO_2 requirement status of any *Brucella* strain.

Introduction

Brucella species are facultative intracellular Gram-negative coccobacilli that cause brucellosis, the most prevalent zoonosis with more than 500,000 human cases reported worldwide every year (Pappas et al., 2006). *Brucella* isolates are routinely identified and classified by biochemical and phenotypical characteristics like urease activity, CO_2 dependence, H_2S production, erythritol and dye-sensitivity, lysis by *Brucella*-specific bacteriophages, agglutination with monospecific sera, or even host preference (Alton et al., 1988). The first observations pertaining *Brucella* and CO_2 were made by Nowak (1908), who noticed that *B. abortus* was more easily isolated from the host tissues when the concentration of oxygen in the atmosphere was reduced, but it was Wilson (1931) who established the requirement of CO_2 for growth in these isolates. This requirement is not universal within *Brucellaceae*, and the different species and biovars show a characteristic pattern of CO_2 dependence. Within the classical species, *B. abortus* biovars 1, 2, 3, 4, and some isolates from biovar 9, as well as *B. ovis*, require an increased concentration of CO_2 for growth, especially in the case of primary cultures obtained directly from infected animals. Within the more recently described species, most strains of *B. pinnipedialis* require supplementary CO_2 for growth, and most of *B. ceti* do not (Foster et al., 1996). The CO_2-dependence may be lost by subculturing *in vitro*, with an estimated frequency of 3×10^{-10} per cell division (Marr and Wilson, 1950), and this is what happened with well-known laboratory *B. abortus* biovar 1 strains like 2308 or S19, that grow in ambient air.

Facultative intracellular bacteria face two environmental conditions with very dissimilar concentrations of carbon dioxide (CO_2). Inside mammalian cells, CO_2 concentration may be as high as 5%, while atmospheric concentration is currently estimated at 0.04%. CO_2 and bicarbonate (HCO_3^-) are essential growth factors for bacteria, and they can be interconverted spontaneously at significant rates. The reversible hydration of CO_2 into HCO_3^- can also be catalyzed by carbonic anhydrase (CA), a ubiquitous metalloenzyme fundamental to many biological functions including photosynthesis, respiration, and CO_2 and ion transport. The CA superfamily (CAs, EC 4.2.1.1) has been found in all the three domains of life (Eubacteria,

Archaea, and Eukarya) and it currently includes seven known families (α-, β-, γ-, δ-, ζ- η-, and θ-CAs) of distinct evolutionary origin (Supuran, 2018). The conversion of CO_2 into HCO_3^- is accelerated in the presence of CA and has the effect of ensuring correct CO_2 concentration for carboxylating enzymes involved in central, amino acid and nucleotide metabolism (Merlin et al., 2003).

CA has been shown to be required to support growth under ambient air in a number of microorganisms like *Ralstonia eutropha* (Kusian et al., 2002), *Escherichia coli* (Hashimoto and Kato, 2003; Merlin et al., 2003), *Corynebacterium glutamicum* (Mitsuhashi et al., 2004), *Saccharomyces cerevisiae* (Aguilera et al., 2005). Growth of CA mutants of these organisms was only possible under an atmosphere with high levels of CO_2,phenomenon that is explained by the availability of bicarbonate, which is substrate for various carboxylation reactions of physiological importance. These reactions are catalyzed by several housekeeping enzymes. like 5'-phosphoribosyl-5-amino-4-imidazole carboxylase (EC 4.1.1.21), phosphoenolpyruvate carboxylase (EC 4.1.1.31), carbamoyl phosphate synthetase (EC 6.3.4.16), pyruvate carboxylase (EC 6.4.1.1), and acetyl-CoA carboxylase (EC 6.4.1.2). They catalyze key steps of pathways for the biosynthesis of not only physiologically essential but also industrially useful metabolites, such as amino acids, nucleotides, and fatty acids (Mitsuhashi et al., 2004). A role for carbonic anhydrase in the intracellular pH regulation has also been demonstrated in some bacteria (Marcus et al., 2005).

..

Brucella species contain two different β-CA, first identified in *B. suis* 1330, as thus named $_{Bs1330}$CAI and $_{Bs1330}$CAII. Both CAs contain the amino acid residues involved in binding of the Zn ion (typical of the β family of CAs), as well as those involved in the catalytic site. Their activity has been verified *in vitro*, and it is slightly higher in $_{Bs1330}$CAII than $_{Bs1330}$CAI (Joseph et al., 2010; Joseph et al. 2011). Pérez-Etayo et al. (2018) compared CAI and CAII activity (activity defined empirically as that allowing growth in a normal atmosphere, the same definition used throughout this study) in several strains of *B. suis*, *B. abortus* and *B. ovis*, and determined that CAII is not

functional in CO_2-dependent *B. abortus* and *B. ovis,* thus establishing a correlation between CA activity and CO_2 dependence. They also observed that CAI is active in *B. suis* 1330 or 513, but not in *B. abortus* 2308W, 292 and 544. Moreover, although an active CAI alone is enough to support CO_2-independent growth of *B. suis* in rich media, it is not able to do it in minimal media, or to support CO_2-independent growth of *B. abortus* at all. A similar result was also obtained by Varesio et al (2019) that identified $BcaA_{BOV}$ (CAII) as the enzyme responsible for the growth of *B. ovis* in a standard, unsupplemented atmosphere (0.04% CO2), in this case, by whole genome sequencing of CO_2-independent mutants. Interestingly, they also reported that a CO2 downshift *B. ovis* initiates a gene expression program that resembles the stringent response and results in transcriptional activation of its type IV secretion system. This shift is absent in *B. ovis* strains carrying a functional copy of carbonic anhydrase.

The classical biotyping mentioned above, despite its limitations and the emergence of new molecular approaches to identify and classify *Brucella* at different taxonomic levels, is still extensively used by reference laboratories, often side by side with the new molecular methods (Garin-Bastuji et al., 2014). However, although there is a known link between phenotype and its genetic cause in some traits like urease activity or erythritol sensitivity (Sangari et al., 2007; Sangari et al., 1994), there is still a gap between the information provided by the molecular methods and the phenotype of *Brucella* isolates. With the availability of more genome sequences, it should be possible to reduce this gap by comparing the phenotypic characteristics of *Brucella* strains with their genome content. Comparative genomics of whole-genome sequences is especially interesting in bacterial pathogenesis studies (Hu et al., 2011). Pathogenomics can be considered as a particular case of comparative genomics, and it has been extensively used for the identification of putative virulence factors in bacteria, by comparing virulent and avirulent isolates (Pallen and Wren, 2007), although in principle could be applied to the elucidation of any phenotypic trait. The genus *Brucella* is a very homogeneous one, with over 90% identity on the basis of DNA-DNA hybridization assays within the classical species, and this results in relatively minor genetic variation between species that sometimes

result in striking differences. As an example, only 253 single nucleotide polymorphisms (SNPs) separate *B. canis* from its nearest *B. suis* neighbour (Foster et al., 2009), but their host specificity differs widely; while *B. canis* is almost entirely restricted to the *Canidae* family, *B. suis* has a wide host range that includes pigs, dogs, rodents, hares, horses, reindeer, musk oxen, wild carnivores and humans. Similarly, there are only 39 SNPs consistently different between the vaccine strain *B. abortus* S19 and strains *B. abortus* 9-941 and 2308, two well-known virulent isolates (Crasta et al., 2008). In the last years a large number of *Brucella* genomes representing all species and biovars have been sequenced, and all this wealth of information is already resulting in new molecular epidemiology and typing methods (O'Callaghan and Whatmore, 2011). We have tested the potential of pathogenomics to unveil phenotypic traits in *Brucella* by defining the pangenome / pseudogenes of a set of *Brucella* strains, and comparing it with the CO_2 dependence of those strains. This process has allowed us to identify Carbonic Anhydrase (CA) II, as the enzyme responsible for growth of the bacteria at atmospheric CO_2 concentrations, and extend the analysis to new species of *Brucella*. All the sequenced genomes of *Brucella* contain two β-CA genes, but only those that carry a defective β-CA II require supplemental CO_2. Reversion of this phenotype happens *in vitro* at a low frequency and is accompanied by a compensatory mutation that results in a full-length β-CAII product. We have also tested the hypothesis that the presence of a truncated β-CAII would have a competitive advantage *in vivo*, as a way to explain why a mutation with such a low frequency could get fixed in some *Brucella* species and biovars. A competitive assay shows that one of such mutants is significantly enriched in a mouse model of infection when compared with its corresponding full-length β-CAII strain. This could explain why CO_2-dependent strains are selected *in vivo*. The polymorphisms affecting β-CAII encoding genes allow the prediction of the CO_2-dependence status of any given strain, thus having the potential to replace the classical assay to characterize *Brucella* isolates.

Materials and Methods

Bacterial strains and growth conditions.

The bacterial strains and plasmids used in this work are listed in Table 1. *Brucella* strains were grown at 37°C for 48–96 hours in a 5% CO_2 atmosphere in *Brucella* broth (BB) or agar (BA) medium (Pronadisa, Spain). Media were supplemented with 10% foetal bovine serum to grow *B. ovis*. All experiments with live *Brucella* were performed in a Biosafety Level 3 facility at the Department of Molecular Biology of the University of Cantabria, and animal infections with *Brucella* were conducted at the University of Cantabria animal facilities, also under BSL3 conditions.

Bioinformatic methods

Genomic and protein sequences of the different *Brucella* species were obtained from GenBank and the Broad Institute (https://www.broadinstitute.org/projects/brucella). To allow easy comparison between the genes and pseudogenes in the different *Brucella* species, we constructed the panproteome of a selected set of 10 strains with the most complete genome annotation at the time (Table S1). To construct this set we started with all the CDS annotated in the *B. suis* 1330 genome. Next we found the most probable functional counterparts for the n pseudogenes annotated in *B. suis* 1330. The pseudogene list was taken directly from the original annotation of the *B. suis* 1330 genome. Finally, we added those CDS in indels from the other genomes not present in *B. suis* 1330. We assigned a new gene name to every CDS in our set following the Bru1_xxxx and Bru2_xxxx nomenclature, depending on the location of the gene in the *B. suis* genome. CDS from indels were also renamed with a nomenclature, BRU1_iXXXX, the “i” indicating their origin from indels absent in *B. suis* 1330. The file pan_pep provided in the supplementary materials is a multifasta protein file containing the sequence of all the 3496 CDS present at least once in any of the used genomes, and constitutes the first version of the *Brucella* pan proteome. The genes and pseudogenes annotated in these

genomes were tabulated and assigned to one of the different gene families present in those genomes. In this way we constructed a spreadsheet with the pseudogenes in each genome using a uniform nomenclature. The analysis of the CA sequences at both the DNA and protein levels was extended to a group of 35 *Brucella* genomes (Table S2 in the supplementary material).

A structural theoretical model of *Brucella* $_{Ba2308}$CAII was generated by molecular threading using the protein homology and recognition engine Phyre2 (Kelley et al., 2015), taking the atomic coordinates of the best hitas template. The pdb model generated was visualized using the PyMOL Molecular Graphics System, version 1.3 (Schrödinger, LLC, Portland, OR, USA).

Primers used in this study (Table 2) were designed with Primer 3 (http://bioinfo.ut.ee/primer3-0.4.0/) and synthesized by Sigma-Aldrich.

Isolation of CO_2-independent mutants in CO_2-dependent *Brucella* strains.

Different CO_2-dependent *Brucella* strains from our collection were streaked onto BA plates and grown in a 5% CO_2 atmosphere. Individual colonies were then re-streaked in duplicate plates, and incubated at 5% CO_2, and ambient atmosphere to check for the correct CO_2-dependence phenotype. They were grown as a lawn in fresh BA plates, and the growth was resuspended in PBS. The suspension was serially diluted and each dilution seeded in duplicate in BA plates. One dilution series was incubated at 5% CO_2 to enumerate the number of bacteria in the inoculum, while the second was incubated at ambient atmosphere to select for CO_2-independent colonies. The mutation rate was expressed as number of mutants per number of initial bacteria. Individual mutants were selected, and genomic DNA was obtained by using InstaGene matrix as described by the supplier (Bio-Rad Laboratories, United Kingdom). *CAI* and *CAII* complete sequences from the different strains were amplified by PCR with oligonucleotides BS192_0456.F/R and BS191_1911.F/R respectively, and sequenced to determine if there was any change compared to the corresponding parental sequence.

Infection and intracellular viability assay of *B. abortus* in J774 cells.

J774.A1 macrophage-like cells (ATCC, TIB-67) were cultured in RPMI medium with 2 mM L-glutamine, and 10% FBS at 37°C in 5% CO_2 and 100% humidity. Confluent monolayers were trypsinized and $2x10^5$ cells/well were incubated for 24 h before infection in 24-well tissue culture plates. Macrophages were infected with *Brucella* strains in triplicate wells at a MOI of 50. After infection for 30 minutes, the wells were washed five times with sterile phosphate-buffered saline (PBS) and further incubated for 30 minutes in RPMI with 2 mM L-glutamine, 10% FCS and 50 µg gentamicin ml^{-1} to kill extracellular bacteria. That was taken as time 0 post-infection, and the medium was changed to contain 10 µg gentamicin ml^{-1}. The number of intracellular viable *B. abortus* was determined at different time points by washing three times with PBS and lysing infected cells with 0.1% Triton X-100 in H_2O and plating a series of 1:10 dilutions on BA plates for colony-forming unit (CFU) determination.

Competitive infection assays.

The following protocol was approved by the Cantabria University Institutional Laboratory Animal Care and Use Committee and was carried out in accordance with the Declaration of Helsinki and the European Communities Council Directive (86/609/EEC). Comparison of fitness between CO_2-dependent and isogenic CO_2-independent strains was done through a competitive infection assay in order to minimize animal-to-animal variation. BALB/c mice (CRIFA, Spain) were injected with 1:1 mixtures of *B. abortus* 292 (CO_2 dependent, wild type) and *B. abortus* 292mut1 (a spontaneous $_{Ba292}$*CAII* CO_2-independent mutant). Two hundred microliters of a suspension containing approximately 10^8 bacteria were administered intraperitoneally to a group (n = 6) of 6- to 8-week-old female BALB/c mice. Mice were sacrificed 8 weeks after infection, and the liver and spleen were removed aseptically and homogenized with 5 ml of BB containing 20% glycerol. Samples were serially diluted and plated in quadruplicate on BA plates. Half of the plates were incubated with 5% CO_2, and the other half at ambient atmosphere. Additionally, colonies grown at 5% CO_2 were replica-plated and incubated at both CO_2 concentrations, to measure the ratio of CO_2-dependent and CO_2-independent colonies in two independent ways. For *in vitro* CI assays, BA plates were seeded forming a lawn with the infection mix, and

incubated at 37°C with 5% CO_2 for eight weeks, with repeated subculture in fresh BA plates every 4-5 days in the same conditions. The ratio of CO_2-dependent and CO_2-independent colonies was determined with the same protocol as the *in vivo* CI. The competitive index (CI) was calculated as the ratio of mutant to wild-type bacteria recovered at the end of the experiment divided by the ratio of mutant to wild-type bacteria in the inoculum, and the differences between groups were analyzed by Student's two-tailed t test with significance set at $P<0.05$.

Results

Identification of the gene responsible for the CO_2-dependence in *B. abortus*

The first evidence of the involvement of Carbonic Anhydrase in the CO_2 dependence phenotype came from the analysis of pseudogenes in the ten fully annotated *Brucella* genomes (Table S1). After tabulation of the pseudogenes, their presence along with the different species was compared with the target phenotype, in this particular case we interrogated the spreadsheet n_pseudos.xls (Supplementary material) to find out which genes are pseudogenes only in those strains in our list that are CO_2 dependent, *B. abortus* 9-941 and *B. ovis*. Three genes met this criterium, namely Bru1_1050 which encodes for a multidrug resistance efflux pump, Bru1_1827 which encodes for carbonic anhydrase II and Bru2_1236, encoding for an Adenosylmethionine-8-amino-7-oxononanoate aminotransferase.

Given the requirement of CA for growth of other microorganisms at ambient CO_2 concentrations, and to check if Bru1_1827 could be responsible for the CO_2-dependence phenotype, we retrieved and aligned the DNA and corresponding amino acid sequences obtained from a set of 35 *Brucella* strains with a known requirement for CO_2 (Wattam *et al*, 2014), (Table S2). Sequences were clustered with VSEARCH (Rognes et al., 2016), resulting in 10 unique sequences that were aligned with ClustalW (Larkin et al., 2007). The CO_2-

267 independent isolates code for full-length identical proteins except for the *B. abortus* 2308 and
268 2308A strains that have an extra amino acid, Ala113. On the contrary, the CO_2-dependent
269 isolates contain different frameshifts or single point mutations, that result in truncated or altered
270 proteins (Figure 1).

271 A group of 3 *B. abortus* strains (86/8/59, 9-941, and 292) shows an extra "C" at position
272 337 in the *CAII* gene when compared with the wild type allele, leading to a frameshift that
273 causes a premature stop, truncating half of the protein. *B. ovis* ATCC 25840 shows an extra "G"
274 at position 523, that similarly leads to a frameshift that alters the last third of the protein at the
275 C-terminus. Finally, 3 *B. pinnipedialis* strains (M163/99/10, M292/94/1, and B2/94) contain a
276 SNP, 557T>C, that causes a non-conservative amino acid substitution, Leu186Pro (Fig. 1B).

277 C337 also appears in CO_2-independent *B. abortus* biovar 1 strains, like S19, 2308, or
278 NTCC 8038, but in these cases there are additional mutations that recover the original ORF;
279 two extra nucleotides in strain 2308, or one nucleotide deletions in *B. abortus* NCTC 8038 and
280 S19. These changes do not affect the conserved amino acid residues typical of β-CAs involved
281 in the catalytic cycle, that is, the four zinc-binding residues, Cys44, Asp46, Hys105, Cys108,
282 and the catalytic dyad Asp46 and Arg48 (Fig. 1B). Some of the strains analyzed here (*B. suis*
283 1330, and *B. abortus* strains 2308W, 292 and 544) were also analyzed by Pérez-Etayo et al,
284 (2018), and our results are in complete agreement.

285 There is one discrepancy involving *B. abortus* Tulya, a biovar 3 strain that according to
286 the literature (Alton et al., 1988) should be CO_2-dependent, but according to our analysis codes
287 for a full-length CAII, thus being grouped with the CO_2-independent isolates. To solve this
288 apparent puzzle, we plated a sample of *B. abortus* Tulya from our laboratory stock and
289 determined its CO_2-dependence. Contrary to the original reference strain phenotype, and in
290 agreement with our *in silico* analysis, this isolate was indeed CO_2-independent. The complete
291 $_{BaTulya}$*CAII* was amplified by PCR from our strain and sequenced, confirming the published
292 sequence. This strain originated from the collection kept in the Centro de Investigación y
293 Tecnología Agroalimentaria of Aragón (CITA), Zaragoza, Spain, where it is also labelled as

being CO_2-independent, suggesting that this is not the result of a contamination or selection of a CO_2-independent mutant in our hands.

As *Brucella* species code for two different carbonic anhydrases (Joseph et al., 2010), we repeated the analysis for the CAI-coding sequences (CDS) . Although several isolates contain a polymorphism consisting of a 24 nt deletion between two 11 nt direct repeats, or different SNPs (Fig S1, Supplemental information), there was no obvious correlation between the presence of these polymorphisms and CO_2-dependence. Pérez-Etayo et al (2018) demonstrated that CAI from *B. abortus* strains 2308W, 292 and 544 is inactive, while that from *B. suis* strains 1330 and 513 is active, although it can only mediate CO_2-independence in complex media, and in a rather prototrophic host. Comparison of $_{Bsuis513}$CAI and $_{Babortus2308W}$CAI reveals a difference of only one amino acid, the valine at position 74 being replaced by a glycine.

Brucella CO2-independent spontaneous mutants present a modified CAII sequence.

Comparison of some of the *CAII* sequences of *B. abortus* biovar 1 CO_2-independent strains like 2308, S19, or NCTC 8038 with those of the other *Brucella* CO_2-dependent and independent isolates suggests that reversion of the CO_2 requirement is coincidental with the introduction of compensatory mutations able to reverse the initial frameshift described above. CO_2-independent mutants have been previously reported to appear at a low frequency (3×10^{-10}) in cultures of CO_2-dependent strains by subculturing *in vitro* in the absence of supplementary CO_2 (Marr and Wilson, 1950). We measured the frequency of the reversion in six CO_2-dependent strains from our laboratory collection, by growing duplicate cultures with or without CO_2. We first checked the phenotype of all the strains by streaking them in a BA that was incubated without added CO_2. All the strains but *B. abortus* Tulya, as reported above, failed to grow in these conditions, in agreement with the published phenotype. We then plated o/n cultures from the CO_2-dependent strains to obtain colonies grown at ambient atmosphere, and calculated the frequency of revertants for those strains (Table 3). The *B. abortus* strains had a similar frequency to the one described by Mar and Wilson, 10^{-8} to 10^{-10}, but *B. ovis* and *B. pinnipedialis* had a higher frequency of reversion, 10^{-6}. In an exploratory effort to identify a possible cause for

these differences in mutation rates, we analyzed the presence and identity between strains of the most obvious proteins that could be involved in this phenotype, like DNA polymerases, MutT, MutS, MutD, etc. Blastp analysis showed that, in all the cases, the protein was not only present in all strains, but had a 100% identity, so we could not find any difference that could explain our results. Maybe the analysis of the frequency of reversion in more CO_2-dependent strains will reveal if this is a species, biovars or even isolate phenotype. We selected a few revertants from each strain, and amplified by PCR the CAI and CAII coding regions. The amplicons were then sequenced to determine if any compensatory mutation had appear in those loci. In all cases we found compensatory mutations in the same region, around nucleotides 333-343. All mutations in this hot spot resulted in full length CAII proteins (Figure 2), or in the case of *B. pinnipedialis*, a C to T change that reverts the Leu to Pro substitution. In this case, we also found the insertion of a nucleotide triplet (CGC or CCG) at the hot spot, that results in the addition of an extra amino acid, either Ala113 or Arg113. That is the same position wherethe extra codon in $_{Ba2308}$CAII is located. Although some of the compensatory mutations appear several times, the most common situation was to find different mutations for the same sequence.

As expected, reversion of the CO_2-dependence phenotype did not produce any change in the coding sequence of CAI, reinforcing the hypothesis that CAII plays the main role in CO_2-independence.

Structural modelling of $_{Babortus2308}$CAI and $_{Babortus2308}$CAII

A single amino acid substitution, Val74 in $_{Bsuis513}$CAI to Gly74 in $_{Babortus2308W}$CAI, putatively renders the protein inactive, while the mutations in CAII in CO_2-dependent *Brucella* isolates do not affect the region where the active center is located, at the N-ter part of the protein (Fig 1B). Moreover, a non-conservative Leu186Pro substitution, far from the active center, is enough as to induce CO_2-dependence in the *B. pinnipedialis* strains analyzed. To better understand the effect of the observed mutations, a structural theoretical model of $_{Ba2308}$CAI and $_{Ba2308}$CAII was

built with Phyre2. The modelled structures closely resembled those of other β-CAs that have been crystalized, displaying matches with a 100% confidence.

The closest structural homologue to $_{Ba2308}$CAI is 1DDZ, a β-CA from the red alga *Porphyridium purpureum* (Mitsuhashi et al., 2000), with a 45% identity. Each 1DDZ monomer contains two internally repeated structures, each one homologous to $_{Ba2308}$CAI. Overlapping of the modelled structures shows how the mutated residue Gly76 lies in close proximity to the coordinated zinc atom, and also to the dimer interface (Figure 3). In the equivalent position of Val76 in $_{Bsuis513}$CAI, 1DDZ contains Ile173 or Ile427, both among the most hydrophobic of amino acids. These residues are stablishing hydrophobic contacts in the interface between the domains; Iso173 with Val441 and Phe442 (upper zoom image) and Iso427 with Phe168 and Tyr190 (lower zoom image). Identical (Phe71, Val90) and similar (Phe93) residues are located in the equivalent positions in *Brucella*$_{Ba2308}$CAI. The presence of a Glycine in *Brucella*$_{Ba2308}$CAI instead of an Isoleucine disrupts these hydrophobic interactions and could impair dimerization. Besides, this substitution could locally alter the folding of this region and affect the nearby residues that are coordinating the Zn atom. In both cases the structure, and consecuently the activity of the protein, would be affected. Indeed a Val to Gly substitution, located in the dimerization surface, was shown to interfere with dimerization of citrate synthase from *Thermoplasma acidophilum* (Kocabiyik and Erduran, 2000), reducing not only its catalytic activity (about 10-fold), but also decreasing its thermal and chemical stability.

The model structure obtained for $_{Ba2308}$CAII is shown in Figure 4, along with the dimer structure of the best hit obtained, 5SWC, showing a 29% of identity and 100% confidence. 5SWC is the β-carbonic anhydrase CcaA from *Synechocystis* sp. PCC 6803. As $_{Ba2308}$CAII contains an extra codon, the residue highlighted in red, Leu187, is the equivalent residue to the Leu186Pro change that is present in the CO_2-dependent *B. pinnipedialis* strains.

In this structure the protein crystalizes as a dimer, with the N-terminal arm composed of two alpha-helical segments (H1 and H2) that extend away from the rest of the molecule and make significant contacts with the last β-sheet with an adjacent monomer (in the case of $_{Ba2308}$CAII His188 with Met1, and Trp191 with Leu4). This interaction between monomers has been

377 determined as crucial for the establishment of the dimer (Cronk et al., 2001). In the case of *B.*
378 *abortus* strains 86/8/59, 9-941, and 292, the premature stop would cause the complete loss of
379 the C-ter end of the protein, including the last β-sheet, involved in the formation of the dimer. *B.*
380 *ovis* ATCC 25840 shows also a completely altered C-terminus, and although the new amino
381 acid sequence would remain folded as a β-sheet, it shows a completely different amino acid
382 composition that would prevent the establishment of the right molecular interactions between
383 the adjacent monomers. Regarding the last mutation observed in CO_2-dependent strains, the
384 SNP present in *B. pinnipedialis* strains M163/99/10, M292/94/1 and B2/94 causes a non-
385 conservative amino acid substitution, Leu186Pro. The model predicts that this change will occur
386 at the last β-sheet, in the area of interaction with the N-terminus of the adjacent monomer.
387 Proline is an amino acid that confers an exceptional conformational rigidity, and as such is a
388 known disruptor of both alpha helices and beta sheets. This being the case, this substitution is
389 predicted to disrupt the dimerization of *Brucella* CAII.
390
391 **Competitive infection assays.**
392 Strain 2308 is not only a CO_2-independent *Brucella* isolate, but also one of the most widely used
393 virulent challenge strains, while S19, also a CO_2-independent *Brucella* isolate is an attenuated
394 vaccine strain. *In vitro* cell assays using J774 macrophages did not detect any difference in
395 virulence between a CO_2-dependent *B. abortus* 292 strain and its corresponding CO_2-
396 independent revertant (Figure 5). Additionally, we could not find any report in the literature that
397 suggests that the CO_2-dependence phenotype is related to virulence, and however there is one
398 puzzling fact; despite the expected low frequency of a frameshift mutation, somehow this mutation
399 is fixed in several species and biovars of *Brucella*. It is then reasonable to think of it as having a
400 biological advantage in specific situations. Competitive index (CI) assays have been used to
401 reveal subtle differences in fitness between two strains, and intra-animal experiments help to
402 minimize inherent inter animal biological variation and also improve the identification of mutations
403 or isolates with reduced or improved competitive fitness within the host (Falkow, 2004). As this
404 could be the case with $_{Ba2308W}$CAII, we performed a CI experiment using *B. abortus* 292 and one

of its CO_2-independent mutants, 292mut1. As a control we grew the same initial mixture in BA plates that were incubated at 37ºC with 5% CO_2, to know if any change in CI could be attributed to just the CO_2 concentration, or there was some other factor that could be attributed to growth within an animal. Results are shown in Figure 6. During the course of the experiments in mice, there was a significant enrichment of the strain carrying the truncated form of $_{Ba2308W}$CAII *B. abortus* 292, when compared with the CO_2-independent revertant able to produce a complete active form of $_{Ba2308W}$CAII. There was not a significant change in the ratio of both strains in liver or spleen, so the colony counts were combined in each mouse to show the ratio in that mice. At the same time, there was no significant enrichment / change in the ratio in cultures grown on plates. This suggests that inactivation of $_{Ba292}$CAII has some fitness advantage *in vivo*, and could eventually result in the displacement of their corresponding CO_2-independent counterpart. This hypothesis could explain why, despite the low frequency of mutation, CO_2-dependent strains appear on primary isolation. As there are some other species and biotypes of *Brucella* that are CO_2-dependent on primary isolation we could infer that the fitness advantage is also present in those species and biotypes.

Discussion

Diagnosis of brucellosis is usually achived by serological detection in both animals and humans. This could be enough to warrant the initiation of response measures, like start of antibiotic therapy in humans, or immovilization or sacrifice of animals. However, isolation, identification and subtyping of brucellae is not only definitive proof of infection, but also allows epidemiological surveillance. Depending on the laboratory, this process is carried out by a combination of classical and modern molecular methods. The classical typing methods consist in the phenotypic characterization of the isolates, using biochemical and immunological tests (CO_2 requirement, H_2S production, urease activity, agglutination with monospecific A, R, and M sera, growth on media with thionin or basic fuchsin, or sensitivity to erythritol), and susceptibility to lytic *Brucella* phages (Alton et al., 1988). These methods require culture of the bacteria, are usually time-consuming and laborious, and they do not offer a good discriminatory power. Moreover, in the last years the field has experienced a revolution with the advent of new molecular methods, resulting in the description of new species, and a better understanding of the population structure of the genus *Brucella*. Thus the classical methods are being replaced or complemented by modern molecular methods. These methods range from PCR detection systems targeting different locus (like *ery*, *bcsp31*, or IS711), that allow species and even biovar differentiation (Mayer-Scholl et al., 2010; López-Goñi et al., 2011), to the multilocus sequence analysis (MLSA) that has been successfully used to describe the phylogenetic relationships of isolates, and the global population structure of the genus *Brucella* (Whatmore et al., 2016). More recently, with the advent of Whole Genome Sequencing (WGS), and especially with the drop in sequencing prices, WGS has been proposed to be the new routine typing method, particularly in groups with a high degree of similarity at the biochemical or serological levels (Chattaway et al. 2017), like *Brucellaceae* is. But these methods are still far from being routine in most brucellosis laboratories, particularly in developing countries, and the classical methods are still routinely used in reference laboratories. Although genomic information offers the potential to unveil most of the phenotypic traits in bacteria, there are still important attributes

that are not evident in the genome sequence. Thus, there is a gap between the classical typing scheme and the molecular methods, and some features still can not be attributed to any specific genetic trait. In the case of *Brucella* it is particularly interesting the host specificity, that it is yet impossible to predict from the genome sequence. It is reasonable to think that as molecular typing improves we should advance in closing the gaps between classical and molecular typing, and we would be able to predict the full virulence and host specificity of a given isolate by analyzing the genome content. We have started to address this gap by looking at the genomic differences between *Brucella* isolates regarding one of the classical test for typing, as it is CO_2 requirement.

B. abortus biovars 1, 2, 3, 4, and some isolates from biovar 9, as well as *B. ovis*, require an increased concentration of CO_2 for growth, as do most strains of *B. pinnipedialis*, but only some of *B. ceti.* We selected 10 *Brucella* strains that have been sequenced and annotated, and which CO_2 dependence status was known, to construct a *Brucella* pangenome based on the *B. suis* 1330 genome annotation. This resulted in a collection of 3496 CDS. We next compared the distribution of pseudogenes (as annotated in the databases) and absent genes with the CO_2 dependence, resulting in only three candidate genes, Bru1_1050 which encodes for a multidrug resistance efflux pump, Bru1_1827 which encodes for carbonic anhydrase II and Bru2_1236, encoding for an Adenosylmethionine-8-amino-7-oxononanoate aminotransferase. The most obvious candidate was CAII, as it has been shown to be required to grow under ambient air in a number of microorganisms. To confirm our initial result, we extracted and aligned the DNA and amino acid sequences of CA II from an extended set of sequenced strains with a known CO_2 phenotype. Those strains that are able to grow in atmospheric concentrations of CO_2 carry a full length copy of the protein, while those that are not contain truncated or mutated versions of the proteins. *Brucella* species also carry a second carbonic anhydrase, CAI, but the polymorphisms found both at the DNA and protein levels do not allow to infer the CO_2-dependence. This result is in agreement of that reported by Pérez-Etayo et al. (2018), and Varesio et al. (2019), and further extends the range of strains tested.

A direct application of this result would be the determination of the CO_2-dependence status of any given strain by determining the sequence at the CAII locus. This is actually the case in *B. abortus* Tulya, where our analysis predicted that our stock should be CO_2-independent, as it was the original stock from CITA. Laboratory determination of the phenotype confirmed the *in silico* result. This approach could be used to determine, or at least narrow down candidate genes for different phenotypes, obviously with monogenic traits being the easier to determine. We have found three different mutations that caused dependence of added CO_2, two independent insertions (C337 and G523) that either cause a premature stop, or change completely the C-terminus of the protein, and a SNP that changes a leucine for a proline in the last β-sheet. All bacterial β-CAs crystallized so far are active as dimers or tetramers, and inactive as monomers, and all of them have the N-terminal α-helix arm that extends away from the rest of the molecule and makes significant contact with the last β-sheet of an adjacent monomer (Supuran, 2016). In all the cases observed in this work, the mutations do not affect the active site, but all of them potentially change the sequence and structure of the protein at the C-terminus so the most obvious hypothesis is that it is the modified structure of the proteins the cause for the loss of activity. Inactive *Brucella* CAII proteins either lack the last β-sheet completely, or have a very different sequence composition that disrupts this last β-sheet. The substitution of a leucine by a proline in the β-sheet is a particular example of this later case, as proline is known to be very disruptive amino acid for both α-helices and β-sheets structures. As these contacts seem to be important for dimerization, we can hypothesize that all the mutations found in CAII will have a strong impact in the dimerization or multimerization of CAII that will remain as a monomer, losing its activity (that we have defined as that allowing growth in a normal atmosphere). But there is a caveat in this reasoning. We, as well as others (Pérez-Etayo et al., 2018) have been unable to obtain a full-length mutant of CAII, despite being able to obtain a CAI (both data not shown). Moreovera transposon sequencing analysis shows that CAII is essential, at least for *B. abortus* 2308 (Sternon et al., 2018). This experiment was apparently carried out without added CO_2, so the result is not unexpected. It would be interesting to know if, performed in the presence of 5-10% CO_2, they would have observed

505 insertions only in the C-ter of the protein, where the mutations in the natural CO_2-dependent
506 isolates accumulate. This means that the C-terminal part of the protein still carries out at least
507 some of its functions as a monomer. We have not found any information regarding the activity of
508 β-carbonic anhydrases as monomers, but in the α-carbonic anhydrase from *Thermovibrio*
509 *ammonificans* the destabilization of the tetramer by reduction of the cysteines results in the
510 dissociation of the tetrameric molecule into monomers with lower activity and reduced
511 thermostability. It seems reasonable to think that this is the case also for *Brucella* CAII.
512 CAII catalizes the fixation of CO_2 with high efficiency when forming dimers, but the low
513 efficiency of the carboxylation reaction when acting as a monomer would require the presence
514 of higher amounts of CO_2.
515 A similar situation could be taking place in the case of CAI. Modelling of the structure of
516 $_{Babortus2308}$CAI allows to hypothesize the role of the only residue of difference with $_{Bsuis513}$CAI, that
517 has to be responsible for the absence of activity in the first one. Its localization close to the Zn
518 atom and to the dimer interface probably results in the destabilization of the dimer, lowering or
519 abolishing its activity. However, it would be necessary to purify and characterized biochemically
520 the monomers of both $_{Babortus2308}$CAI and $_{Babortus2308}$CAII to confirm our model.
521
522 These mutations can only be selected in high CO_2 environments, like those present
523 inside animals, where high CAII activity would be dispensable, as this atmosphere generates
524 enough bicarbonate in solution as to fullfil the metabollic requirement of the bacteria (Nishimori
525 2009). We have determined the frequency of appearance of CO_2-independent isolates, and
526 although there is a huge variation between strains, it ranges from 10^{-6} to 10^{-10}, as previously
527 described. Despite its low frequency, somehow these mutations got selected in several species
528 and biovars of *Brucella*, suggesting that they provide some biological advantage. To test this
529 hypothesis, we performed a competitive assay both *in vitro* and *in vivo*. This assay resulted in a
530 significant enrichment of the strain carrying an inactive carbonic anhydrase in animals, but not
531 in cultured plates. Pérez-Etayo et at (2018) assayed the bacterial loads of *B. ovis* PA and *B.*
532 *ovis* PA Tn7$_{Ba2308W}$CAII in the spleens of BALB/c mice at 3 and 8 weeks post-infection, and

found that there was no significant difference between a CO_2-dependent and its corresponding CO_2-independent strain at the level of multiplication in the mouse model. This apparent contradiction with our own results could be due to the different species used, or to the different experiment used to test this hypothesis. When trying to determine subtle differences in fitness between two given strains, a competitive assay has a higher discrimination power (Eekels et al., 2012; Shames et al, 2018), as any effect is amplified over time. Although the ultimate reason behind this competitive advantage is currently unknown, it would explain why some strains and biovars of *Brucella* are dependent of CO_2 in primary isolation, despite the low frequency of mutation. It is also noteworthy that this phenotype is only observed in certain species and biovars, suggesting that the competitive advantage of the CAII mutants only applies to a subset of host/pathogen pairs. As CAII is essential, the mutant strains still would have to produce the protein, and thus the metabolic gain should be negligible for them. Another possibility would be that the dimer form of the enzyme is too active in a high CO_2 environment, and causes a deleterious acidification in the bacteria. By evolving this sophisticated system that reversibly alters the dimerization state of the protein, *Brucella* is able to adjust to the different requirements encountered during its biological cycle.

Acknowledgements

This work was supported by grants BFU2011-25658 from the Spanish Ministry of Science and Innovation, and by grant 55.JU07.64661 from the University of Cantabria to FJS. BAR was supported by a Scholarship received from DGAPA-UNAM. The authors want to acknowledge help from María J. Lucas and Elena Cabezón in the drawing and interpretation of crystallographic data.

561 **References**
562

563 Aguilera**,** J., Van Dijken, J. P., De Winde, J. H. and Pronk, J. T. (2005). Carbonic anhydrase
564 (Nce103p): an essential biosynthetic enzyme for growth of *Saccharomyces cerevisiae* at
565 atmospheric carbon dioxide pressure. *Biochem J* **391**: 311-316.
566 Alton, G. G., Jones, L. M., Angus, R. D., and Verger, J. M. (1988). Techniques for the
567 Brucellosis Laboratory. Paris: INRA.
568 Buck JM. Studies on vaccination during calfhood to prevent bovine infectious abortion. (1930). *J*
569 *Agri Res*. **41**:667–689.
570 Chain PS, Comerci DJ, Tolmasky ME, Larimer FW, Malfatti SA, et al. (2005) Whole-genome
571 analyses of speciation events in pathogenic *Brucellae*. *Infect Immun* **73**(12): 8353–8361.
572 Chattaway MA, Schaefer U, Tewolde R, Dallman TJ, Jenkins C. (2017). Identification of
573 *Escherichia coli* and *Shigella* species from Whole-Genome Sequences. *J Clin Microbiol*.
574 **55**(2):616-623. doi: 10.1128/JCM.01790-16.
575 Crasta OR, Folkerts O, Fei Z, Mane SP, Evans C, Martino-Catt S, et al. (2008). Genome
576 Sequence of *Brucella abortus* Vaccine Strain S19 Compared to Virulent Strains Yields
577 Candidate Virulence Genes. *PLoS ONE* **3**(5): e2193. doi:10.1371/journal.pone.0002193
578 Cronk, J. D., Endrizzi, J. A., Cronk, M. R., O'neill, J. W., and Zhang, K. Y.J. (2001). Crystal
579 structure of *E. coli* β–carbonic anhydrase, an enzyme with an unusual pH–dependent activity.
580 *Protein Sci*. **10**(5): 911–922. doi: 10.1110/ps.46301.
581 Eekels, J. J., Pasternak, A. O., Schut, A. M., Geerts, D., Jeeninga, R. E., and Berkhout, B.
582 (2012). A competitive cell growth assay for the detection of subtle effects of gene transduction
583 on cell proliferation. Gene Ther. **19**(11):1058-64. doi: 10.1038/gt.2011.191
584 Falkow S. (2004). Molecular Koch's postulates applied to bacterial pathogenicity–a personal
585 recollection 15 years later. Nat Rev Microbiol. 2: 67-72. doi:10.1038/nrmicro799.
586 Foster, G., Jahans, K. L., Reid RJ, Ross HM. (1996). Isolation of *Brucella* species from
587 cetaceans, seals and an otter. Vet Rec. **138**:583–586.

588 Foster JT, Beckstrom-Sternberg SM, Pearson T, et al. (2009). Whole-genome-based phylogeny
589 and divergence of the genus *Brucella*. J Bacteriol 191:2864–70.
590 Garcia-Lobo, J. M., and F. J. Sangari. 2004. Erythritol metabolism and virulence in *Brucella*. In I.
591 Lopez-Goñi and I. Moriyon (ed.), *Brucella*: molecular and cellular biology. Horizon Bioscience,
592 Norfolk, United Kingdom.
593 Garin-Bastuji B, Mick V, Le Carrou G, Allix S, Perrett LL, Dawson CE, Groussaud P,
594 Stubberfield EJ, Koylass M, Whatmore AM. (2014) Examination of taxonomic uncertainties
595 surrounding *Brucella abortus* bv. 7 by phenotypic and molecular approaches. Appl Environ
596 Microbiol. 80(5):1570-9. doi: 10.1128/AEM.03755-13.
597 Gerhardt, P. & J. B. Wilson, (1950) Attempts to replace the added carbon dioxide required by
598 some strains of *Brucella abortus*. J Bacteriol 59: 311-312.
599 Gladstone, G. P., P. Fildes, and G. M. Richardson (1935). Carbon dioxide as an essential factor
600 in the growth of bacteria. Br. J. Exp. Pathol. 16:335-348.
601 Halling SM, Peterson-Burch BD, Bricker BJ, Zuerner RL, Qing Z, et al. (2005) Completion of the
602 genome sequence of *Brucella abortus* and comparison to the highly similar genomes of *Brucella*
603 *melitensis* and *Brucella suis*. J Bacteriol 187 8: 2715–2726.
604 Horton RM, Cai ZL, Ho SN, Pease LR. 1990. Gene splicing by overlap extension: tailor-made
605 genes using the polymerase chain reaction. Biotechniques 8(5):528-535.
606 Hu B, Gary Xie, Chien-Chi Lo, Shawn R. Starkenburg, Patrick S. G. Chain (2011) Pathogen
607 comparative genomics in the next-generation sequencing era: genome alignments,
608 pangenomics and metagenomics. *Briefings in Functional Genomics*, 10(6): 322–333.
609 doi:10.1093/bfgp/elr042
610 Joseph P., Turtaut F., Ouahrani-Bettache S., Montero J. L., Nishimori I., Minakuchi T., Vullo D.,
611 Scozzafava A., Köhler S. et al. (2010). Cloning, characterization, and inhibition studies of a
612 beta-carbonic anhydrase from *Brucella suis*. *J Med Chem* **53**, 2277–2285.
613 Joseph, P., Ouahrani-Bettache, S., Montero, J. L., Nishimori, I., Minakuchi, T., Vullo, D.,
614 Scozzafava, A., Winum, J. Y., Köhler, S., and Supuran, C. T. (2011). A new β-carbonic
615 anhydrase from *Brucella suis*, its cloning, characterization, and inhibition with sulfonamides and

sulfamates, leading to impaired pathogen growth. Bioorg Med Chem. 19(3):1172-8. doi: 10.1016/j.bmc.2010.12.048.

Köhler, S., Safia Ouahrani-Bettache & Jean-Yves Winum (2017). *Brucella suis* carbonic anhydrases and their inhibitors: Towards alternative antibiotics?, Journal of Enzyme Inhibition and Medicinal Chemistry, **32**:1, 683-687, doi:10.1080/14756366.2017.1295451

Kocabiyik, S., and Erduran, I. (2000). The effect of valine substitution for glycine in the dimer interface of citrate synthase from *Thermoplasma acidophilum* on stability and activity. Biochem Biophys Res Commun. **275**(2):460-5. DOI: 10.1006/bbrc.2000.3310.

Kupriyanova, E., Pronina, N. & Los, D. (2017). Carbonic anhydrase — a universal enzyme of the carbon-based life. *Photosynthetica* 55: 3. doi:10.1007/s11099-017-0685-4

Kurtz, S, A. Phillippy, A.L. Delcher, M. Smoot, M. Shumway, C. Antonescu, et al. 2004. Versatile and open software for comparing large genomes. Genome Biol., 5 (2004), p. R12

Kusian, B., D. Sultemeyer & B. Bowien, (2002) Carbonic anhydrase is essential for growth of *Ralstonia eutropha* at ambient CO_2 concentrations. J Bacteriol 184: 5018-5026.

Larkin, M. A., Blackshields, G., Brown, N. P., Chenna, R., McGettigan, P. A., McWilliam, H., Valentin, F., Wallace, I. M., Wilm, A., Lopez, R., Thompson, J. D., Gibson, T. J., and Higgins, D. G. (2007). Clustal W and Clustal X version 2.0. Bioinformatics. **23**(21):2947-8. doi: 10.1093/bioinformatics/btm404.

Le Flèche P., I. Jacques, M. Grayon, S. Al Dahouk, P. Bouchon, F. Denoeud, K. Nöckler, H. Neubauer, L.A. Guilloteau, G. Vergnaud. (2006). Evaluation and selection of tandem repeat loci for a *Brucella* MLVA typing assay. BMC Microbiol., 9:6–9.

López-Goñi, I., García-Yoldi, D., Marín, C. M., de Miguel, M. J., Muñoz, P. M., Blasco, J. M., Jacques, I., Grayon, M., Cloeckaert, A., Ferreira, A. C., Cardoso, R., Corrêa de Sá, M. I., Walravens, K., Albert, D., Garin-Bastuji, B. (2008). Evaluation of a multiplex PCR assay (Bruce-ladder) for molecular typing of all *Brucella* species, including the vaccine strains. J Clin Microbiol. **46**(10):3484-7. doi: 10.1128/JCM.00837-08.

López-Goñi, I., García-Yoldi, D., Marín, C. M., de Miguel, M. J., Barquero-Calvo, E., Guzmán-Verri, C., Albert, D., Garin-Bastuji, B. (2011). New Bruce-ladder multiplex PCR assay for the

644 biovar typing of *Brucella suis* and the discrimination of *Brucella suis* and *Brucella canis*. Vet
645 Microbiol. **154**(1-2):152-5. doi: 10.1016/j.vetmic.2011.06.035
646 Marcus, E. A., A. P. Moshfegh, G. Sachs & D. R. Scott, (2005) The periplasmic alpha-carbonic
647 anhydrase activity of *Helicobacter pylori* is essential for acid acclimation. J Bacteriol 187: 729-
648 738.
649 Marr, A. G., and Wilson, J. B. (1950). Genetic aspects of the added carbon dioxide
650 requirements of *Brucella abortus*. Proc Soc Exp Biol Med. **75**(2):438-40.
651 Mayer-Scholl, A., Draeger, A., Göllner, C., Scholz, H. C., and Nöckler, K. (2010). Advancement
652 of a multiplex PCR for the differentiation of all currently described *Brucella* species. *J. Microbiol.*
653 *Methods* 80, 112–114. doi: 10.1016/j.mimet.2009.10.015.
654 McGurn, L. D., Moazami-Goudarzi, M., White, S. A., Suwal, T., Brar, B., Tang, J. Q., Espie, G.
655 S., and Kimber, M. S. (2016). The structure, kinetics and interactions of the beta-carboxysomal
656 beta-carbonic anhydrase, CcaA. Biochem. J. **473**: 4559-4572. doi: 10.1042/BCJ20160773.
657 Merlin, C., Masters, M., McAteer, S., and Coulson, A. (2003) Why is carbonic anhydrase
658 essential to *Escherichia coli*? *J Bacteriol* **185**: 6415-6424. doi: 10.1128/jb.185.21.6415-
659 6424.2003.
660 Mitsuhashi, S., Mizushima, T., Yamashita, E., Yamamoto, M., Kumasaka, T., Moriyama, H.,
661 Ueki, T., Miyachi, S., and Tsukihara, T. (2000). X-ray structure of beta-carbonic anhydrase from
662 the red alga, *Porphyridium purpureum*, reveals a novel catalytic site for CO(2) hydration. J. Biol.
663 Chem. **275**: 5521-5526. doi: 10.1074/jbc.275.8.5521.
664 Mitsuhashi, S., Ohnishi, J., Hayashi, M., and M. Ikeda. (2004) A gene homologous to beta-type
665 carbonic anhydrase is essential for the growth of *Corynebacterium glutamicum* under
666 atmospheric conditions. Appl Microbiol Biotechnol 63: 592-601.
667 Newton, J. W. & J. B. Wilson, (1954) CO_2 requirements and nucleic acid synthesis by *Brucella*
668 *abortus*. J Bacteriol 68: 74-76.
669 O'Callaghan D, Whatmore AM. (2011). *Brucella* genomics as we enter the multi-genome era.
670 Brief Funct Genomics 10(6):334-41. doi: 10.1093/bfgp/elr026

671 Pallen M.J., Wren B.W. Bacterial pathogenomics. Nature. 2007;449:835–842. doi:
672 10.1038/nature06248.
673 Pappas G, Papadimitriou P, Akritidis N, Christou L, Tsianos EV. (2006). The new global map of
674 human brucellosis. Lancet Infect Dis. 6(2):91-9.
675 Pérez-Etayo. L., de Miguel, M. J., Conde-Álvarez, R., Muñoz, P. M., Khames, M., Iriarte, M.,
676 Moriyón, I., and Zúñiga-Ripa, A. (2018). The CO_2-dependence of *Brucella ovis* and *Brucella*
677 *abortus* biovars is caused by defective carbonic anhydrases. Vet Res. **49**(1):85. doi:
678 10.1186/s13567-018-0583-1.
679 Philippe N, Alcaraz JP, Coursange E, Geiselmann J, Schneider D. (2004). Improvement of
680 pCVD442, a suicide plasmid for gene allele exchange in bacteria. Plasmid. 51(3):246-55. doi:
681 10.1016/j.plasmid.2004.02.003.
682 Rognes, T., Flouri, T., Nichols, B., Quince, C., and Mahé, F. (2016) VSEARCH: a versatile open
683 source tool for metagenomics. *PeerJ* **4**: e2584. doi: 10.7717/peerj.2584.
684 Sangari FJ, García-Lobo JM, and Agüero, J. (1994). The *Brucella abortus* vaccine strain B19
685 carries a deletion in the erythritol catabolic genes. FEMS Microbiol Lett. **121**(3):337-42.
686 Sangari FJ, Seoane A, Rodríguez MC, Agüero J, García Lobo JM. 2007. Characterization of the
687 urease operon of *Brucella abortus* and assessment of its role in virulence of the bacterium.
688 Infect Immun. 75(2):774-80. doi: 10.1128/IAI.01244-06.
689 Sangari, F. J., Cayón, A. M., Seoane, A., and García-Lobo, J. M. (2010). *Brucella abortus ure2*
690 region contains an acid-activated urea transporter and a nickel transport system. *BMC*
691 *Microbiol.* **10**: 107. doi: 10.1186/1471-2180-10-107.
692 Sievers F, Higgins DG. 2014. Clustal Omega, accurate alignment of very large numbers of
693 sequences. Methods Mol Biol. **1079**:105-16. 10.1007/978-1-62703-646-7_6
694 Smith, K.S., Jakubzick, C., Whittam, T.S., and Ferry, J.G. (1999). Carbonic anhydrase is an
695 ancient enzyme widespread in prokaryotes. Proc. Natl. Acad. Sci. 96: 15184–15189.
696 Sternon, J. F., Godessart, P., Gonçalves de Freitas, R., Van der Henst, M., Poncin, K., Francis,
697 N., Willemart, K., Christen, M., Christen, B., Letesson, J. J., De Bolle, X. (2018). Transposon

Sequencing of *Brucella abortus* Uncovers Essential Genes for Growth In Vitro and Inside Macrophages. Infect Immun. **86**(8). pii: e00312-18. doi: 10.1128/IAI.00312-18.

Suárez-Esquivel, M., Ruiz-Villalobos, N., Castillo-Zeledón, A., et al. (2016). *Brucella abortus* Strain 2308 Wisconsin Genome: Importance of the Definition of Reference Strains. *Frontiers in Microbiology*. **7**:1557. doi:10.3389/fmicb.2016.01557.

Supuran, C. T. (2016). Structure and function of carbonic anhydrases. Biochem J **473**:2023–32.

Supuran, C. T. (2018). Carbonic Anhydrases and Metabolism. Metabolites. **8**(2). pii: E25. doi: 10.3390/metabo8020025.

Valdivia, R. H., and Falkow, S. (1997). Fluorescence-based isolation of bacterial genes expressed within host cells. Science 277: 2007–2011.

Varesio LM, Willett JW, Fiebig A, Crosson S. 2019. A carbonic anhydrase pseudogene sensitizes select *Brucella* lineages to low CO2 tension. J Bacteriol. pii: JB.00509-19. doi: 10.1128/JB.00509-19. [Epub ahead of print]

Veitch, F.P. and Blankenship, L.C. (1963) Carbonic anhydrase activity in bacteria. Nature 197, 76-77.

Wattam AR, Foster JT, Mane SP, et al. (2014). Comparative Phylogenomics and Evolution of the Brucellae Reveal a Path to Virulence. *Journal of Bacteriology*. **196**(5):920-930. doi:10.1128/JB.01091-13.

Whatmore, A. M., Mark S. Koylass, Jakub Muchowski, James Edwards-Smallbone, Krishna K. Gopaul, and Lorraine L. Perrett. (2016). Extended Multilocus Sequence Analysis to Describe the Global Population Structure of the Genus *Brucella*: Phylogeography and Relationship to Biovars. Front Microbiol. 7: 2049. doi:10.3389/fmicb.2016.02049.

Wilson, G. S. (1931). The gaseous requirements of *Br. abortus* (Bovine type). Brit. J. Exper. Path., 12, 88.

Tables and Figure Legends

Table 1. Strains and plasmids used in this study

Strains	Main characteristics	Reference
Brucella		
B. abortus 544	Biotype 1, CO_2-dependent	Alton et al., 1988
B. abortus 86/8/59	Biotype 2, CO_2-dependent	Alton et al., 1988
B. abortus Tulya	Biotype 3, CO_2-dependent	Alton et al., 1988
B. abortus 292	Biotype 4, CO_2-dependent	Alton et al., 1988
B. abortus A-579	Biotype 3, CO_2-dependent	Alton et al., 1988
B. abortus 2308W	Biotype 1, CO_2-independent	Suárez-Esquivel et al. 2016
B. ovis 63/290	CO_2-dependent	Alton et al., 1988
B. pinnipedialis B2/94	CO_2-dependent	Foster et al., 1996
B. abortus 2308 $\Delta_{Ba2308w}$*CAI* mutant	CO_2-independent	This study
B. abortus 292 mut 1	CO_2-independent	This study

730 **Table 2. Oligonucleotides used in this work**

BS192_0456.F	CATGCTGGAACCAAAGTTGA
BS192_0456.R	CGTTTCCGCAAGCTGTAAAT
BS191_1911.F	GGGTTCCACAGGGTTCATTT
BS191_1911.R	GACGGCAAATAATTGCATGA
U_BAB2_0449.*SacI*.F	GAGCTCTGAGCACAACCTGCAAAATC
U_BAB2_0449.R	GGCGAATGATCGTTCTTCAT
D_BAB2_0449.F	ATGAAGAACGATCATTCGCCGGATCCTGCCAACCG GCAGAATAAT
D_BAB2_0449.*XbaI*.R	TCTAGAGGGGGAGGCTTCCTAGTTT

731
732

733

734 **Table 3.** Observed frequency of appearance of CO_2-independent
735 mutants in different *Brucella* strains.
736

737 Strain	Frequency of mutants
738	
739 *B. abortus* 292	2.72×10^{-8}
740	
741 *B. abortus* 544	5.95×10^{-8}
742	
743 *B. abortus* 86/8/59	1.14×10^{-9}
744	
745 *B. abortus* A-579	2.29×10^{-10}
746	
747 *B. ovis* 63/290	3.38×10^{-6}
748	
749 *B. pinnipedialis* B2/94	5.5×10^{-6}

750

751

A

```
                          1
B.ovis_ATCC25840          ATGGCTGATCTTCCAGATTCACTTCTTGCTGGTTACAAAACCTTCATGAGCGAGCATTTC
B.neotomae_5K33           ATGGCTGATCTTCCAGATTCACTTCTTGCTGGTTACAAAACCTTCATGAGCGAGCATTTC
B.suisBv1_1330            ATGGCTGATCTTCCAGATTCACTTCTTGCTGGTTACAAAACCTTCATGAGCGAGCATTTC
B.suisBv3_686             ATGGCTGATCTTCCAGATTCACTTCTTGCTGGTTACAAAACCTTCATGAGCGAGCATTTC
B.pinnipedialis_M163/99/10 ATGGCTGATCTTCCAGATTCACTTCTTGCTGGTTACAAAACCTTCATGAGCGAGCATTTC
B.melitensisBv2_63/9      ATGGCTGATCTTCCAGATTCACTTCTTGCTGGTTACAAAACCTTCATGAGCGAGCATTTC
B.abortusBv6_870          ATGGCTGATCTTCCAGATTCACTTCTTGCTGGTTACAAAACCTTCATGAGCGAGCATTTC
B.abortusBv2_86/8/59      ATGGCTGATCTTCCAGATTCACTTCTTGCTGGTTACAAAACCTTCATGAGCGAGCATTTC
B.abortusBv1_NCTC8038     ATGGCTGATCTTCCAGATTCACTTCTTGCTGGTTACAAAACCTTCATGAGCGAGCATTTC
B.abortusBv1_2308         ATGGCTGATCTTCCAGATTCACTTCTTGCTGGTTACAAAACCTTCATGAGCGAGCATTTC
                          ************************************************************

                          61
B.ovis_ATCC25840          GCGCATGAAACGGCACGCTACAGGGACTTGGCTGAAAAAGGGCAATCGCCGGAAACTCTG
B.neotomae_5K33           GCGCATGAAACGGCACGCTACAGGGACTTGGCTGAAAAAGGGCAATCGCCGGAAACTCTG
B.suisBv1_1330            GCGCATGAAACGGCACGCTACAGGGACTTGGCTGAAAAAGGGCAATCGCCGGAAACTCTG
B.suisBv3_686             GCGCATGAAACGGCACGCTACAGGGACTTGGCTGAAAAAGGGCAATCGCCGGAAACTCTG
B.pinnipedialis_M163/99/10 GCGCATGAAACGGCACGCTACAGGGACTTGGCTGAAAAAGGGCAATCGCCGGAAACTCTG
B.melitensisBv2_63/9      GCGCATGAAACGGCACGCTACAGGGACTTGGCTGAAAAAGGGCAATCGCCGGAAACTCTG
B.abortusBv6_870          GCGCATGAAACGGCACGCTACAGGGACTTGGCTGAAAAAGGGCAATCGCCGGAAACTCTG
B.abortusBv2_86/8/59      GCGCATGAAACGGCACGCTACAGGGACTTGGCTGAAAAAGGGCAATCGCCGGAAACTCTG
B.abortusBv1_NCTC8038     GCGCATGAAACGGCACGCTACAGGGACTTGGCTGAAAAAGGGCAATCGCCGGAAACTCTG
B.abortusBv1_2308         GCGCATGAAACGGCACGCTACAGGGACTTGGCTGAAAAAGGGCAATCGCCGGAAACTCTG
                          ************************************************************

                          121
B.ovis_ATCC25840          GTTGTTGCCTGCTGCGATTCCCGCGCTGCGCCGGAAACCATCTTCAATGCCGCACCGGGC
B.neotomae_5K33           GTTGTTGCCTGCTGCGATTCCCGCGCTGCGCCGGAAACCATCTTCAATGCCGCACCGGGC
B.suisBv1_1330            GTTGTTGCCTGCTGCGATTCCCGCGCTGCGCCGGAAACCATCTTCAATGCCGCACCGGGC
B.suisBv3_686             GTTGTTGCCTGCTGCGATTCCCGCGCTGCGCCGGAAACCATCTTCAATGCCGCACCGGGC
B.pinnipedialis_M163/99/10 GTTGTTGCCTGCTGCGATTCCCGCGCTGCGCCGGAAACCATCTTCAATGCCGCACCGGGC
B.melitensisBv2_63/9      GTTGTTGCCTGCTGCGATTCCCGCGCTGCGCCGGAAACCATCTTCAATGCCGCACCGGGC
B.abortusBv6_870          GTTGTTGCCTGCTGCGATTCCCGCGCTGCGCCGGAAACCATCTTCAATGCCGCACCGGGC
B.abortusBv2_86/8/59      GTTGTTGCCTGCTGCGATTCCCGCGCTGCGCCGGAAACCATCTTCAATGCCGCACCGGGC
B.abortusBv1_NCTC8038     GTTGTTGCCTGCTGCGATTCCCGCGCTGCGCCGGAAACCATCTTCAATGCCGCACCGGGC
B.abortusBv1_2308         GTTGTTGCCTGCTGCGATTCCCGCGCTGCGCCGGAAACCATCTTCAATGCCGCACCGGGC
                          ************************************************************

                          181
B.ovis_ATCC25840          GAAATCTTTGTCCTTCGCAATGTGGCCAATCTCATTCCGCCCTATGAGCCGGATGGTGAA
B.neotomae_5K33           GAAATCTTTGTCCTTCGCAATGTGGCCAATCTCATTCCGCCCTATGAGCCGGATGGTGAA
B.suisBv1_1330            GAAATCTTTGTCCTTCGCAATGTGGCCAATCTCATTCCGCCCTATGAGCCGGATGGTGAA
B.suisBv3_686             GAAATCTTTGTCCTTCGCAATGTGGCCAATCTCATTCCGCCCTATGAGCCGGATGGTGAA
B.pinnipedialis_M163/99/10 GAAATCTTTGTCCTTCGCAATGTGGCCAATCTCATTCCGCCCTATGAGCCGGATGGTGAA
B.melitensisBv2_63/9      GAAATCTTTGTCCTTCGCAATGTGGCCAATCTCATTCCGCCCTATGAGCCGGATGGTGAA
B.abortusBv6_870          GAAATCTTTGTCCTTCGCAATGTGGCCAATCTCATTCCGCCCTATGAGCCGGATGGTGAA
B.abortusBv2_86/8/59      GAAATCTTTGTCCTTCGCAATGTGGCCAATCTCATTCCGCCCTATGAGCCGGATGGTGAA
B.abortusBv1_NCTC8038     GAAATCTTTGTCCTTCGCAATGTGGCCAATCTCATTCCGCCCTATGAGCCGGATGGTGAA
B.abortusBv1_2308         GAAATCTTTGTCCTTCGCAATGTGGCCAATCTCATTCCGCCCTATGAGCCGGATGGTGAA
                          ************************************************************

                          241
B.ovis_ATCC25840          TACCACGCGGCTTCGGCGGCTTTGGAATTTGCCGTGCAGAGCCTCAAGGTAAAACATATC
B.neotomae_5K33           TACCACGCGGCTTCGGCGGCTTTGGAATTTGCCGTGCAGAGCCTCAAGGTAAAACATATC
B.suisBv1_1330            TACCACGCGGCTTCGGCGGCTTTGGAATTTGCCGTGCAGAGCCTCAAGGTAAAACATATC
B.suisBv3_686             TACCACGCGGCTTCGGCGGCTTTGGAATTTGCCGTGCAGGGCCTCAAGGTAAAACATATC
B.pinnipedialis_M163/99/10 TACCACGCGGCTTCGGCGGCTTTGGAATTTGCCGTGCAGAGCCTCAAGGTAAAACATATC
B.melitensisBv2_63/9      TACCACGCGGCTTCGGCGGCTTTGGAATTTGCCGTGCAGAGCCTCAAGGTAAAACATATC
B.abortusBv6_870          TACCACGCGGCTTCGGCGGCTTTGGAATTTGCCGTGCAGAGCCTCAAGGTAAAACATATC
B.abortusBv2_86/8/59      TACCACGCGGCTTCGGCGGCTTTGGAATTTGCCGTGCAGAGCCTCAAGGTAAAACATATC
B.abortusBv1_NCTC8038     TACCACGCGGCTTCGGCGGCTTTGGAATTTGCCGTGCAGAGCCTCAAGGTAAAACATATC
B.abortusBv1_2308         TACCACGCGGCTTCGGCGGCTTTGGAATTTGCCGTGCAGAGCCTCAAGGTAAAACATATC
                          ************************************ ********************

                          301
B.ovis_ATCC25840          GTGGTGATGGGCCACGGGCGTTGCGGTGGCATCAAGGC---GGCGCTCGACACTGAAAGC
B.neotomae_5K33           GTGGTGATGGGCCACGGGCGTTGCGGTGGCATCAAGGC---GGCGCTCGACACTGAAAGC
B.suisBv1_1330            GTGGTGATGGGCCACGGGCGTTGCGGTGGCATCAAGGC---GGCGCTCGACACTGAAAGC
B.suisBv3_686             GTGGTGATGGGCCACGGGCGTTGCGGTGGCATCAAGGC---GGCGCTCGACACTGAAAGC
B.pinnipedialis_M163/99/10 GTGGTGATGGGCCACGGGCGTTGCGGTGGCATCAAGGC---GGCGCTCGACACTGAAAGC
B.melitensisBv2_63/9      GTGGTGATGGGCCACGGGCGTTGCGGTGGCATCAAGGC---GGCGCTCGACACTGAAAGC
B.abortusBv6_870          GTGGTGATGGGCCACGGGCGTTGCGGTGGCATCAAGGC---GGCGCTCGACACTGAAAGC
B.abortusBv2_86/8/59      GTGGTGATGGGCCACGGGCGTTGCGGTGGCATCAAGGCC--GGCGCTCGACACTGAAAGC
```

```
827  B.abortusBv1_NCTC8038          GTGGTGATGGGCCACGGGCGTTGCGGTGGCATCAAGGCCG--GC-CTCGACACTGAAAGC
828  B.abortusBv1_2308              GTGGTGATGGGCCACGGGCGTTGCGGTGGCATCAAGGCCGCGGCGCTCGACACTGAAAGC
829                                 ************************************    ** ***************
830
831                                 361
832  B.ovis_ATCC25840               GCCCCGCTTTCACCGAGCGATTTTATCGGAAAATGGATGAGCCTCATTTCGCCCGCGGCA
833  B.neotomae_5K33                GCCCCGCTTTCACCGAGCGATTTTATCGGAAAATGGATGAGCCTCATTTCGCCCGCGGCA
834  B.suisBv1_1330                 GCCCCGCTTTCACCGAGCGATTTTATCGGAAAATGGATGAGCCTCATTTCGCCCGCGGCA
835  B.suisBv3_686                  GCCCCGCTTTCACCGAGCGATTTTATCGGAAAATGGATGAGCCTCATTTCGCCCGCGGCA
836  B.pinnipedialis_M163/99/10     GCCCCGCTTTCACCGAGCGATTTTATCGGAAAATGGATGAGCCTCATTTCGCCCGCGGCA
837  B.melitensisBv2_63/9           GCCCCGCTTTCACCGAGCGATTTTATCGGAAAATGGATGAGCCTCATTTCGCCCGCGGCA
838  B.abortusBv6_870               GCCCCGCTTTCACCGAGCGATTTTATCGGAAAATGGATGAGCCTCATTTCGCCCGCGGCA
839  B.abortusBv2_86/8/59           GCCCCGCTTTCACCGAGCGATTTTATCGGAAAATGGATGAGCCTCATTTCGCCCGCGGCA
840  B.abortusBv1_NCTC8038          GCCCCGCTTTCACCGAGCGATTTTATCGGAAAATGGATGAGCCTCATTTCGCCCGCGGCA
841  B.abortusBv1_2308              GCCCCGCTTTCACCGAGCGATTTTATCGGAAAATGGATGAGCCTCATTTCGCCCGCGGCA
842                                 ************************************************************
843
844                                 421
845  B.ovis_ATCC25840               GAGGCCATCAGCGGAAATGCGCTCATGACGCAAAGCGAGCGTCATACGGCGCTGGAGCGT
846  B.neotomae_5K33                GAGGCCATCAGCGGAAATGCGCTCATGACGCAAAGCGAGCGTCATAGGGCGCTGGAGCGT
847  B.suisBv1_1330                 GAGGCCATCAGCGGAAATGCGCTCATGACGCAAAGCGAGCGTCATACGGCGCTGGAGCGT
848  B.suisBv3_686                  GAGGCCATCAGCGGAAATGCGCTCATGACGCAAAGCGAGCGTCATACGGCGCTGGAGCGT
849  B.pinnipedialis_M163/99/10     GAGGCCATCAGCGGAAATGCGCTCATGACGCAAAGCGAGCGTCATACGGCGCTGGAGCGT
850  B.melitensisBv2_63/9           GAGGCCATCAGCGGAAATGCGCTCATGACGCAAAGCGAGCGTCATACGGCGCTGGAGCGT
851  B.abortusBv6_870               GAGGCCATCAGCGGAAATGCGCTCATGACGCAAAGCGAGCGTCATACGGCGCTGGAGCGT
852  B.abortusBv2_86/8/59           GAGGCCATCAGCGGAAATGCGCTCATGACGCAAAGCGAGCGTCATACGGCGCTGGAGCGT
853  B.abortusBv1_NCTC8038          GAGGCCATCAGCGGAAATGCGCTCATGACGCAAAGCGAGCGTCATACGGCGCTGGAGCGT
854  B.abortusBv1_2308              GAGGCCATCAGCGGAAATGCGCTCATGACGCAAAGCGAGCGTCATACGGCGCTGGAGCGT
855                                 ************************************************ ************
856
857                                 481
858  B.ovis_ATCC25840               ATTTCGATCCGCTATTCGCTGGCTAATCTGCGCACTTTCCCTTGGCGTGGATATTCTGGA
859  B.neotomae_5K33                ATTTCGATCCGCTATTCGCTGGCTAATCTGCGCACTTTCCCTTG-CGTGGATATTCTGGA
860  B.suisBv1_1330                 ATTTCGATCCGCTATTCGCTGGCTAATCTGCGCACTTTCCCTTG-CGTGGATATTCTGGA
861  B.suisBv3_686                  ATTTCGATCCGCTATTCGCTGGCTAATCTGCGCACTTTCCCTTG-CGTGGATATTCTGGA
862  B.pinnipedialis_M163/99/10     ATTTCGATCCGCTATTCGCTGGCTAATCTGCGCACTTTCCCTTG-CGTGGATATTCTGGA
863  B.melitensisBv2_63/9           ATTTCGATCCGCTATTCGCTGGCTAATCTGCGCACTTTCCCTTG-CGTGGATATTCTGGA
864  B.abortusBv6_870               ATTTCGATCCGCTATTCGCTGGCTAATCTGCGCACTTTCCCTTG-CGTGGATATTCTGGA
865  B.abortusBv2_86/8/59           ATTTCGATCCGCTATTCGCTGGCTAATCTGCGCACTTTCCCTTG-CGTGGATATTCTGGA
866  B.abortusBv1_NCTC8038          ATTTCGATCCGCTATTCGCTGGCTAATCTGCGCACTTTCCCTTG-CGTGGATATTCTGGA
867  B.abortusBv1_2308              ATTTCGATCCGCTATTCGCTGGCTAATCTGCGCACTTTCCCTTG-CGTGGATATTCTGGA
868                                 ********************************************** ***************
869
870                                 541
871  B.ovis_ATCC25840               GAAGAAGGGCAAGCTCACCCTGCATGGCGCATGGTTCGATATTTCGACCGGCGAATTGTG
872  B.neotomae_5K33                GAAGAAGGGCAAGCTCACCCTGCATGGCGCATGGTTCGATATTTCGACCGGCGAATTGTG
873  B.suisBv1_1330                 GAAGAAGGGCAAGCTCACCCTGCATGGCGCATGGTTCGATATTTCGACCGGCGAATTGTG
874  B.suisBv3_686                  GAAGAAGGGCAAGCTCACCCTGCATGGCGCATGGTTCGATATTTCGACCGGCGAATTGTG
875  B.pinnipedialis_M163/99/10     GAAGAAGGGCAAGCTCACCCCGCATGGCGCATGGTTCGATATTTCGACCGGCGAATTGTG
876  B.melitensisBv2_63/9           GAAGAAGGGCAAGCTCACCTTGCATGGCGCATGGTTCGATATTTCGACCGGCGAATTGTG
877  B.abortusBv6_870               GAAGAAGGGCAAGCTCACCCTGCATGGCGCATGGTTCGATATTTCGACCGGCGAATTGTG
878  B.abortusBv2_86/8/59           GAAGAAGGGCAAGCTCACCCTGCATGGCGCATGGTTCGATATTTCGACCGGCGAATTGTG
879  B.abortusBv1_NCTC8038          GAAGAAGGGCAAGCTCACCCTGCATGGCGCATGGTTCGATATTTCGACCGGCGAATTGTG
880  B.abortusBv1_2308              GAAGAAGGGCAAGCTCACCCTGCATGGCGCATGGTTCGATATTTCGACCGGCGAATTGTG
881                                 ******************  ************************************
882
883                                 601
884  B.ovis_ATCC25840               GGTGATGGATCACCAGACCGGTGATTTCAAACGCCCTGAACTTTGA
885  B.neotomae_5K33                GGTGATGGATCACCAGACCGGTGATTTCAAACGCCCTGAACTTTGA
886  B.suisBv1_1330                 GGTGATGGATCACCGGACCGGTGATTTCAAACGCCCTGAACTTTGA
887  B.suisBv3_686                  GGTGATGGATCACCAGACCGGTGATTTCAAACGCCCTGAACTTTGA
888  B.pinnipedialis_M163/99/10     GGTGATGGATCACCAGACCGGTGATTTCAAACGCCCTGAACTTTGA
889  B.melitensisBv2_63/9           GGTGATGGATCACCAGACCGGTGATTTCAAACGCCCTGAACTTTGA
890  B.abortusBv6_870               GGTGATGGATCACCAGACCGGTGATTTCAAACGCCCTGAACTTTGA
891  B.abortusBv2_86/8/59           GGTGATGGATCACCAGACCGGTGATTTCAAACGCCCTGAACTTTGA
892  B.abortusBv1_NCTC8038          GGTGATGGATCACCAGACCGGTGATTTCAAACGCCCTGAACTTTGA
893  B.abortusBv1_2308              GGTGATGGATCACCAGACCGGTGATTTCAAACGCCCTGAACTTTGA
894                                 ************** ******************************
```

895

B

```
                                                                  ▼ ▼
                          1                                       ▼ ▼
B.ovis_ATCC25840          MADLPDSLLAGYKTFMSEHFAHETARYRDLAEKGQSPETLVVACCDSRAAPETIFNAAPG
B.neotomae_5K33           MADLPDSLLAGYKTFMSEHFAHETARYRDLAEKGQSPETLVVACCDSRAAPETIFNAAPG
B.suis Bv1_1330           MADLPDSLLAGYKTFMSEHFAHETARYRDLAEKGQSPETLVVACCDSRAAPETIFNAAPG
B.suis Bv3_686            MADLPDSLLAGYKTFMSEHFAHETARYRDLAEKGQSPETLVVACCDSRAAPETIFNAAPG
B.pinnipedialis M163/99/10 MADLPDSLLAGYKTFMSEHFAHETARYRDLAEKGQSPETLVVACCDSRAAPETIFNAAPG
B.melitensis Bv2_63/9     MADLPDSLLAGYKTFMSEHFAHETARYRDLAEKGQSPETLVVACCDSRAAPETIFNAAPG
B.abortus Bv6_870         MADLPDSLLAGYKTFMSEHFAHETARYRDLAEKGQSPETLVVACCDSRAAPETIFNAAPG
B.abortus Bv2_86/8/59     MADLPDSLLAGYKTFMSEHFAHETARYRDLAEKGQSPETLVVACCDSRAAPETIFNAAPG
B.abortus Bv1_NCTC8038    MADLPDSLLAGYKTFMSEHFAHETARYRDLAEKGQSPETLVVACCDSRAAPETIFNAAPG
B.abortus Bv1_2308        MADLPDSLLAGYKTFMSEHFAHETARYRDLAEKGQSPETLVVACCDSRAAPETIFNAAPG

                          61                                    ▼ ▼
B.ovis_ATCC25840          EIFVLRNVANLIPPYEPDGEYHAASAALEFAVQSLKVKHIVVMGHGRCGGIK-AALDTES
B.neotomae_5K33           EIFVLRNVANLIPPYEPDGEYHAASAALEFAVQSLKVKHIVVMGHGRCGGIK-AALDTES
B.suis Bv1_1330           EIFVLRNVANLIPPYEPDGEYHAASAALEFAVQSLKVKHIVVMGHGRCGGIK-AALDTES
B.suis Bv3_686            EIFVLRNVANLIPPYEPDGEYHAASAALEFAVQGLKVKHIVVMGHGRCGGIK-AALDTES
B.pinnipedialis M163/99/10 EIFVLRNVANLIPPYEPDGEYHAASAALEFAVQSLKVKHIVVMGHGRCGGIK-AALDTES
B.melitensis Bv2_63/9     EIFVLRNVANLIPPYEPDGEYHAASAALEFAVQSLKVKHIVVMGHGRCGGIK-AALDTES
B.abortus Bv6_870         EIFVLRNVANLIPPYEPDGEYHAASAALEFAVQSLKVKHIVVMGHGRCGGIK-AALDTES
B.abortus Bv2_86/8/59     EIFVLRNVANLIPPYEPDGEYHAASAALEFAVQSLKVKHIVVMGHGRCGGIK--AGARH*
B.abortus Bv1_NCTC8038    EIFVLRNVANLIPPYEPDGEYHAASAALEFAVQSLKVKHIVVMGHGRCGGIK-AGLDTES
B.abortus Bv1_2308        EIFVLRNVANLIPPYEPDGEYHAASAALEFAVQSLKVKHIVVMGHGRCGGIKAAALDTES

                          121
B.ovis_ATCC25840          APLSPSDFIGKWMSLISPAAEAISGNALMTQSERHTALERISIRYSLANLRTFPWRGYSG
B.neotomae_5K33           APLSPSDFIGKWMSLISPAAEAISGNALMTQSERHRALERISIRYSLANLRTFPCVDILE
B.suis Bv1_1330           APLSPSDFIGKWMSLISPAAEAISGNALMTQSERHTALERISIRYSLANLRTFPCVDILE
B.suis Bv3_686            APLSPSDFIGKWMSLISPAAEAISGNALMTQSERHTALERISIRYSLANLRTFPCVDILE
B.pinnipedialis M163/99/10 APLSPSDFIGKWMSLISPAAEAISGNALMTQSERHTALERISIRYSLANLRTFPCVDILE
B.melitensis Bv2_63/9     APLSPSDFIGKWMSLISPAAEAISGNALMTQSERHTALERISIRYSLANLRTFPCVDILE
B.abortus Bv6_870         APLSPSDFIGKWMSLISPAAEAISGNALMTQSERHTALERISIRYSLANLRTFPCVDILE
B.abortus Bv2_86/8/59     ............................................................
B.abortus Bv1_NCTC8038    APLSPSDFIGKWMSLISPAAEAISGNALMTQSERHTALERISIRYSLANLRTFPCVDILE
B.abortus Bv1_2308        APLSPSDFIGKWMSLISPAAEAISGNALMTQSERHTALERISIRYSLANLRTFPCVDILE

                          181
B.ovis_ATCC25840          EEG--QAHPAWRMVRYFDRRIVGDGSPDR......
B.neotomae_5K33           KKGKLTLHGAWFDISTGELWVMDHQTGD-FKRPEL
B.suis Bv1_1330           KKGKLTLHGAWFDISTGELWVMDHRTGD-FKRPEL
B.suis Bv3_686            KKGKLTLHGAWFDISTGELWVMDHQTGD-FKRPEL
B.pinnipedialis M163/99/10 KKGKLTPHGAWFDISTGELWVMDHQTGD-FKRPEL
B.melitensis Bv2_63/9     KKGKLTLHGAWFDISTGELWVMDHQTGD-FKRPEL
B.abortus Bv6_870         KKGKLTLHGAWFDISTGELWVMDHQTGD-FKRPEL
B.abortus Bv2_86/8/59     ................................
B.abortus Bv1_NCTC8038    KKGKLTLHGAWFDISTGELWVMDHQTGD-FKRPEL
B.abortus Bv1_2308        KKGKLTLHGAWFDISTGELWVMDHQTGD-FKRPEL
```

Figure 1. Alignment of sequences of Carbonic Anhydrase II from representative *Brucella* isolates. The genomes shown here are the representative species for each of the clusters of identical sequences obtained from the selected 35 *Brucella* strains. Those clusters formed by species that are CO_2-dependent are shown in blue a) Partial DNA sequences, with nucleotides that differ from the consensus wild type sequence highlighted in red, and b) protein sequences, with amino acids that differ from the consensus wild type sequence highlighted in red. Red triangles indicate the four zinc-binding residues, Cys42, Asp44, His98, and Cys101 and blue triangles the catalytic dyad Asp44–Arg46

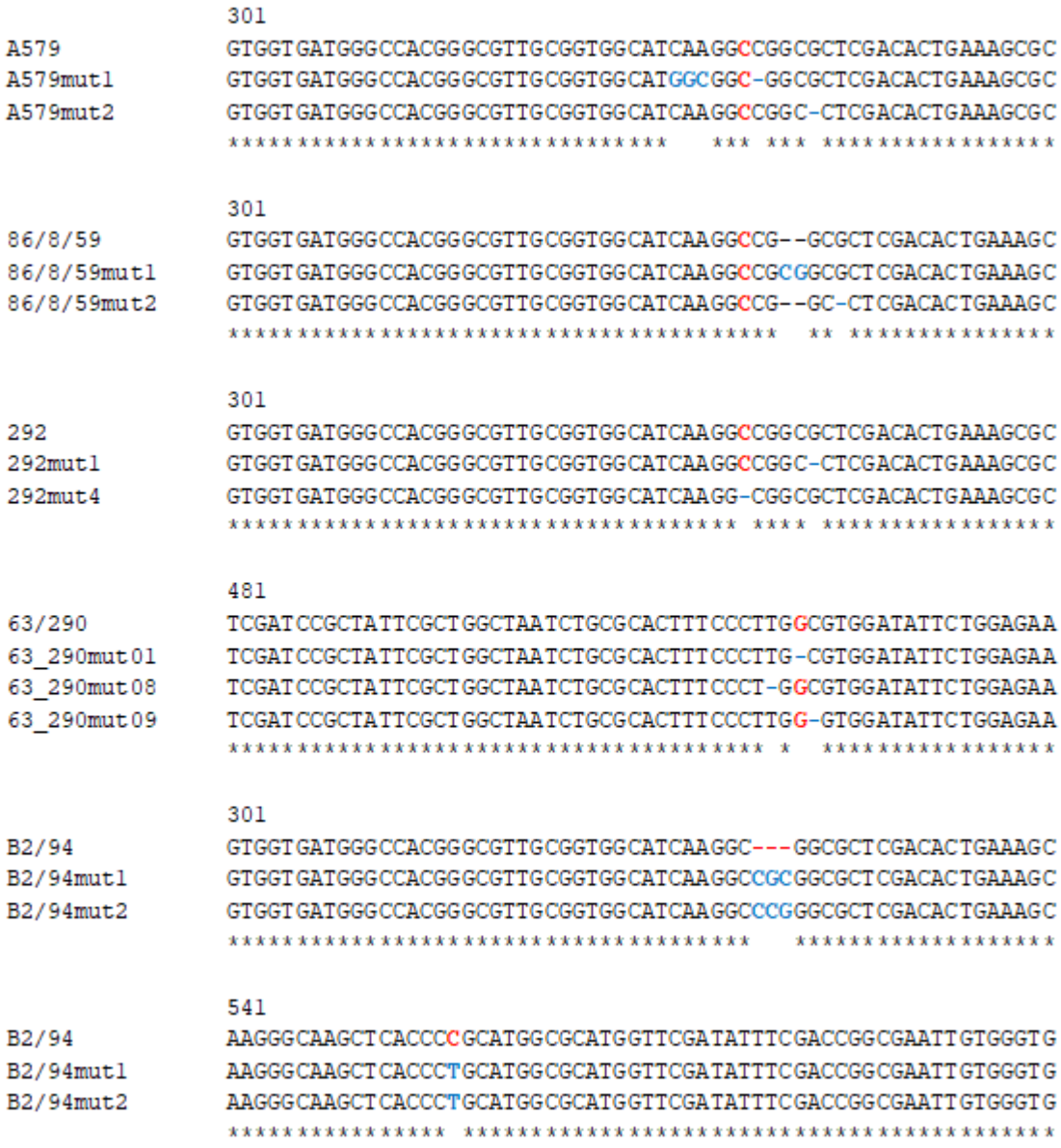

Figure 2. Nucleotide changes in CAII from selected CO_2-independent mutants of different *Brucella* strains. Partial sequence of the regions where the original CO_2-dependent strains had the mutations that caused the defective phenotype (shown in red), and the changes observed after selection and sequencing of different spontaneous CO_2-independent mutants (shown in blue).

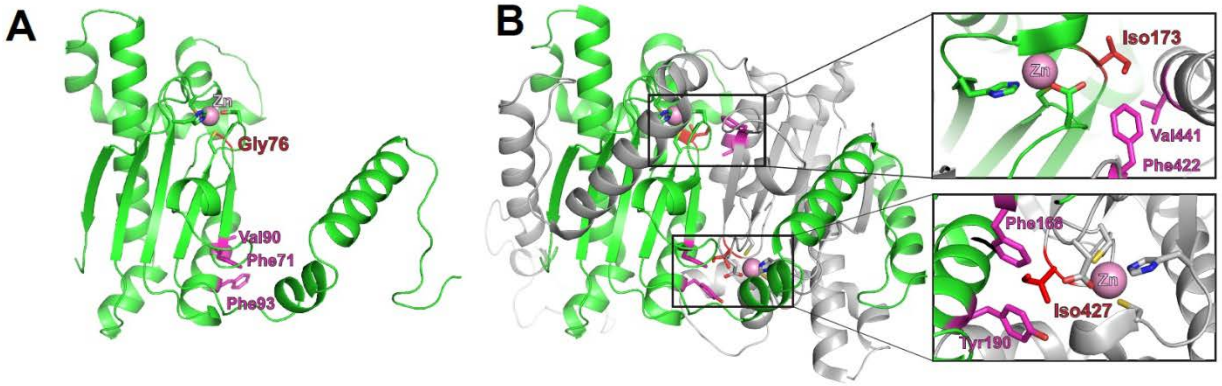

Figure 3. Structural model of *Brucella* $_{Ba2308}$CAI. (A) Predicted structure of a monomer of Q2YL41, the CAI from *B. abortus* 2308, created using Phyre2 and the structure from the β-carbonic anhydrase from the red alga *Porphyridium purpureum* (1ddz) as template. Gly76 is depicted in red and the nearby zinc atom as a pink ball. (B) X-ray structure of the *Porphyridium purpureum* monomer, composed of two internally repeated structures. The N-terminal half (residues 1-308, equivalent to the sequence of monomeric $_{Ba2308}$CAI) is colored in green and the C-terminal half (residues 309-564, equivalent to the second molecule of a putative dimer from $_{Ba2308}$CAI) is colored in grey. In the equivalent position of Gly76 from $_{Ba2308}$CAI in *Porphyridium purpureum* is located Iso173 (in the N-terminal half) or Iso427 (in the C-terminal half). These residues are stablishing hydrophobic contacts in the interface between the domains; Iso173 with Val441 and Phe442 (upper zoom image) and Iso427 with Phe168 and Tyr190 (lower zoom image). Identical (Phe71, Val90) and similar (Phe93) residues are located in the equivalent positions in *Brucella*$_{Ba2308}$CAI (A). The presence of a glycine in *Brucella*$_{Ba2308}$CAI instead of an isoleucine disrupts these hydrophobic interactions and could impair dimerization. Besides, this substitution could alter locally the folding of this region and affect the nearby residues that are coordinating the Zn atom.

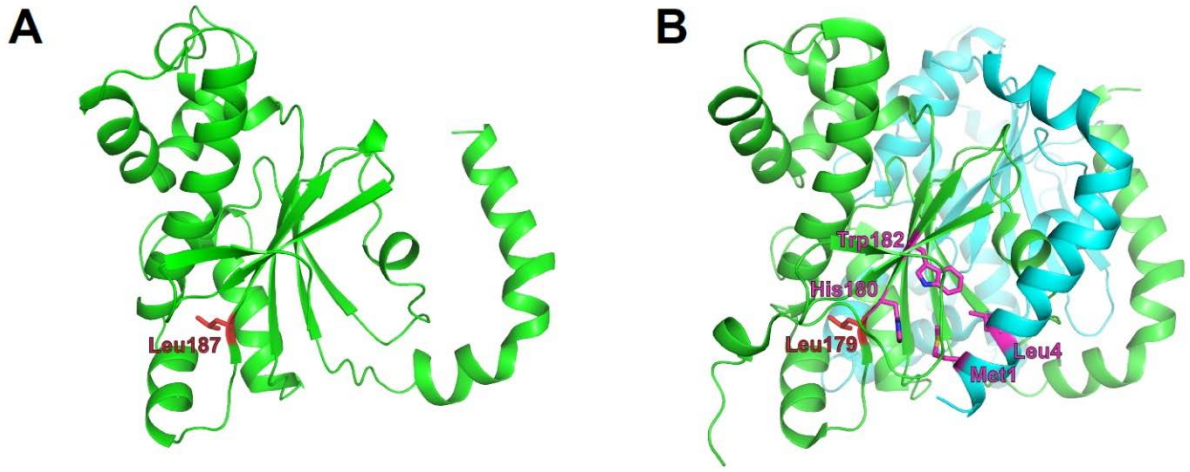

983

984 **Figure 4. Structural theoretical model of *Brucella* $_{Ba2308}$CAII.** A) Model structure of a
985 monomer of Q2YLK1, the CAII from *B. abortus* 2308, created using Phyre2 and structure 5SWC
986 from *Synechocystis* sp as a template. Leu187 is depicted in red colour. (B) The X-ray structure
987 of the *Synechocystis* sp CA dimer, showing an equivalent leucine residue in position 179.
988 Adjacent residues His180 and Trp182 from the C-terminal β-sheet are in close contact with
989 residues Met1 and Leu4 from the N-terminal H1-H2 helix, respectively, and are involved in
990 monomer-monomer interactions. Zinc atoms are depicted as pink balls.

991

992

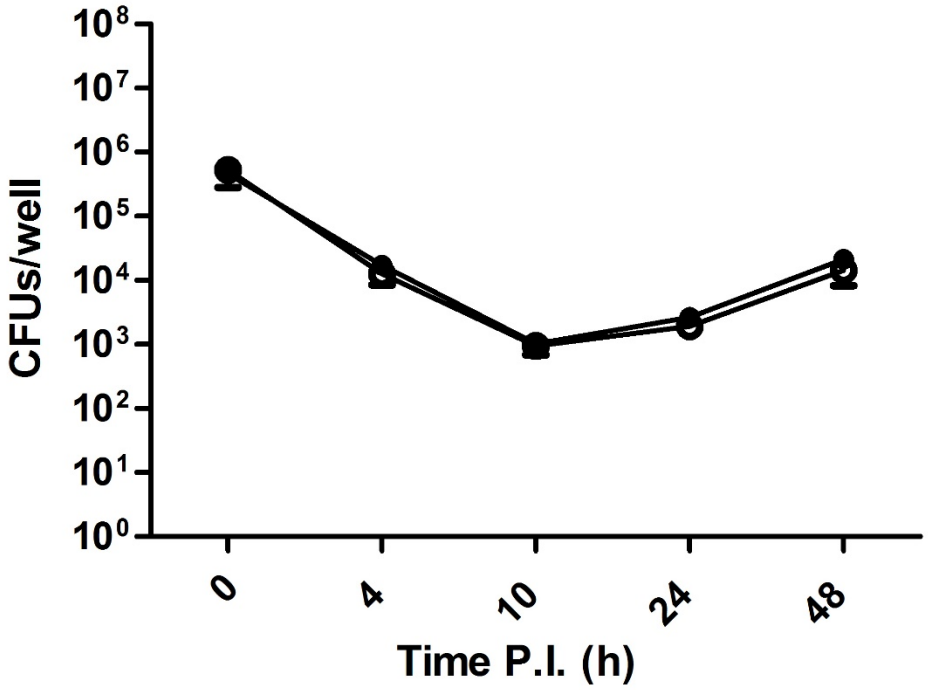

Figure 5. Infection and intracellular viability assay of *B. abortus* in J774 mouse macrophages *in vitro*. J774 macrophages were infected with either *B. abortus* 292 or the CO_2-independent spontaneous mutant *B. abortus* 292mut1, at a MOI of 50. Samples from triplicate wells were obtained at 0, 4, 10, 24 and 48 h post infection, and enumerated by dilution and plating. ● *B. abortus* 292 ○ *B. abortus* 292mut1.

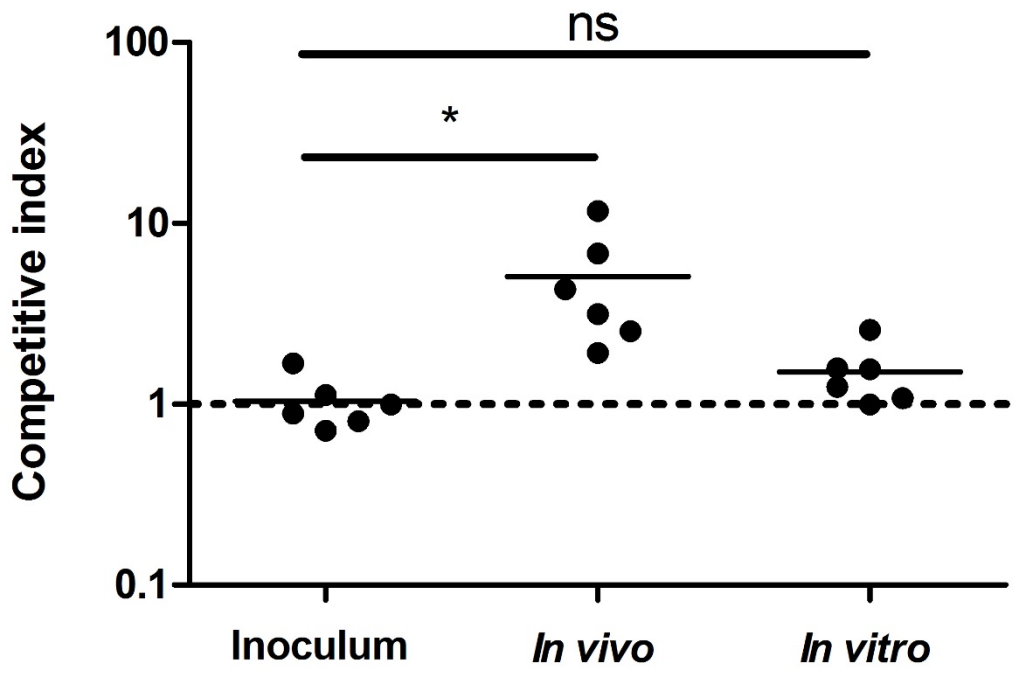

Figure 6: Competitive Index assay of a mixture of *B. abortus* 292, and its corresponding CO_2-independent spontaneous mutant *B. abortus* 292 mut1. The competitive index was calculated by dividing the output ratio of mutant to wild-type bacteria by the input ratio of mutant to wild-type bacteria, in the two groups tested, regarding the original inoculum. Thus, for strains with the same fitness, the result should be 1. The differences between groups were analyzed by Student's two-tailed t test with significance set at $P<0.05$ (*). ns, non significant.